Computational Principles of Neural Processing: modulating neural systems through temporally structured stimuli

Dissertation zur Erlangung des Grades
'Doktor der Kognitionwissenschaft' im
Fachbereich Humanwissenschaften der
Universität Osnabrück

vorgelegt von

Marta Castellano [1]

Osnabrück, October 2014

[1] m@martacastellano.eu

To Ian, Papa and Mama,
whose support made this possible

Dissertation Committee

Gordon Pipa
Institute of Cognitive Sciences, University of Osnabrück.
Address: Albrechtstrasse 31, 49076 Osnabrück, Germany.

Raul Vicente
Institute of Computer Science, University of Tartu.
Address: Juhan Liivi 2, 50409 Tartu, Estonia

Ulla Martens
Institute of Psychology, University of Osnabrück..
Address: Seminarstrasse 20, 49074 Osnabrück, Germany.

Declaration of Authorship

I, Marta Castellano Palomino, hereby declare that this thesis titled, "Computational Principles of Neural Processing: Modulating neural systems through temporally structured stimuli", and the work presented in it are my own. I confirm that:

- Where information has been derived from other sources or through collaborative work, it has been indicated in the thesis.
- This work was done while in candidature for a research degree at this University and the work has not been submitted previously, in whole or in part, to qualify for any other academic award.
- All experiments reported in this thesis were approved by the local ethics committee and conducted in accordance with the Declaration of Helsinki and National and Institutional Guidelines.

Signed: _____

October 2014

Acknowledgements

When I sat down to write the acknowledgements, I realized I had no idea where to begin. So many different people have contributed to make this thesis happen, and in so many diverse ways, I felt at a loss for words for what to say. Moreover, it has been extremely difficult figuring who to begin with: does listing Mama and Papa first mean they were more important than Gordon in creating this document? Of course not. With that said, in no particular order (and I mean that!) I would like to thank...

- Gordon Pipa, on both a personal and professional level, who gave constant support and encouragement, with his great ability to keep seeing interesting scientific questions and his enthusiasm for scientific research.
- The Neuroinformatics gang, in particular Hazem Toutounji, Patrick Putzky, Johannes Schumacher, Vikash Peesapati, Johannes Leugering and Mina Sahi, whose intelligence is never gonna stop surprising me. Great colleagues and friends.
- A long list of researchers within the Max Planck Institute of Brain Research, in particular Prof. Wolf Singer, Kai Gansel, Dr. Lucia Melloni, Dr. Will Barnes and Dr. Raul Vicente, for great discussions and guidance.
- Close friends who accompanied me through this time, in particular Laura Tatjer, Alba Trallero, Sascha Alexeyenko and Gabriella Lapesa. Here and there, you have been my family.
- Jordi Planas, Joan Bertran and Malu Calle among others, another long list of professors, this time from the University of Vic, who, with their enthusiasm and rigurosity, introduced me to the exciting world of science.
- Mama and Papa, my aunts, uncle and cousin, my dearest family who provided emotional and moral support in ways that are impossible to describe. Thanks for being who you are.
- When talking about family, I shall involve the Kavanagh family, in particular Nancy Kavanagh who managed to keep me going and whose participation was invaluable.
- Ian, my love, for everything, in every way, shape or form.
- To the Max Planck Institute for Brain Research, the Frankfurt Institute for Advanced Studies, the University of Osnabrück and the Pool Frauenförderung from the Gleichstellungsbüro for providing financial support at some point during the process.

I couldn't have done it without the love and support that I have received from all of you. From every fiber of my being, thank you.

No podria haver-ho fet sense l'amor i suport que he rebut de tots vosaltres. Des del fons del meu cor, us estimo!

Marta Castellano October 2014

'Begin at the beginning,' the King said, gravely, 'and go on till you come to an end, then stop.'

– Lewis Carroll, *Alice in Wonderland*

La labor de un pianista [. . .] es inaccesible para el hombre ineducado ya que la adquisición de nuevas habilidades requiere muchos años de práctica mental y física. Para entender plenamente este complejo fenómeno se hace necesario admitir, además del refuerzo de vias orgánicas preestablecidas, la formación de vias nuevas por ramificación y crecimiento progresivo de la arborización dendrítica y terminales nerviosas. (p. 296)

– Santiago Ramon y Cajal

Socrates: ...let us suppose that every mind contains a kind of aviary stocked with birds of every sort, some in flocks apart, some in small groups, and some solitary, flying among them all. Theaetetus: Be it so. What follows? Socrates: Whenever a person acquires any piece of knowledge and shuts it up in his enclosure, we may say that he has learned or discovered the thing of which this is the knowledge, and that is what 'knowing' means. Now think of him hunting once more for any piece of knowledge that he wants, catching, holding it and letting it go again.

– Plato. Theaetetus

[...] We may conclude that the complexity of a stone should increase with the length of its observation.

– Peter Erdi. Complexity Explained

UNIVERSITY OF OSNABRÜCK

Abstract

Institute of Cognitive Sciences
Department of Neuroinformatics

Dr. rer. nat

Computational Principles of Neural Processing: modulating neural systems through temporally structured stimuli

by Marta Castellano

In order to understand how the neural system encodes and processes information, research has focused on the study of neural representations of simple stimuli, paying no particular attention to it's temporal structure, with the assumption that a deeper understanding of how the neural system processes simplified stimuli will lead to an understanding of how the brain functions as a whole [84]. However, time is intrinsically bound to neural processing as all sensory, motor, and cognitive processes are inherently dynamic. Despite the importance of neural and stimulus dynamics, little is known of how the neural system represents rich spatio-temporal stimulus, which ultimately link the neural system to a continuously changing environment. The purpose of this thesis is to understand whether and how temporally-structured neural activity modulates the processing of information within the brain, proposing in turn that, the precise interaction between the spatio-temporal structure of the stimulus and the neural system is particularly relevant, particularly when considering the ongoing plasticity mechanisms which allow the neural system to learn from experience.

In order to answer these questions, three studies were conducted. First, we studied the impact of spiking temporal structure on a single neuron spiking response, and explored in which way the functional connections to pre-synaptic neurons are modulated through adaptation. Our results suggest that, in a generic spiking neuron, the temporal structure of pre-synaptic excitatory and inhibitory neurons modulate both the spiking response of that same neuron and, most importantly, the speed and strength of learning. In the second, we present a generic model of a spiking neural network that processes rich spatio-temporal stimuli, and explored whether the processing of stimulus within the network is modulated due to the interaction with an external dynamical system (i.e. extracellular media), as well as several plasticity mechanisms. Our results indicate that the memory capacity, that reflects a dynamic short-term memory of incoming stimuli, can be extended on the presence of plasticity and through the interaction with an external dynamical system, while maintaining the network dynamics in a regime suitable for information processing. Finally, we characterized cortical signals of human subjects (electroencephalography, EEG) associated to a visual categorization task. Among other aspects, we studied whether changes in the dynamics of the stimulus leads to a changes in the neural processing at the cortical level, and introduced the relevance of large-scale integration for cognitive processing. Our results suggest that the dynamic synchronization across distributed cortical areas is stimulus specific and specifically linked to perceptual grouping.

Taken together, the results presented here suggest that the temporal structure of the stimulus modulates how the neural system encodes and processes information within single neurons, network of neurons and cortical areas. In particular, the results indicate that timing modulates single neuron connectivity structures, the memory capability of networks of neurons, and the cortical representation of a visual stimuli. While the learning of invariant representations remains as the best framework to account for a number of neural processes (e.g. long-term memory [70, 174]), the reported studies seem to provide support the idea that, at least to some extent, the neural system functions in a non-stationary fashion, where the processing of information is modulated by the stimulus dynamics itself. Altogether, this thesis highlights the relevance of understanding adaptive processes and their interaction with the temporal structure of the stimulus, arguing that a further understanding how the neural system processes dynamic stimuli is crucial for the further understanding of neural processing itself, and any theory that aims to understand neural processing should consider the processing of dynamic signals.

List of Figures

1.1 Neural processing involves the activation of spatially distributed neural sources . . . 2

2.1 Generation of an action potential . . . 13
2.2 Biological basis of activity-dependent cortical plasticity . . . 15
2.3 Stimulus-specific spiking activity of a single neuron, modulated by the stimulus statistics and its changes due to the presence of ongoing plasticity 18

3.1 Spatial structure of neurons within cortical networks . . . 40
3.2 Population activity is stimulus-specific and adapts to the temporal structure of stimulus . . . 44
3.3 Spiking activity in a spiking neural network is stimulus specific . . . 56
3.4 Time-dependent stimulus encoding in SNN and a plastic SNN . . . 57
3.5 Computational Performance and Memory Trace of a SNN and plastic SNN . . . 58
3.6 Computational Performance and Memory Trace of SSN coupled to DDS (k=0.04) . . . 59

4.1 Macroscopic neural signals recorded by EEG . . . 67
4.2 Hierarchical organization of the visual cortex . . . 70
4.3 Local representation of contour perception: static versus morphing contour integration tasks . . . 89
4.4 Long-range phase synchronization during contour integration for different frequency intervals . . . 90

A.1 Visualization of a graphical (A) and matrix (B) representation of a regression problem . . . 103
A.2 Visualization of A) data partition on training and testing sets and B) overfitting of an estimated model . . . 115

Abbreviations

2AFC	2 **A**lternative **F**orced **C**hoice
AMPA	α**A**mino-3-hydroxy-5-**M**ethyl-4-isoxazole**P**ropionic **A**cid, excitatory neurotransmitter
CDF	**C**umulative **D**istribution **F**unction
DDS	**D**elayed **D**ynamical **S**ystem
EEG	**E**lectro**E**ncephalo**G**raphy
EPSP	**E**xcitatory **P**ost-**S**ynaptic **P**otential
GABA	**G**amma **A**mino**B**utyric **A**cid, inhibitory neurotransmitter
HP	**H**omeostatic **P**lasticity
ICA	**I**ndependent **C**omponent **A**nalysis
IPSP	**I**nhibitory **P**ost-**S**ynaptic **P**otential
ISI	**I**nter **S**spike **I**nterval
LFP	**L**ocal **F**ield **P**otential
LIF	**L**eaky **I**ntegrate **F**ire
MEG	**M**agneto**E**ncephalo**G**raphy
RC	**R**eservoir **C**omputing
RNN	**R**ecurrent **N**eural **N**etworks
SNN	generic **S**piking **N**eural **N**etwork
STA	**S**pike **T**riggered **A**verage
STDP	**S**pike **T**ime **D**ependent **P**lasticity
PCA	**P**rincipal **C**omponent **A**nalysis
PLV	**P**hase **L**ocking **V**alue
V1	Primary visual cortex

Contents

Abstract viii

List of Figures x

Abbreviations xiii

Contents xv

1 General Introduction 1

2 Microscopic scale: Single Neuron 9
- 2.1 Fundamentals of single neurons . . . 11
  - 2.1.1 From neurons to single neuron models . . . 11
  - 2.1.2 Cortical plasticity: biological basis and computational models . . . 12
- 2.2 Context . . . 16
- 2.3 Paper I: Spike train auto-structure impacts post-synaptic firing and timing-based plasticity . . . 19

3 Mesoscopic scale: Networks of Neurons 37
- 3.1 Fundamentals of neural networks . . . 38
  - 3.1.1 From single neurons to neural networks . . . 39
  - 3.1.2 Computational models of spiking neural networks: reservoir computing . . . 41
- 3.2 Context . . . 42
- 3.3 Paper II: Extending the memory trace in spiking neural networks through the coupling with an external slow delayed dynamical system . . . 45
- 3.4 Complementary simulations to Paper II: Extending the memory trace in spiking neural networks through the synergistic presence of several plasticity mechanisms. Impact of coupling with an external slow delayed dynamical system . . . 54

4 Macroscopic scale: Cortical areas 63
- 4.1 Fundamentals of cortical processing . . . 65
  - 4.1.1 From neural networks to macroscopic neural activity . . . 65
  - 4.1.2 Anatomical and functional basis of visual processing . . . 69
- 4.2 Context . . . 71

4.3 Paper III: Neuronal oscillations form parietal/frontal networks during contour integration. 73
4.4 Complementary analysis to Paper III: Static vs Dynamic Contour Integration: When Timing Matters 87

5 General Discussion and Conclusions **93**
5.1 Summary of the presented studies 94
5.2 Dynamic neural responses are stimulus-specific and are modulated by the stimulus dynamics 96
5.3 Characterizing dynamic neural responses in a time-resolved fashion . . . 98
5.4 Perspectives and open issues 101

A Appendices **103**
A.1 Appendix I: Regression models 103
A.1.1 Parameter Estimation 107
A.1.2 Model Validation - Goodness of Fit 112
A.1.3 Model Comparison and Model Selection 115
A.1.4 Regularization Methods 115
A.1.5 References 116

Bibliography **117**

Curriculum Vitae **135**

1

General Introduction

The neural system is an adaptive system that interacts with a continuously changing world, producing behaviour that ensures the survival of the organism. Spatio-temporal signals from the visual, tactile, auditory, and olfactory systems are continuously integrated into the ongoing brain dynamics to produce said behaviour. Simultaneously, plasticity mechanisms in the brain allow the neural system to learn and recognize the statistics of patterns, and adapt its responses to incoming stimulus. In such a complex system, how can we study the diverse physiological mechanisms that lead to cognition?

One of the main paradigms in cognitive science to understand cognition is the representationalist, or cognitivist framework, which posits that cognition arises through the manipulation of symbolic representations of the external world. As such, cognition is a form of computation, in which information - a symbolic representation of concepts on the physiological substrate - is encoded, stored, manipulated, and retrieved, generally referred to as neural processing [84]. As well as perception and action, cognition is reduced to the manipulation of representational states, where stimulus-specific representations are created and manipulated in terms of formal relations. In essence, determining stimulus-specific representations and how they are manipulated is the key to understanding cognitive function. This approach have resulted in years of research aiming to associate persistent neural activity with measurable features of the external world. For instance, intracraneal recordings report an enhancement of spiking activity within single neurons in the inferiotemporal cortex as in response to complex shapes or whole objects, carrying shape information from visual stimuli [27]. Similar feature-specific response has been reported on single neurons within prefrontal cortex [32], as well as within several regions within the temporal cortices that, for instance, specifically respond to faces [146]. But it is not only the neural representations of sensory stimulus that have been studied. Great efforts have been done to understand the neural basis of higher-level cognitive functions, including neural representations of values or rewards [112], attentional demands [244] or concept formation [147].

There are two crucial aspects to consider when characterizing neural representations empirically or studying neural processing in general: space and time [233, 251]. On the spatial aspect of neural processing, neural processing involves the activation of spatially distributed neural sources that can be recorded at spatially different scales, ranging

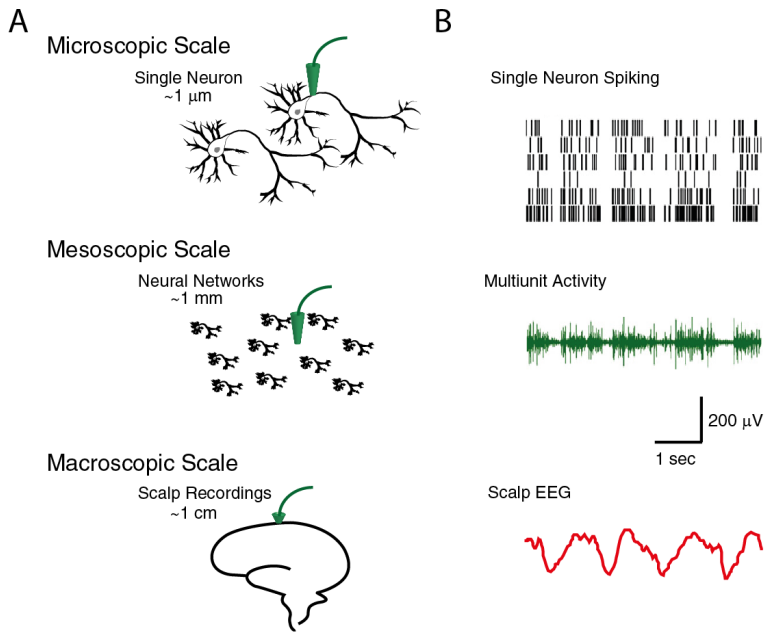

FIGURE 1.1: **Neural processing involves the activation of spatially distributed neural sources**. The neural system is a self-organized dynamical system that processes continuous streams of stimulus, producing complex output that contains information at multiple spatio-temporal scales, depicted in panel A. An approach to study such a complex system is to reduce its complexity by studying the constituting elements. Panel B reflects the spatially different neural signals that convey information about a common behavioural stage: REM sleep (adapted from [188]).

from single neurons within the same population, to large populations of neurons spread across the brain [137, 195]. This aspect of spatial distribution can be better illustrated with a specific example (see Figure 1), where the activity of single neurons, populations of neurons, and distant cortical areas has been recorded during sleep: slow waves and spindles, the most prominent neural features arising during sleep, can be recorded in both population activity (reflecting neural activity within ~ 1 mm^3) and scalp EEG (~ 1 cm^3) at several spatial locations across the brain, and are associated with ON/OFF periods of spiking activity within single neurons ($\sim 1\mu$m^3), that have a tendency to propagate through distal cortical areas [188]. Therefore, the most prominent features of neural activity associated to a given behavioural state can be decoded from signals that reflect neural activations at spatially different scales and from several spatial locations. Through the analysis of neural activity at disperse spatial locations, we arrive to one of the main features of the neural system: the brain is a modular structure that consists of several discrete functional systems [89, 109, 137, 178]. Though the degree of functional specialization and the discretization within neural circuits is under debate [226], it is generally accepted that different brain regions have some degree of functional specialization within disperse spatial locations, as evidenced by a large body of physiological, psychophysical and neuroimaging studies [89, 109, 137, 178].

Along with the spatial dimension of neural processing, a crucial aspect of the neural system is the temporal component: neural responses are dynamic, and the inherent temporal structure of neural activity conveys information [38, 46, 231]. The relevance of temporal coding has been evidenced by a large body of studies that report that

single neurons can generate precise spike-times patterns with milliseconds precision as a response to stimulus [107, 207, 232], spiking patterns of activity within a population of neurons [205, 231]. Most importantly, it has been proposed that precise temporal coordination of neural activity is the most plausible candidate for the dynamic information routing across the neural system, where spatially distinct neural sources code information in a synergistic manner [231, 268]. This aspect of temporal coding, where the precise coordination of spike times serves neural processing, has been largely discussed in literature under the name of temporal coding or the assembly hypothesis [229, 231]. Other examples of temporal coding are the latency code, where the precise timing of the first spike arising after stimulus onset carries most of the stimulus information [266], or phase coding, where the spikes that contain most information are those which fire in a relative phase in reference of an internal neural oscillation [183] (see [63, 65, 195, 215] for reviews). Simultaneously, in the cortical level ($\sim$ 1 cm^3) the relevance of temporal coding is classically studied within the context of the large-scale integration problem [86, 268], where distributed brain activity is coordinated to produce behaviour.

The relevance of neural dynamics and their temporal structure for neural processing becomes more evident in light of the recent body of studies that aim to directly characterize the spatio-temporal patterns of activity arising within the neural system [38]: reproducible spatio-temporal patterns of activity within sensory cortices has been reported as a response to static visual [187], olfactory [28, 172] or auditory stimuli [16], as well as within somatosensory system [5, 23]. Spike times become relevant as they trace a particular neural trajectory on the space, transcient signals whose dynamics encode information about a stimulus or cognitive event. Those signals that associate to specific stimuli also contain information from past stimuli, leading to a history-dependent representation of the outside world [55]. Importantly, as neurons seem inherently capable of encoding stimulus in spatio-temporal patterns of activity, it has become clearer that the temporal structure of neural activity can only be neglected at the cost of loosing information [205]. But it is not only the neural responses that are dynamic. At every instance, time-varying stimuli from visual, tactile, auditory and olfactory systems are integrated to produce behaviour, such that the timing of the stimulus is intrinsically bound to the completion of cognitive tasks [118]. For example, in the visual modality, the integration of the temporal information of a stimuli is not only crucial for the estimation of its direction and speed, but also its duration and its invariance over spatial rotations [164, 284]. However, the importance of time and the integration of temporal structures may be better shown by the auditory system and its ability to process and produce auditory/speech patterns, and where removing either spatial or temporal information impairs processing [16, 19, 75, 147]. Similarly, such behavioural impairment has been reported within other sensory modalities, such as the somatosensory system (e.g. grasping behaviour) [5, 23, 38] or visual sequentail learning [57, 93, 154, 177].

However, despite the physiological and behavioural relevance of temporal structures within neural signals and stimuli, little is known on how the neural system processes rich spatio-temporal stimuli. Any neuroscience textbook would provide a detailed explanation of how the visual cortex discriminates specific features of visual stimuli, such as orientation selectivity in early visual cortical areas (V1) or speed selectivity of the middle-temporal visual cortex (MT or V5) [137]. However, there is no clear mechanistic explanation on how the visual cortex discriminates the duration of such

stimuli, as current models of spatio-temporal processing cover dramatically different physiological mechanisms [34, 98, 100, 108, 129, 130, 265] (see section 4.2).

The lack of knowledge concerning how the neural system extracts temporal information from the stimulus can be attributed to several factors. First off, most of the neuroscience research studies neural responses associated to a simplistic and static stimulus, under the assumption that the physiological mechanisms that encode and process static stimuli can be generalized to those that are deal with dynamic stimuli [36–38]. Supporters of this idea argue that the temporal structures within the stimulus do not modulate the perception or the processing of the stimulus itself, as invariant representations of stimuli are learned [202, 209]. Second, there is a dearth of experimental methods which would allow for the clear segregation of cognitive processes in space and time. As such, the segregation of cognitive processes has to be done through simplifying the tasks and conditions tested [137]. For example, in estimating the trajectory of a visual stimuli in a noisy environment (i.e. a wine glass that is falling in a party environment), several cognitive processes are recruited, including object recognition, attentional selection and sustainment of sensory information within short-term memory: in such complex environment, how do we distinguish neural signals that are associated to each of these processes? Third and finally, the variability of cortical responses to a repeated stimulation is often as large as the response itself [11], and while considering that neural variability reflects the noise of the system, neural signals are averaged across several trials to increase the signal to noise ratio. However, the neural system processes time-varying stimuli on a continuous fashion while making sense of noisy single events, two crucial aspects that cannot be studied by the usage of static stimuli nor through the averaging across trials.

While invariant representations (and its implicit statement that the physiological mechanisms that encode and process static stimuli can be generalized to those that are deal with dynamic stimuli [36–38]) remain as the best framework to account for a number of cognitive processes (e.g. long-term memory [70, 174]), the reported studies seem to evidence that dynamics within the stimulus at the neural system are crucial for neural processing. To this end, understanding how the neural system processes dynamic stimuli is crucial, at a minimum, for the following reasons. First, it would allow for the verification of whether the physiological mechanisms that process simplified static stimulus can be generalized to the processing of dynamical stimulus or whether the temporal structure of stimulus is a relevant feature that modulates the neural processing itself [100]. Second, it would allow for the study of several cognitive tasks that cannot be addressed without considering temporal aspects, such as sequential learning tasks [57, 92], interval estimation [38] or for control and execution of body movements [55, 145].

In this thesis, we focus on the dynamic aspects of neural representations, studying how time-varying signals modulate neural responses. To that end, given the spatial complexity of the neural system, the modulation of neural responses via time-varying signals and other complementary aspects of spatio-temporal processing will be discussed at separate spatial scales: at the scale of single neurons, within populations of neurons, and involving activation of distributed large cortical areas. At each spatial scale, we will discuss how time-varying signals modulate the neural responses and other complementary aspects by reviewing recent literature and presenting three different studies. In a general sense, the first study analyses the impact of temporal

structure within pre-synaptic spike-times in the spiking activity of a plastic single neuron, introducing the relevance of plasticity on shaping the neural system and discussing spatio-temporal processing on self-organizing systems. The second study presents a neural population that processes spatio-temporal stimuli, introducing the relevance of population coding on the processing of spatio-temporal patterns, and discussing its properties and limitations. The third study characterizes the dynamics of EEG-signals associated to visual perception, introducing the relevance of large-scale integration for cognitive processing, among several other aspects.

With these studies, we aim to provide further evidence that neural responses are strongly dependent on the temporal features of the stimulus, suggesting that understanding the interplay between stimulus dynamics and the neural activity is crucial for the further understanding of neural processing itself. In particular, complementing studies that report a selective response of neurons to specific spatio-temporal structures within stimuli, [38, 222], this thesis proposes that any theory that aims to understand neural processing should account for the processing of time-varying stimuli. Furthermore, we argue that experimental and methodological limitations can be overcome by the usage of decoding algorithms that predict the presence of a given stimulus or behaviour from the pattern of neural responses [142, 237]. Decoding techniques have proven particularly useful for analysing cognitive tasks in a time-resolved fashion such as odour representation [28, 172], different stages of object recognition [49], among others [142]. Finally, we discuss how considering spatio-temporal structures is specially relevant within adaptive systems, as plasticity alters neural representations while enabling the neural system to learn and recognize spatio-temporal patterns of a continuously changing world [79].

Statement of the problem

Research aimed at understanding neural processing, and neural mechanisms that underlie stimulus representation and manipulation, has proceeded with the assumption that further understanding of how the neural system processes simplified stimulus is key to address brain functioning [84]. While this assumption may remain as the best framework to study the mechanisms by which invariant representations of stimuli are generated, time is intrinsically bound to neural processing as a) neurons seem inherently capable of encoding stimulus in spatio-temporal patterns of activity and b) sensory, motor and cognitive processes rely spatio-temporal patterns of neural activity, that ultimately, link the neural system to a continuously changing environment. However, despite the behavioural and physiological relevance of temporal structures in both stimulus and neural activity, little is known on how the neural system processes rich spatio-temporal signals or whether and how stimulus dynamics modulate neural representations.

Purpose of the dissertation

The purpose of this dissertation is to study how time-varying signals modulate the neural responses at different spatial scales: at the single neuron or microscopic scale, within networks of neurons or mesoscopic scale, and within cortical areas or macroscopic scale, . We argue that understanding the interplay between stimulus dynamics

and the neural activity is crucial for the further understanding of neural processing itself.

Outline of the dissertation

Given the spatial complexity of neural systems, the processing of time-varying signals will be discussed at three separate spatial scales: at the scale of single neurons, within population of neurons and within distributed coding through large cortical areas, each comprising its own chapter.

The first study in chapter 2 will analyse the impact of the temporal structure of incoming spikes on the spiking activity of a single neuron and its synaptic weights. Given that the study is based on single neuron activity, we define this study as the microscopic scale of analysis. In chapter 3, the second study is presented, which aims to characterize the capability of an spiking neural network to process and retain stimulus with rich temporal structure. This will be the mesoscopic scale of analysis. In chapter 4, the final study will be presented, which analyses the dynamics of scalp-recorded neural data (electroencephalogram or EEG) of human subjects performing a visual categorization task, the macroscopic level of analysis. This study aims to characterize a) whether the temporal structure within stimulus modulates cortical responses, b) whether oscillatory activity within visual cortex predicts the integration of visual features and its further categorization and c), we tested whether and how this categorization process modulates communication (i.e synchronization) across distal EEG sources.

These chapters 2,3 and 4 are divided in several sections. Each chapter starts with a short summary of the following study, with the aim to clarify the research question(s) and hypotheses. Following that, each chapter contains a 'context' section that revisits how the neural system represents and processes stimuli at that specific spatial scale, with special emphasis on how those neural representation are modulated by the temporal structure of the stimulus. Next, the section 'fundamentals' aims to present the background concepts used on the corresponding studies for readers lacking a neuroscience training. The following sections contain a detailed introduction, method section, results, discussion and conclusions as appear on the corresponding published journals and conferences.

Note that parts of this dissertation were presented and published as following:

Study 1: Single Spiking Neurons

Parts of this study were presented in the following events: *International Neuroinformatics Coordinating Facility Congress (INCF)* (August 30 - September 1, 2010, Kobe, Japan) and on *Computational and Systems Neurosciences Meeting - COSYNE* (February 25-28, 2010, Salt Lake City, UT, USA)

This study was published after peer-review process in *Frontiers in Computational Neuroscience*, and is found under the following reference:

Scheller, B.∗, **Castellano**, M.∗, Vicente, R., and Pipa, G. (2011). Spike train auto-structure impacts post-synaptic firing and timing-based plasticity. *Front. Comput. Neurosci.* 5, 60.

∗ These authors contributed equally

Study 2: Network of Spiking Neurons

Part of this study was presented and published after peer-review process as a talk and conference proceeding on the *International Conference on Artificial Neural Networks*, and is found under the following reference:

Castellano, M., and Pipa, G. (2013). Memory trace in spiking neural networks. In Artificial Neural Networks and Machine Learning – ICANN 2013, *Lecture Notes in Computer Science*, (Springer Berlin Heidelberg), pp. 264–271.

Study 3: Cortical Areas performing a Contour Categorization Task

Parts of this study were presented in the following events: *Osnabrück Computational Cognition Alliance Meeting - OCCAM* on *"Mechanisms for Probabilistic Inference"* (May 7-9, 2014, Osnabrück, Germany)

This study has been published after a peer-reviewed process in *Frontiers in Integrative Neuroscience*, and is found under the following reference:

Castellano, M., Plöchl, M., Vicente, R., and Pipa, G. (2014). Neuronal oscillations form parietal/frontal networks during contour integration. *Front. Integr. Neurosci.* 8, 1–13.

Significance of the dissertation

Understanding how the neural system processes dynamic stimuli is crucial, at a minimum, for the following reasons. First, it would allow for the verification of whether the physiological mechanisms that process simplified static stimulus can be generalized to the processing of dynamical stimulus or whether the temporal structure of stimulus is a relevant feature that modulates the neural processing itself [100]. Second, it would allow for the study of several cognitive tasks that cannot be addressed without considering temporal aspects, such as sequential learning tasks [57, 92], interval estimation [38], control and execution of body movements [55, 145] or spatial navigation tasks [69].

The literature exploring the processing of temporally structured stimulus is sparse. The relevance of temporal information within the neural signals has been evidenced by a large body of studies that report the presence of precise spike patterns within single neuron responses [107, 207, 232], as well as population [205, 231] and a precise coordination of cortical responses within distal cortical areas [268], and it has been proposed that precise temporal coordination of neural activity is the most plausible candidate for the formation of dynamic information routing across the neural system [86, 231, 268]. However, the relevance of temporal information within the stimulus itself is largely neglected, with the assumption that understanding the mechanisms by which the neural system processes simplified static stimulus would generalize to stimulus with rich spatio-temporal structures [84, 202, 209].

Here, we argue that, despite the advancement of experimental methods that allow for the time-resolved analysis of cognitive stages, there is little research that bridges

how temporally-structured stimulus are processed at separate spatial scales, nor there are many studies that investigate how the temporal structure of the incoming stimulus modulate neural processing in comparison to static stimuli. This thesis attempts to further knowledge in the field concerning the processing of dynamic stimuli, arguing that understanding neural processing may be crucial in order to understand the processing of dynamic signals.

Limitations of the dissertation

1. Different spatial scales (single neurons, population of neurons and distributed cortical areas) are studied as independent processing scales, disregarding any possible interaction or dependencies among them that have been reported and studied elsewhere [46, 195].

2. The method to decode used within populations of neurons and within cortical areas to decode stimulus/behaviour assume a linear relationship between the that the relationship between stimulus/behaviour and the neural signal is linear (see section A.1 for details). Such constraint on linear dependencies can be potentially made non-linear.

Delimitations of the dissertation

The studies presented on this dissertation neither seek to provide a mathematical formulation of neural processing mechanisms nor to develop novel computational models. Although these would be very interesting possibilities, rigorous computational models that aim to provide a mechanistic explanation of the physiological mechanisms by which the neural system processes spatio-temporal stimulus are provided elsewhere (see [38, 71] for an example).

2

Microscopic scale: Single Neuron

The purpose of this dissertation is to study how time-varying signals modulate the neural responses at different spatial scales: at the single neuron or microscopic scale, within networks of neurons or mesoscopic scale and within cortical areas or macroscopic scale.

This chapter presents the first study that aims to analyse the impact of the temporal structure of incoming spikes on the spiking activity of a single neuron and its synaptic weights, the microscopic scale of analysis. The chapter is divided in three sections, and starts with a short summary of the corresponding study with the aim to provide a broad idea of the research questions and hypothesis. Following, the section 'fundamentals' aims to present the background concepts used on the corresponding studies. Next, each chapter contains a 'context' section that revisits how the neural system represents and processes stimuli at that specific spatial scale, with special emphasis on how those neural representation are modulated by the temporal structure of the stimulus. The third section, contains the published journal article, as appears in *Frontiers in Computational Neuroscience* with the following citation: Scheller, B.∗, **Castellano**, M.∗, Vicente, R., and Pipa, G. (2011). Spike train auto-structure impacts post-synaptic firing and timing-based plasticity. *Front. Comput. Neurosci.* 5, 60.

∗ These authors contributed equally

Short summary of the study

Cortical neurons typically receive stimulus on the form of spike trains at several thousands of synapses. The precise coincidence of pre-synaptic spikes may lead to the generation of a spike on the post-synaptic neuron, so that the temporal pattern of incoming pre-synaptic spikes can modulate the spiking response of the post-synaptic neuron [101, 137, 238].

However, when studying several thousands neurons, the temporal pattern of pre-synaptic spikes is assumed to be a renewal process with no temporal structure [81, 115, 193].While recorded spiking activity of pyramidal neurons typically deviates from

Poisson-processes [12, 165, 185, 186, 201, 249], it is generally argued, that, when the pre-synaptic spike trains, arriving at a neuron are independent, the temporal structure is washed out [81, 193].

The purpose of this study was to investigate how the temporal structure of pre-synaptic spiking modulates the post-synaptic firing through the modelling of a spiking neuron that is receiving pre-synaptic activity from inhibitory and excitatory neurons. As previously suggested by theoretical studies [51, 155, 200], our study reveals that the temporal structure of both inhibitory and excitatory pre-synaptic spike trains, together with its relative firing rate, modulate the firing probability of the post-synaptic neuron in a non trivial fashion.

Furthermore, through this first chapter, we also introduce the concept of plasticity and activity-dependent plasticity mechanisms, that can be influenced by the precise temporal order between the pre- and post-synaptic spiking [151, 167, 234]. While the relevance of precise spike times is widely recognized experimentally [107, 207, 231, 232, 268], the temporal structure in computational models, which study plasticity, is still approximated by a *Poisson* process. Through the modelling of spike-timing dependent plasticity (STDP), we explored how the temporal structure within pre-post synaptic spike trains modulates the synaptic weight that connect the single neuron with its pre-synaptic neurons. In short, our results suggest that the synaptic weight distribution is modulated by the temporal structure at three different temporal scales. First, we described how the fast changes on synaptic weight directly reflect the repetitive structure of the pre-synaptic spike trains. Second, we found that temporally structured spike trains modulate the speed at which synaptic weight occur, as long as the firing rate of excitation/inhibition keeps a simple *n:m* relation. Third and finally, our results show that the temporal structure within excitatory pre-synaptic trains modulates the equilibrium distribution of synaptic weights. In summary, our first study suggest that the modelling of real neural firing might require a non-*Poisson* assumption, as structural changes associated to activity-dependent plasticity are modulated by the regularity and frequency of spiking activity.

References

Parts of this study were presented in the following events: *International Neuroinformatics Coordinating Facility Congress (INCF)* (August 30 - September 1, 2010, Kobe, Japan) and on *Computational and Systems Neurosciences Meeting - COSYNE* (February 25-28, 2010, Salt Lake City, UT, USA)

This study was published after peer-review process in *Frontiers in Computational Neuroscience*, and is found under the following reference:

Scheller, B.∗, **Castellano**, M.∗, Vicente, R., and Pipa, G. (2011). Spike train auto-structure impacts post-synaptic firing and timing-based plasticity. *Front. Comput. Neurosci.* 5, 60.

∗ These authors contributed equally

2.1 Fundamentals of single neurons

This section aims to provide background knowledge of the concepts used on this and following chapters. In particular, this section presents an overview of the physiological properties of cortical neurons and plasticity mechanisms, briefly presenting computational models that describe both phenomena.

2.1.1 From neurons to single neuron models

About 10% of cells in the brain are nerve cells or neurons [137]. Although other cells in the nervous system (e.g. glia cells) may play a role in synaptic plasticity and learning [6, 9] or neuromodulation [7, 119], neurons are still regarded as the main information processing units in the brain. Correspondingly, we will concentrate on the physiology and modelling of neurons.

Neurons are electrically excitable cells that integrate and transmit electrochemical signals, also called *action potentials* or *spikes*, within and to the central nervous system [137]. Neurons produce spikes that have a rather similar intensity and duration [101, 238, 241], in contrast to other electrically excitable cells (i.e. muscle cells), whose response amplitude is dependent on the intensity of stimulus. As such, the variability of action potentials is then disregarded, and the spiking activity of a neuron is described a set of events in time or spike trains, a sequence of data points or point process.

Although the morphology of a neuron can be widely different depending on its location in the brain [137], its general structure can be divided into three parts: the dendritic tree, the axons and the cell body or soma (Figure 2.1). A neuron receives electrochemical signals from other neurons through its synapses, highly specialized junctions connecting two neurons, that spread over the axons (pre-synapse, the efferent side) and the dendritic tree (post-synapse, the afferent side).

An action potential is an extremely precise event in which the membrane potential of a cell rapidly changes voltage, lasting for 1-2 ms and inducing a voltage change of about 100 mV, see Figure 2.1. An action potential on the efferent side (pre-synaptic neuron) will induce the release of several molecules at the synapses that will activate ion channels on the post-synaptic neurons, allowing an influx of ions within the neuron or membrane potential change. Depending on the type of molecule or neurotransmittor released at the pre-synaptic side, a pre-synaptic signal can induce either an excitatory or inhibitory potential on the post-synaptic neuron (Figure 2.1). Excitatory pre-synaptic signals (EPSP) induce a depolarization or decrease of the membrane potential by activating mechanisms that allow the entrance/escape of Na^+/K^+ ions respectively. Inhibitory pre-synaptic signals (IPSP) induce an hyperpolarization or increase the membrane potential by allowing the escape/ entrance of Na^+/K^+ ions respectively. If the total incoming ionic flux overcomes a threshold, this leads to the production of an action potential within the post-synaptic neuron, that would travel along the axons until the synaptic cleft, where it would act as a signal for the following neuron. After an action potential is generated, the membrane potential of the afferent neuron is resat to the equilibrium membrane potential, typically 65 mV difference from the extracellular potential. The action potential would travel along the axon with an

average velocity of about 1 to 100 m/s[1], depending mainly on the diameter of the axon and the thickness of the Myelin sheath (a electrically insulating material that forms a layer around axons, an outgrowth from glial cells). For few ms after an action potential, there is a refractory period during which no spike can be evoked.

The biophysical mechanisms underlying action potential generation can be formalized in phenomenological models that describe the spiking behaviour of single neurons. As the cell membrane separate ions between the intra and extra cellular medium, it can be described as a capacitor (the capacitance C_m is the ability of a substance to keep apart charged particles) and thus, measure its resistance as $R_m = 1/C_m$. The membrane potential V relates to the membrane capacitance C_m and the incoming currents I through Ohm's law $I = C_m \cdot V$ where I is the current through the conductor. The time-evolution of the membrane potential can be describe by $\tau_m \cdot \frac{dV}{dt} = -V(t) + R_m \cdot I(t)$, where τ_m, the membrane time constant, describes the speed of change. Accompanied with a threshold value θ that defines the moment at which the membrane potential is resat to the resting potential V_{rest}. The variability of the membrane potential at equilibrium V_{rest} (and initial conditions V_0) and the threshold θ is not very high within biological systems [101, 238, 241] and models usually assume that those parameters can be modelled as constants. This description of the membrane potential is the *integrate and fire model*, and was developed in the 1907 by Lapicque [149]. Further developments lead to a wide range of single neuron models, varying from highly detailed descriptions of biophysical signals to extremely simplified models with two discrete states [96]. Detailed models require higher number of variables and are usually computationally heavy, while simplified models are computationally more efficient but may lead to wrong biological results. For a widespread review, see [63, 96, 121]. In the studies comprised within this dissertation, the integrate and fire model will be used. If there is any modification from the integrate and fire model, it will be indicated.

2.1.2 Cortical plasticity: biological basis and computational models

In the context of neuroscience, plasticity was first introduced by William James on 1890, in reference to the susceptibility of human behaviour to adapt. It was until 1906 that Ramon y Cajal argued for the neural basis of this adaptability, presenting activity-dependent plasticity as an intrinsic mechanism of the newly found neurons that could serve as a substrate for learning and memory [206]. Since Bliss and Lomo first demonstrated activity-dependent modification of synaptic efficiency within hippocampus (Long Term Potentiation or LTP) [24], it is widely accepted that during learning, the efficiency of synaptic transmission between neurons changes, and that those changes must be stabilized in order for memory to persist [70, 174], creating a

[1]The first measure of the conduction velocity was performed in the middle of the 19th century by Hermann von Helmholtz through a reaction-time experiment: he touched the foot of one of his subjects and instructed him to report the feeling of the touch. Then, he repeated the experiment, this time by touching the subject thigh. He knew the distance between the foot and the thigh, and after performing several trials, he could also compute the average reaction time. By subtracting the foot reaction times from the thigh times, he could arrive to an estimation of neural conduction time. That was indeed, the first time that it was shown that sensations are not simultaneous with stimulation [118]

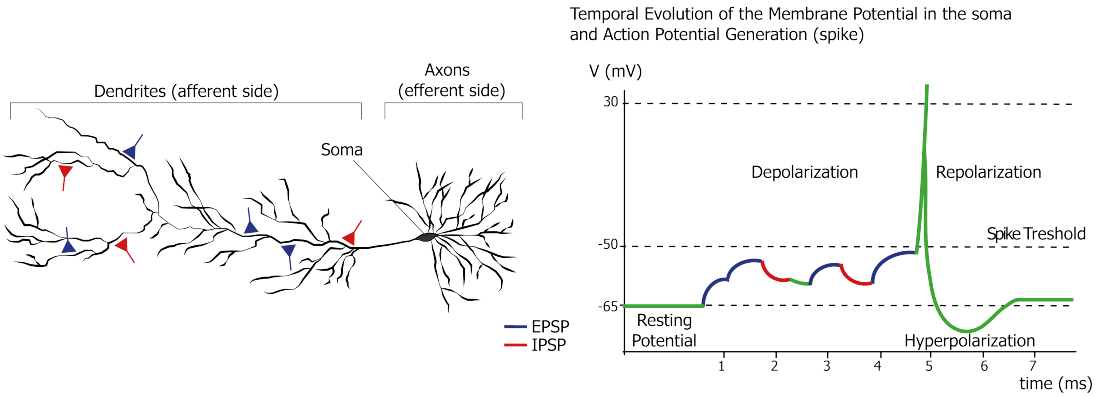

FIGURE 2.1: **Generation of an action potential**. Left: Morphology of a pyramidal neuron. Right: Temporal evolution of the membrane potential of a pyramidal neuron (green), where an action potential is generated through the convergence of excitatory pre synaptic potentials (EPSP, blue trace) and inhibitory pre synaptic potential (IPSP, red trace).

direct link between structural modifications within single neurons and learning and memory.

But not all cortical plasticity mechanisms are functionally responsible of making structural changes that constitute stimulus-specific memories. The relevance of cortical plasticity in cognitive processing and general brain functioning is widely recognized by both experimental and computational studies. Experimentally, long-term modifications of synaptic weights and structural or morphological changes within neural systems have been observed as a result of cognitive processing [56]. For instance, acute and chronic stress disorders associate anxiety-like behaviour and mood alterations to structural modifications of specific amygdala nuclei, hippocampus and prefrontal cortex [211]. On a similar fashion, addiction and drug abuse seem to modulate neural circuits involved in reinforcement and reward-modulated learning, inducing long-term adaptations in the dopamine system, involving the Nucleus Accumbens (NAc), the Ventral Tagmental Area (VTA), hippocampus, and other brain regions involved in the mesolibmic dopamine system [138].

What are the physiological mechanisms that mediate such adaptation? Experimental studies on synaptic modifications between neurons have revealed the presence of a large body of plasticity mechanisms that affect the synaptic transmission efficacy and the intrinsic excitability of neurons (see for reviews [39, 96, 259]). Plasticity mechanisms can be grouped in several classes, depending on the timescale at which synaptic modification occurs (e.g. ms to years), depending on whether the mechanism affects a neuron pair or several neurons (e.g. global neuromodulatory signals) or whether the change in synaptic strength involves changing the properties of the synapse (e.g. vesicle release) or the neuron intrinsic properties (e.g. ion channel redistribution). Other mechanisms are *metaplasic*, implying that regulate the location and intensity of synaptic plasticity, modulating the probability of inducing subsequent plasticity [2]. Some other mechanisms are *homeostatic*, ensuring that the neural activity does not exceed metabolic constraints, stabilizing neural activity towards a stable fixed-point activity [61, 259]. Ultimately, cortical plasticity arises through the complex interplay of all these plasticity mechanisms which are ubiquitous within the neural system.

Despite the efforts on designating a specific function for different plasticity mechanisms, little is known about the precise functional relevance of different plasticity mechanisms. The most important limitation is the fact that different plasticity mechanisms share common molecular pathways and receptors, and inhibition or manipulation of receptors or secondary messengers block multiple forms of plasticity [141]. Here is where computational models, that can isolate different plasticity mechanisms, can contribute on the understanding of how plasticity modulates information processing.

Computationally, synaptic plasticity was first proposed by Hebb in 1949 as a model for learning and memory [117], even before the experimental evidence of LTP was reported [24]. In short, Hebb postulated that when two neurons activate simultaneously, their synaptic strength increased, while decreased when active independently. This Hebbian plasticity is self-amplifying and acting on the timescale of sec to minutes, and through the positive-feedback loop, synapses would saturate rapidly as memories are directly stored on the synaptic weights. On the same way, ineffective synapses are weakened to the point of quiescence, an overall dynamics that tends to destabilize post-synaptic firing which either saturates or becomes silent. Together with the advancement of experimental studies, several computational models of plasticity arise that, when considered with Hebbian learning, lead to the control of such instabilities: some of the mechanisms are homeostatic (regulating the overall neuron's excitability), some of them are time-dependent (where the precise time of a spike matters) and some of them involve a modulation of the overall network excitability (neuromodulatory plasticity) [1, 56, 96, 181, 277]. Following, an overview of those cortical plasticity mechanisms that will be used in this dissertation.

Spike-timing dependent plasticity

Spike-timing dependent plasticity is a form of Hebbian plasticity where the precise order of pre-post spikes determines the amount and direction (potentiation or depression) of the plastic change, within a critical window of few ms [48]. In a simplified manner, if the pre-synaptic spike precedes a post-synaptic spike, there is a potentiation of the synaptic strength which is reflected as an increase in EPSP amplitude; the reverse order of spikes leads to a depressive synapses, as long as the timing difference between pre-post spikes is beneath 40-80 ms (Figure 2.2 A). Since the discovery of this temporal dependency in Hebbian plasticity, the study of the STDP has become one of the most active in the area of synaptic plasticity and learning (see [1, 48, 60] for review). Besides the simplicity of the learning principle, the temporal-dependent modification of synaptic weight has been observed in a wide variety of brain areas, species and induction protocols (Figure 2.2 A, lower plots), suggesting that, regardless the direction of the synaptic modification, learning temporal dependencies within the precise pre-post spike times is a crucial feature within the neural system.

Physiologically, it is generally accepted that such modulations in the EPSP amplitude result from changes in the post-synaptic concentration of calcium, recruited by several Ca-transporters involved in the intracellular singling pathways that are classically activated after synaptic activation within LTP and LTD protocols [48, 181]. In short, high concentrations of calcium within the post-synaptic neuron before the arrival of a EPSP result in a potentiated response to future EPSP (LTP), leading to a self-potentiation of EPSP amplitude. Additionally, the emission of an EPSP can temporally modify

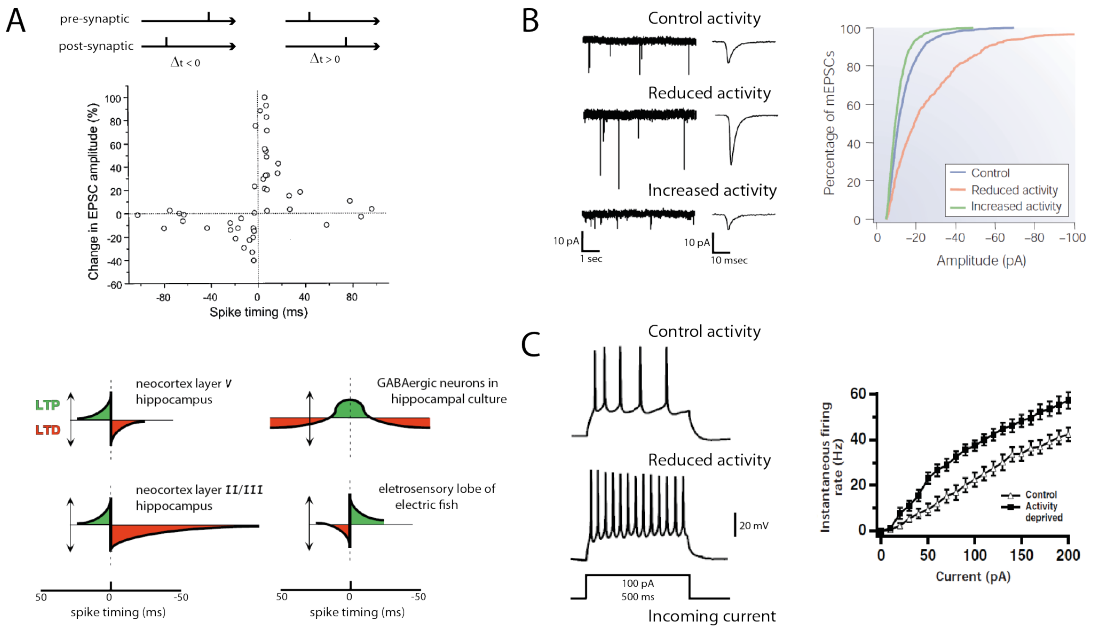

FIGURE 2.2: **Activity-dependent cortical plasticity** A) Spike-timing dependent plasticity leads to a modification of the EPSP amplitude induced by repetitive pairing of pre-post-synaptic spikes (upper plot, hippocampal neurons, adapted from [21]). The strength and direction of the synaptic modulation (potentiation or depression) varies in different brain areas, species and induction protocols (adapted from [1]) B) Synaptic scaling leads to a change in the membrane potential amplitude after the arrival of an EPSP. While chronic increase of incoming activit reduce the amplitude of EPSP, reduced incoming stimulus has the opposite effect. Adapted from [258, 259] C) Intrinsic Plasticity leads to an increased firing frequency and lower spiking threshold after reduced or decreased input of pyramidal neurons, adapted from [66]

the excitability of the dendritic tree within the same neuron (back-propagation potential, BAP), resulting in a low influx of Ca within the cell that leads to depression or reduction of the amplitude of the future EPSP (LTD) [48, 60].

Computationally, it has been proposed that STDP encourages synaptic competition, as effective synapses are enhanced, while introducing stability and sensitivity to future incoming stimuli [235]. On a similar fashion, several studies propose that temporal asymmetry within synaptic plasticity allows for the cortical remapping observed in learning studies [234].

Homeostatic plasticity

Homeostatic plasticity describes a set of plasticity mechanisms that bring the overall network activity towards a certain fixed point, avoiding quiescence or runaway excitation regimes of activity and implementing some kind of metabolic regulation of spiking activity [61, 62, 259]. Homeostatic processes have been largely studied in biology and more recently, it has become apparent that those mechanisms are crucial not only to stabilize spiking activity due to incoming stimulus, but also, as a stabilizing mechanism on neural systems where synaptic plasticity is taking place [255, 259]. Computationally, the relevance of homeostatic plasticity was apparent from the first studies on Hebbian

learning rules, where a normalizing term to regulate the total synaptic strength and avoid the neural system from runaway excitation or quiescence [1]. The exact physiological mechanisms by which the spiking activity of neurons is regulated through homeostatic mechanisms remain to be characterized, mostly due to the fact that an homeostatic regulation of the firing rate may result from the modulation of several physiological features, including a change on the strength of synaptic connections between neurons or a change on the intrinsic excitability of neurons [61, 62, 259]. In this section, we focus on synaptic scaling and intrinsic plasticity and its models, both homeostatic mechanisms that have been studied within the computational neuroscience community.

Synaptic scaling Through synaptic scaling, the strength of all neuron's synaptic input is modulated as a function of the incoming activity [61, 62, 259]. As such, the total synaptic drive is scaled up to a specific value, while the relative strength of each synapse is kept constant (Figure 2.2 B). Computational studies were the first to show that the scaling of synaptic weight stabilizes Hebbian plasticity, highlighting the relevance of homeostatic plasticity for the stabilization of spiking activity [62]. Experimentally, synaptic scaling has been observed over repeated single neuron recordings, while its physiological mechanisms have not been uncovered yet [259].

Intrinsic plasticity Through intrinsic plasticity, the intrinsic excitability of neurons is modified as a function of the incoming activity [61, 62, 259]. As such, the neuron spiking response to a stimulus will change, so that the neuron is more excitable during periods of low stimulation, and less excitable after long periods of stimulation (Figure 2.2 C). Computational studies have shown that as a result of active intrinsic plasticity, single neuron's firing rate becomes exponential and argued that through IP, a single neuron maximizes stimulus information [56]. Experimentally, multiple forms of intrinsic plasticity have been observed, differing on the physiological mechanisms involved, brain regions or species [289], and such persistent changes in the neuron's intrinsic excitability can be observed in behaving animals [289].

2.2 Context

The question on how single neurons encode and transmit information has been a central issue in neuroscience research: the neural coding problem [46, 97, 224, 233], or the search of the smallest neural response that is capable of representing stimulus features.

The search for the neural code started after it was observed that the firing rate of a single neuron changes as a response to a change of a stimulus, as reported first in 1926 by E.D Adrian [4], who observed a steady increase of the spiking activity of nerve cells when a muscle was stretched. It was until 1962 that Hubel and Wiesel reported the first modulation of firing rate within central nervous system of anaesthetized cats: the firing rate of neurons within the primary visual cortex (V1) depended strongly on the orientation of a moving bar (Figure 2.3 A), becoming one of the hallmarks in neuroscience research [125]. Their findings were accompanied by the rising of the grandmother cell idea, a term coined in the 1960s by Koronoski and Lettvin, which

propose that each neuron represents only one certain type of information about the stimulus [103]. Since then, the coding of information as a change of the spiking rate, or **rate coding**, has been related to the processing of sensory information, as well as to cognitive processing in general [132, 137, 137, 210, 215]. Among others, sustained firing rate has been proposed as the mechanism by which the neural system retains and sustains items that can be manipulated through working memory [134]. Also, sustained firing rate has been proposed to be crucial for decision making processes, where the average firing rate is thought to represent the accumulation of sensory evidence that is required to perform a decision [102].

The precise spike times of a neuron can similarly represent information about the stimulus or its features, according to the **temporal coding** hypothesis [232], where precise temporal spiking patterns can be triggered by the presence of stimuli [64, 166] or by behavioural events [107, 207, 271]. For example, individual cells in the lateral geniculate nucleus (LGN) are found to respond with the same spike pattern (with 1 ms precision, in cat cortex) to repeated flickering stimulus, and spiking responses with similar temporal precision can be found in somatosensory cortices encoding spatial location of a rat [196]. On a similar fashion, an individual neuron has been shown to represent information about the stimulus by means of the time intervals between spikes (latency code, see [266]) or by the phase difference to ongoing oscillatory activity (phase code, see [183]).

Accompanying this body of experiments that report several mechanisms by which information is encoded and processed by single neurons, it should be noted that the spiking response of a single neuron to a specific stimuli is far more complex than expected: the spiking response of a single neuron to a specific stimulus has been reported to change as a function of both the spatio-temporal context of the stimulus and due to the presence of plasticity mechanisms.

On the first place, the responses of a single neuron to a specific stimuli depend strongly on both its spatial context (what surrounds a given stimulus or stimulus feature) and its temporal context (what has been observed in the past). For instance, while neurons in the primary visual cortex (V1) are selective for specific orientation of a bar stimuli [125], the presence of a surround spatial context with an orientation of a least 15^{o} induces a suppression of the spiking response to the preferred orientation, while orthogonal orientation of the context leads to spike facilitation [52]. The modulation of spiking activity of single neurons due to changes in the properties of the stimulus been similarly reported in the study of motion, brightness, blur and faces [222], as well as within auditory cortex [139], where the spiking activity carry activity of not only the identity of the tone, but of its temporal evolution.

On the second place, and due to the presence of plasticity mechanisms, the responses of a single neuron to a specific stimuli depend strongly on prior experiences [60, 79]. The classical example of adaptation studies comes from the visual system, where monocular deprivation shifts V1 ocular dominance [282]: an eye-closed kitten becomes blind in the closed eye, while retina and pre-cortical areas remain physiologically healthy. Such adaptation has been similarly reported in the spiking response of the preferred stimulus in auditory [279] and somatosensory cortices [23], where repeated exposure to a particular stimulus shifts the preferred stimulus-response of a specific neuron (Figure 2.3 B).

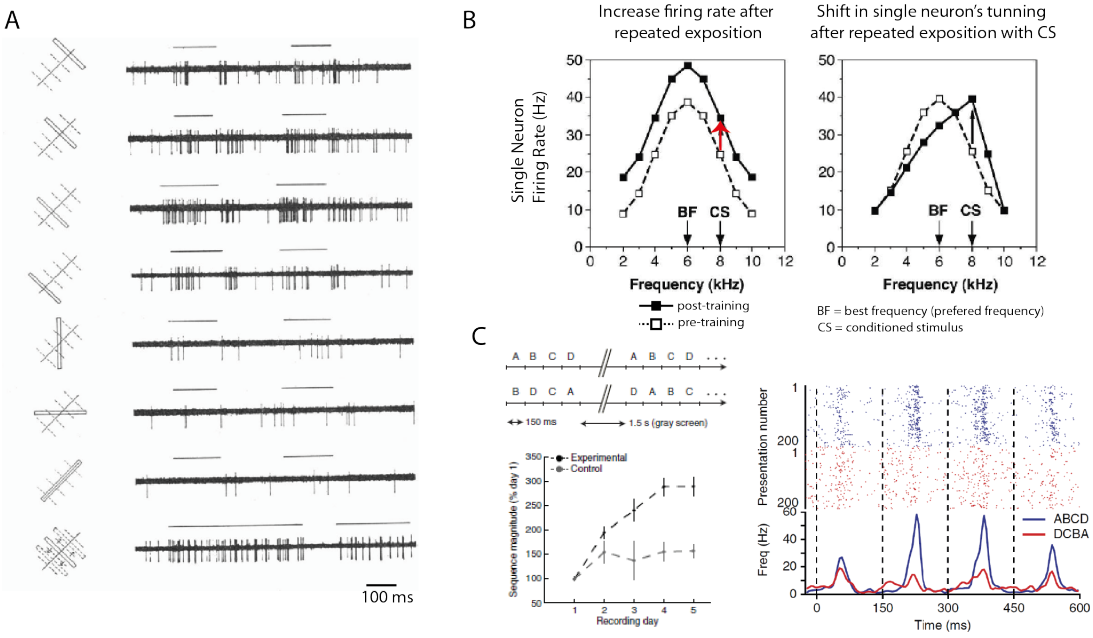

FIGURE 2.3: **Stimulus-specific spiking activity of a single neuron, which is modulated by the stimulus statistics and changes due to the presence of ongoing plasticity**. A) Stimulus-specific spiking activity in visual cortex of anaesthetized cats to a specific orientation of a moving bar, adapted from [125] B) Stimulus-specific representations are modulated by the behavioural demands of the task and change as a function of frequency of stimulation, as evidence by this classical conditioning studies in early auditory areas [279]. Note that such shifts on the single neuron response has been observed through sensory cortices, including visual and somatosensory cortices (see [23, 282]). C) Stimulus-specific representations are sensitive to the temporal structure of the stimulus, as exemplified by sequence learning in adult mice V1: experimental mice are exposed to ABCD sequence, while control mice are exposed to random combinations of ABCD, leading to an increased spiking activity for ABCD sequence exemplified by the two lower plots. Adapted from [93]

But it is not only the presence or absence of sensory stimulation that leads to change in the spiking activity of single neurons, but also the temporal structure of sensory stimulation. Studies focusing in sequential learning showed that neural responses in monkey V4 [177], monkey IT [154], along with mice V1 [93] learn temporal dependencies of incoming input. These studies report that temporally-structured stimuli can lead to systematic shifts in spiking activity, modulated by both the length of stimulation and the shifts on the temporal structure within the stimulus (Figure 2.3 C). On a similar fashion, systematic shifts in the spiking response of V1 cells in adult rats occur after exposure to temporally correlated stimulus [60], while in humans, the orientation selectivity of single neurons to gratings can be changed through pairing two gratings with distinct orientation [286], as previously shown in cat visual cortex [221]. Even non-sensory areas can be influenced by the temporal dynamics of the stimulus: several studies report spike reliability in neocortical neurons after repeated stimulation increases, further reporting that the precision of precise spike times increases as stimuli fluctuations resemble synaptic activity [64, 166].

Ultimately, these observations suggest that temporal structure of the stimulus is intrinsically bound to modulate the single neuron responses, and as such, the processing of temporal information should not be disregarded in the study of neural processing.

However, the mechanisms by which the temporal structure of the stimulus modulate the spiking responses within adaptive single neurons remain unclear. Part of the difficulty is that little is known about the precise interactions between the dynamic stimuli and the underlying plasticity mechanisms that lead to adaptation. This limitation is mostly due to two factors. On the one hand, the modulations reported within behavioural experiments are induced and observed at slow timescales (min to days), while the physiological timescales of plasticity are much faster (ms). On the other hand, cortical plasticity mechanisms themselves are very difficult to study experimentally, since different plasticity mechanisms share expression pathways. As such, it is practically impossible to perform pharmacological or genetic modifications specific to a single plasticity mechanisms. In this context, computational models provide an advantage as plasticity mechanisms can be treated as independent processes, providing a clear way to dissociate effects of each plasticity mechanisms.

In this study, we aim to characterize whether and how temporally-structured stimulus modulate the spiking response of a single neuron, as well as characterize how this temporal structures within the pre-synaptic spike train modulates the fast-changing synaptic connections due to the presence of plasticity.

2.3 Paper I: Spike train auto-structure impacts post-synaptic firing and timing-based plasticity

frontiers in
COMPUTATIONAL NEUROSCIENCE

ORIGINAL RESEARCH ARTICLE
published: 16 December 2011
doi: 10.3389/fncom.2011.00060

Spike train auto-structure impacts post-synaptic firing and timing-based plasticity

***Bertram Scheller*[1†], *Marta Castellano*[2,3,4†], *Raul Vicente*[3,4] *and Gordon Pipa*[2,3,4*]**

[1] *Clinic for Anesthesia, Intensive Care Medicine and Pain Therapy, Johann Wolfgang Goethe University, Frankfurt am Main, Germany*
[2] *Institute of Cognitive Science, University of Osnabrück, Osnabrück, Germany*
[3] *Department of Neurophysiology, Max-Planck-Institute for Brain Research, Frankfurt am Main, Germany*
[4] *Frankfurt Institute for Advanced Studies, Johann Wolfgang Goethe University, Frankfurt am Main, Germany*

Edited by:
Hava T. Siegelmann, Rutgers University, USA

Reviewed by:
Markus Diesmann, RIKEN Brain Science Institute, Japan
Alessandro Villa, University of Lausanne, Switzerland

***Correspondence:**
Gordon Pipa, Institute of Cognitive Science, University of Osnabrück, Albrechtstraße 28, 49069 Osnabrück, Germany.
e-mail: mail@g-pipa.de

[†]*Bertram Scheller and Marta Castellano have contributed equally to this work.*

Cortical neurons are typically driven by several thousand synapses. The precise spatiotemporal pattern formed by these inputs can modulate the response of a post-synaptic cell. In this work, we explore how the temporal structure of pre-synaptic inhibitory and excitatory inputs impact the post-synaptic firing of a conductance-based integrate and fire neuron. Both the excitatory and inhibitory input was modeled by renewal *gamma* processes with varying shape factors for modeling regular and temporally random *Poisson* activity. We demonstrate that the temporal structure of mutually independent inputs affects the post-synaptic firing, while the strength of the effect depends on the firing rates of both the excitatory and inhibitory inputs. In a second step, we explore the effect of temporal structure of mutually independent inputs on a simple version of Hebbian learning, i.e., hard bound spike-timing-dependent plasticity. We explore both the equilibrium weight distribution and the speed of the transient weight dynamics for different mutually independent *gamma* processes. We find that both the equilibrium distribution of the synaptic weights and the speed of synaptic changes are modulated by the temporal structure of the input. Finally, we highlight that the sensitivity of both the post-synaptic firing as well as the spike-timing-dependent plasticity on the auto-structure of the input of a neuron could be used to modulate the learning rate of synaptic modification.

Keywords: spike train, auto-structure, STDP, temporal correlations, integrate and fire, non-*Poissonian*

INTRODUCTION

The processing of information within the cortex crucially depends on the neuronal self-organization and structure formation of neuronal networks. While studying such networks and their structure formation, the spatiotemporal patterns of neuronal activity is often ignored and spike activity is modeled by *Poisson*-point processes. One argument for assuming *Poissonian* firing has been that neurons can receive input from up to several thousand pre-synaptic neurons (Destexhe et al., 2001; Faisal et al., 2008). With the further assumption that the firing of these pre-synaptic neurons is mutually independent, it has been argued that any auto-structure in the individual processes is washed out once the activity is integrated and forms a single so called compound process reaching the soma of the cell (original publication Hanson and Tuckwell, 1983; related publications please see Fellous et al., 2003; Ostojic et al., 2009). However, analytically it has been demonstrated that only the inter-spike interval (ISI) distribution and the ISI correlations of the compound process can be well approximated by a *Poisson* process (Lindner, 2006). The auto-correlation of the compound process, however, does not vanish in general (please note: a *Poisson* process has zero auto-correlation; Câteau and Reyes, 2006; Lindner, 2006). For the extreme case where all point processes are identically distributed, the auto-correlation of the compound process shows an overall reduction in amplitude compared to the auto-correlation of each individual process, with the shape being preserved (Lindner, 2006). Furthermore, it has been shown that individual non-*Poissonian* pre-synaptic activity might also result in a non-*Poissonian* compound activity, which holds true even if thousands of spike trains are added up (Pipa et al., 2008).

Structure formation due to synaptic plasticity has been discussed to be reliant on the precise timing of spiking events (Markram et al., 1997; Song and Abbott, 2001; Lazar et al., 2007, 2009). Since real neuronal activity typically deviates from *Poisson* processes (Smith, 1954a,b; Burns and Webb, 1976; Levine, 1991; Iyengar and Liao, 1997; Teich et al., 1997; Pipa et al., 2006; Nawrot et al., 2007, 2008; Averbeck, 2009; Maimon and Assad, 2009), the modeling of real neuronal firing and structure formation might require a more realistic assumption, including non-*Poissonian* pre-synaptic firing.

Here, the simulation of a conductance-based integrate and fire neuron is used to determine how deviations from a *Poissonian* structure of pre-synaptic spike trains affect the firing probability of a post-synaptic cell. We show that a non-*Poissonian* structure of pre-synaptic spike trains and the resulting changes in post-synaptic firing modulate structure formation in a network with synaptic plasticity modulated by spike-time-dependent plasticity (STDP). In particular, we show that even in the case of mutually independent inputs, both the equilibrium distribution of synaptic weights and the temporal evolution of the weight of individual synapses depend on the precise temporal auto-structure of

pre-synaptic neurons. Finally, we discuss possible consequences of these results on structure formation in recurrent networks, as well as potential modulators of plasticity arising just by the sensitivity on the structure (i.e., regularity as well as rate distribution across pre-synaptic neurons).

MATERIALS AND METHODS

MODELING THE PRE-SYNAPTIC ACTIVITY

We modeled pre-synaptic activity as a set of mutually independent renewal processes. The ISI (ξ) of each process followed a *gamma* distribution with an integer shape factor (γ)

$$p_\gamma(\xi) = \xi^{\gamma-1}\frac{(\gamma\lambda)^\gamma \exp(-\gamma\lambda\xi)}{\Gamma(\gamma)} \text{for } \xi > 0$$

where $\gamma = 1/\langle\xi\rangle$ stands for the rate of the point process. Note that a *Poisson* process is then a special case of a *gamma* process with a shape factor of $\gamma = 1$. In order to simulate spike trains, we sampled ISIs from the corresponding *gamma* distribution. To prevent correlations with respect to the initial condition, i.e., simulation time t_0, we simulated a warm-up period containing 1000 spikes. For the simulation shown here, we used spikes subsequent to the warm-up period. To test whether spikes are equilibrated after the warm-up period, we performed a test on the homogeneity of the spiking probability in the first 100 ms after simulation start.

MODELING THE POST-SYNAPTIC NEURON

We simulated a conductance-based integrate and fire neuron (IF) which receives input from an excitatory and an inhibitory neuronal population, consisting of N_e and N_i spike trains, respectively. A detailed description of the model can be found in Salinas and Sejnowski (2001) and the exact values of the parameters are described on **Table 1**. The equation governing the membrane potential reads:

$$\tau_m g_{\text{leak}}\frac{dV}{dt} = -g_{\text{leak}}(V(t) - V_L) - I_{\text{AMPA}} - I_{\text{GABA}}$$

where

$$I_{\text{AMPA}} = \sum_{i=1}^{N_e} g^i_{\text{AMPA}}(V - E_{\text{AMPA}}) \text{ and}$$

$$I_{\text{GABA}} = \sum_{i=1}^{N_i} g^i_{\text{GABA}}(V - E_{\text{GABA}})$$

Table 1 | Implementation details of the neural network model (as described in Nordlie et al., 2009).

Parameter	Description of the parameter	Parameter values
INTEGRATE AND FIRE NEURON		
τ_m	Membrane time constant	$\tau_m = 20$ ms
g_{leak}	Conductance of the leakage currents, modulated by g_{total}	See text and **Table 2** for details
g_{total}	Total conductance contributed by excitatory and inhibitory synapses	See text and **Table 2** for details
g^i_{AMPA} g^i_{GABA}	Synaptic conductances for both excitatory (AMPA) and inhibitory synapses (GABA)	See text for details
E_{AMPA}	Reversal potential for both excitatory (AMPA) and inhibitory synapses (GABA)	$E_{\text{AMPA}} = 0$ mV
E_{GABA}		$E_{\text{GABA}} = -70$ mV
E_L	Resting potential	$E_L = -74$ mV
V_θ	Threshold of the membrane potential at which a spike is elicited	$V_\theta = -54$ mV
V_{reset}	Voltage at which the membrane potential is reset after an action potential	$V_{\text{reset}} = -60$ mV
SYNAPTIC CONDUCTANCES		
τ_{AMPA}	Exponential decay of excitatory and inhibitory synaptic conductances, respectively	$\tau_{\text{AMPA}} = 2$ ms
τ_{GABA}		$\tau_{\text{GABA}} = 5.6$ ms
$\bar{g}_{\text{AMPA}}$	Average synaptic strength for excitatory and inhibitory synaptic conductances	See text and **Table 2** for details
$\bar{g}_{\text{GABA}}$		
SYNAPTIC PLASTICITY		
A_+	Synaptic modification constant for synaptic potentiation and depression, respectively	$A_+ = 0.009$
A_-		$A_- = 1.05 \cdot A_+$
τ_+	Temporal decay constant of the auxiliary variables P_{pre} and P_{post} respectively	$\tau_+ = \tau_- = 20$ ms
τ_-		
PRE-SYNAPTIC ACTIVITY		
γ	Shape factor which determines the distribution of the inter-spike-interval distribution	$\gamma = 1$ for *Poisson* process
		$\gamma > 1$ and $\gamma \in \mathbb{N}$ for *gamma* process
λ	Firing rate produced by the point process, different for inhibitory and excitatory populations, in spikes per second	$\lambda_{\text{inh}} = \alpha\lambda_{\text{exci}}$
α	Firing rate ratio between excitatory and inhibitory population	See text and **Table 2** for details
N_e	Size of excitatory pre-synaptic population	See text and **Table 2** for details
N_i	Size of inhibitory pre-synaptic population	See text and **Table 2** for details

Additionally, when $V(t)$ exceeds a threshold V_θ, an action potential is elicited. The membrane potential is then clamped to the value V_{reset}. The membrane time constant was set to $\tau_m = 20$ ms. Numerical integration with forward Euler method was used to solve the differential equation (step size of 0.05 ms). AMPA and GABA mediated receptors were modeled by exponentially decaying synaptic conductances with time constants $\tau_{\text{AMPA}} = 2$ ms and $\tau_{\text{GABA}} = 5.6$ ms.

$$g^i_{\text{AMPA}} = \bar{g}_{\text{AMPA}} \exp\left(-\frac{t - t^i_0}{\tau_{\text{AMPA}}}\right) \quad \text{and}$$

$$g^i_{\text{GABA}} = \bar{g}_{\text{GABA}} \exp\left(-\frac{t - t^i_0}{\tau_{\text{GABA}}}\right) \quad \text{for } t > t^i_0.$$

Maximal synaptic conductance strengths $\bar{g}_{\text{GABA}}$ and $\bar{g}_{\text{AMPA}}$ were chosen to be identical across all synapses of the same type.

In this modeling study, we want to control four main criteria: First, we want to regulate the ratio between the leak conductance g_{leak} and the total conductance contributed by both excitatory and inhibitory synapses g_{total} (Destexhe and Paré, 1999). Second, we want to control the firing rate of the post-synaptic neuron. Third, we want to have an approximated balance between excitation and inhibition (average net synaptic drive approx. compensating the leak; Haider et al., 2006; Rudolph et al., 2007). Fourth, we want to control the input firing rate of both inhibitory and excitatory synapses so that we can control the auto-structure of the incoming activity. Regarding this last case, the ratio between the firing rate of the excitatory and inhibitory population is always described by:

$$\lambda_{\text{inh}} = \alpha\lambda_{\text{exci}}$$

Next, we outline how these four constraints were met by choosing appropriate parameters. To control the ratio between the leak conductance g_{leak} and the total conductance, we introduce the scaling factor S, so that $g_{\text{total}} = Sg_{\text{leak}}$ (see Salinas and Sejnowski, 2001). Further simulation values of $S = 2$, 4, 20, 40 are used. However, motivated by experimental studies (e.g., Destexhe and Paré, 1999) for most parts of the simulations, we choose the total conductance to be four times higher than the leakage ($S = 4$), otherwise stated.

As follows, for controlling the post-synaptic firing rate, the average membrane potential and the sub-threshold fluctuations have to be considered. The average membrane potential in our model is determined by the balance between excitation and inhibition. The fluctuations are determined by the number of synapses and the average conductance $\bar{g}_{\text{GABA}}$ and $\bar{g}_{\text{AMPA}}$. Moreover, note that increasing the number of synapses while keeping the total conductance g_{total} the same, leads to a reduction in the amount of membrane fluctuations and therefore to a reduction in the post-synaptic firing rate. Thus, to control the firing rate, given a certain number of pre-synaptic synapses and a certain S determining the total conductance, we adapted the balance of the average conductance $\bar{g}_{\text{GABA}}$ and $\bar{g}_{\text{AMPA}}$ via numerical simulations such that the average post-synaptic firing rate was 10 spikes/s (pre-synaptic *Poisson*). Exact combinations of parameters can be taken from the **Table 2**.

MODELING SPIKE-TIME-DEPENDENT PLASTICITY

Spike-time-dependent plasticity was modeled as originally introduced by Abbott and Nelson (2000) and Song and Abbott (2001). The synaptic connectivity between excitatory neurons is modified depending on the temporal difference δ_t between pre- and post-synaptic spikes. The synaptic modification, described by A_+ and A_-, is given by

$$\Delta w(\delta_t) = \begin{cases} A_+ \exp\left(\frac{\delta_t}{\tau_+}\right) & \text{for } \delta_t < 0 \\ -A_- \exp\left(\frac{\delta_t}{\tau_-}\right) & \text{for } \delta_t \geq 0 \end{cases}$$

The exact values of the parameters are described in **Table 1**. This STDP curve describes the synaptic modification in pyramidal neurons of the layer 5 in neocortex as described in experiments by Markram et al. (1997). Although variable STDP learning curves have been found, such pair-based STDP models already represent the temporal causality relation between neurons. Moreover, it is widely used in theoretical studies, keeping results comparable across studies (Song and Abbott, 2001; Lazar et al., 2007; Morrison et al., 2008). For an efficient implementation, we keep track of the entire history that contributed to STDP at an individual synapse by defining an auxiliary P_{pre} and P_{post} that satisfy:

$$\tau_+ \frac{dP_{\text{pre}}}{dt} = -P_{\text{pre}} \text{ and } \tau_- \frac{dP_{\text{post}}}{dt} = -P_{\text{post}}.$$

Every time an excitatory pre-synaptic terminal emits a spike, Ppre is increased by A_+ otherwise, exponential decay with time constant τ_-), resulting in a change in the conductances of excitatory neurons as follows:

$$g^i_{\text{AMPA}} \rightarrow g^i_{\text{AMPA}} + g^i_a \text{ and } g^i_a \rightarrow g^i_a + P_{\text{pre}} g_{\max}$$

Thus, $P_{\text{pre}}(t)$ determines how much a synapse is weakened if the pre-synaptic neuron fires an action potential at time t. Otherwise, P_{post} is decreased by A_- every time the post-synaptic neuron fires an action potential and $g^i_a \rightarrow g^i_a + P_{\text{pre}} g_{\max}$, so that $P_{\text{post}}(t)$ determines how much the synapse is strengthened if the pre-synaptic terminal receives a spike at time t. Following Song and Abbott (2001), the conductances are a measure of the strengths of the weights. Finally, g^i_a is bounded such that $0 < g^i_a < g_{\max}$ (hard bound).

RESULTS

First, we show that the auto-structure of pre-synaptic spiking can modulate the auto-structure of post-synaptic activity. In particular, we present the relation between pre- and post-synaptic firing for *Poisson* and *gamma* processes. In the last section of the results, we show the impact of non-*Poissonian* pre-synaptic activity on structure formation induced by spike-timing-dependent plasticity. Note that throughout the paper, when comparing results across different auto-structures of the pre-synaptic activity (different shape parameter of the ISI distribution γ), all other parameters are kept constant.

Table 2 | Parameter specification.

$\bar{g}_{AMPA}$ (nS)	$\bar{g}_{GABA}$ (nS)	α	λ_{post}* (Hz) *Poisson case*	N_e	N_i	S
0.1025	0.5679	1	5.47	200	50	2
	0.4057	1.4	4.60			
	0.3155	1.8	4.30			
	0.2840	2.0	4.12			
0.0115	0.0550	1	6.84	2000	500	
	0.0393	1.4	6.35			
	0.0306	1.8	5.80			
	0.0275	2.0	5.70			
0.1352	1.2354	1	10.61	200	50	4
	0.8824	1.4	8.51			
	0.6863	1.8	7.48			
	0.6177	2.0	6.98			
0.0135	0.1235	1	12.99	2000	500	
	0.0882	1.4	11.33			
	0.0686	1.8	10.33			
	0.0617	2.0	10.03			
0.3975	6.5749	1	60.25	200	50	20
	4.6964	1.4	45.79			
	3.6527	1.8	37.22			
	3.2875	2.0	34.12			
0.0484	0.6452	1	61.83	2000	500	
	0.4609	1.4	52.73			
	0.3584	1.8	46.57			
	0.3226	2.0	44			
0.7254	13.009	1	115.86	200	50	40
	9.4639	1.4	88.22			
	7.3608	1.8	71.48			
	6.6247	2.0	65.87			
0.08934	1.3009	1	117.52	2000	500	
	0.9292	1.4	98.97			
	0.7227	1.8	87.14			
	0.6505	2.0	82.64			

**Average firing rate over 50 simulations.*

IMPACT OF PRE-SYNAPTIC AUTO-STRUCTURE ON POST-SYNAPTIC FIRING

To study how the temporal structure of either excitatory or inhibitory drive modulates the post-synaptic firing of a neuron, we simulated an Integrate and Fire neuron receiving inputs from $N_e = 200$ excitatory (AMPA) and $N_i = 50$ inhibitory (GABA) synapses. Each individual synapse transmits a spike train with mean firing rate λ_{exci} or λ_{inh}, depending on whether they are excitatory or inhibitory (see Materials and Methods for a more detailed description of the model). Throughout this paper, the temporal structure of each individual pre-synaptic train has been modeled as a *gamma* point-process with shape factor of either 1, corresponding to *Poissonian* activity (referred to as *Poissonian*) or $\gamma = 100$,which corresponds to oscillatory regimes (referred to as *gamma*). The impact of *Poissonian* and *gamma* processes for both excitatory and inhibitory activity will be addressed by comparing four different cases: *Poissonian* excitation and inhibition; *gamma* type excitation and *Poissonian* inhibition, *Poissonian* excitation and *gamma* type inhibition, and finally, *gamma* type excitation and inhibition.

We start by characterizing the relation between pre- and post-synaptic firing by means of the post-synaptic spike-triggered average of the pre-synaptic population activity (referred to as STA, **Figure 1**). The STA shows the pre-synaptic population activity, i.e., excitatory (black) and inhibitory (red), relative to the timing of a post-synaptic spike. For each of the combinations of *Poissonian* and *gamma*-process activity for inhibitory and excitatory neurons (**Figure 1**, row 1–4), there is a prominent increase of average excitatory activity and decrease of inhibitory population activity preceding a post-synaptic spike, since a post-synaptic spike is more likely to occur if inhibition is reduced (see red lines, **Figure 1**) and excitation increased (see black lines, **Figure 1**). For the *gamma* processes, we additionally find a repetitive structure, an increase/decrease of spiking density preceding and following the post-synaptic spike

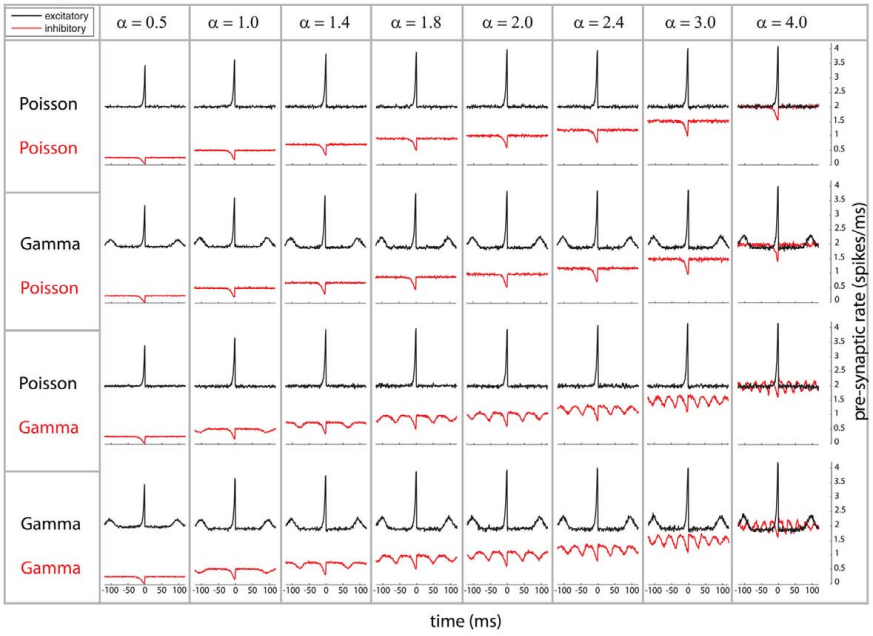

FIGURE 1 | Spike-triggered average (STA) as relation between the compound process of 250 mutually independent pre-synaptic spike trains and post-synaptic firing. Variations of the relative firing rates of inhibitory/excitatory are reflected in α (columns), and different combinations of firing statistics (*gamma* $\gamma = 100$/*Poisson* $\gamma = 1$) are presented for the pre-synaptic excitatory ($N_e = 200$) and inhibitory ($N_i = 50$) population (rows). Total conductance was $S = 4$ and bin size 1 ms. Firing rates for excitatory neurons were kept at 10 Hz, whereas the firing rates of the inhibitory population was varied in the steps 5, 10, 14, 18, 20, 24, 30, and 40 Hz, corresponding to values of $\alpha = 0.5$, 1.0, 1.4, 1.8, 2.0, 2.4, 3.0, and 40. Increasing the firing rates of the inhibitory pre-synaptic activity leads to a higher spike-triggered average. For a pre-synaptic *gamma*-process, the modulation in the STA shows peaks in a distance of the peaks representing the expected inter-spike interval.

for excitatory/inhibitory populations, respectively. This reduction and increase of firing density are both occurring at a distance which corresponds to the individual average ISI of the pre-synaptic spike trains. Moreover, these peaks observed on the spiking density are a reflection of the modulation of the auto-correlation of the compound process (e.g., for excitatory neurons, see black lines in row 2 and 4 of **Figure 1**). The same modulation of pre-synaptic activity preceding a spike happens for the inhibitory population, but the direction of the modulation is opposite (see red lines in row 3 and 4 of **Figure 1**). In other words, the firing density of both excitatory and inhibitory populations is locked to a post-synaptic event. This could be explained by the fact that the neuron may fire if any relatively small subpopulation produces either a synchronized increase of excitatory activity or a synchronized decrease of inhibitory activity.

In summary, as a first point, post-synaptic firing is sensitive to the pre-synaptic auto-structures of mutually independent spike trains. Secondly, post-synaptic firing is locked to periods with increases of excitatory firing and decreases of inhibitory firing. Third, in the case that either of the two types is composed of *gamma* processes, these increases and decreases reoccur with a temporal structure given by the auto-correlation of the compound process, which again is identical to an amplitude-reduced auto-correlation of the individual pre-synaptic processes.

After characterizing the relation between the pre- and post-synaptic firing, we now explore its implication on the auto-structure of the post-synaptic firing. To that end, we computed the auto-correlogram of the post-synaptic firing for the different combinations of excitatory and inhibitory pre-synaptic drives while modifying the relative firing rate between the two populations, the α factor (**Figure 2**). Therefore, note that the inhibitory rate is different for any column since α ranges from 0.5 to 4. The auto-correlation of the post-synaptic firing becomes flat (for time intervals larger than the refractory time of a few milliseconds) only when all of the pre-synaptic spike trains are *Poissonian* (**Figure 2**, row 1) or if α is large and only the inhibitory activity is temporally structured (**Figure 2**, row 3, last three columns). Otherwise, the auto-correlation of the post-synaptic firing is periodically modulated by at least one non-*Poissonian* pre-synaptic population (**Figure 2**). The period of the oscillatory modulation is determined by the expected ISI of the non-*Poissonian* processes (e.g., **Figure 2**, row 2, this modulation is 10 Hz (where Hertz stands for spikes per second) corresponding to an average ISI of 100 ms on the excitatory population). In the case where only the excitatory drive is temporally structured, the modulation of the auto-correlation has the same period as the expected ISI of the excitatory process (**Figure 2**, row 2). If both the excitatory and the inhibitory populations are composed of *gamma* processes with different rates, as shown in **Figure 2** (row 4), the modulation of the post-synaptic auto-correlation is a mixture of modulations of both compound processes.

Effect of different rates for individual pre-synaptic populations

Next, we investigate the effect of the excitatory and inhibitory input structure on the post-synaptic spike train while interacting at different firing rates. We model both excitatory and inhibitory

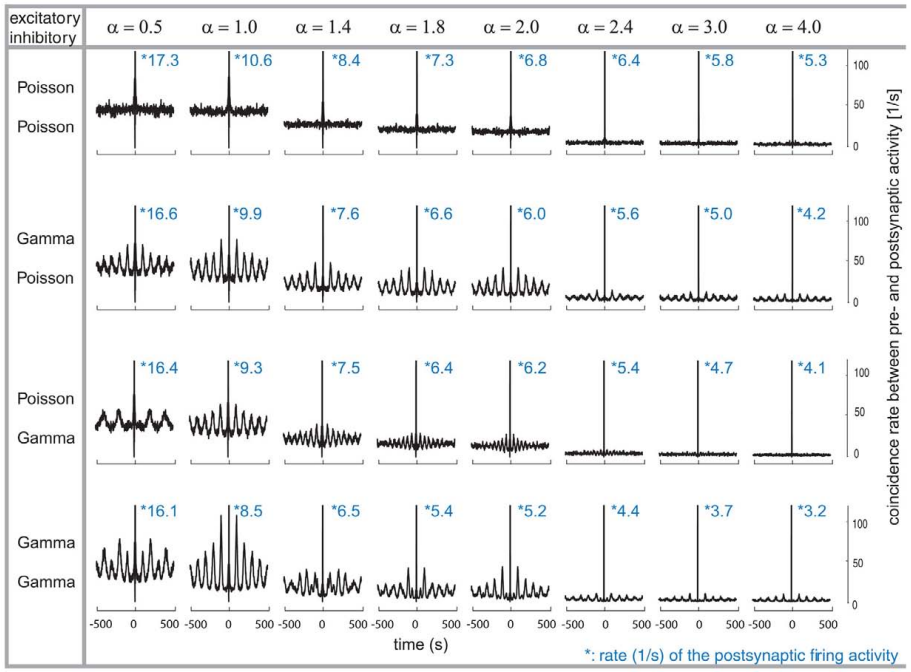

FIGURE 2 | Correlograms and firing rates of the post-synaptic spiking activity. Variations of the relative firing rates of inhibitory/excitatory are reflected in α (columns), and different combinations of firing statistics (*gamma* $\gamma = 100$/*Poisson* $\gamma = 1$) are presented for the pre-synaptic excitatory ($N_e = 200$) and inhibitory ($N_i = 50$) population (rows). Total conductance was set to $S = 4$. With higher pre-synaptic inhibitory firing rates (α), the post-synaptic firing rates decrease. At each α, the post-synaptic firing rate decreases when the pre-synaptic firing is *gamma*-distributed, while the lowest post-synaptic firing rate is present when both pre-synaptic inhibitory and excitatory distributions are *Poissonian*. Modulations in the post-synaptic firing pattern are more prominent when the excitatory population is given a *gamma*-shaped firing modality, are missing when both inhibitory and excitatory firing show a *Poisson*-distributed pattern and is inhomogeneous in its appearance when the post-synaptic activity is driven by both inhibitory and excitatory *gamma*-shaped distributions.

populations by mutually independent *gamma* processes ($\gamma = 100$) and we vary the relative firing rate between them. The rate for the excitatory population is set to 10 Hz while the rate of the inhibitory population is varied systematically, based on the ratio between the firing rate of the inhibitory and excitatory population α. We explore a value of $\alpha = 1$ and variations between 0.5 and 4.

In the case of $\alpha = 1$, where excitatory and inhibitory neurons have the same firing rates, the interaction between the two auto-structures is restricted to a locked increase and decrease of activity in both populations (**Figure 1**, row 4 and column 2), as measured by the STAs. Nevertheless, the pre-synaptic spike-triggered average for regular *gamma* processes and different firing rates between populations shows a damped oscillation for all tested values of α, i.e.,$\alpha = 0.5$, 1.4, 1.8, 2.0, 3.0, and 4.0 (**Figure 1**, row 4). Note that the STA of the excitatory population remains unchanged for different values of α, which is expected, since pre-synaptic activity is composed of mutually independent processes. The periods of the oscillatory modulations for both populations is determined by the expected ISI of the respective point processes.

Damped oscillations are also visible on the auto-correlation of the post-synaptic activity (**Figure 2**, row 4). In the case of $\alpha = 1$ (**Figure 2**, row 1–4 and column 2), the post-synaptic auto-correlation function essentially reflects the auto-correlation of each of the individual processes, either excitatory or inhibitory. However, in the other cases of α, i.e.,$\alpha = 0.5$, 1.4, 1.8, 2.0, 3.0, and 4.0, where the firing rates are not the same between excitation and inhibition, the interaction between both populations becomes more important. An $\alpha = 2$ value induces a modulation with a strong component at 10 Hz coming from the excitatory expected ISI and a smaller component with 20 Hz arising by the inhibitory population (**Figure 2**, column 5). This modulation for $\alpha = 2$ still leads to a clear damped periodic pattern of the auto-correlation. However, for other values of α the interaction is more complicated. For these values, the period length of the modulation in the STA of the excitatory and inhibitory drive does not follow as a simple *n*:*m* relation anymore, as for $\alpha = 0.5$, 1, 2 corresponding to 1:2, 1:1, and 2:1 relation, respectively.

The cases of α (i.e.,$\alpha = 1.4$, 1.8, 2.0, 3.0, and 4.0) induce more complex modulations, dominated by a rhythm of 10 Hz, arising by the expected ISI of the excitatory population. This becomes evident, for example, in the case of $\alpha = 1.4$, for which the first side peak of the post-synaptic auto-correlation is lower than the second and the third (**Figure 2**, column 3).

Effect of population size

Additionally, we explored the effects of population size on the auto-structure of post-synaptic firing. In **Figure 3**, we show the STA and in **Figure 5** the auto-correlation of the post-synaptic spike train for the same population size that was used in all other simulations previously discussed ($N_e = 200$ excitatory as

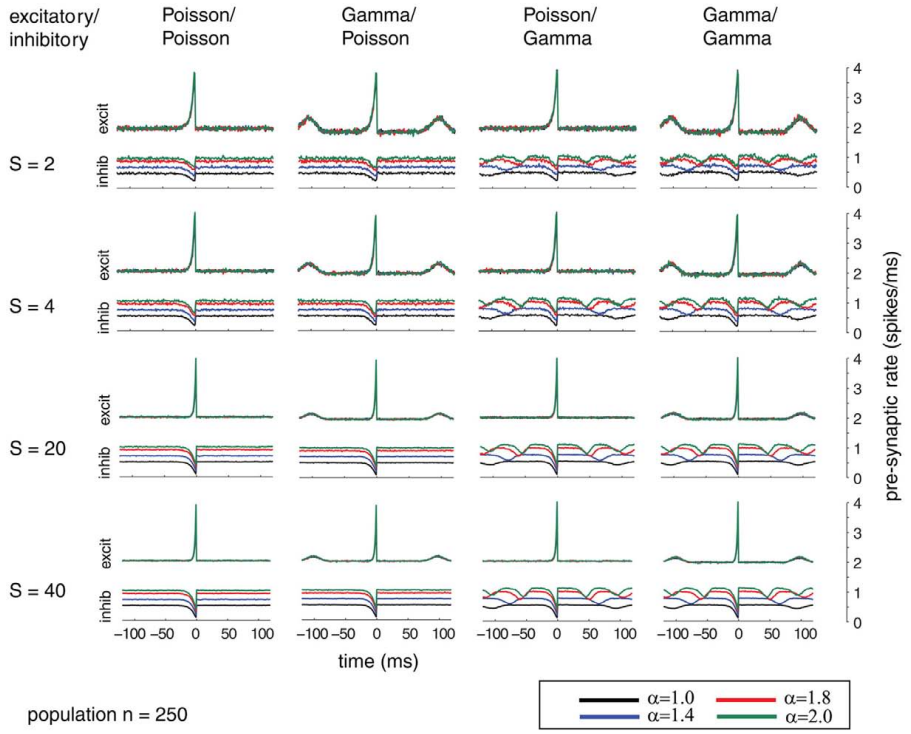

FIGURE 3 | Spike-triggered average (STA) as relation between the compound process of 250 mutually independent pre-synaptic spike trains and post-synaptic firing. Variations of the relative firing rates of inhibitory/excitatory are reflected in α (color coded). Variable conductance of *S* (rows) is compared to different combinations of firing statistics (*gamma* $\gamma = 100$ and *Poisson* $\gamma = 1$) for the pre-synaptic excitatory ($N_e = 200$) and inhibitory ($N_i = 50$) population (columns). Firing rates for excitatory neurons were kept at 10 Hz, whereas the firing rates of the inhibitory population was varied in the steps 10, 14, 18, and 20 Hz, corresponding to values of $\alpha = 1.0$, 1.4, 1.8, 2.0. Increasing the firing rates of the inhibitory pre-synaptic activity leads to higher values of the spike-triggered average. For *gamma* processes in the pre-synaptic activity, the modulation in the STA shows peaks with the distance of the peaks representing the expected inter-spike interval. The appearance of this modulation is irrespective of the conductance values *S*.

gamma-process and $N_i = 50$ inhibitory *Poisson* process with rate $\lambda_{inh} = \lambda_{exci} = 10$ Hz, and a total synaptic weight $S = 4$ times the leak conductance). To assess the effect of the population size and the synaptic strength, we increased the population by a factor of 10 so that $N_e = 2000$ and $N_i = 500$ (STAs shown in **Figure 4** and auto-correlogram shown in **Figure 6**). To distinguish the contribution of the increase in population size from that of the total synaptic weight, we scale at the same time the individual synaptic weights (different rows with $S = 2$, 4, 20 2, 4, 20, and 40 in the **Figures 3–6**). Note that the individual synaptic weight of a model with $S = 2$ and 250 synapses is equivalent to the model with $S = 20$ and 2500 synapses. The same holds true for $S = 4$ and $S = 40$ in the case of 250 and 2500 synapses, respectively. In contrast, other combinations of the number of synapses and *S* induce changes in the synaptic strength distribution. To identify the effect of an increase in the number of synapses keeping the individual strength of each synapse identical, one can compare the case $S = 20$ or 40 for the 250 synapses with the case $S = 20$ or 40 for 2500 synapses (compare row 1 and 2 from **Figure 3** with row 3 and 4 from **Figure 4**). Irrespective of the choice of *S* and the number of synapses, all cases exhibit the same pattern, qualitatively. All show modulations with a frequency given by the ISI of the excitatory population. This indicates that the temporal structure of non-*Poisson* activity is modulating post-synaptic firing even for large pre-synaptic populations and rather small weights.

EFFECTS OF NON-*POISSONIAN* INPUT ON STRUCTURE FORMATION DUE TO STDP

After having evaluated the role of non-*Poissonian* pre-synaptic input in the firing properties of a post-synaptic neuron, we are now in a position to discuss the potential impact of non-*Poissonian* pre-synaptic activity on structure formation and learning via STDP. This form of plasticity has been applied to sequence learning and has been discussed to be involved in spontaneous and activity-driven pattern formation (Markram et al., 1997; Song et al., 2000; Lazar et al., 2007, 2009). STDP can strengthen potentially causal relations between pre-synaptic drive and post-synaptic activity by increasing the synaptic strength of all synapses that have been activated immediately before a post-synaptic spike is generated.

Equilibrium distribution of synaptic weights under STDP

We performed simulations on a single IF neuron (same as described above) with the addition of an exponential STDP rule to its excitatory synapses (see Materials and Methods). Inhibitory synapses were not involved in the plasticity dynamics and were initialized with the same synaptic strength. We then monitored, for each individual synapse, the temporal evolution of the changes

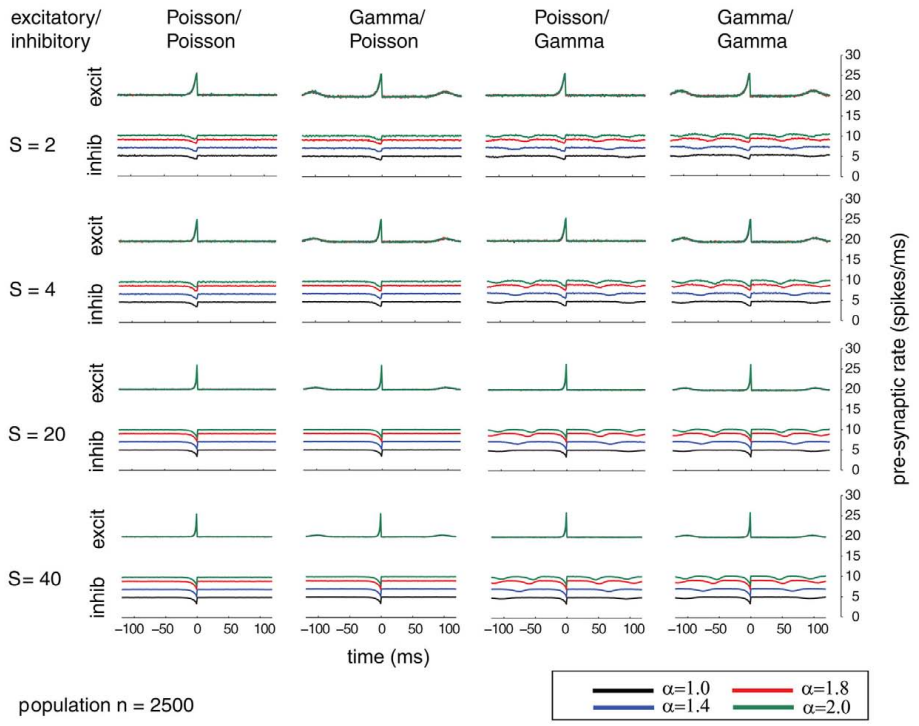

FIGURE 4 | Spike-triggered average (STA) comparable to Figure 3 but for a population size of 2500 mutually independent spike trains. Figure 4 shows the dependence of varying relative firing rates for the inhibitory/excitatory spike trains α (color coded) and variable conductances *S* (rows) for the different combinations of firing statistics (*gamma* $\gamma = 100$ and *Poisson* $\gamma = 1$) for the excitatory ($N_e = 2000$) and inhibitory ($N_i = 500$) population. Firing rates for excitatory neurons were kept at 10 Hz, whereas the firing rates of the inhibitory population was varied in the steps 10, 14, 18, and 20 Hz, corresponding to values of $\alpha = 1.0, 1.4, 1.8, 2.0$. Increasing the firing rates of the inhibitory pre-synaptic activity leads again to higher values of the spike-triggered average. For *gamma* processes in the pre-synaptic activity, the modulation in the STA shows peaks with the distance of the peaks representing the expected inter-spike interval. The appearance of the modulation is irrespective of the conductance values *S*.

on the synaptic strength for a period of 500 s. As in the previous sections, we used mutually independent renewal *gamma* processes as input. After ensuring that the distribution of synaptic strength was stable at the end of the simulation period, we used the last 50 s of the simulation time to estimate the equilibrium distribution of the synaptic conductances.

The cumulative equilibrium distributions of conductance for four combinations of *Poissonian* and *gamma* activity for the inhibitory and excitatory population are shown in **Figure 7A**. In general, the shape of the synaptic weight distribution is bimodal, as shown in Song and Abbott (2001). Remarkably, temporally structured and yet mutually independent activity of the excitatory population leads to different medians (corresponding to a value of 0.5 on the *y* axis in **Figure 7A**) and different shapes of the distributions. The median of the synaptic weight is typically larger for the case of excitatory *Poisson* processes, independent of the temporal structure of the inhibitory population. The difference in the median can be as large as ∼20%. For all tested cases, the tails of the bimodal distribution of weights became heavier in the case of excitatory *Poisson* processes regardless of the temporal structure of the inhibitory population. Both effects of the median and the shape are independent of the relative rate for the excitatory and inhibitory drives (compare different rows of **Figure 7A**). To test whether this difference is indeed caused by an interaction of the temporal structure of the pre- and post-synaptic spiking activity, we performed a control, for which we destroyed this interaction, while keeping the pre-synaptic temporal structure the same. To this end, we randomized the post-synaptic spike timing. Using this control, the cumulative distribution function (CDF) for temporally structured and unstructured pre-synaptic synapses became identical (CDFs were compared with a two-sample Kolmogorov–Smirnov test, test level 5%, see **Figure 8**), indicating that temporal structure in the pre-synaptic activity alone is insufficient to explain the differences observed in **Figure 7**.

In a second step, we studied the temporal structure of synaptic weight changes. In particular, we tested whether synaptic changes of the same synapse reoccur on a short time scale, as expected by the repetitive structure of the STAs (see **Figures 1**, **3**, and **4**). To this end, we performed a spike-triggered average of the synaptic changes of the STDP so that we could observe the averaged conductance changes triggered on the post-synaptic firing (**Figure 7B**). The analysis was performed for the same period (last 50 s) of the simulation as used for the CDFs where the total distribution of weights is already in a dynamic equilibrium. In the averaged STA of the conductances, we found a clear periodic component. The exact temporal structure of the synaptic is a function of both the temporal structure of the excitatory and the inhibitory activity. This was expected, based on the results regarding temporal

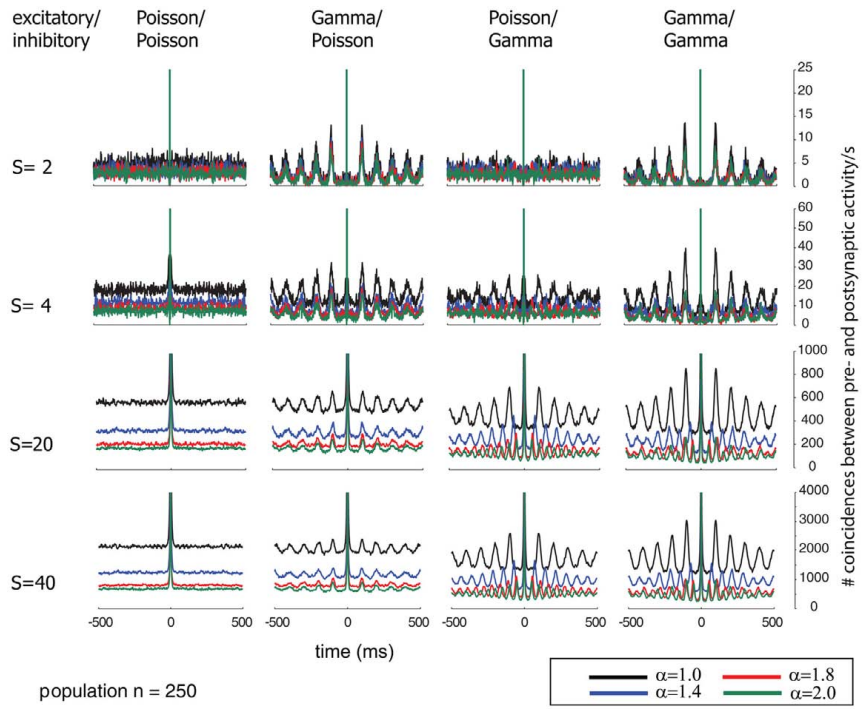

FIGURE 5 | Correlograms of the post-synaptic spiking activity in dependence of varying relative pre-synaptic firing rates for the inhibitory/excitatory spike trains α (color coded) and variable conductances *S* (rows) for the different combinations of firing statistics (*gamma* $\gamma = 100$ and *Poisson* $\gamma = 1$) for the pre-synaptic excitatory ($N_e = 200$) and inhibitory ($N_i = 50$) population (columns).

structure of the post-synaptic firing (compare **Figures 2**, **5**, and **6**). If only either the excitatory or inhibitory activity is temporally structured (**Figure 7B**, blue and green curves, respectively), then the temporal structure of the post-synaptic changes is completely determined by the temporal structure of the non-*Poissonian* pre-synaptic process (notice the differences in the periodic component for variations of the inhibitory firing rate defined by α). However, if both the excitatory and inhibitory pre-synaptic drive is temporally structured, the temporal structure of the synaptic changes is a mix of the two pre-synaptic temporal structures (**Figure 7B**, black curve). Remarkably, the strength of repetitive changes, especially of the first satellite peaks in the STAs of the conductance, depends on α. For $\alpha = 1$ (that corresponds to an *n*:*m* relation of 1:1) and still rather simple *n*:*m* relations of 1:2 and 2:1 for $\alpha = 0.5$ and $\alpha = 2$, the first side peak of the changes of the conductance are larger than for more complex *n*:*m* relations based on $\alpha = 1.4$, 1.8, 2.4, 3.0 and 4.0. This indicates that synaptic modifications reoccur on a short timescale in the range of a few ISIs, which boost changes associated with the same reoccurring spiking pattern. It needs to be emphasized that this occurrence of the same spiking pattern is just caused by the temporal auto-structure of the pre-synaptic drive. This highlights that the auto-structure of pre-synaptic activity might be relevant for modulating synaptic learning.

Temporal evolution of weight changes caused by STDP

Next, we compared the temporal evolution of the distribution of individual synaptic weights as a function of the simulation time. In particular, we study whether the auto-structure of the pre-synaptic population also has an impact on the transient period of the distribution of weights and the speed of the weights' changes. We compare the temporal evolution of weights for each case by means of observing the CDF. On the one hand, we present the CDF in the case where both pre-synaptic drives are *Poisson* processes (**Figure 9A**). This figure shows how the synaptic weight evolves over time due to STDP, from the initial point at $t = 0$, where all the weights are the same, up to a bimodal distribution at the end of the simulation ($t = 100$ s).

On the other hand, we present the differences between the CDF of synaptic weights between two cases: *Poisson/Poisson* and *gamma/gamma* (**Figure 9B**). Both measures were explored for different values of the relative firing rate α. We found that for identical rates ($\alpha = 1$), synaptic weights change faster during the transition toward the equilibrium distribution. This effect is especially strong in the first 70 s of the simulation where the case of both populations being *gamma* leads to more extreme values, as indicated by the negative areas. Remarkably, we observe the same effect also for $\alpha = 0.5$ and $\alpha = 2$, which are both corresponding to a rather simple *n*:*m* relation of the period length of the modulation of the STAs (**Figures 1**, **3**, and **4**). For the more complicated relations, $\alpha = 1.4$, 1.8, 2.4, 3.0, and 4.0, this faster change of the CDFs for temporally structured pre-synaptic activity disappears. This suggests that the temporal structure and the interaction between the rates of excitatory and inhibitory processes can modulate the speed with which synaptic weights are changing, which is the learning rate of the STDP. For simulation times longer than 100 s, the distributions are

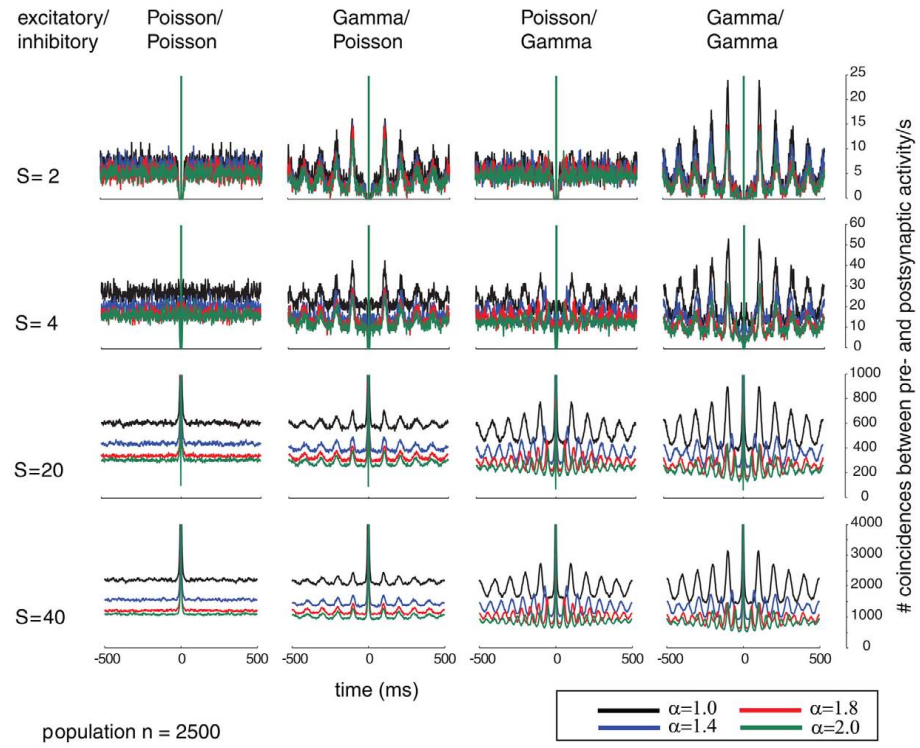

FIGURE 6 | In analogy to Figure 5, This Figure shows the correlograms of the post-synaptic spiking activity in dependence of varying relative pre-synaptic firing rates for the pre-synaptic excitatory ($N_e = 2000$) and inhibitory ($N_i = 500$) population (columns for the inhibitory/excitatory spike trains α (color coded) and variable conductances S (rows) for the different combinations of firing statistics (*gamma* $\gamma = 100$ and *Poisson* $\gamma = 1$).

close to the equilibrium and consistent with the results reported in the previous section.

COMPARISON TO *GAMMA* PROCESSES WITH $\gamma = 10$

Further, we replicated the results mentioned in the case when the pre-synaptic activity has been modeled as a gamma point process where $\gamma = 10$. We first describe the impact of the pre-synaptic structure on the post-synaptic firing. Along this line, we observed that the effects were reduced but still present. The relation between the pre- and post-synaptic firing is characterized via the STA (**Figure 10A1**) and its implications can be observed on the auto-correlation function (**Figure 10A2**), which reflects the temporal structure of the post-synaptic firing. For that, we simulated the pre-synaptic activity with $\alpha = 1$, so that the firing rate of both inhibitory and excitatory pre-synaptic neurons equals 10 Hz, and the overall conductances are scaled by $S = 4$. In the case where $\gamma = 10$, both STA and the auto-correlation are showing a modulation of the pre- and post-synaptic activity occurring at a distance which corresponds to the average ISI of the pre-synaptic spike trains. These peaks also reflect the modulation on the auto-correlation of the pre-synaptic compound process.

Second, we investigate the effects of non-*Poissonian* input on structure formation due to STDP. For that, the cumulative distribution of synaptic weights as a function of time was presented so that we could estimate the temporal evolution of synaptic weights caused by STDP. In **Figure 10B**, we present the differences between the CDF of synaptic weights between two cases: *Poisson/Poisson* and *gamma/gamma* (for $\gamma = 10$). Similar to the case where the *gamma* process was described by a shape factor of $\gamma = 10$ (see **Figure 9B**), we found that the synaptic weights change faster during the transition period (the first 70 s). Moreover, the synaptic weights shift toward more extreme values when both populations are modeled by *gamma* processes (with $\gamma = 10$). Note that the effects for both $\gamma = 10$ and $\gamma = 100$ are very similar regarding the strength and the temporal evolution of the synaptic weight distribution (compare **Figure 10B** with **Figure 9B**, row 2).

DISCUSSION

We demonstrate that auto-structure, such as regularity and temporal structure of pre-synaptic activity, can induce temporal structure on the post-synaptic neuron, such as spatial temporal pattern of post-synaptic activity, even when spike trains are mutually independent. We also show that such a patterning can change the learning rates as well as the equilibrium distribution of synaptic weights in a model of synaptic plasticity, such as STDP. We will now discuss potential implications of these findings as well as their generalizability.

INTERPLAY OF STRUCTURE IN PRE- AND POST-SYNAPTIC SPIKE TRAINS

A first step in understanding the interplay between pre- and post-synaptic activity is to describe the temporal structure of

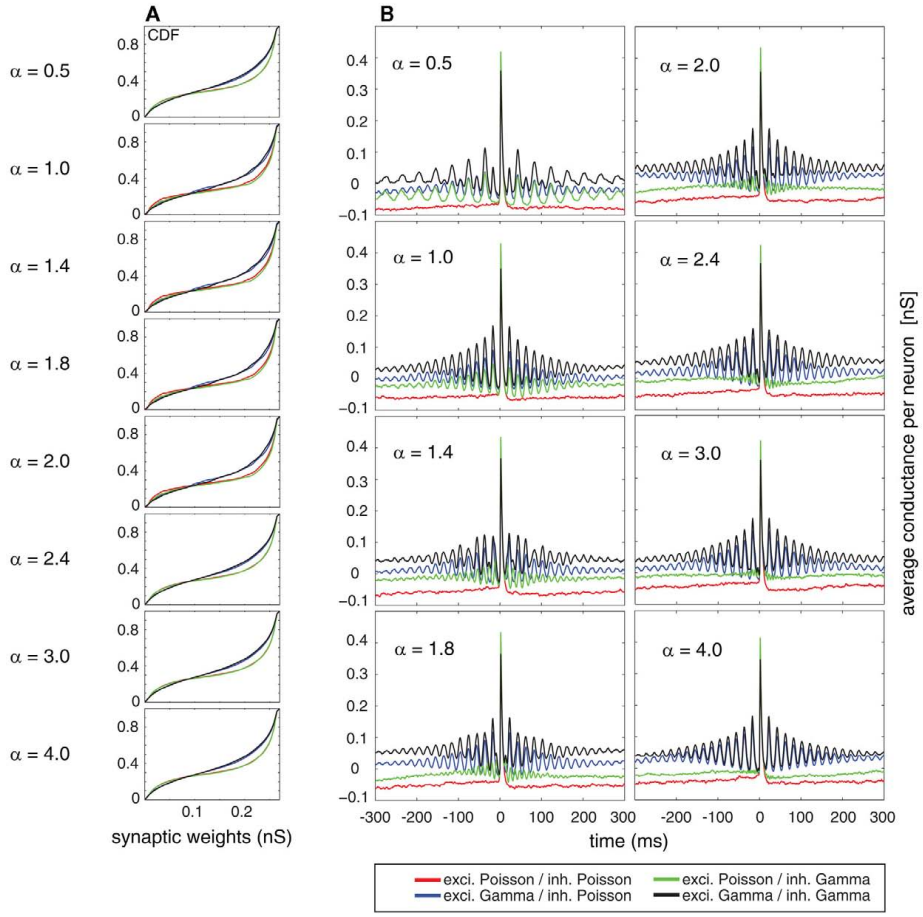

FIGURE 7 | (A) Cumulative distribution function of the synaptic weights averaged on the stable period of simulation (last 50 s from a total simulation time of 300 s). **(B)** Spike-triggered average (STA) as a relation between the average synaptic weights of 250 mutually independent pre-synaptic spike trains $N_e = 200$ and $N_i = 50$) and the post-synaptic firing. Color coded for different combinations of firing statistics (*gamma* $\gamma = 100$ and *Poisson* $\gamma = 1$). Excitatory firing rate λ_{exci} was kept constant at 10 Hz and variations of inhibitory firing rate λ_{inh} correspond to values of $\alpha = 0.5$, 1.0, 1.4, 1.8, 2.0, 2.4, 3.0, and 4.0 where $\lambda_{inh} = \alpha\lambda_{exci}$.

the compound process that is the overall input being delivered to the soma of the cell. From previous work (Câteau and Reyes, 2006; Lindner, 2006; Tetzlaff et al., 2008), it is known that the compound process of a set of spike trains has a remaining temporal structure, reflecting the temporal structure of the individual trains. Based on that, we study whether temporal structure in the inhibitory and excitatory drive of a neuron can affect the post-synaptic firing using numerical simulations of a leaky integrate and fire neuron model. We thus studied both the temporal structure of the post-synaptic spike train based on auto-correlograms and the interaction between the pre- and post-synaptic structure based on spike-triggered averages. We show that auto-structure of both the excitatory and inhibitory pre-synaptic population can induce temporal patterns in the post-synaptic activity (**Figure 2**). Even more, the impact of the temporal structure of the excitatory and inhibitory drive can lead to different post-synaptic firing patterns. This means that only if either excitatory or inhibitory activity is temporally structured (i.e., *gamma*-process), the post-synaptic spiking activity will reflect the same temporal modulation. For the case where both excitatory and inhibitory activities are *gamma*, the temporal structure of the post-synaptic activity is mainly determined by the excitatory drive for low and intermediate conductance values. For higher conductance values, both the structure of the excitatory and inhibitory population is relevant such that the temporal structure of the post-synaptic firing appears to be a superposition of both modulations.

Here, we studied a single neuron. However, there might be implications of our findings concerning temporally structured activity on the propagation of activity in large and recurrent networks. To this end, Câteau and Reyes (2006) studied feed-forward networks and the propagation of pulse packets as a function of different temporal structures of the spiking activity. Using the Fokker Planck approach and a leaky integrate and fire model, the authors demonstrate that temporal structure of excitatory *gamma* activity remains to be structured while propagating through layers of the network. Further evidence for the importance of auto-structure on the activity from a recurrent network is provided in the study by Tetzlaff et al. (2008). They first demonstrate the

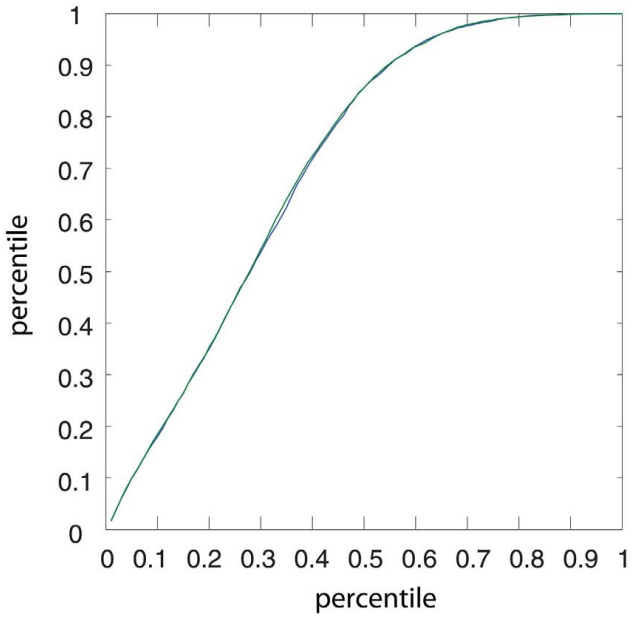

FIGURE 8 | Quantile–Quantile plot of the CDFs of the surrogate STDP rule for *Poisson* and regular *gamma* pre-synaptic spiking activity. Two simulations were performed with identical parameters, but different auto-structure in the pre-synaptic activity. In one case, the excitatory drive was composed of regular *gamma*-spike trains (green), in the other case the excitatory activity was *Poisson* (blue). For both, the inhibitory activity was *Poisson*. For the surrogate STDP rule, the post-synaptic spike timing was randomized, i.e., a random *Poisson* process with fixed post-synaptic firing of 10 spikes/s. The result is a control showing that the CDFs for temporally structured and unstructured pre-synaptic activity become identical, indicating that temporal structure in the pre-synaptic activity alone is insufficient to explain the differences observed in **Figure 7A**.

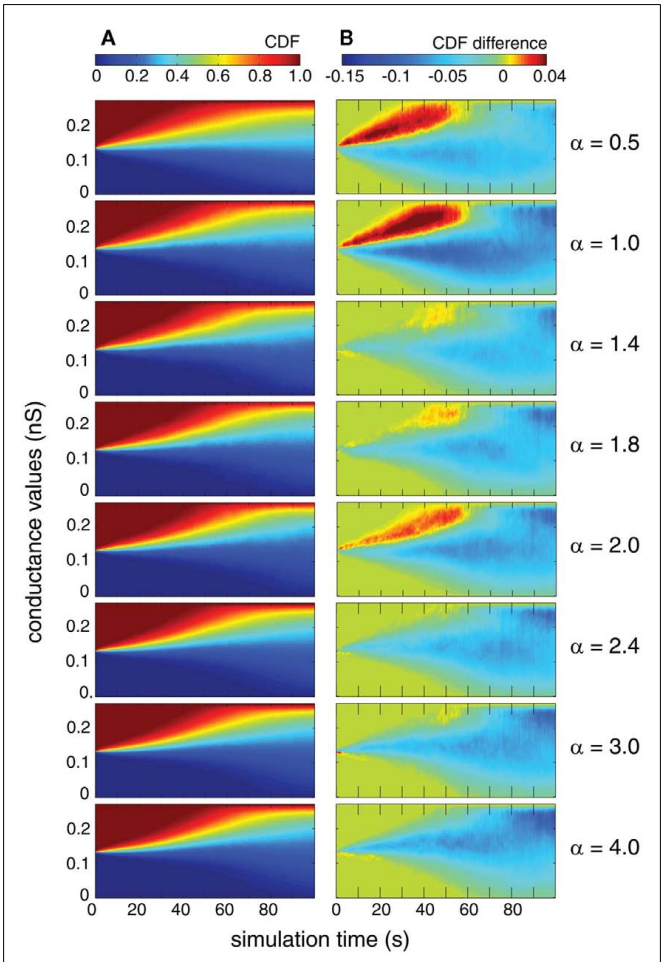

FIGURE 9 | Distribution of synaptic weights of 250 mutually independent pre-synaptic spike trains ($N_e = 200$ and $N_i = 50$). Excitatory firing rate λ_{exci} was kept constant at 10 Hz and variations of inhibitory firing rate λ_{inh} correspond to values of $\alpha = 0.5$, 1.0, 1.4, 1.8, 2.0, 2.4, 3.0, and 4.0 where $\lambda_{inh} = \alpha\lambda_{ecxi}$. **(A)** Time-resolved CDF of synaptic weights where the pre-synaptic firing statistics are *Poissonian* ($\gamma = 1$). **(B)** Time-resolved difference in the CDF of synaptic weights between the cases in which the pre-synaptic drive is *gamma* ($\gamma = 100$) and *Poisson* ($\gamma = 1$).

importance of auto-structure for individual neurons using an alternative approach based on the Fourier domain and second, they use numerical simulations to study the importance of auto-structure when neurons are embedded in a recurrent network. Combining the evidence presented by Câteau and Reyes (2006) and Tetzlaff et al. (2008), along with the results presented here, we suspect that temporal structure in excitatory and inhibitory activity is at least partially preserved through many layers.

SPIKE-TIMING-DEPENDENT NEURONAL PLASTICITY AND TEMPORAL STRUCTURE

Neuronal plasticity links structure formation in recurrent neuronal networks with its spiking activity. Given the results that the temporal structure of pre-synaptic activity affects the post-synaptic firing (see first part of this publication) and therefore can propagate through a larger network (Câteau and Reyes, 2006), the question arises whether temporal structure of spiking can also effect neuronal plasticity. To study this question, we use a spike-timing-dependent type of neuronal plasticity (STDP) which uses the exact timing of the pre- and post-synaptic firing to change individual synaptic weights.

To test the impact of various pre-synaptic temporal structures of excitatory and inhibitory activity, we observe the equilibrium distribution of the synaptic weights. We find that at equilibrium the distribution of synaptic weights depends solely on the auto-structure of the excitatory population. One possible explanation could be the fact that the synapses of the excitatory population are the only ones subjected to STDP. However, auto-structure of the inhibitory population has an effect on the transient period of the synaptic changes. This can be explained by the fact that the auto-structure of the inhibitory population changes the firing pattern of the post-synaptic neuron. In particular, the interplay between pre-synaptic auto-structures can modulate the post-synaptic firing such that the structure formation also depends on the inhibitory firing patterns. We showed that not only the regularity of renewal processes, but also the rate of the individual processes, modulates the dynamics of the synaptic weights. For the case that rates of inhibitory and excitatory population match a simple *n*:*m* relation, i.e., 1:1, 1:2, 2:1, modulations of the auto-correlation of the

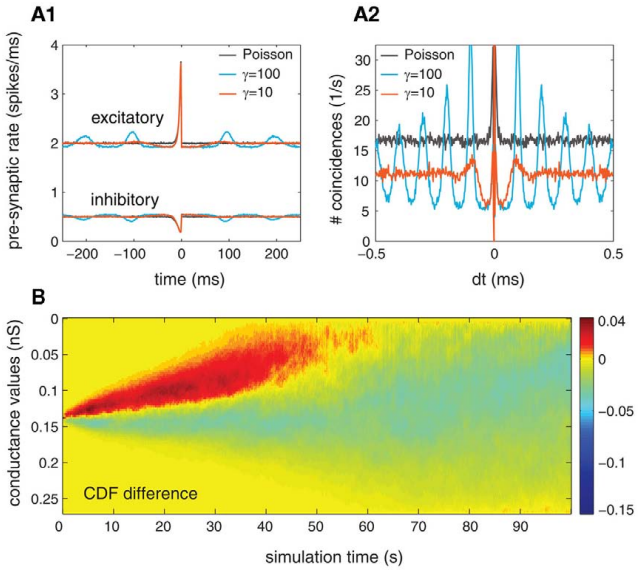

FIGURE 10 | Exploring the effects of auto-structure in *gamma* processes where the ISI is drawn from a *gamma* distribution with a shape parameter $\gamma = 10$ for a population of 250 mutually independent pre-synaptic spike trains ($N_e = 200$, $N_i = 50$, and $\alpha = 1.0$). In **(A1, A2)**, the STA and auto-correlation of post-synaptic activity are presented, respectively. The different colors correspond to the comparison between three cases: *gamma*-spike trains $\gamma = 10$ (light blue), *gamma*-spike trains $\gamma = 100$ (red) and *Poisson* spike train $\gamma = 1$ (black). **(B)** Time-resolved difference in the CDF of synaptic weight distribution between the cases in which the pre-synaptic drive is *gamma* ($\gamma = 10$) and *Poisson* ($\gamma = 1$).

post-synaptic firing are rather strong, while they are considerably reduced for other more complex relations.

In a next step, we test the temporal structure of synaptic modifications and the temporal evolution of the distribution of weights. As shown in the first part, temporal structure of even mutually independent spike trains induces temporal structure in the occurrence of spike patterns across neurons that take place just by chance. This temporal modulation can be repetitive, as observed for regular firing *gamma* processes. We find that such a repetitive pattern modulates the synaptic change by STDP. We additionally find that the auto-structure and the rate of the two types, i.e., excitatory and inhibitory pre-synaptic processes, interact and can both be used to regulate the speed with which STDP changes synaptic weights (**Figure 9**). There, the speed of changes in the weight distribution in the initial period between 0 and 70 s is strongest for a rate ratio between excitatory and inhibitory processes of 1:1 and 1:2. For other ratios between 1:1 and 1:2, this effect is strongly reduced. Such results highlight that both the rate and changes in the auto-structure can be used to modulate STDP.

GENERALIZABILITY FOR OTHER FORMS OF PLASTICITY AND OTHER PROCESSES

Can the findings presented here be generalized to other STDP models as well as to different population sizes, point process models and models other than a conductance-based integrate and fire neuron?

In this study, we used a rather simple model of spike-timing-dependent plasticity. This form, also known as STDP with hard bounds, has an equilibrium weight distribution that is strongly bimodal with mainly weak or strong synapses. An alternative model is the soft-bound STDP which can lead to an equilibrium weight distribution that is uniform with most synapses having intermediate strength (Gütig et al., 2003). So the question is whether the results reported in this paper can be generalized for the soft-bound or other STDP models. We found that the auto-structure changes both the equilibrium distribution but also the evolution of the weight distribution over time. Especially the strong change in the first 70 s of the simulation (**Figure 9**), for which the weight distribution is still uniform, indicates that the auto-structure influences the structure formation based on STDP for both uniform and bimodal weight distribution. Since soft-bound STDP promotes unimodal distributions, we expect that also soft-bound STDP is sensitive to the auto-structure of pre-synaptic activity.

Similarly, this comparison could be made with other STDP models proposed. Modulations of synaptic weights due to STDP are observable, independent of the weight distribution. Structure formation depends on the temporal relations of the spiking activity rather than on the distribution of synaptic weights itself. Other STDP rules, such as the ones presented by van Rossum et al. (2000), Pfister and Gerstner (2006), Morrison et al. (2007), or Clopath et al. (2010), discuss the temporal relation among pre- and post-synaptic spike trains. Thus, we expect our model also to reflect the temporal structure of pre-synaptic spike trains.

We now address whether our findings are generalizable regarding population size and conductance strength. Based on the analytical results from Lindner (2006), it is known that the auto-correlation of a compound process of scaled point processes, i.e., scaled delta peaks $\delta(t)/N$, is of order $1/N$. In contrast, the auto-correlation of standard point processes, i.e., non-scaled delta peaks $\delta(t)$, grows linearly with N. However, it is important to note that the shape of the auto-correlation stays identical independent of N and whether the point processes are scaled or not. Especially in the case where synapses are weak, one could argue that the remaining auto-correlation is too small to drive the neuron. However, we know that neurons can be close to their threshold. This makes neurons sensitive, such that a small number of pre-synaptic events in a short temporal window can make a neuron fire. This highlights that it is not the total number of synapses but the number of pre-synaptic events that is necessary to drive the neuron, which determines the dampening of the auto-structure in a subpopulation of neurons. In other words, since the neuron is a thresholding device, it can receive noise inputs from a pre-synaptic population with no temporal structure, while being driven by a structured subset of such pre-synaptic neurons. Our results support this argumentation, since we found, for both a small and large population of the order of several thousand pre-synaptic events that the auto-structure of the pre-synaptic spike trains drives the post-synaptic neuron nearly equally well.

We next addressed the generalizability of our findings regarding the choice of the point process model. We chose *gamma* processes which are renewal processes and which can be entirely described by the ISI distribution. Here, we presented results for *gamma*

processes that strongly deviate from *Poissonian* firing. Compared to data obtained from electrophysiology, the regularity used in the paper is rather high (Baker and Lemon, 2000; Nawrot et al., 2007, 2008). However, we chose this regime to demonstrate the rather strong impact auto-structure can have on structure formation based on neuronal plasticity. To test whether the effects are also existing for more biologically plausible ISI distribution, we used *gamma* processes with a shape parameter of $\gamma = 10$. We observed that the effects were reduced but still present (**Figure 10**). This demonstrates that the presented results can be generalized to less extreme deviations from *Poissonian* firing. However, we used renewal processes which are just a first step toward more realistic neuronal firing statistics. Such more realistic firing might also require to model serial correlation in between ISIs and therefore make the processes non-renewal. Analytically, one can show (Pipa et al., 2010), that the average frequency of spike patterns across neurons is independent of the exact ISI distribution of the renewal process, while deviation from this renewal property can also influence the average frequency of spike pattern across neurons. Since neuronal plasticity based on STDP is directly linked to the pattern frequency we expect that non-renewal point processes lead to even stronger changes of learning and structure formation as reported here.

LIMITATIONS

This study and neural model relies on three principle assumptions. First, that the membrane potential dynamics can be sufficiently described by a point neuron via an ordinary differential equation describing a conductance-based integrate and fire neurons. Second, that neural firing can be described by a gamma-renewal process which captures the neuron refractoriness on the ISI distribution. Third, that synaptic plasticity can be modeled by a rather simple additive STDP rule. Given that by definition such assumptions are wrong, we should raise the question to what degree can we expect these results to be generalizable for biological neurons?

The first assumption we made is that neurons can be modeled by a simple point neuron with conductance-based integrate and fire dynamics. That means that we ignored any non-linear dendritic computations. Predicting the effect of those non-linearities seems to be impossible in general since they depend on the very complex and specific topology of individual dendritic trees. However, it has been shown that non-linearities may act as coincidence detectors based on super-linear integration on local segments of the dendrites (London and Häusser, 2005). Since those effects are happening in a confined area with a relatively small number of synapses, and the modulations of auto-structure that we show here grow with decreasing population sizes, we therefore expect that non-linear properties of dendritic trees may boost the sensitivity to changes in the auto-structure. Further, such a conductance-based integrate and fire neuron is a simple one-dimensional model with a fixed threshold. More realistic neuronal models can manifest complex sub-threshold dynamics and may have thresholds that can depend on the state of the neuron (such as Hodkin-Huxley, Izhikevich or the exponential integrate and fire, see Izhikevich, 2003). For such neurons, we expect that structure imposed by the pre-synaptic activity and dynamics of the neuron model may interact. Therefore, we expect, as shown for example by Asai et al. (2008), that different neuronal models may lead to different results. However, we also expect that differences between *Poissonian* and non-*Poissonian* pre-synaptic activity survives in one way or the other.

Second, experimental studies indicate that *gamma* processes are better models that *Poisson* processes when describing the temporal structure of neuronal firing. Alternatively, the ISI distribution can be modeled by log-normal distributions. Common to both is that they are renewal processes, meaning that subsequent ISI are independent. Such assumption of independence on the ISI may be wrong (Farkhooi et al., 2009; Nawrot, 2010). Here, we did not test for the effect of non-renewal activity. Therefore, whether specific models of non-renewal processes can change the effect of STDP, still remains an open question for future research.

Finally, this study assumes that STDP can be modeled by a simple additive rule, while experimental findings show that this model oversimplifies the real spike-timing-dependent plasticity (Abbott and Nelson, 2000). Alternatively, multiplicative STDP rules or STDP rules which take patterns of spikes into account may be more biologically plausible (see Morrison et al., 2008 for review). However, it needs to be stressed that all these rules appear to be oversimplifications, if one considers that real neurons have multiple neuronal plasticity forms (i.e., homostatic plasticity, synaptic rescaling or short term modulations, like short term depression or facilitations), acting at the same time. Any of these interacting plasticity forms may change the reported results and may even lead to new emergent properties that cannot be predicted by any of the individual rules alone (Lazar et al., 2007, 2009). Despite these general complications which all modeling studies suffer from, it remains an issue whether the findings shown here can be generalized for other STDP rules mentioned before. We expect that most of the effects would be found when using other STDP rules, since all consider the exact temporal structure of the pre–post-synaptic firing. For example, one could argue that since different STDP rules would lead to different steady-state distributions of synaptic weights, it could destroy the effects reported on in this paper. However, we analyzed the changes in the strength of weights undergoing additive STDP in the early phase of learning (**Figure 9B**), where the weight distribution is still unimodal (i.e., period between 0 and 50 s of simulation time). We found that auto-structure-induced modulations in the effective strength of neuronal plasticity have been especially strong during this period. This suggests that the auto-structure modulates the effective strength of neuronal plasticity for both bimodal and unimodal weight distributions. Further, this indicates that the effects may be even stronger for multiplicative STDP.

POTENTIAL IMPLICATIONS FOR STRUCTURE FORMATION IN RECURRENT NETWORKS

For learning in recurrent networks, a modulation of neuronal plasticity can be useful. Such modulation can be used to control self-organization via spontaneous structure formation of the network and the learning of certain trajectories of neuronal activities. One such mechanism for modulation was implemented as reward-modulated STDP, where a global teacher signal regulates the self-organization of the system (Florian, 2007; Izhikevich, 2007; Legenstein et al., 2008).

Here, we propose an alternative modulation of spontaneous structure formation based on the control of the auto-structure of the pre-synaptic activity. We showed that temporal structure in the pre-synaptic activity of both the excitatory and inhibitory activity can modulate the effective strength of neuronal plasticity as well as the speed with which synapses change their synaptic weights in the case of STDP. Therefore, this suggests that controlling the auto-structure of pre-synaptic activity can be used to control the effective strength of neuronal plasticity. For example, we showed that changes in the regularity of renewal processes and changes in the relation between the excitatory and inhibitory firing rates can be used to control the learning of structure in individual neurons. Alternative mechanisms of controlling the effective strength of neuronal plasticity via changes in the auto-structure could be making pre-synaptic activity non-renewal, e.g., by oscillatory firing or long-lasting temporal dependencies.

From a biological perspective, such control of the auto-structure could be realized by many intrinsic or extrinsic mechanisms. Potential intrinsic mechanisms are neuromodulator or top-down signals that shape the temporal structure of neuronal activity in the target population. Alternatively, temporal structure in the target population may be shaped by oscillatory activity emerging by synchronization of different populations. Extrinsic modulations may occur via stimulus-driven changes in the balance and rate relation of excitatory and inhibitory activity. Also, temporal structure induced by the stimulus may be a potential candidate to modulate the effective strength of neuronal plasticity.

In conclusion, our work suggests that variation in the auto-structure and the rate of activity in a recurrent network may be exploited by nature to modulate the sensitivity for spontaneous formation of structure and therefore learning.

CONCLUSION

Structure formation and neuronal self-organization in networks is crucial for information processing within the cortex. We demonstrate that both the speed and strength of structural changes induced by spike-timing-dependent plasticity can be modulated by the temporal structure of mutually independent spiking activity. This highlights the possibility that the modulation of auto-structure of larger groups of neurons could be used to modulate the sensitivity of spontaneous structure formation in networks. Especially the regularity in combination with the firing rates of the neurons seems to be a promising new concept for such a modulation of synaptic plasticity. Interestingly, changes in the firing rate and in the auto-structure of spiking activity are often modulated during cognitive tasks, such as attention and memory, which may indicate that nature exploits these mechanisms for modulation of structure formation and neuronal self-organization in neuronal circuits (Engel et al., 2001; Fries et al., 2001; Pesaran et al., 2002; Uhlhaas et al., 2009; Düzel et al., 2010).

ACKNOWLEDGMENTS

We thank Carl van Vreeswijk for his support and very constructive discussions. We also thank Sonja Grün and Markus Diesman who helped in developing the initial ideas of this paper. And finally, we would like to thank Larry Abbott who inspired Gordon Pipa during his time at Brandeis University. This work was partially financed by the Phocus EU project (FP7-ICT-2009-C).

REFERENCES

Abbott, L. F., and Nelson, S. B. (2000). Synaptic plasticity: taming the beast. *Nat. Neurosci.* 3, 1178–1183.

Asai, Y., Guha, A., and Villa, A. E. P. (2008). Deterministic neural dynamics transmitted through neural networks. *Neural Netw.* 21, 799–809.

Averbeck, B. B. (2009). Poisson or not poisson: differences in spike train statistics between parietal cortical areas. *Neuron* 62, 310–311.

Baker, S. N., and Lemon, R. (2000). Precise spatiotemporal repeating patterns in monkey primary and supplementary motor areas occur at chance level. *J. Neurophysiol.* 84, 1770–1780.

Burns, B. D., and Webb, A. C. (1976). The spontaneous activity of neurones in the cat's cerebral cortex. *Proc. R. Soc. B Biol. Sci.* 194, 211–223.

Câteau, H., and Reyes, A. (2006). Relation between single neuron and population spiking statistics and effects on network activity. *Phys. Rev. Lett.* 96, 1–4.

Clopath, C., Büsing, L., Vasilaki, E., and Gerstner, W. (2010). Connectivity reflects coding: a model of voltage-based STDP with homeostasis. *Nat. Neurosci.* 13, 344–352.

Destexhe, A., and Paré, D. (1999). Impact of network activity on the integrative properties of neocortical pyramidal neurons in vivo. *J. Neurophysiol.* 81, 1531–1547.

Destexhe, A., Rudolph, M., Fellous, J.-M., and Sejnowski, T. J. (2001). Fluctuating synaptic conductances recreate in vivo-like activity in neocortical neurons. *Neuroscience* 107, 13–24.

Düzel, M., Penny, W. D., and Burgess, N. (2010). Brain oscillations and memory. *Curr. Opin. Neurobiol.* 20, 143–149.

Engel, A. K., Fries, P., and Singer, W. (2001). Dynamic predictions: oscillations and synchrony in top–down processing. *Nat. Rev. Neurosci.* 2, 704–716.

Faisal, A. A., Selen, L. P. J., and Wolpert, D. M. (2008). Noise in the nervous system. *Nat. Rev. Neurosci.* 9, 292–303.

Farkhooi, F., Strube-Bloss, M., and Nawrot, M. (2009). Serial correlation in neural spike trains: experimental evidence, stochastic modeling, and single neuron variability. *Phys. Rev. E Stat. Nonlin. Soft Matter Phys.* 79, 1–10.

Fellous, J.-M., Rudolph, M., Destexhe, A., and Sejnowski, T. J. (2003). Synaptic background noise controls the input/output characteristics of single cells in an in vitro model of in vivo activity. *Neuroscience* 122, 811–829.

Florian, R. V. (2007). Reinforcement learning through modulation of spike-timing-dependent synaptic plasticity. *Neural Comput.* 19, 1468–1502.

Fries, P., Reynolds, J. H., Rorie, A. E., and Desimone, R. (2001). Modulation of oscillatory neuronal synchronization by selective visual attention. *Science* 291, 1560–1563.

Gütig, R., Aharonov, R., Rotter, S., and Sompolinsky, H. (2003). Learning input correlations through nonlinear temporally asymmetric Hebbian plasticity. *J. Neurosci.* 23, 3697–3714.

Haider, B., Duque, A., Hasenstaub, A. R., and McCormick, D. A. (2006). Neocortical network activity in vivo is generated through a dynamic balance of excitation and inhibition. *J. Neurosci.* 26, 4535–4545.

Hanson, F. B., and Tuckwell, H. C. (1983). Diffusion approximations for neuronal activity including synaptic reversal potentials. *J. Theor. Neurobiol.* 2, 127–153.

Iyengar, S., and Liao, Q. (1997). Modeling neural activity using the generalized inverse Gaussian distribution. *Biol. Cybern.* 77, 289–295.

Izhikevich, E. M. (2003). Simple model of spiking neurons. *IEEE Trans. Neural Netw.* 14, 1569–1572.

Izhikevich, E. M. (2007). Solving the distal reward problem through linkage of STDP and dopamine signaling. *Cereb. Cortex* 17, 2443–2452.

Lazar, A., Pipa, G., and Triesch, J. (2007). Fading memory and time series prediction in recurrent networks with different forms of plasticity. *Neural Netw.* 20, 312–322.

Lazar, A., Pipa, G., and Triesch, J. (2009). SORN: a self-organizing recurrent neural network. *Front. Comput. Neurosci.* 3:23. doi:10.3389/neuro.10.023.2009

Legenstein, R., Pecevski, D., and Maass, W. (2008). A learning theory for reward-modulated spike-timing-dependent plasticity with application to biofeedback. *PLoS Comput. Biol.* 4, e1000180. doi:10.1371/journal.pcbi.1000180

Levine, M. W. (1991). The distribution of the intervals between neural impulses in the maintained discharges of retinal ganglion cells. *Biol. Cybern.* 65, 459–467.

Lindner, B. (2006). Superposition of many independent spike trains is generally not a Poisson process. *Phys. Rev. E Stat. Nonlin. Soft Matter Phys.* 73, 022901.

London, M., and Häusser, M. (2005). Dendritic computation. *Annu. Rev. Neurosci.* 28, 503–532.

Maimon, G., and Assad, J. A. (2009). Beyond Poisson: increased spike-time regularity across primate parietal cortex. *Neuron* 62, 426–440.

Markram, H., Lubke, J., Frotscher, M., and Sakmann, B. (1997). Regulation of synaptic efficacy by coincidence of postsynaptic APs and EPSPs. *Science* 275, 213–215.

Morrison, A., Aertsen, A., and Diesmann, M. (2007). Spike-timing-dependent plasticity in balanced random networks. *Neural Comput.* 19, 1437–1467.

Morrison, A., Diesmann, M., and Gerstner, W. (2008). Phenomenological models of synaptic plasticity based on spike timing. *Biol. Cybern.* 98, 459–478.

Nawrot, M. P. (2010). "Analysis and interpretation of interval and count variability in neural spike trains," in *Analysis of Parallel Spike Trains*, Chap. 3, eds S. Grün and S. Rotter (Boston, MA: Springer US), 1–22.

Nawrot, M. P., Boucsein, C., Rodriguez Molina, V., Aertsen, A., Grün, S., and Rotter, S. (2007). Serial interval statistics of spontaneous activity in cortical neurons in vivo and in vitro. *Neurocomputing* 70, 1717–1722.

Nawrot, M. P., Boucsein, C., Rodriguez Molina, V., Riehle, A., Aertsen, A., and Rotter, S. (2008). Measurement of variability dynamics in cortical spike trains. *J. Neurosci. Methods* 169, 374–390.

Nordlie, E., Gewaltig, M.-O., and Plesser, H. E. (2009). Towards reproducible descriptions of neuronal network models. *PLoS Comput. Biol.* 5, e1000456. doi:10.1371/journal.pcbi.1000456

Ostojic, S., Brunel, N., and Hakim, V. (2009). How connectivity, background activity, and synaptic properties shape the cross-correlation between spike trains. *J. Neurosci.* 29, 10234–10253.

Pesaran, B., Pezaris, J. S., Sahani, M., Mitra, P. P., and Andersen, R. A. (2002). Temporal structure in neuronal activity during working memory in macaque parietal cortex. *Nat. Neurosci.* 5, 805–811.

Pfister, J. P., and Gerstner, W. (2006). Triplets of spikes in a model of spike timing-dependent plasticity. *J. Neurosci.* 26, 9673–6982.

Pipa, G., Riehle, A., and Grün, S. (2006). Validation of task-related excess of spike coincidences based on NeuroXidence. *Neurocomputing* 70, 2064–2068.

Pipa, G., van Vreeswijk, C., and Grün, S. (2010). Impact of spike-train auto-structure on probability distribution of joint-spike events. (Submitted).

Pipa, G., Vicente, R., and Tikhonov, A. (2008). Auto-structure of presynaptic activity defines postsynaptic firing statistics and can modulate STDP-based structure formation and learning. *Lecture Notes in Comput. Sci.* 5164, 413–422.

Rudolph, M., Pospischil, M., Timofeev, I., and Destexhe, A. (2007). Inhibition determines membrane potential dynamics and controls action potential generation in awake and sleeping cat cortex. *J. Neurosci.* 27, 5280–5290.

Salinas, E., and Sejnowski, T. J. (2001). Correlated neuronal activity and the flow of neuronal information. *Nat. Neurosci.* 2, 539–550.

Smith, W. (1954a). Asymptotic renewal theorems. *Proc. R. Soc. Edinb. A* 64, 9–48.

Smith, W. (1954b). On the cumulants of renewal processes. *Biometrika* 64, 1–29.

Song, S., and Abbott, L. F. (2001). Cortical development and remapping through spike timing-dependent plasticity. *Neuron* 32, 339–350.

Song, S., Miller, K. D., and Abbott, L. F. (2000). Competitive Hebbian learning through spike-timing-dependent synaptic plasticity. *Nat. Neurosci.* 3, 919–926.

Teich, M. C., Heneghan, C., Lowen, S. B., Ozaki, T., and Kaplan, E. (1997). Fractal character of the neural spike train in the visual system of the cat. *J. Opt. Soc. Am. A Opt. Image Sci. Vis.* 14, 529–546.

Tetzlaff, T., Rotter, S., Stark, E., Abeles, M., Aertsen, A., and Diesmann, M. (2008). Dependence of neuronal correlations on filter characteristics and marginal spike train statistics. *Neural Comput.* 20, 2133–2184.

Uhlhaas, P. J., Pipa, G., Lima, B., Melloni, L., Neuenschwander, S., Nikolic, D., and Singer, W. (2009). Neural synchrony in cortical networks: history, concept and current status. *Front. Integr. Neurosci.* 3:17. doi:10.3389/neuro.07.017.2009

van Rossum, M. C., Bi, G. Q., and Turrigiano, G. G. (2000). Stable Hebbian learning from spike timing-dependent plasticity. *J. Neurosci.* 20, 8812–8821.

Conflict of Interest Statement: The authors declare that the research was conducted in the absence of any commercial or financial relationships that could be construed as a potential conflict of interest.

Received: 17 November 2010; accepted: 29 November 2011; published online: 16 December 2011.

Citation: Scheller B, Castellano M, Vicente R and Pipa G (2011) Spike train auto-structure impacts post-synaptic firing and timing-based plasticity. Front. Comput. Neurosci. ***5****:60. doi: 10.3389/fncom.2011.00060*

3

Mesoscopic scale: Networks of Neurons

The purpose of this dissertation is to study how time-varying signals modulate the neural responses at different spatial scales: at the single neuron or microscopic scale, within networks of neurons or mesoscopic scale, and within cortical areas or macroscopic scale.

This chapter presents the second study, which aims to analyse the impact of the temporal structure of the inputs within networks of neurons, known as the mesoscopic scale. The chapter is divided into four sections. It begins with a short summary of the corresponding study, with the aim to provide the broad context of the research questions and hypothesis. Following that, the section 'fundamentals' aims to present the background concepts used in the corresponding studies. Next, the chapter contains a 'context' section that revisits how the neural system represents and processes stimuli at the specific spatial scale under discussion, with special emphasis on how those neural representation are modulated by the temporal structure of the stimulus. The third section contains the study as published in the journal *Lecture Notes in Computer Science*, as a peer-reviewed conference publication under the reference Castellano, M., and Pipa, G. (2013). Memory trace in spiking neural networks. In Artificial Neural Networks and Machine Learning – ICANN 2013, *Lecture Notes in Computer Science*, (Springer Berlin Heidelberg), pp. 264–271. Following, the 4th section contains complementary simulations that frame the published research to the context of the thesis. Finally, the section 5 provides a summary and discussion of the obtained results, while section 6 concludes the study and contextualizes the obtained results with the general goal of the dissertation.

Short summary of the study

Spiking neural networks that process time-varying stimulus have a limited capacity to store and recall past inputs, what we call the memory trace [161]. Intuitively, a

stimulus arriving at an active neural network (e.g. spontaneously spiking) will induce a pattern of spiking activity that could be decoded for a few ms after its arrival [161]. The ability to keep such stimulus-specific dynamics distinguishable from spontaneous spiking activity for longer time intervals is crucial for several cognitive tasks, including motor preparation [55, 145] or working memory tasks [72], where stimulus representations must be available over periods of few hundreds of milliseconds. However, a generic spiking neural network can only retain stimulus within few ms after its arrival and cognitive tasks involving short-term memory are thus unsolvable.

The purpose of this study is to characterize and extend the memory trace of a generic spiking neural network that is processing time-varying stimulus. As a first step, we will characterize the dynamics of the spiking neural network model (SNN) by testing whether it shows stimulus specificity, whether cortical plasticity modulates such stimulus representations and its impact on the memory trace. For the second step, we aim to extend the memory trace of the spiking neural network through the coupling to an external delayed-dynamical system (DDS), which attempts to be an abstract representation of slow currents that are present in the external medium where spiking neural networks are embedded. Finally, we will further characterize the memory trace of a plastic-SNN with the external DDS to test whether there can be any synergetic interaction between the systems that lead to the further extension of the memory trace. Taken together, this study aims to be a proof of principle that highlights possibility that the dynamics of neural units are modulated through interaction with external dynamical systems.

References

Part of this study was presented and published after peer-review process as a talk and conference proceeding on the *International Conference on Artificial Neural Networks*, and is found under the following reference:

Castellano, M., and Pipa, G. (2013). Memory trace in spiking neural networks. In Artificial Neural Networks and Machine Learning – ICANN 2013, *Lecture Notes in Computer Science*, (Springer Berlin Heidelberg), pp. 264–271.

3.1 Fundamentals of neural networks

This section aims to provide background knowledge of the concepts used on this and following chapters. Specifically, this section presents an introduction to the modelling of neural networks, followed by a description of reservoir computing, a recently developed framework for the processing of time-varying signals.

3.1.1 From single neurons to neural networks

The human brain consists of about 10^{11} neurons with highly diverse morphology and dendritic tree structures. The connectivity pattern between those neurons strongly determines the flow of information through the system [117], as its structure affects function.

Connectivity patterns within neural populations has long been studied within the neuroscientific community with different contexts: anatomical connectivity, functional connectivity and effective connectivity, which builds on functional connectivity by describing a directional dependency or causality between signals [90, 225, 228].

The first line of research, anatomical connectivity, is concerned with the specific structural connections within the network (i.e. synapses or fiver paths) that form particular connectivity patterns or topologies. Despite the simplicity of the idea, the establishment of an anatomical connectivity is one of the major challenges in neuroscience, as complexity of the connectivity increases with the number of neurons to be studied [109]. In particular to the cerebral cortex, anatomical analysis suggest that neurons are organized in six layers of different cellular density, each containing inhibitory and excitatory neurons that spread their axons within and across layers (Figure 3.1 A). The cerebral cortex is refereed to as gray matter, as it contains neurons in high density when compared to the underlying white matter, which mostly contain glial cells and myelinated axons that connect the cerebral cortex and other brain regions.

The second major line of network research is concerned with the functional connectivity of the neural system. From this perspective, connectivity measures aim to capture the statistical dependencies between neural activity, specifically making reference to transient communication between neurons that arise within cognitive processing. In particular to the cerebral cortex, functional analysis suggest that cortical layers are functionally organized in **cortical columns**, aggregates of 10^6-10^8 neurons that have a nearly nearly identical response to a stimulus. A classical example of functionally defined cortical columns is the orientation of selective columns within early visual cortex (V1), where nearby neurons would have a rather similar receptive field to oriented bars (Figure 3.1 B).

But what can be learned about neural information processing by studying the anatomical and functional connectivity of the cerebral cortex? Given its anatomical and functional complexity, the study of such complex networks may benefit from computational studies where some of the biological complexity can be simplified [131, 243]. However, modelling biologically inspired spiking neural networks which process stimulus is far from trivial. In particular, what is the adequate level of simplification that should be included in the computational model? In regards to biological systems, complexity within the networks can arise due to several factors:

1. Single neuron dynamics (nodes): the neurons itself show structural and temporal dynamics, which could be different in different neurons.
2. Anatomical connections (edges): the connection between the neurons establish routes for information transmission between neurons. At the same time, the

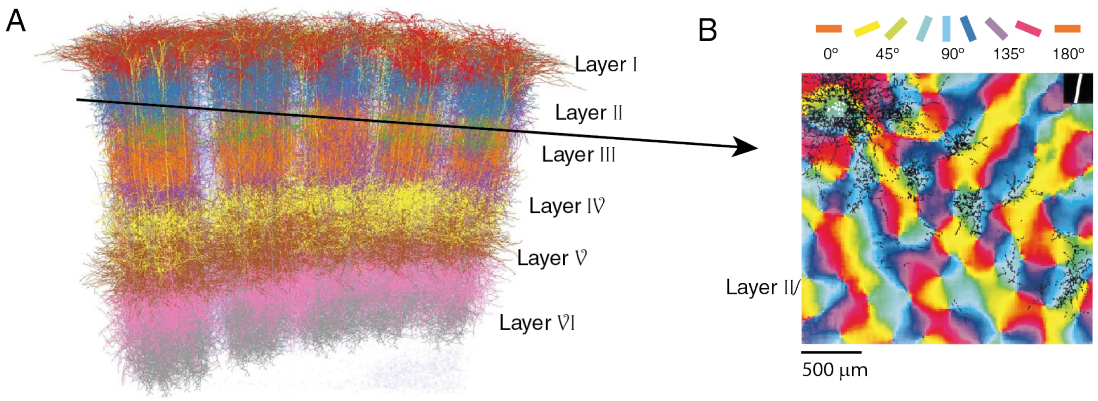

FIGURE 3.1: **Spatial structure of neurons within cortical networks.** A) Cortical layers can be further organized in cortical columns involving tens of thousands neurons (modified from [191]). B) An orientation preference map of macaque visual cortex in layer 2/3, reflecting receptive fields of several cortical columns. Horizontal connections from a column with 80^{o} orientation preference (white dots) to neighbouring columns are visible through staining (black lines). Modified from [26].

strength of connections between neurons establish directionality and make some connections more relevant than others.

3. Adaptability (edges): the connections between neurons change over time due to synaptic plasticity mechanisms, leading to changes on the strength of connections or leading to the creation/loss of connections.

From this prospective, simplification of some of these factors may facilitate the study of how information is transmitted through a neural network. Which simplifications would be adequate? Which models could be used for the study of spiking neural networks? Ultimately, the model chosen must replicate some aspects of biological systems and most importantly, the simplifications and assumptions on computational models would ultimately delimit the outcome of the studies and must always be considered for discussion.

In this study, we focus on an intermediate level of simplification, where biologically inspired neurons (both inhibitory and excitatory) are randomly connected forming a recurrent network (see section 3.4 for further details on the model). In our model, the neuron dynamics are described by a single differential equation, reducing variability on network dynamics due to single neuron variations (reduction of variability type 1). The connections between the neurons are drown randomly, leading to an anatomical variability found in recurrent networks (RNN), a class of neural networks where connections between neurons can form directed cycles. As such, the modulations of neural dynamics due to specific anatomical connections is simplified to those dynamics arising within RNN (reduction of variability type 2). Finally, the connections between neurons are plastic, as in this study we are going to explore how several adaptation mechanisms, through changes in the network dynamics, change the computational capabilities of neural circuits [150, 151].

Why did we choose this particular model? As the goal of the study is to further understand whether and how an external delayed-dynamical system will modulate the network properties, (in particular memory trace), we started by simplifying the dynamics of single spiking neurons, and continued by simplifying the anatomical variability by using recurrent neural networks. Furthermore, the specific neuron and plasticity models were chosen based on a trade-off between its biological plausibility and its computational costs (further discussed and presented in section 3.4).

3.1.2 Computational models of spiking neural networks: reservoir computing

Computational models of spiking neural networks started to develop shortly after spiking neuron models were well established [113]. However, mimicking neural population dynamics by means of spiking neural network models has been shown to be difficult. The first models that were capable to process time-varying stimulus did so by incorporating an explicit representation of time within the spatial structure [75]. Recurrent neural networks (RNNs), developed in the 1980s, were the first models to represent time implicitly [74, 124]. RNN consist of a set of neurons (nodes, units or processing elements) connected in a recurrent manner, whose connections (or links) are trained to solve specific tasks. Within the machine learning field, RNNs became powerful tools for solving tasks that required the processing of information over time [114] (e.g. time series prediction, speech recognition or adaptive control). To use a RNN to solve a specific task, the connections between neurons have to be trained, so that the task can be decoded from a subset of neurons. Despite its simplicity, RNNs have been shown to be Turing equivalent, namely, universal approximations of dynamical systems [140, 280]. However, the usage of RNN to solve real-world tasks is not always feasible since the training of the connections is computationally very high and converges slowly (see [158] for an overview).

The reservoir computing framework (RC) overcomes the difficulties of RNNs in learning dependencies of time-dependent stimulus [133, 162], developed in parallel by Jaeger [133], as an Echo State Network (ESN), and Maass [162] as a Liquid State Machine (LSM), the latter being proposed as a model of a cortical column and cortical processing. Within RC, the training required to solve a computational task it is not performed on the connections between neurons, but by an external decoder. In this case, the recurrent network is regarded as a complex kernel (see chapter 5 and 6 in [22]) that projects the time-varying stimulus onto a high-dimensional space from which the stimulus, or a function of the stimulus, can be decoded. This paradigm has indeed improved upon the performance of classical RNNs in solving a wide set of benchmark tasks in the machine learning community (see [158] for an overview).

Conceptually within the RC-cortical circuits framework (LSM), the time-varying stimulus are combined with the spiking activity of the network in a time resolved fashion. As such, the spiking neural network provides a high-dimensional, non-linear transformation of the time-varying signal, from which a task can be decoded by an external decoder. Maass and Markram [160] showed that under certain constraints, a spiking

neural network is an universal function approximator: any function of the stimulus can be decoded from the network activity if a) the dimensionality of the network is higher than the dimensionality of the stimulus, b) the several stimulus are mapped onto a spiking activity that can be differentiated by the decoder (separation property) and if c) the network activity maintains information about past events (fading memory). In other words, the RC framework proposes that the capability of a spiking neural network to perform a computation on a time-varying stimulus will depend on its ability to retain information about past events and its ability to project stimulus into separable spiking patterns, what we call the memory trace.

Strikingly, the memory trace of spiking neural networks that process time-varying stimulus have a limited capacity to store and recall past inputs [161]. Intuitively, a stimulus arriving at an active neural network (e.g. spontaneously spiking) will induce a pattern of spiking activity that could be decoded for a few ms after its arrival. Accordingly, computations that involve or require the storage and recall of memory for longer times that the fading memory of the network will not be solvable. Take for example a working memory task, in which a set of items with spatio-temporal structure must be recalled after a delay period [72]. The ability to keep such stimulus-specific dynamics distinguishable from spontaneous spiking activity for longer time intervals is crucial for several cognitive tasks, including motor preparation [55, 145] or working memory tasks [72], where stimulus representations must be available over periods of few hundreds of milliseconds. However, a generic spiking neural network can only retain stimulus within few ms after its arrival and cognitive tasks involving short-term memory are thus unsolvable.

In the following study, we aim to extend the memory trace of a generic spiking neural network while processing time-varying stimulus. Specifically, our study is divided in four stages. First, we will characterize the dynamics of the spiking neural network model (SNN) by testing whether it shows stimulus specificity, whether cortical plasticity modulates such stimulus representations and its impact on the memory trace. For the second step, we aim to extend the memory trace of the spiking neural network through the coupling to an external delayed-dynamical system (DDS), which attempts to be an abstract representation of slow currents that are present in the external medium where spiking neural networks are embedded. Finally, we will further characterize the memory trace of a plastic-SNN with the external DDS to test whether there can be any synergetic interaction between the systems that lead to the further extension of the memory trace.

3.2 Context

Although there are studies that associate the spiking activity of a single neuron to a precise function [110, 125], in several cases, the response of a population of neurons is a better predictor of the function (see [13, 128, 203] for review).

The relevance of population activity on information processing has gained relevance as the experimental techniques allow for the parallel recording of neural activity [30, 53].

An striking example of the importance of population coding can be observed in the hippocampus of a rat: while single neurons encode the particular location of the animal, the whole population activity seem to encode the location of the animal within the space that this animal exists [182]. In other words, as each neuron encodes a place field (which is a small region of the space that, when occupied by the rat, induces a response of the cell), and different neurons will have a place fields on different locations, large population of cells will respond to any given location, encoding in a distributed manner, the spatial location of the animal (see Figure 3.2A for an schematic representation). The encoding of stimulus within the **population rate code** (or the probabilistic population code), where each neuron represents a particular stimulus feature [13, 128, 203], has been similarly proposed to encode stimulus information within several cortical areas, including frontal eye fields, where precise saccadic movements are better predicted by the weighted sum of the activity of a large populations of less finely tuned neurons [236]; visual discrimination within early visual areas [104]; or the control of arm movements within motor cortex [8].

But it is not only through the establishment of feature-specific neurons that populations of neurons encode stimulus information. Since the development of experimental techniques that allow for the parallel recording of spiking activity, several studies hint at the relevance of precise spike timing on the population level, the **assembly hypothesis** [205, 231], where populations of neurons are thought to coordinate their precise spike times to tag particular stimulus or events. In this framework, neurons code information in a synergistic manner, where assemblies or groups of neurons that code particular stimulus are formed through the precise synchronization of their spike times. Accordingly, spike-time patterns with millisecond precision can be found in the spike trains of multiple neurons in both *in-vitro* and *in-vivo* [156, 204, 250, 271].

A different framework for population coding is the **spatio-temporal coding framework** or reservoir computing, where populations of neurons encode stimulus information on the spatio-temporal dynamics of the population activity [38]. The basic idea of this framework is that, on arrival of a signal, the neural system generates a pattern of activity that contains information about stimulus, where spike times become relevant as they belong to the population activity that describes a particular trajectory on the space. The neural system as such, acts as a filter where the stimulus is mapped to a high dimensional space, where information about the stimulus becomes decodable (Figure 3.2B). Accordingly, transient and highly dynamic neural responses have been observed on several sensory cortices, including olfactory [28, 172], auditory [16, 19], and visual cortices [187], as well as in parietal cortex while involved in working memory tasks [14].

Taken together, it seems that in the neuroscience community, it is becoming clear that the temporal structure of neural activity can only be neglected at the cost of loosing information [205]. However, and despite the significant advances on understanding population coding, population responses are far more complex than expected, as they are shaped by experience [39, 96, 259].

Computational and experimental studies bring light on how, due to the presence of ongoing plasticity mechanisms, populations responses change and adapt to the incoming stimuli. By analyzing the spiking activity of a population of generic spiking neurons,

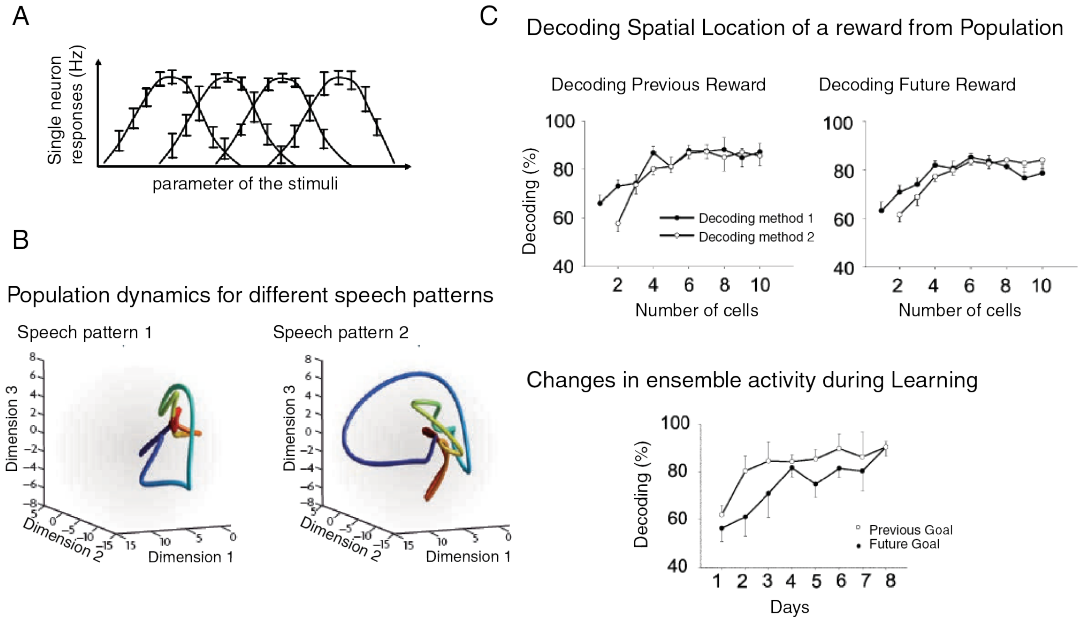

FIGURE 3.2: **Population activity is stimulus-specific and adapts to the temporal structure of stimulus**. A) Population rate code framework, or the probabilistic population code, where the tuning curves of single neurons span the whole stimulus parameter range, allowing a population of neurons to encode the entire stimulus space, adapted from [203] B) Visualization of spatio-temporal patterns arising within a simulated network of spiking neurons that arise as a representation of two different spoken words, adapted from [38] as an example of the spatio-temporal coding framework, where a population of neurons encodes stimulus information within its transient spatio-temporal of activity C) (upper) The spatial location of past rewards (left), as well as the future or expected rewards (right) can be decoded from the spatio-temporal patterns of spiking activity within a population of neurons within rat's prefrontal cortex, which have been learned through repeated exposure to an environment (lower). Adapted from [14]

computational studies propose that, through the combination of both homeostatic and activity-dependent plasticity, populations or neurons adapt their responses to the statistics of the stimulus in a self-organized fashion, necessary for the creation of robust and stable neural representations of the stimulus [150, 151, 255]. Experimentally, the changes of transient patterns that arises through learning has been reported in few studies [14, 253]. A particularly interesting example was reported in [14], where the spatio-temporal patterns arising within rat's prefrontal neurons as a result of exposure to novel stimuli changes after few sessions of training, along with their ability to remember the spatial location of a reward [14].

Ultimately, these observations suggest that the spatio-temporal properties of neural signals as well as its modulations in response to stimuli is crucial for the further understanding of population coding. However, and despite the significant advances on understanding population coding, the basic principles governing population coding remains to be determined. The most important limitation is the fact that, while recent technological advances allow for the recording of many neurons in parallel [45, 59], the establishment of methods that allow for a quantitative description of the effective connectivity between those neurons is still under research [95, 192]. To this point,

computational models hold a great potential to advance our knowledge of how a population activity processes and manipulates rich spatio-temporal stimuli, and ultimately produce specific predictions on population dynamics that can be tested experimentally.

Computational models of spiking neural networks that allow for the processing of stimulus with rich spatio-temporal dynamics started to develop shortly after models of spiking neurons were presented (see section 3.1 for further discussion). However, mimicking the dynamics of neural populations and linking those dynamics to behavioral tasks or cognitive functions has proven to be very difficult for several reasons. First, a great difficulty lies in bridging the temporal scales of spiking responses within neural populations and those of the tasks to be solved. For instance, consider delayed-reward tasks, where the chosen action (press red button) can only be rewarded after a relatively long time interval (get a cookie at the next office), so that the action must be retained over this delay period [112]. Second, while computational models facilitate the study of plasticity mechanisms that allow for the adaptation of population dynamics, little is known on the specific roles of diverse spatial mechanisms and its precise interaction with stimulus and population dynamics.

In this study, we start by analyzing whether and how different plasticity mechanisms modulate population dynamics within a generic spiking neural network, with the ultimate goal of extending the capability of a generic spiking neural network to retain stimulus-specific responses (the memory trace). Next, we follow by proposing a computational model where the memory trace of a spiking neural network is extended through the interaction with an external slow-dynamical system, with the aim of empathizing the relevance of delays within biological systems, as well as raise awareness of a possible synergistic interaction between spike dynamics and local field potentials (LFP) within the neural system.

3.3 Paper II: Extending the memory trace in spiking neural networks through the coupling with an external slow delayed dynamical system

Memory trace in spiking neural networks

Marta Castellano, Gordon Pipa

Institute of Cognitive Sciences,
University of Osnabrueck, Germany
{mcastellano,gpipa}@uos.de

Abstract. Spiking neural networks have a limited memory capacity, such that a stimulus arriving at time t would vanish over a timescale of 200-300 milliseconds [1]. Therefore, only neural computations that require history dependencies within this short range can be accomplished. In this paper, the limited memory capacity of a spiking neural network is extended by coupling it to an delayed-dynamical system. This presents the possibility of information exchange between spiking neurons and continuous delayed systems.

Keywords: spiking neural networks, memory trace, delayed-dynamical systems, reservoir computing

1 Introduction

Neurons communicate through action potentials, while the represented cognitive processes operate at slower timescales. The neural system, then, must have some way of storing the short term information required for the cognitive processes.

Classical paradigms for short-term memory state that memory arises through persistent patterns of neural activity, which stabilize through synaptic modification [3]. A relatively new paradigm proposes that spiking neural networks (SNN) encode and store information in their transient dynamics, while computations emerge through the continuous interaction of external stimulus with the internal states of the network [2]. This concept is generalized within the reservoir computing community: any non-linear dynamical system with fading memory, the reservoir, can be used as a computational system that processes stimulus in its transient trajectories [4, 5].

If information is retained within neural trajectories, how quickly are those traces forgotten? A spiking neural network, with no slow processes associated, (such as adaptation or synaptic plasticity), has a memory trace of few ms, which is on the same timescale of the intrinsic time constant of single neurons [6]. As a result, computations, that require information to be retained over longer timescales, are not be solvable; for example motor preparation [7, 8] or working memory tasks [3].

Several studies have tried to overcome the limited memory trace. Through the addition of feedback connections, [9] brought a generic spiking neural network to develop high-dimensional attractor-like sub-manifolds that solved working memory tasks. Likewise, [10] extended the memory trace by introducing

working memory units, neurons connected to the recurrent network by means of plastic synapses that mark the presence of an event as on/off states, bringing the network towards multiple point attractors.

While these two studies propose a model by which the memory trace of the reservoir is extended by the interaction with adjacent neural units, we propose a model by which the memory trace of the reservoir is extended by a non-linear coupling of the network to an external delayed-dynamical system (DDS), which is a general term for a dynamical system that change over time depends on its current and past states.

Our proposal is based on two primary observations. First, delays are ubiquitous in biological systems and including them within mathematical models extend the range of dynamics observed in the system [11]. Second, DDSs can, in a similar fashion, be used as a reservoir to solve computational tasks (first proposed in the PHOCUS European project FP7-ICT-2009-C).

This paper is organized as follows. The method section presents SNN and DDS, with emphasis on the methods of encoding and decoding used to estimate computational performance and the memory trace. In the results section, we first present both SNN and DDS dynamics, together with their computational performance and memory trace. Afterwhich, the results are compared to the case, in which SNN is coupled to DDS, showing that the memory trace of an SNN can be extended by the non-linear coupling with a delayed-dynamical system.

2 Methods

Spiking Neural Network The spiking neural network (SNN) is modeled with the modeling toolbox CSIM [12]. In short, a set of $N_n = 135$ leaky integrate and fire neurons are placed on a 3x3x15 grid and 20% of them are randomly selected to be inhibitory. The membrane potential V_m^i of a neuron i is described by:

$$\tau_m \frac{dV_m^i}{dt} = -(V_m - E_{rest}) + R_m \cdot (I_{in}^i + I_{syn}^i) \tag{1}$$

with a membrane time constant $\tau_m = 30$ ms, a resting potential $E_{rest} = 0$ and an input resistance $R_m = 1M\Omega$. The spiking threshold is set to 15 mV; the absolute refractory period is 3 ms (excitatory) and 2 ms (inhibitory). The membrane potential is reset to a voltage uniformly drawn from the interval [13.8 mV, 14.5 mV], same values used to initialize V^i each simulation [12]. I_{syn}^i is the sum of recurrent connections currents that arrive at the membrane, while I_{in}^i are the sum of the stimulus currents. Numerical approximation is obtained by the Euler's method with fixed integration step ($\delta t = 0.001$) sec. The neurons are randomly connected with a probability of connection c, which is different among inhibitory (in) and excitatory (ex) neurons: 0.3 ex-ex, 0.2 ex-in, 0.4 in-ex and 0.1 in-in, leading to a total of 2325 synapses.

Delay-Dynamical System A non-linear system with delayed feedback of the general form $\dot{x}(t) = f(x(t)) + g(x(t-\tau))$, is here named delay-dynamical system (DDS) and implemented by the Mackey-Glass equation [13, 14]:

$$\frac{dx(t)}{dt} = \beta \frac{x(t-\tau) + \alpha I_{DDS}(t)}{1 + (x(t-\tau) + \alpha I_{DDS}(t))^n} - x(t) \tag{2}$$

with $\beta = 0.4$ being the coupling factor of the feedback, $n = 1$ the non-linearity exponent, $\alpha = 0.05$ the history dependence, $\tau = 80$ the delay time and $I_{DDS}(t)$ receives the external stimuli. Numerical approximation of the delayed differential equation is obtained by the Heun's method with fixed integration step ($h = 0.001$).

Stimulus To The Reservoir The reservoir receives $R = 2$ dimensional time-varying stimulus r_1 and r_2, an non-homogeneous Poisson process with uniformly distributed rates $\lambda = [10, 20, 40]$ Hz, so that at each point in time t the Poisson process is drawn from $r_i(t) \approx \lambda(t) \cdot \delta t$ with $\lambda(t)$ being uniformly distributed from the set $[10, 20, 40]$, see Figure 2 A).

Encoding The Stimulus The DDS encodes stimulus as follows: the delay term τ is divided into M virtual nodes, i.e., a set of M points equidistant distributed over the delay τ, see Figure 2. The virtual nodes are those time points that encode the stimulus $r_i(t)$. The stimulus $r_i(t)$ is previously preprocessed, referred as the masking procedure. Masking can be seen as a multiplication of the stimulus $r_i(t)$ with the masking function $m(t)$, so that the stimulus that each of the virtual nodes receive $I_{DDS}(t)$, is defined as $I_{DDS}(t) = \sum_{i=1}^{R} r_i(t) \cdot m(t)$, where $m(t)$ is a binary random vector so that $m(t) \in [-1, 1]^M$. Masking the stimulus has three goals: to multiplex the stimulus over the delay line, to ensure that every virtual node of the delayed line receives a linear combination of different dimensions of the stimulus R and ensures that the delayed dynamical system is constantly in a transient regime. Furthermore, the encodign of the stimulus on the delay line is modulated by the parameter k, here called encoding scheme, which reflects the number of time steps t of the stimulus that are going to be encoded within a delay line. In short, a delay line encodes $1/k$ time steps of the stimulus and a time step t is projected onto $N_{in} = 200$ virtual nodes. In this way, the total number of virtual nodes within a delay line scales by the parameter k so that $M = \frac{1}{k} \cdot N_{in}$.

The SNN encodes external stimulus by means of spike trains. The stimulus $r_1(t)$ and $r_2(t)$ are time-varying firing rates from which Poisson spike trains are drawn, and each of them is mapped to an independent subset of 8 neurons $j \in N_n$. The spike probability on the interval δt is given by $p(spike = 1(t - \delta t, t + \delta t)) = r_i(t)\delta t$. The spike trains are converted into currents by the convolution of the spikes with an exponential decay term, so that the current I_{in} resembles an EPSP. Specifically $I_{in} = W * e^{-1/\tau_s}$, where $\tau_s = 4$ is the decay time of the EPSP and $W = 0.15$ scales the EPSP amplitude.

Decoding The Stimulus The reservoir activation $z(t)$, which can be either the SNN or the delayed-dynamical system, for N nodes and total simulation time Q is denoted $\mathbf{A}$, and the expected output signal of the reservoir (the target signal to be approximated) as $y(t)$ for $t \in (t_0, ..., t_Q)$. The aim of the linear regression (i.e. maximum likelihood with normal distributed residuals) is to find the set of weights w that fulfill $y = wA$, obtained by applying the pseudo-inverse, so that $w = y(\mathbf{A})^{-1}$. The target signal is defined in this paper as the sum of the two-dimensional stimulus, so that $y(t) = r_1(t) + r_2(t)$. Learning the weights w is denoted as the training phase. Next, in the testing phase, the weights w are kept fixed and an output $u(t)$ is obtained from the network activity,so that $u(t) = wA$. Finally, the accuracy of the linear regression is evaluated on the testing set as described in the computational performance section. Intuitively, the weights w of the readout can be trained in a task specific way, so that for every task, there is a linear combination of nodes in the reservoir that can be used to approximate the target signal $y(t)$.

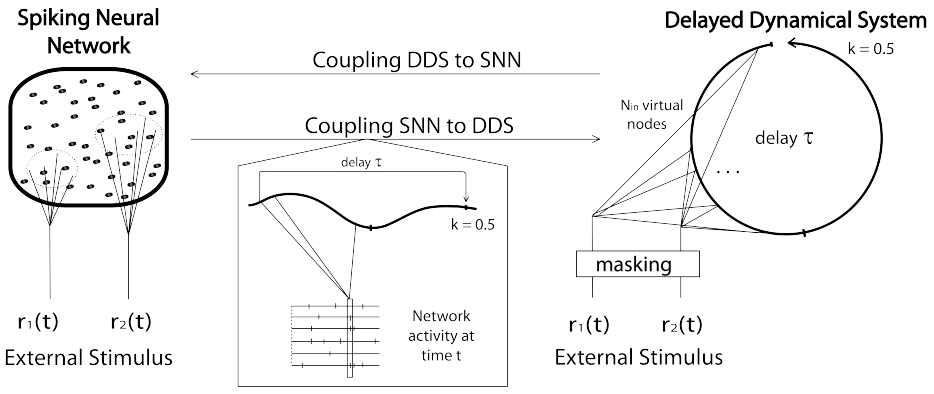

Fig. 1: Visualization of the non-linear coupling between DDS and SNN

Computational task The task of the reservoir consists in reconstructing a time-dependent stimulus $r_i(t)$ by reading out the activity of the reservoir at later times t_{lag}.

Computational Performance and Memory Trace Computational performance $CP(t)$ is defined as the correlation coefficient between target $y(t)$ and estimated output $u(t_{lag})$ at time $t = t_{lag}$, so that $CP(t_{lag}) = corr(y(t), u(t_{lag}))$. Memory trace MT is defined as the maximum time at which the input can be decoded from the network with a correlation coefficient higher than 0.5, so that $MT = max\ \rho_i$, where ρ_i is the time lag t_{lag} at which $CP(t_{lag})$ becomes lower than 0.5.

Coupling Between Delayed-Dynamical System and Spiking Neural Network The non-linear coupling can be visualized in Figure 2. The SNN encodes the signal of the DDS, $x(t)$, by means of 16 analog synapses, represented in the I&F neurons as a current in the term $I_{in} = W_{DDS} \cdot x(t)$, where $W_{DDS} = 0.01$.

3 Results

This section is divided in two different parts. First, we characterize both SNN and DDS dynamics and present its computational performance and memory trace, providing a qualitative and quantitative description of the two models. Second, we compare the results to the case in which SNN is coupled to DDS, showing that the memory trace of an SNN can be extended by the non-linear coupling with a delayed-dynamical system.

3.1 Memory trace of SNN and DDS

The dynamic responses of the two systems when processing the stimulus are presented in Figure 2 B) and Figure 2 C). The system operates in a fixed point regime (i.e. single fixed point, Figure 2 D, left), perturbed by external stimulus (see Figure 2 D, right).

The computational performance at different time lags and the memory trace of the SNN and DDS are quantified in Figure 2 E). The simulated SNN (parameter specification in methods section) has a maximum computational performance of 0.9 at time lag zero and a memory trace of 0.11 sec, consistent with results presented in [1].

The memory trace and computational performance of the DDS varies together with the variation of the parameter k, which controls the projection of the stimulus to the DDS (encoding scheme). At $k = 1$, $\delta t = 1$ ms of stimulus $r_i(t)$ is mapped to the $M = 200$ virtual nodes contained in a delayed loop $\tau = 80$. In this encoding scheme, the DDS has a maximum computational performance of 0.87 at time lag zero and a memory trace of 0.067 sec. Increase of k leads to the increase of the time steps δt of the stimulus that are mapped within the delay line. The higher the k, the longer the memory trace of the DDS. Consider for example the case where $k = 0.04$, where a single delay loop encodes 25 δt of the stimulus in a total of 5000 virtual nodes (note that the number of virtual nodes increases as $1/k \cdot N_{in}$). This encoding scheme has a maximum computational performance of 0.93 at time lag zero and a memory trace of 0.27 sec.

The increase in memory trace observed by the increase of k cannot be explained by the increase on the number of virtual nodes: a DDS with an encoding parameter $k = 1$ and $M = 5000$ virtual nodes has a maximum computational performance of 0.9 at time lag zero and a memory trace of 0.07 sec. The results obtained in this section are used as a baseline to compare the computational performance and memory trace of the following simulations.

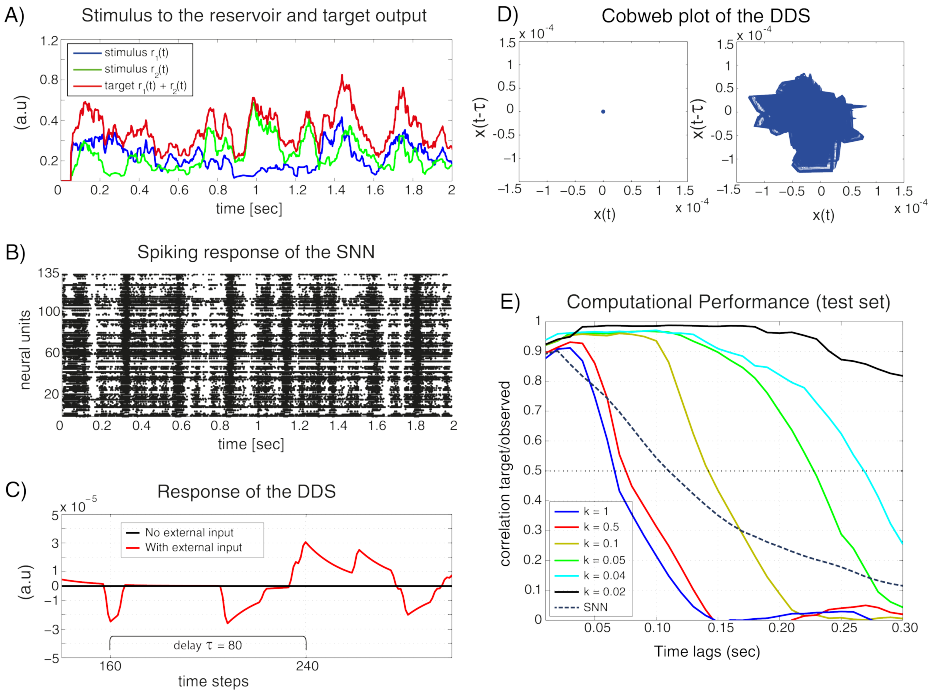

Fig. 2: A) Stimulus and target output for the reservoir. B) Spiking response of the SNN. C) Response of the DDS within a delay line (see equation 2). D) Cobweb plot of the DDS (left) and the DDS receiving external stimulus $r_1(t)$ and $r_1(t)$ (right). E) Estimation of the computational performance at different time lags for the SNN *(dotted blue line)* and the DDS, where k changes the encoding to the DDS.

3.2 Memory trace of SNN coupled to DDS

This section aims to estimate whether the SNN shows an increased memory trace when coupled to the DDS. Accordingly, we performed two different simulations: on the one hand, the SNN receives input from the DDS, and on the other hand, the SNN receives input from both DDS and external stimulus.

In the first case, the DDS encodes stimulus r_1 and r_2 and the signal from the DDS is sent to the SNN. With this, we test whether the SNN extracts information from the stimulus that is being processed by the DDS. In this case, the computational performance of the SNN at zero time lag is lower compared to the baseline, while the memory trace of the SNN is longer than baseline as long as the DDS encodes the input at $k > 0.5$ (for instance, at $k = 0.04$ $CP(t_{lag=0}) = 0.62$ and $MT = 0.16$ sec).

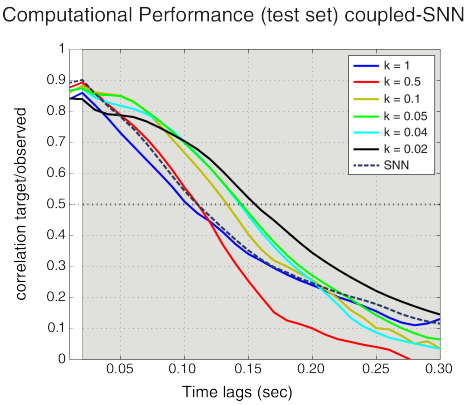

Fig. 3: Computational performance and memory trace of the coupled-SNN for different k, compared to the non-coupled SNN *(dotted line)*.

In the second case, the SNN receives stimulus from both DDS and external stimulus (r_1 and r_2), referenced as coupled-SNN. With this simulation we aim to estimate whether the SNN can integrate DDS signals to the ongoing stimulus processing. Results presented in Figure 3 show that the coupling to the DDS does not change the computational performance of the SNN at time lag zero. Nevertheless, as long as the DDS encodes stimulus at $k > 0.5$, the coupled-SNN has longer memory trace than the baseline SNN (0.11 sec baseline memory trace versus 0.14 sec at $k = 0.04$). The gray shadow in Figure 3 indicates that the difference to the non-coupled SNN is statistical significant ($p = 1.7 \cdot 10^{-16}$, one way ANOVA for 20 observations).

4 Discussion

Previous models for short-term memory in spiking neural networks (SNN) proposed that low-dimensional attractors in the circuit dynamics store stimulus information [3]. Here we explored a new paradigm, whereby short-term memory is implemented in the transient dynamics. Within this framework, the memory trace is limited by the length of the neural trajectory, modulated by features such as intrinsic neuron time constants [6] or network topology [15]. We propose a modification of the framework by which a SNN extends its memory trace by a non-linear coupling with a delayed-dynamical system (DDS).

As a proof of principle, we defined a generic DDS and proposed a non-linear coupling with the SNN, which lead to the increase of the memory trace of the spiking neural network. This highlights an essential feature: including delayed coupling within a spiking neural network extended the memory trace, which could not be maintained by the spiking network alone.

The relevance of this finding relies upon neural systems being delayed dynamical systems. Often spiking neuron models are simplified up the point where delays play no role. The addition of delays, not only increase the dynamic range of mathematical models [11], but also increases the range of timescales at which the system processes and retains stimulus.

Acknowledgments This research was partially supported by the EU grant PHOCUS European project FP7-ICT-2009-C. The authors declare that there is no conflict of interests.

References

1. Maass, W., Natschläger, T. & Markram, H. Fading memory and kernel properties of generic cortical microcircuit models. Journal of Physiology 98, 31530 (2004).
2. Buonomano, D. V & Maass, W. State-dependent computations: spatiotemporal processing in cortical networks. Nature Reviews Neuroscience 10, 113125 (2009).
3. Durstewitz, D., Seamans, J. K. & Sejnowski, T. J. Neurocomputational models of working memory. Nature Neuroscience 3 Suppl, 118491 (2000).
4. Maass, W., Natschläger, T. & Markram, H. Real-time computing without stable states : a new framework for neural computation based on perturbations. Neural Computation 14, 25312560 (2002).
5. Jäger, H. The echo state approach to analysing and training recurrent neural networks. GMD Report 147 (2001).
6. Mayor, J. & Gerstner, W. Signal buffering in random networks of spiking neurons: Microscopic versus macroscopic phenomena. Physical Review E 72, 15 (2005).
7. Körding, K. P. & Wolpert, D. M. Bayesian integration in sensorimotor learning. Nature 427, 2447 (2004).
8. Churchland, M. M. et al. Neural population dynamics during reaching. Nature 487, 516 (2012).
9. Maass, W., Joshi, P. & Sontag, E. D. Computational aspects of feedback in neural circuits. PLoS Comput. Biol. 3, e165 (2007).
10. Pascanu, R. & Jäger, H. A Neurodynamical Model for Working Memory. Neural Networks 1, 123 (2010).
11. Forde, J. E. Delay Differential Equation Models in Mathematical Biology. PhD Thesis
12. Natschläger, T., Markram, H. & Maass, W. Computer Models and Analysis Tools for Neural Microcircuits. Neuro- science databases. A practical guide 121136 (2003).
13. Mackey, M. C. & Glass, L. Oscillation and Chaos in Phisiological Control Systems. Science (1977).
14. Appeltant, L. et al. Information processing using a single dynamical node as complex system. Nature Communications 2, 468 (2011).
15. Ganguli S, Huh D, Sompolinsky H. Memory traces in dynamical systems. PNAS. 2008;105:1897018975.

3.4 Complementary simulations to Paper II: Extending the memory trace in spiking neural networks through the synergistic presence of several plasticity mechanisms. Impact of coupling with an external slow delayed dynamical system

If the stimulus information is retained within neural trajectories, how quickly are those traces forgotten? A spiking neural network, with no slow processes associated, (such as synaptic plasticity), has a memory trace of few hundred of ms, depending on the network size and connectivity, the input of the incoming stimuli, and the amount of spontaneous spiking activity present in the system [161]. As discussed in several studies, the length of the memory trace within generic spiking neural networks is determined by the intrinsic time constants of single neurons, and longer memory traces can only arise due to heterogeneities within the neuron time constants, in the network connections, or through the explicit inclusion of slow processes within the neuron or network (e.g. synaptic plasticity, connection delays) [92, 171]. Cortical plasticity, an ubiquitous mechanism within neural systems, operates in a slower timescales than spiking activity itself [197]. As such, the presence of cortical plasticity within generic spiking neural networks has been shown to modulate the memory trace (extended over few hundred of ms), altering the overall network dynamics in a stimulus-specific manner and its ability to process and perform tasks on rich spatio-temporal stimulus [150, 151, 255].

In this study, we aim to extend the memory trace of a generic spiking neural network (SNN) through the coupling of the SNN to an external dynamical system (DDS), comparing them to the dynamical changes that arise due to cortical plasticity. For that, we will first show that cortical plasticity modulates the SNN dynamics by quantifying the fading memory of a SNN with and without plasticity. Second, we will proceed to test whether the ability to store past information of a SNN can be extended coupling a plastic SNN to the slow-external DDS.

Methods

The spiking neural network, synapses and DDS were modelled as described in the previous section.

Modelling Spike-Timing Dependent Plasticity

With spike-timing dependent plasticity, the strength of the connection between two neurons m is modified on the relative timing between the neuron's spike and the pre-synaptic spike time (see section 2.1.2). As such, modulating the synaptic weight, will

lead to the change of the overall synaptic currents, as $I^i_{syn} = \sum_{k=1}^{K} A_k exp(-\Delta_k/\tau_s)$ and $A_k = m \cdot u_k \cdot R_k$ The activity-dependent modification of the synaptic weights m was modulated as follows:

$$\Delta m_{i,j} = \epsilon_i^{pre} \epsilon_j^{post} F(\Delta_t) \tag{3.1}$$

$$F(\Delta_t) = \begin{cases} A_+ exp\left(\frac{\Delta_t}{\tau_+}\right) & \text{for } \Delta_t < 0 \\ -A_- exp\left(\frac{\Delta_t}{\tau_-}\right) & \text{for } \Delta_t \geqslant 0 \end{cases} \tag{3.2}$$

as presented in [91]. The synaptic efficacy changes $\Delta m_{i,j}$ due to the ith pre-synaptic spike ϵ_i^{pre} and the jth post-synaptic spike ϵ_j^{post}. This change is weighted by the function $F(\Delta_t)$, which represents the temporal window for STDP plasticity (see Figure 3.1). Time constants τ determine the decay of LTP τ_+ and LTD τ_-, respectively, while A_- and A_+ scale the weight change. Values of the parameters are $A_+ = 7$, $A_- = 0.003$, $\tau_+ = 17$ ms and, $\tau_- = 34$ ms, as defined in [263]. Note that this specific STDP leads to an asymmetric weight change, resulting in an overall facilitation. Furthermore, note that STDP is only acting on excitatory synapses.

Modelling Homeostatic mechanisms through Intrinsic Plasticity

Homeostatic plasticity describe a set of plasticity mechanisms that bring the overall network activity towards a certain fixed point, avoiding silent or saturated regimes of activity and implementing some kind of metabolic regulation of spiking activity [62]. Homeostatic regulation can be implemented through several plasticity rules that will, at the end, lead to a regulation of the overall firing activity. Here, the homeostatic effect is implemented through intrinsic plasticity that modulate the synaptic weight between neurons [136]. In short, the strength of the connection between two neurons m is modified as a function of the output firing rate of the post-synaptic neuron, to ensure that the post-synaptic firing rate converges to a base level (i.e. does not exceed values which are not biologically plausible). An optimal firing rate $v_{base} = 30$ Hz is set according to experimental studies, which modulates the synaptic weight as:

$$\Delta m \cdot \alpha \cdot \tau_w = v_{pre}(t) \cdot v_{post}(t) \cdot (v_{base} - v_{pre}(t)) \tag{3.3}$$

for $\tau_w = 10$ ms and $\alpha = 0.01$, where α scales the speed of change of the synaptic weight. The pre-synaptic and post-synaptic firing rates $v_{pre}(t)$ and $v_{post}(t)$ are computed as the average number of spike trains within a integration window of 30 ms. With the explicit dependence between pre-post synaptic firing rates, the post-synaptic firing rate $v_{post}(t)$ is shown to converge to v_{base}. Finally, the synaptic weight m modulates the overall amplitude of synaptic currents $I^i_{syn} = \sum_{k=1}^{K} m \cdot u_k \cdot R_k \cdot exp(-\Delta_k/\tau_s)$.

Results

This section is divided into several parts. First, we are interested in showing that cortical plasticity modulates neural processing by quantifying the fading memory of a SNN. Second, we will introduce cortical plasticity to the SNN and test whether the fading memory of an adaptive-SNN can be extended through the interacting with an external DDS.

Stimulus specific dynamics of Spiking Neural Networks are modulated due to the presence of plasticity

To better understand the encoding of time-varying stimulus onto spiking activity of a neural population, we started by analysing the neural response to several stimulus.

To this end, we measured the mean firing rate of both single neuron and neural network when receiving three different stimulus. The average firing rate of 86.17% of the single neurons within the network is significantly different for different stimulus, exhibiting stimulus specificity. The percentage of single neurons that show a significantly different firing rate for different stimulus was computed via z-score (comparing a neuron's firing for stimulus i with the firing rate of the other stimulus j, for $i, j \in [1, 2, 3]$). Examples of such stimulus specificity encoded on the firing rate of single neurons can be visualized in Figure 3.3 B. These results conform to experimental studies showing that neurons respond to stimulus in a specific manner [103, 125, 208, 272].

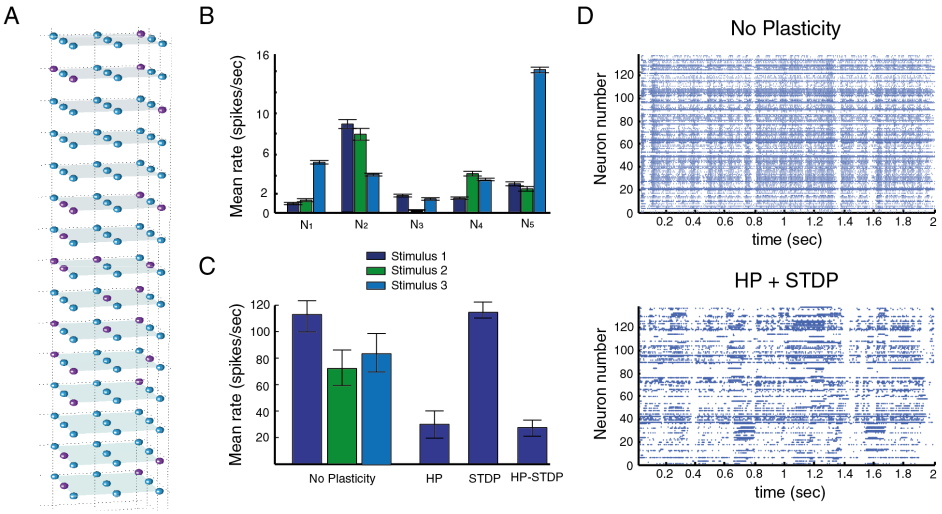

FIGURE 3.3: **The spiking activity in a SNN is stimulus specific**. A) Spiking Neural Network topology, a total of 135 randomly connected neurons, 20% inhibitory (see Method section for details). B) Mean firing rate and standard deviation of 5 network neurons (over 10 simulations, different colors indicate different stimuli) C) Average firing of the SNN for different stimulus (colorcoded) and for networks with different cortical plasticity (HP = homeostatic plasticity, STDP = Spike-Time Dependent Plasticity). D) Raster plot, reflecting the spiking response of the SNN to stimulus 1, both for non-plastic (upper) and plastic SNN

We proceeded by computing the average firing rate of the neural population and found that the average firing rate of the network it is not modulated in a stimulus specific manner, see Figure 3.3 C. Note that in our simulation, the different stimulus are modeled as a set of 8 spike trains whose firing probability is randomly changing between 0.1, 0.2 or 0.4. As such, all the stimulus have the same firing rate but a different spatio-temporal structure and the resulting network dynamics result from the interaction of the stimulus with the intrinsic dynamics of the network. For the sake of completeness, the spiking response of the spiking neural network in response to stimulus 1 is presented in Figure 3.3 C. These results suggest that time-varying stimulus are encoded into the network dynamics, as previously observed in experimental studies [28, 38, 71, 94, 172, 187].

Single and multicellular recordings have shown that neurons and networks of neurons encode stimulus as a pattern of activity that changes in time [28, 172, 187]. This dynamic activation can be visualized by computing the principal components of the network activity (PCA), which allows for the reduction of the dimensionality of the neural system to two/three dimensions. The stimulus specific neural trajectory are presented in Figure 3.4 A, for a spiking neural network that is processing Stimulus 1 (color indicate time, in steps of 200 ms).

Next, we performed the same analysis with plastic SNN that had either homeostatic plasticity (HP), spike-timing dependent plasticity (STDP) or both plasticity mechanisms active while processing different stimuli. As in non-plastic SNN, neurons present a stimulus-specific firing rate which is significantly different across stimulus and compared to the non-plastic SNN (z-score, $p<0.01$). As such, the average firing rate of the plastic SNN is modulated by the stimulus, and it is significantly different from the non-plastic network. Specifically, networks which are regulated by HP show a down-regulation of the firing rate towards the target firing rate (see section 3.4), keeping the network with spiking activity within biological constraints. As such, these observations indicate that cortical plasticity modulates the neural processing through the modification of the connectivity between neurons and the corresponding mapping between stimulus to network activity.

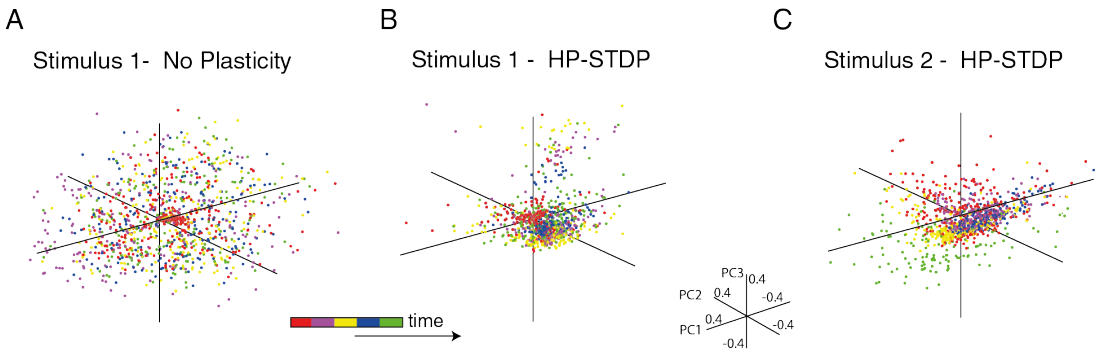

FIGURE 3.4: **Time-dependent stimulus encoding in SNN and a plastic SNN**. SNN encode stimulus as a pattern of activity that changes in time and is modulated by cortical plasticity. Spatio-temporal trajectories of a on non-plastic (A) and plastic SNN (B) that were processing Stimulus 1. C) Spatio-temporal trajectories of a plastic SNN that processes Stimulus 2. Time is visualized as a color (HP = homeostatic plasticity, STDP = Spike-Timing Dependent Plasticity). change.

We proceed by exploring whether the the time-dependent representation of a stimulus is modulated by the cortical plasticity through the visualization of its principal components, see Figure 3.4. Similar to non-plastic networks, plastic networks create a stimulus-dependent trajectory (Figure 3.4 B and C), creating a neural representation for different stimulus.

Through the comparison of the neural trajectories of a non-plastic with a plastic SNN (Figure 3.4 panels A and B), our results seem to suggest that the variability of the stimulus-specific neural trajectories seems to decrease in presence of both plasticity mechanisms. The clustering of neural trajectories within nearby spatio-temporal regions, may facilitate the decoding of the stimulus by an external decoder.

Computational Task and Memory Trace of plastic and non-plastic Spiking Neural Networks

Our spiking neural network correctly performs the computational task in hand: addition of two sets of spike trains. The stimulus spike trains were generated by the spiking probabilities visualized in Figure 3.5 A, and the computational performance of the network can be visualized in Figure 3.5 B, at time lag zero.

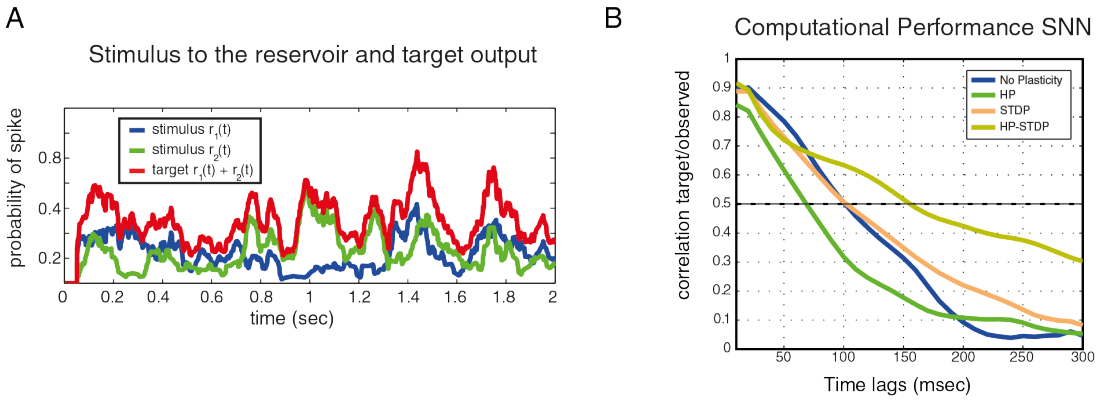

FIGURE 3.5: **Computational Performance and Memory Trace of a SNN and plastic SNN**. All SNN can successfully solve the computational task in hand with a performance (correlation coefficient between target and estimated decoding output) above 85%. The Memory Trace measures the fading memory of the SNN and is corresponds to the time point at which the computational performance decays below change level (correlation of 0.5).

Following that, we characterized the fading memory of the generic SNN (non-plastic and plastic) by means of the memory trace. Our results replicate previous studies that propose that the combination of homeostatic plasticity and spike-timing dependent plasticity yields to the extension of a SNN memory performance [150]. The memory trace in a network operating with STDP is very poor, while a non-plastic and a HP network have a comparable memory trace of about 110 ms, consistent with results presented in [161]. Interestingly, a spiking neural network that operates with both HP-STDP shows an increased memory trace of about 152 ms.

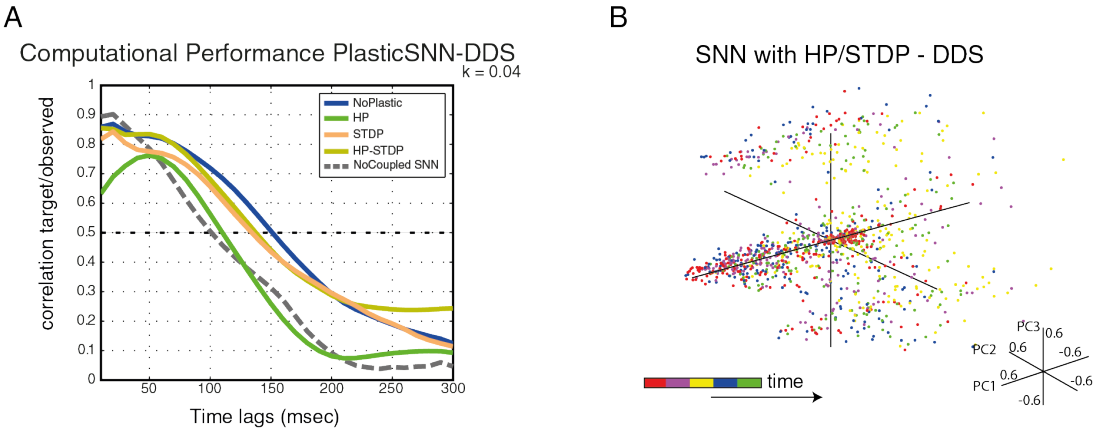

FIGURE 3.6: **Computational Performance and Memory Trace of SSN coupled to DDS (k=0.04)**. All SNN can successfully solve the computational task in hand with a performance (correlation coefficient between target and estimated decoding output) above 85%. The Memory Trace measures the fading memory of the SNN and is corresponds to the time point at which the computational performance decays below change level (correlation of 0.5).

Memory trace of self-organizing spiking neural networks coupled to delayed dynamical systems

So far, we have seen that fading memory of a generic spiking neural network can be modulated through the presence of cortical plasticity and through the interaction with an external delayed dynamical system. This last section aims to characterize whether the memory trace of a plastic SNN can be modulated through the interaction with the external DDS. For that, we couple a plastic SNN with a DDS at $k = 0.04$, which we found to be the encoding scheme yielding to an increased memory trace for non-plastic SNN (25 ms of stimulus $r_i(t)$ is mapped to the $M = 200$ virtual nodes contained in a delayed loop $\tau = 80$). Figure 3.6A shows both the Computational Performance and Memory Trace of SSN coupled to DDS.

The computational performance of the plastic SNN-DDS at zero time lag does not change in comparison to the non-plastic SNN-DDS, except for the plastic SNN that undergoes homeostatic plasticity. On a similar fashion, the memory trace of the plastic SNN-DDS is comparable to the memory trace of the non-plastic SNN-DDS of about 160 ms. In order to further understand the lack of improvement, we visualized the trajectory of the spiking activity of the plastic SNN-DDS (both HP and STDP), which seem to increase separability as in comparison to the plastic SNN (see 3.4 B). These results suggest that the coupling of a plastic SNN to an external DDS do result in a modulation of the time-dependent trajectory of the spiking neural network, though this modification does not directly modulates the memory trace.

Next, we proceed by visualizing the dynamic activation of the system by plotting the first three principal components of the network activity (PCA), see Figure 3.6B. Similar to non-coupled plastic-SNN, plastic-SNN coupled to DDS networks create a stimulus-dependent trajectory. Through the comparison of the neural trajectories of a non-coupled plastic-SNN with a coupled-DDS plastic-SNN (Figure 3.4 panels A and

Figure 3.6B), our results seem to suggest that, through the interaction with the DDS, the stimulus-specific neural trajectories seem to distribute in space.

Discussion

Modeling spiking neural networks (SNN) that process time-varying stimulus is far from trivial, as a SNN that presents time-varying activity will very fast forget past information. The availability of stimulus within short-term memory is crucial for solving tasks that require past stimulus information, such as sequence learning [57], motor preparation [55, 145] or working memory tasks [72].

The goal of the study was three fold. First, we aimed to characterize the dynamics of a SNN that is processing time-varying stimulus and estimate whether and how these dynamics adapt to the stimulus properties through cortical plasticity. Second, we quantified the short-term memory of a SNN by means of the memory trace and estimated whether the memory trace is modulated by cortical plasticity. Third and finally, we aimed to extend the memory trace of a SNN though the interaction of a SNN with an external delayed dynamical system (DDS).

Temporal structure of stimulus modulates neural processing within plastic and non-plastic spiking neural networks

Experimental studies show that a neural population can encode stimulus as a stimulus-specific time-varying spiking pattern [28, 172, 187]. Our simulation captures these properties and provides evidence that a generic recurrent network of spiking neurons can generate time-dependent representation of stimulus, and that such representation is modulated by cortical plasticity mechanisms. The results obtained in this study explores a little further the mechanisms by which cortical plasticity modulates neural processing and proposes that both activity-dependent and homeostatic plasticity are necessary mechanisms to learn task-specific structures (STDP) and keeping high sensitivity to new incoming stimuli (HP). Note that all the stimulus-specific network dynamics arise spontaneously, as there is no constraints or tagging on how the stimulus identity should be represented.

In order to further understand how stimulus are processed in adaptive spiking neural networks, we characterized neural processing by means of the computational performance and the memory trace. The computational performance tests whether the dynamical system can solve a computational task (addition of two time-varying stimulus) while the memory trace characterizes the fading memory of the system. The fading memory of the system describes the ability of a neural network to retain information about past events, a crucial property of SNN that limits which tasks can be actually solved by a SNN (e.g. working memory, motor control)[57, 72, 161]. Our results show that the computational performance on solving the sum of rates task is barely modulated by addition of cortical plasticity on a generic spiking neural network that is solving the 'sum of rates' task. This may be due to the simplicity of the task:

the computational performance of a generic spiking neural network is ceil to the maximum performance. On the other hand, the fading memory of the SNN is extended in presence of both HP and STDP (from 110 ms to 160ms). This result support previous studies that propose a non-trivial interaction between HP and STDP leading to an increased performance of a SNN to detect temporal structures of the stimulus [150].

Coupling of a plastic and non-plastic spiking neural networks to a slow-delayed dynamical system

Finally, the change in the spiking dynamics within the plastic-SNN-DDS suggest that there is a non trivial interaction between cortical plasticity and the DDS system, though this interaction did not led to increased fading memory.

Limitations and generalizability

This study serves as a proof of principle where the neural processing within a spiking neural network interacts with an external dynamical system. However, this study is limited to the analysis of a single interaction or coupling scheme. Further studies could be done to explore different coupling schemes, as the interaction between the system would also modulate the information being exchanged. Most importantly, it would be interesting to proceed by establishing a biological basis for the concept of an external-slow delayed dynamical system.

From a more machine-learning perspective, it may be interesting to relate this study to the reservoir computing framework, whose link to neural computation is established through the Liquid State Machine framework [162]. Within the reservoir computing community, the connections between the elements of the reservoir are static and randomly drawn. The parameters of that networks are then carefully tuned so that the networks are optimized for solving tasks [162, 219]. This optimization of the network properties for a task seems to be crucial as the reservoir connectivity greatly influences its computational performance. For example, studies on SNN have shown that increasing sparsity on the network connectivity increases the computational performance of the SNN on solving a couple of benchmark tasks [20]. As such, the question on how to optimize reservoirs to solve specific problems or classes of problems is largely unanswered within the reservoir community [25, 217]. In the framework of our generic spiking neural network, we have seen that cortical plasticity mechanisms modulate the spatio-temporal representation of the stimulus, changing in turn the computational properties of the SNN, supporting the idea that cortical plasticity may be plausible learning rules to adapt the reservoir in a task specific manner [25, 150, 151]. Furthermore, we have shown that those computational properties are also modulated through the coupling of the SNN to an external reservoir, the DDS, with relatively different processing dynamics. As such, our study predicts an increased computational performance where reservoirs with different processing dynamics interact in a symbiotic manner. It would be interesting to further generalize our findings with an study of the computational properties of a reservoir where the dynamics of each of the elements can be modulated to span over a wide temporal range.

Conclusions

The presented spiking neural network model has been able to reproduce several essential properties that have been observed in experiments. First, that network activity is stimulus specific and that stimulus is encoded as a temporally-varying pattern of activity [38, 71, 94]. Second, that the observed stimulus-specific neural trajectory is modulated by the presence of cortical plasticity mechanisms [14, 151, 255]. In particular, by characterizing the fading memory of the system and its changes due to the presence of plasticity, our study highlights the relevance on considering adaptation and plasticity of the neural system when analysing stimulus-specific neural responses, as we have shown that a stimulus with a certain and persistent dynamics alter the connectivity between neurons, modulating the neural processing and the computational capabilities of that neural circuit.

Furthermore, our results suggest that the neural representation of time-varying stimulus within a spiking neural network, as well as its memory trace, can be modulated through the interaction with of the spiking neural network with an external delayed-dynamical system (DDS). To this end, this study acts as a proof of principle showing that the computational properties of a generic spiking neural network may be modulated through the interaction with an external dynamical system. As neurons are surrounded by an extracellular medium, this raises the question of whether the electric field fluctuations observed in the neural systems are merely an epiphenomena or whether they also have a functional role by modulating the spiking activity of neurons and networks of neurons.

4

Macroscopic scale: Cortical areas

The purpose of this dissertation is to study how time-varying signals modulate the neural responses at different spatial scales: at the single neuron or microscopic scale, within networks of neurons or mesoscopic scale and within cortical areas or macroscopic scale.

This chapter presents the third study that aims to analyse the impact of the variable stimulus statistics within cortical areas and intra-cortical communication, the mesoscopic scale. The chapter is divided in four sections, and starts with a short summary of the corresponding study with the aim to provide a broad idea of the research questions and hypothesis. Following, the section 'fundamentals' aims to present the background concepts used on the corresponding studies. Next, each chapter contains a 'context' section that revisits how the neural system represents and processes stimuli at that specific spatial scale, with special emphasis on how those neural representation are modulated by the temporal structure of the stimulus. The third section, contains the introduction, methods, results and discussion of the study as published in *Frontiers in Integrative Neurosciences*, see **Castellano**, M., Plöchl, M., Vicente, R., and Pipa, G. (2014). Neuronal oscillations form parietal/frontal networks during contour integration. *Front. Integr. Neurosci.* 8, 1–13. Following, the 4th section contains introduction, results and discussion of the study as presented as a poster in *Osnabrück Computational Cognition Alliance Meeting - OCCAM* on *"Mechanisms for Probabilistic Inference"* (May 7-9, 2014, Osnabrück, Germany). Finally, the section 5 concludes the study and contextualizes the obtained results with the general goal of the dissertation.

Short summary of the study

The processing of visual information involves activation of both visual cortices and higher cortical areas (i.e. temporal and frontal cortices) whose implication depend on the cognitive requirements of the task in hand [106, 109, 126, 137, 163]. While widespread advances have been done on the understanding of the local mechanism by

which cortical areas respond to visual stimulation [68, 244, 245], it remains difficult to characterize how the cortical areas and its communication patterns lead to the integration of visual features into a coherent percept. Part of the difficulty is that both cortical activity and long-range communication patterns are not only shaped by the cognitive task in hand [41, 198, 227, 246], but they have been reported to change as the spatio-temporal structure within the stimulus changes. While such effects have been studied within the framework of contextual effects [222], hysteresis [73], after-effects [252] or sequentail learning [57], the exact mechanisms by which cortical areas respond and processes rich spatio-temporal signals is still under debate [34, 98, 108, 129, 130, 265]. Through this study, we will characterize whether and how cortical activity changes as the spatio-temporal structure of the stimulus changes, and we will further argue that a crucial step on understanding neural responses to visual stimulus relies on the understanding on how dynamic stimulus are processed.

In particular, we studied the processing of visual information through a contour categorization task, where local visual features are integrated into a coherent visual percept and further categorized. Through the analysis of recorded human-EEG performing this this perceptual grouping task, we aimed to test three different hypothesis: first, we tested whether the temporal structure within stimulus modulates cortical responses, hypothesizing that cortical responses to a stimulus are modulated by the temporal structure of the stimulus itself. Second, we tested whether oscillatory activity within visual cortex predicts the integration of visual features and its further categorization, hypothesizing that perceptual grouping entails an enhancement of oscillatory activity within distributed cortical areas, not constrained to early visual cortex. Third, we tested whether and how this categorization process modulate long-range synchronization, hypothesizing that perceptual integration may be associated to long- range synchronization in the high frequency range. To this end, the task was specifically designed to control the temporal structure within contour formation, which allowed, for the first time, for the disentanglement between visual stimulation onset and perceptual integration onset.

Taken together, our results indicate that light changes in the sequence of events within a visual stimulus would modulate cortical activity associated to visual stimulus within parietal/frontal cortex, empathizing the relevance of stimulus dynamics on sensory processing. Additionally, our results suggest while oscillatory activity within occipital cortex predicts the linking of visual features into a coherent contour, the further manipulation and categorization of the visual stimulus involves both local synchronization within parietal/frontal cortices, as well as a transient synchronization among them. In particular, cortical areas within parietal/frontal cortices that were recruited for the categorization task synchronize within theta (4-8 Hz), alpha (8-13), and gamma (>30 Hz) frequencies, while long-range synchronization at beta frequency (13-30 Hz) arises between those parietal and frontal cortical areas that are not especially recruited to execute the task. Altogether, our study empathizes the relevance of a transient synchronization across distal cortical areas as a form of dynamic control of information flow through distal sources, in a frequency specific manner.

References

Parts of this study were presented in the following events: *Osnabrück Computational Cognition Alliance Meeting - OCCAM* on *"Mechanisms for Probabilistic Inference"* (May 7-9, 2014, Osnabrück, Germany)

This study has been submitted for journal publication and it is currently under peer-review. For the time being, it is referenced by:

Castellano, M., Plöchl, M., Vicente, R., and Pipa, G. (2014). Neuronal oscillations form parietal/frontal networks during contour integration. Front. Integr. Neurosci. 8, 1–13.

4.1 Fundamentals of cortical processing

This section is organized to present a short introduction on the recording of macroscopic neural activity that reflect activations within cortical areas, followed by a review of the related literature regarding visual stimulus processing.

4.1.1 From neural networks to macroscopic neural activity

Neural activity from large neuron ensembles (within the scale of $> 10^6$ neurons) can be recorded by a variety of methods, such as optical imaging, near-infrared spectroscopy (NIRS), functional magnetic resonance (fMRI), or electro/magneto-encephalogram (EEG/MEG), among other methods [137, 190, 214]. As the main study on this chapter records macroscopic activity through electroencephalography or EEG, this section starts by revisiting the general characteristics of this method, and finishes by reviewing the physiological correlates of the electric field oscillations.

The EEG records electrical activity or electric field produced by a large population of neurons from a set of electrodes located at the scalp. For the sake of completeness, if the electric field is recorded by subdural grid electrodes is known as electrocorticogram (ECoG), and local field potential (LFP) when recorded by electrodes located within the neural tissue, while the magnetic field that arises from the electric field can be recorded by the magnetoencephalogram (MEG). When recorded by the EEG, the electric field potential has an amplitude on the range of 100 μV and reflects the co-activation of $10^6 - 10^8$ neurons within cortical layers (corresponding to 1 cm^3 of cortical volume) [45].

What is exactly the electric field of a neural tissue? The electric field recorded by EEG at the scalp level is thought to be result from the superposition of all active cellular process which generate electrical currents when trespassing the cell membrane: currents from the same polarity that are co-aligned to the recording electrode would add up and result in a electric field modulation, while adding currents from randomly

oriented sources or current fluctuations that are not synchronized, would cancel out and lead to a small fluctuation of the resulting field (Figure 4.1 A).

The electric field potentials are often studied and classified according to the frequency range at which the signals oscillate, namely, based on its rhythmic or repetitive dynamics for an observed period of time. Oscillations within neural signals are classified over a wide range of frequencies, including delta (δ: 0.5-4 Hz), theta (θ: 4-8 Hz), alpha (α: 8-13 Hz), beta (β: 13-30 Hz) and gamma (γ: 30-100 Hz), see Figure 4.1 B, and they are thought to reflect various aspects of cortical processing: slow oscillations with strong delta component are present during sleep and are thought to be crucial for memory formation [173], theta-band oscillations phase-encode spatial information in rat hippocampus [42, 170] and awake states are dominated by beta and gamma oscillatory activity, which have been correlated with perceptual binding, attention and multi-sensory integration [88, 230, 268].

Of particular interest for the following study, are the neural oscillations in the γ range. Oscillatory activity within this range was first reported in the LFP recordings of the auditory system of anaesthetized cats, rabbits and rats, as a response to auditory stimulation [3], leading to the proposal that γ oscillatory activity encodes information within the auditory system [85]. From then, sustained γ oscillatory activity, or γ synchronization, has been reported in numerous experiments in animals and humans in both invasive and non-invasive recordings of neural activity, and it is associated to several cognitive processes, including perceptual grouping [107, 246], attentional selection [227], perception of mutistable stimulus [123, 152], working memory maintenance [198, 247] and sensory-motor integration [261].

Although sustained γ oscillations are observed in neural systems in association to cognitive functions, its exact functional relevance is still under strong debate [175, 287, 288], reflecting a lack of understanding on the physiological mechanisms that generate such oscillations. Part of the difficulty on understanding the physiological mechanisms that lead to oscillatory activity at the macroscopic level is that the physiological mechanisms and its observed phenomena can only be studied within very different spatial scales (i.e. spiking neurons, cortical oscillations and behaviour). The few evidences and hypothesis that link spiking activity to global oscillations within the resulting electric fields are discussed below, with special emphasis on the generation of γ oscillations.

What are the mechanisms that lead to the generation of oscillatory activity within electric fields? Oscillatory activity in electric fields is ought to reflect synchronized activity within the underlying neural population [45, 137, 190, 214]. Synchronized activity within a population of neurons can be generated in several ways: through common drive, where distributed neurons synchronize as a consequence of being driven by same input (remote pacemakers); through direct coupling between individual neurons, where a set of neurons drive the population to oscillate; or through coupling of neural populations where synchronization emerge from the population dynamics and no single neuron acts as a pacemaker [44, 276].

In particular to oscillatory activity in the γ frequency, the current view in neuroscience is that γ oscillations emerge through the interaction of inhibitory and excitatory neurons, discarding the idea that an external pacemaker or common drive is necessary for

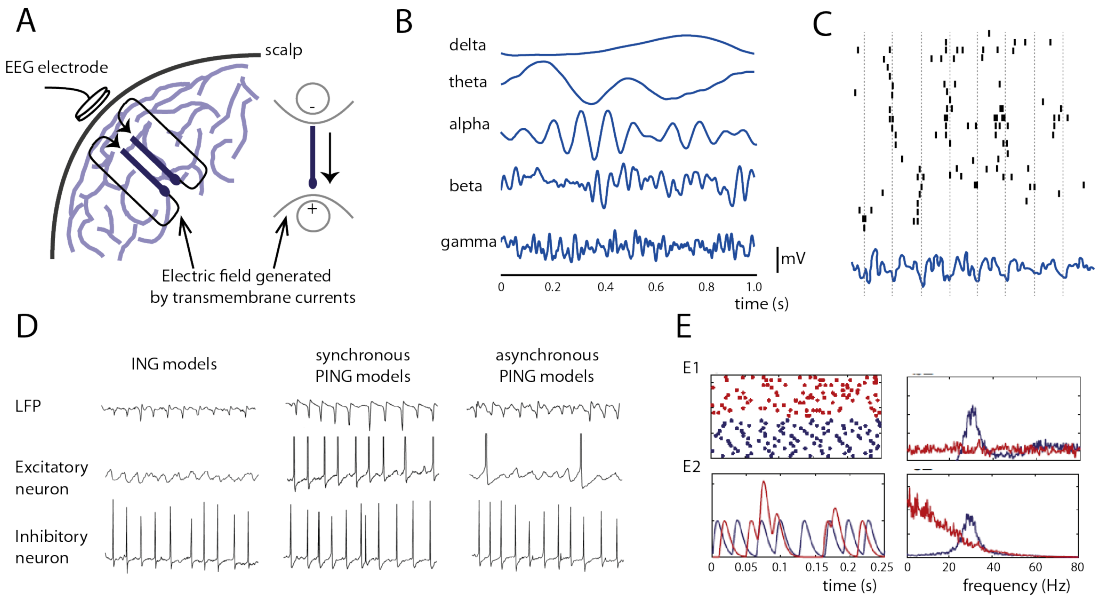

FIGURE 4.1: **Macroscopic neural signals recorded by EEG**. A) The electric field recorded at the scalp results from the superimposed electrical currents arising from co-aligned neurons that are active in a coherent manner B) Electric field fluctuations classified according to its oscillatory frequency C) Gamma oscillatory activity may arise through the coincident firing of action potentials with millisecond precision. Adapted from [45] D) Example of LFP and neural responses during ING/PING models of oscillatory activity, adapted from [281]. E) Asynchronous PING model, where the frequency of oscillation is determined by the synaptic dynamics and the firing frequency: E1 (left) shows the spike trains of inhibitory (red) and excitatory (blue) neurons with an average firing rate of 30 Hz, as reflected by the power-spectrum (log scale, right). E2 shows the synaptic currents derived from the spike trains (left), whose power-spectrum peaks at the average firing rate of the spike trains (log-scale, right), while the power of higher frequencies is not modulated by the temporal structure. Adapted from [260]

the generation of oscillations [47, 87]. In other words, γ oscillations in the macroscopic electric field directly reflect cell assemblies that dynamically organize in γ cycles (Figure 4.1 C), as observed by electrophysiological recordings within the cortex [107, 198, 260], hippocampal areas [42, 170], auditory cortices [3, 85], olfactory bulb and thalamus, as well as other areas (see [47, 87, 256] for review). Common to all these brain regions is the presence of both inhibitory interneurons (basket cells or GABAergic interneurons) and pyramidal cells (glutamate-based excitatory neurons), while connectivity between this neurons remains highly variable [47]. As spiking activity of cortical neurons are usually reported to be very irregular and close to an asynchronous process (see chapter 2), the question can be reduced to what are the mechanisms that bring spiking activity of a neural population to cluster in time. Computational models that aim to study how synchrony can emerge in recurrent networks groups in two main classes, depending on whether synchronization emerges due to mutual inhibition (ING) or mutual excitation (PING), see Figure 4.1 D.

Interneuronal Gamma (ING) models specifically describe oscillatory activity that arises through synaptically coupled basket cells [17, 18, 256, 264, 269, 281]. Through mutual inhibition, basket cells fire periodically in response to tonic excitatory drive, while

stochastic drive leads to equally periodic firing as long as the connection between neurons is strong enough [47]. Given this constraints, the frequency of the resulting field oscillation is determined by the parameters that determine the length of the inhibitory volley where no excitation occurs: the decay time of the IPSPs, the strength of the recurrence between interneurons, and the strength of the drive [33, 254, 256, 264]. Given the decay time of a generic chemical synapses, oscillation frequency generated on a population of inhibitory and excitatory neurons through mutual inhibition is limited to 80 Hz [54], contrasting the high frequency oscillatory activity observed in electric fields. However, in considering the fast synaptic interactions that have been observed between basket cells (which are fast spiking neurons), oscillatory frequencies on networks of isolated interneurons can go up to 110 Hz [17]. Furthermore, oscillatory frequencies up to 200 Hz can be observed in models where gap junctions between inhibitory interneurons are considered (gap junctions allow for direct electrical communication between cells, leading to nearly instantaneous coupling) [18]. Concurrently, pharmacological blockade of gap junctions and GABA receptors abolishes γ oscillations [257, 269], suggesting that activation of basket cell population is a necessary condition for the generation of gamma oscillatory activity. In summary, activation of inhibitory interneurons is crucial for the generation of gamma oscillatory activity, which can arise based on mutual inhibition between basket cells. However, oscillatory activity arising due to mutual inhibition is highly sensitive to the strength and the dynamics of excitatory drive, not completely consistent with the spiking activity in experimental studies [17]. As such, ING models alone are unlikely to reflect physiological mechanisms generating oscillatory activity, as mutual inhibition can only be relevant when interacting with the firing patterns of the excitatory neurons.

Pyramidal Interneuron Gamma (PING) models specifically describe oscillatory activity arising through mutual excitation between pyramidal neurons (excitatory) that modulate basket cells activity (inhibitory) [281]. Synchrony in these networks may arise due to two dynamic modes: single neurons firing periodically or asynchronously. On the first case, neurons can behave as oscillators that fire at the oscillatory frequency that is observed in the resulting electric field. Such models predict the emergence of a several ms delay between pyramidal and basket cells activity, consistent with several *in vivo* recordings [285]. Within this model, the frequency of the resulting oscillation is determined by the synaptic delays between excitatory and inhibitory populations [31, 47], which can sustain oscillations up to 100 Hz. In further support of this model, pharmacological blockade of AMPA receptors results in the reduction of the amplitude of gamma oscillation [47]. Note that this kind of synchronization has been extensively studied by models of coupled oscillators (see [10, 67, 242] for further information). On the second case, oscillatory activity may arise through asynchronous spiking activity: oscillations in gamma have been observed in LFP, together with a excitatory neurons that fire between 5 and 20% of the oscillation period [31, 281]. As such, oscillatory activity in electric field do not arise due to synchronized spiking activity, but from the superposition of the synaptic currents of the local population. Computational models suggest that the frequency of the resulting oscillatory activity as such is determined by the synaptic dynamics of excitatory neurons, and can reach up to 200 Hz [31]. Finally, note that this observations can be generalized as follows (as suggested in [200, 260]): small deviations from asynchronous activity introduces an oscillation in the population activity, and the strength or power that oscillation scales with the firing frequency of

the spiking process (the more firing, the stronger the oscillation); while the oscillations in the population activity at higher frequencies than the neuron's firing rate may be present, they do not reflect the temporal structure of the underlying spiking activity, see Figure 4.1 E. Altogether, these studies propose several mechanisms by which oscillatory activity in the γ frequency arise through the precise interplay between excitation and inhibition within recurrent networks. Note, however, that oscillatory activity in γ frequency may as well arise from other physiological mechanisms, as suggested elsewhere [260].

4.1.2 Anatomical and functional basis of visual processing

At a general level, the processing of visual stimulus entails the participation of multiple and widespread brain areas, from the primary visual cortex via spatially segregated processing streams, to higher cortical areas where information is thought to be associated with higher cognitive functions [106, 109, 126, 137, 163]. In essence, the classical description of visual processing states that those different regions of the visual cortex involved in visual processing are thought to be specialized to carry out different functions and to communicate information in a hierarchical fashion [105, 137]. In this section, we aim to raise awareness about the functional specialization of the visual system, as well as its hierarchical organization, presenting experimental evidences that both support and oppose this view.

Within the hierarchical framework, the neural system consist of several discrete functional systems that directly discriminate the different sensory modalities (touch, vision, etc...), and each of this divisions can be equally divided into smaller modules that perform particular functions within the sensory processing itself. One of the most striking examples of this framework are the studies within peripheral areas or early sensory areas, where stimulus is represented topologically: neighbouring cells in the retina project to neighbouring cells in the V1, and successively [125]. Through years of research, there has been established over 30 brain regions that selectively respond to specific features of the visual stimulus, forming a complex hierarchy of visual processing areas, the cortical visual pathways (Figure 4.2 A). Each of the layers within the system processes different information from the stimulus and, through the convergence of this distributed process, the sensory information becomes available as a percept [106, 137]. Different cortical areas in the pathway are selective for different features of the stimulus (shape, color, texture, etc...), and within higher levels, cortical areas respond to higher order properties of the stimulus (e.g.object identity in IT). Remarkably, this functional organization of visual early cortex was reported under natural stimuli viewing: changes in color, presence of faces, bodies or languages induced an activation of particular regions of early visual cortices [15].

How strict is this hierarchical distribution of information during the processing visual stimulus? On the one hand, it has been suggested that the latency of response onset varies across brain areas within the visual system, and is not congruent with the position of that area within the hierarchy [218]. On the other hand, a detailed

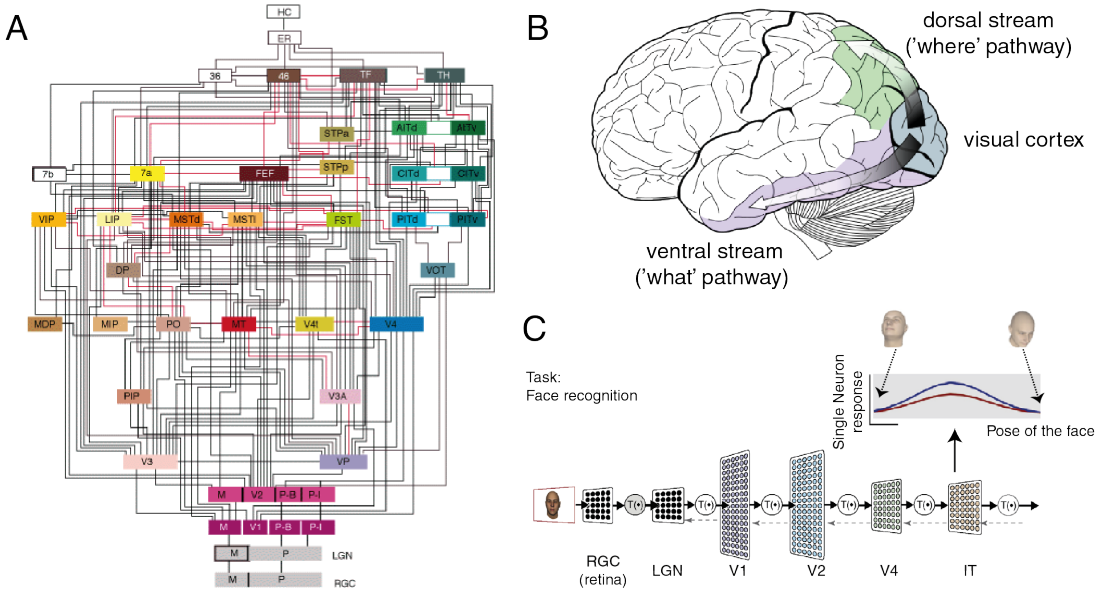

FIGURE 4.2: **Hierarchical organization of the visual cortex**. A) Detailed functional architecture of the visual cortex, adapted from [80] B) The two stream hypothesis, or the what and where pathways, which propose an organization of the visual cortex in two processing streams originating in the occipital cortex. The dorsal pathway (towards the parietal cortex) is specialized in object recognition, while the ventral pathway (towards the temporal cortex) strongly responds to object spatial location. Adapted from [283] C) The strong hierarchical framework lead to several object-recognition models, where each of the layers within the system processes different information from the stimulus and, through the convergence of this distributed process, the sensory information becomes available as a percept. Adapted from [68].

analysis on the anatomical connections between and within visual cortex suggest that, due to the variability observed in the experiments, several hierarchies could be deduced from the data [216]. One of the possible resulting hierarchies is a two-pathway hierarchy: the dorsal (what) and ventral (where) pathways, as proposed by Ungerleider and Mishkin proposed in 1982 [179] (Figure 4.2 B). Together with behavioural, lesions and physiological studies, Ungerleider and Mishkin proposed the existence of two processing streams for visual processing [179]: recognition of objects depends on the primary visual cortex and the parietal cortex (dorsal pathway), while localization of objects depends on the primary visual cortex and the medial temporal cortex (ventral pathway). From such studies, several computational models for object recognition appeared, proposing a mainly feed-forward transmission of sensory information, where object recognition arises from self-organized responses within the visual system (Figure 4.2 C).

Although the two-stream hypothesis and the resulting models may be an useful scheme to simplify the processing and stimulus representation within the visual system, several studies challenge such simplification. For instance, while the categorical information is expected to be represented in the ventral pathway, regions in the dorsal stream are indeed involved object categorization tasks [223]. On the same line, recent studies report that complex viewing situations can be decoded from the dynamic activity distributed through the visual cortex [189]. Finally, early visual cortical areas (V1) in

adult rats has been shown to be reward-modulated, challenging the understanding of a strict functional organization of the cortex, and highlight the remarkable plasticity in adult sensory areas [226].

So far, despite the widespread knowledge on the anatomical, physiological and psychological basis of visual processing, there are several questions that remain unanswered: how do visual features of the visual stimulus bound together to form a percept? how can this process lead to an invariant object recognition? how does the brain segregates and perceives 'relevant' information from such complex stimulus? Of particular interest to our study is the question of perceptual binding, or how the neural system integrates information from disperse areas to form a coherent percept. This question will be further presented and discussed in the section 4.4. For further readings on theories of visual processing or its neurobiological basis, see [106, 137, 274].

4.2 Context

The question of how cortical areas encode and transmit information has been a central issue in neuroscience research since the development of techniques that allow for the recording of large neural ensembles in a non-invasive manner [137, 190, 214]. In this section we will review how populations of neurons on the range of $10^6 - 10^8$ neurons, the macroscopic scale, respond to stimulus or cognitive tasks. We will continue by discussing whether and how these signatures are modulated by the spatio-temporal structure of the stimulus, as well as its modulations due to the task requirements. Finally, this section ends by discussing some of the frameworks that aim to explain how the neural system represents and processes time-varying signals.

Activity within cortical layers, as well as the patterns of communication across them, are stimulus-specific as evidenced by a large body of physiological, psychophysical and neuroimaging studies that evidence a functional specialization of cortical areas [89, 109, 137, 178]. Of particular interest to this dissertation are the cortical regions that are involved in the processing of visual stimuli: neuroimaging, lesion, and electrophysiology studies provide evidence that the processing and perception of visual stimulus entails the participation of multiple and widespread brain areas, emphasizing the selective role of visual cortices [125, 179], parietal cortex [246, 273] and frontal cortices [83, 180] on this process. But cortical areas do not only respond to specific sensory stimulus, but lots of efforts have been made to functionally delineate which cortical areas represents and processes cognitive tasks. The first reference of the brain being associated to a behaviour appears in an Egyptian papyrus about 1700 BCE, that describes several clinical cases of cognitive impairments due to a skull/neural tissue damage [109]. Since then, huge efforts have been done in characterizing cortical responses associated to cognitive tasks. For instance, acute stress activates the amygdala [211], while impairment on language comprehension arises as a result of lesions within Wernike's area (while speech remains normal)[137].

Accompanying this body of experiments that report a functional organization of the cortex, it should be noted that cortical responses to specific stimulus or cognitive

tasks are far more complex than expected, as cortical responses, and the patterns of communication across them, have been reported to change as a function of both the spatio-temporal structure of the stimulus and the cognitive requirements associated with the task in hand.

On the first place, cortical responses have been reported to be modulated by shifts in the physical properties of the stimulus (i.e. low level features). For instance, and in particular to the visual system, responses in visual cortices are stronger for salient stimuli, and increase with stimulus size, contrast and spatial integrity of the visual stimuli [40]. This modulation of cortical responses, as well as modulations on the perception of a particular stimulus, have been studied within different fields and can be found under different names: contextual effects [222], hysteresis [73], after-effects [252], and sequential learning or priming [57]. On the second place, cortical responses have been reported to be modulated by the cognitive requirements associated with the task in hand, including attentional selection [41, 176, 227, 262], working memory maintenance [198, 247], the expectation of a reward [226], memory matching of familiar stimuli ([120] or the targeting of the stimulus [163, 267].

Of particular interest of this thesis are the cortical responses to stimulus with rich-spatio temporal structures: as timing and structure in time is an intrinsic property of both the stimulus and the neural system, how does cortical areas represent and process stimulus with rich temporal structure? The processing of temporal information has been largely discussed within the context of psychology [34, 58, 98, 108, 129, 130, 265] and, within this context, the theories that aim to explain the processing of temporal signals can be divided into three classes: dedicated, intrinsic or stationary.

Within the dedicated framework, the processing of time is performed through a specialized mechanisms that explicitly represent time. Accordingly, neuroimaging studies report activation within specific cortical areas in response to temporally structured stimulus. For instance, auditory cortex activates specifically to a pair or sequence of tones [19], superior temporal sulcus activate selectively to particular full-body or hand movements [99], while the fusiform gyrus activate to the presence of facial expressions in complex viewing situations [15]. Within the intrinsic framework, the representation of time is considered an inherent property of the dynamics of the system [100]. As such, a stimulus with rich spatio-temporal properties will be encoded within the neural system as a neural signal with rich spatio-temporal dynamics. Some of the most compelling evidences supporting intrinsic timing comes from the fact that lesion and transcranial magnetic stimulation (TMS) studies have shown that the perception of time-varying signals is modality specific, as TMS silenced V5/MT does not impair the detection of the duration of tone, while impairs the detection of visual motion [58, 129]. Finally, within the stationary framework, time is described as a low-level feature of the stimulus that is ruled out through the processing stages, leading to an invariant representation of stimuli [68]. Experimental studies report this invariant learning on the temporal dimension, such as the activation of the fusiform gyrus to the presence of face expressions in complex viewing situations [15] or place cells in the hippocampus [182]. Along these lines, several studies presented computational mechanisms where the temporal structure within stimulus is explicitly ruled out through processing stages, as

hierarchical models of invariant object recognition [68], hierarchical models of body movement perception [99] or slow feature analysis [284].

Ultimately, the lack of a unifying theory that explains the processing of rich spatio-temporal signals mostly reflects a lack of an understanding on how signals with rich temporal structure are processed. The study within this chapter aims to further understand the visual processing of a stimulus with rich spatio-temporal structure and among other hypothesis, test whether modulations in the temporal structure within the stimulus modulates the neural representation and processing of the stimulus, as predicted by the intrinsic framework of temporal processing.

4.3 Paper III: Neuronal oscillations form parietal/frontal networks during contour integration.

frontiers in
INTEGRATIVE NEUROSCIENCE

ORIGINAL RESEARCH ARTICLE
published: 13 August 2014
doi: 10.3389/fnint.2014.00064

Neuronal oscillations form parietal/frontal networks during contour integration

Marta Castellano[1]*, Michael Plöchl[1], Raul Vicente[2] and Gordon Pipa[1]

[1] *Department of Neuroinformatics, Institute of Cognitive Sciences, University of Osnabrück, Osnabrück, Germany*
[2] *Faculty of Mathematics and Computer Science, Institute of Computer Science, University of Tartu, Tartu, Estonia*

Edited by:
Micah M. Murray, University Hospital Center and University of Lausanne, Switzerland

Reviewed by:
Tatiana Alexandrovna Stroganova, Moscow State University of Psychology and Education, Russia
Gregor Volberg, Universität Regensburg, Germany

***Correspondence:**
Marta Castellano, Department of Neuroinformatics, Institute of Cognitive Sciences, University of Osnabrück, Albrechtstrasse 31, 49076 Osnabrück, Germany
e-mail: m@martacastellano.eu

The ability to integrate visual features into a global coherent percept that can be further categorized and manipulated are fundamental abilities of the neural system. While the processing of visual information involves activation of early visual cortices, the recruitment of parietal and frontal cortices has been shown to be crucial for perceptual processes. Yet is it not clear how both cortical and long-range oscillatory activity leads to the integration of visual features into a coherent percept. Here, we will investigate perceptual grouping through the analysis of a contour categorization task, where the local elements that form contour must be linked into a coherent structure, which is then further processed and manipulated to perform the categorization task. The contour formation in our visual stimulus is a dynamic process where, for the first time, visual perception of contours is disentangled from the onset of visual stimulation or from motor preparation, cognitive processes that until now have been behaviorally attached to perceptual processes. Our main finding is that, while local and long-range synchronization at several frequencies seem to be an ongoing phenomena, categorization of a contour could only be predicted through local oscillatory activity within parietal/frontal sources, which in turn, would synchronize at gamma (>30 Hz) frequency. Simultaneously, fronto-parietal beta (13–30 Hz) phase locking forms a network spanning across neural sources that are not category specific. Both long range networks, i.e., the gamma network that is category specific, and the beta network that is not category specific, are functionally distinct but spatially overlapping. Altogether, we show that a critical mechanism underlying contour categorization involves oscillatory activity within parietal/frontal cortices, as well as its synchronization across distal cortical sites.

Keywords: oscillations, parietal cortex, feature binding, contour integration, visual perception

INTRODUCTION

A fundamental ability of the neural system is to integrate visual features into coherent percepts, whereby the segments belonging to an object boundary are perceptually grouped (Wertheimer, 1923; Field et al., 1993). One particular instance of perceptual grouping, where a coherent percept arises through the integration of a single stimulus feature, is contour integration, where a set of local elements are integrated to a common contour due to its relative orientation (Field et al., 1993). Evidence from psychophysical (Field et al., 1993; Li and Gilbert, 2002; Mathes et al., 2006), physiological (Li et al., 2006), and neuroimaging studies (Altmann et al., 2003; Kourtzi et al., 2003) report enhanced activity within early visual cortex, suggesting that contour integration can be mediated within the primary visual cortex itself, giving form to the saliency hypothesis. A complementary set of studies that argue for this hypothesis is that contour detection performance strongly depends on the spatial organization of the local elements (reviewed in Hess and Field, 1999), up to the extent that behavioral performance is thought to be explained by the anatomy of the visual cortex (Field et al., 1993).

Simultaneously, neuroimaging, lesion, and electrophysiology studies provide evidence that the processing and perception of visual stimulus entails the participation of multiple and widespread brain areas, emphasizing the selective role of early visual cortices (Hubel and Wiesel, 1962; Mishkin et al., 1983), parietal cortex (Tallon-Baudry et al., 1997; Volberg and Greenlee, 2014), and frontal cortices (Foxe and Simpson, 2002; Morgan et al., 2013) on this process. In particular to perceptual grouping, several studies suggest the involvement of higher-order areas the integration process as contour detection and its neural signatures arising in early visual cortex seem to be modulated by the task requirements, including attentional demands (Roelfsema et al., 2004), perceptual learning (Li et al., 2006), or perceptual noise within the contour (Mathes et al., 2006). Altogether, these studies suggest that perceptual grouping, as well as contour integration, seem to involve the processing within non-primary visual cortex.

Of particular interest for the understanding of the neural mechanisms that mediate perceptual grouping is neural oscillatory activity. Local enhancement of oscillatory activity within early visual cortices has been associated with visual processing

and perceptual grouping itself through intracranial recordings (Gray et al., 1989; Fries, 2009; Uhlhaas et al., 2009), and human EEG/MEG studies (Lutzenberger et al., 1995; Tallon-Baudry et al., 1997; Hoogenboom et al., 2006; Donner et al., 2007; Volberg et al., 2013). But it is not only synchronization in local cortical areas that is relevant for perceptual grouping. Recent studies report transient synchronization between parietal and frontal cortices: low frequency oscillations (7–14 Hz) have been proposed to coordinate activity between disperse cortical areas during visual processing (Tallon-Baudry et al., 2001; Sehatpour et al., 2008), while enhanced synchronization within the gamma frequency band (>30 Hz) has been associated with visual integration of segregated features and cross-modal integration across independent processing streams (Palva et al., 2005; Hipp et al., 2011). To this end, neural synchronization has been proposed as the mechanism by which visual information is integrated into a percept, grouping visual features at both localized cortical areas and across distributed cortical areas (Singer, 1999; Varela et al., 2001).

Despite the widespread advances to understand the mechanisms by which the neural system performs perceptual grouping tasks, it is not yet clear how both local and long-range oscillatory activity leads to the integration of visual features into a coherent percept (Engel et al., 2001). Here, we investigate whether oscillatory activity within visual cortex predicts perceptual grouping of a visual stimuli, and whether and how perceptual grouping modulates synchronized activity across distributed neuronal populations. To test this, we recorded EEG from human subjects performing a contour categorization task, where co-aligned local elements (i.e., Gabor elements) must be linked and further classified (see **Figure 1**, Field et al., 1993). Our assumption is that with the use of a contour categorization task, perceptual grouping is be described as a two-stage process, where the local elements that form contour must be linked into a coherent structure, which is then further processed and manipulated to perform the categorization task. Our assumption can be framed in both the incremental grouping theory (Roelfsema, 2006) and perceptual matching theories (Herrmann et al., 2004; Watt et al., 2008), where perceptual grouping is described as a two stage process where the linking of the local elements is followed by a further processing that require high-order cortical areas (see also Mack and Palmeri, 2010; Kourtzi and Connor, 2011). As such, the usage of a categorization task as a framework for the study of perceptual grouping allows for a disentanglement of the linking process of local elements (Contour Linking Process) and the further contour processing for its categorization (Contour Processing), which may involve several secondary processes, such as top-down attentional selection (Mesulam, 1999; Buschman and Miller, 2007; Siegel et al., 2008; Van Ede et al., 2012), memory matching (Herrmann et al., 2004), or the targeting of the contour (VanRullen and Thorpe, 2001). In particular, we expect the involvement of fronto-parietal areas that are proposed to mediate the formation and selection of behaviorally relevant stimulus (Sato and Schall, 2003). Furthermore, in our task, contour formation is a dynamic process where contour is continuously morphing (see Video 1 for a contour trial and 2 for a non-contour trial), so that the appearance of the contour is, for the first time, not associated with a sudden onset of the visual stimuli. This paradigm, in combination with a new analysis approach, allows for the identification of cortical areas that are associated with different behavioral events, such as the processing of visual stimulus,

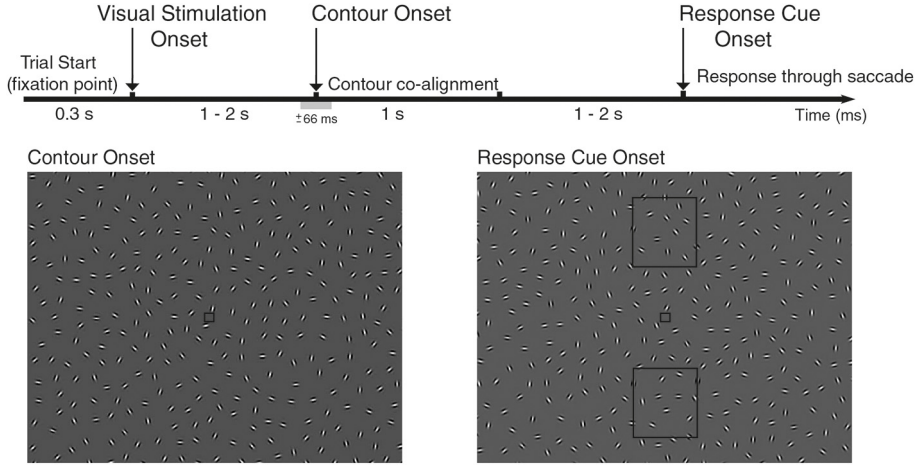

FIGURE 1 | Experimental design of the study. EEG was recorded while subjects performed a contour integration task, where participants were instructed to identify two different orientations of an oval contour. The contour would appear on half the trials (contour vs. non-contour trials), randomly on the left/right hemifield in varying locations in respect to horizontal view, lasting for 1 s. Each trial starts with the appearance of a fixation point, followed with a field of Gabor elements (Visual Stimulation Onset, VS) that were continuously changing its orientation (see Video 1 for contour trials and 2 for non-contour trails). After a delay period, a subset of Gabor elements co-align forming an oval-like contour that pointed up/down (Contour Onset, CO; ±66 ms range of contour visibility). Note that in this diagram, the contour is shadowed to increase visibility. Subjects reported identification of the contour via saccade after the response cue onset, indicated with the appearance of two rectangles (up/down) that mark the target location of the saccade (Response Cue Onset, RC). Subjects were instructed to maintain fixation until the appearance of the report cue onset and forced to perform saccade in non-contour trials. Throughout the study, we analyzed neural activity associated with the different behavioral events: VS-CO-RC and with two behavioral conditions associated with CO event (contour and non-contour trials).

the linking of contour elements, the further contour processing for correct categorization and saccade planning. In the following, we describe the oscillatory mechanisms involved in these processes and their modulations within and across spatially distinct cortical networks.

MATERIALS AND METHODS

PARTICIPANTS AND STIMULI

A total of 15 participants (9 female and 6 male, aged 18–32 years) gave informed written consent to participate in the study, approved by the local ethics committee and conducted in accordance with the Declaration of Helsinki and national guidelines. Participants reported normal or corrected-to-normal vision, with no history of neurological or psychiatric illness. At each trial, participants were presented with a frame of 335 randomly oriented Gabor elements (each spanning 0.5° of visual angle) whose orientation was continuously changing [2° ± 2.6° (mean ± std) per frame], leading to the perception of smoothly rotating Gabor elements. During the trial, Gabor elements would keep rotating and, on half of the trials, the orientation of 22 Gabor elements would co-align to form an oval-like contour that spans 11.3° of the visual field (see Video 1 for contour trials and Video 2 for non-contour trials,.avi and.mpeg format). The modulation of the angle of Gabor elements introduces temporal evolution on the contour formation, so that collinear contours are continuously morphing and perceived as dynamic stimuli with smooth progression between stimulation frames. The contour is an oval-like shape, so that the curvature at both asymmetric ends was rather similar (see **Figure 1**). Contours appeared in 50% of the trials, on either the left or right hemifield (25% of total trials) on five different positions relative to the horizon (see Figure S1). Stimuli were displayed on a DELL UltraSharp LCD monitor, VGA mode, 1024 × 768 pixel resolution, frame rate 60 Hz. The participants viewed the screen binocularly at 60 cm distance in a room with dim light and constant luminance.

BEHAVIORAL TASK

The task of the participants was to identify two different spatial orientations of the same oval-like contour, and report its orientation in a two-alternative forced choice task (2AFC, up/down response, Mathes et al., 2006). Contours appear 50% of the trials, and the narrow side of the oval corresponds to the pointing direction of the contour (oriented either up or down the screen). The identification of the contour's direction was reported through a voluntary saccade toward the pointing direction of the oval after the response cue (see **Figure 1**), and subjects were required to make a random choice of an up or down eye movement in the case where no contour was identified, which include non-contour and false negative trials due to high noise. This last constraint forces the participant to plan and execute an eye movement in every trial, so that trials where contour orientation is reported cannot be distinguished from the other trials based on the resulting eye movement. Each trial starts with the appearance of a fixation dot (spanning 0.3° of visual angle, see **Figure 1**). After a 300 ms, visual stimulation starts with a full-frame field of randomly oriented Gabor elements, and lasts either 1.03, 1.50, or 1.97 s. This is the first behavioral event, namely, the visual stimulation onset or VS event. After this period, a subset of 22 Gabor elements co-align to form the described oval contour, and stay in co-alignment for 1.03 s. Note that while the orientation of Gabor elements changes at the same rate (2° ± 2.6° (mean ± std) per frame), they remain aligned to the underlying contour path, see Video 1 for an example of a contour trial. This is the second behavioral event considered for analysis: the contour onset (CO) event. As contours appear on 50% of the trials, the CO event has two behavioral conditions associated: contour vs. non-contour trials. After a random period (either 1.03, 1.50, or 1.97 s), the response cue appears (two rectangular shapes up/down the fixation point, see **Figure 1**), marking the moment when participants are required to report the categorization of the contour by performing a saccade toward the response rectangles, located either up/down of the fixation point (RC event). Each participant was required to respond to a total of exactly 720 valid trials, during which EEG and eye movements were recorded. Each trial starts with the appearance of a fixation point, where participants were instructed to fixate on during the total length of the trial. Loss of fixation lead to a premature end of the trial, where loss of fixation is defined as saccades with an amplitude larger than 1.25°. Analyses were performed in Matlab (MathWorks, Natick, MA) with custom code and several open-source toolboxes: field trip (Oostenveld et al., 2011) and EEGLab (Delorme and Makeig, 2004).

CONTOUR VISIBILITY AS A FUNCTION OF GABOR ORIENTATION NOISE

Given that the contour within contour trials arises through continuously morphing Gabor elements, the time at which the contour is identified at each trial may vary. We account for this variability around the CO event in two ways. First, we define that the CO time $t = 0$ marks the time point at which the contour can be identified with a probability of 0.7, on average over subjects. Second, we define a range of contour visibility, which delineates the time interval within the trial at which the contour will be identified with a probability above chance. For that, we estimated a psychometric curve that defined the subject's performance in the contour categorization task for the different degrees of co-alignment of the Gabor elements. This experiment was conducted with a different set of 7 male participants, aged 24–29 who gave informed consent to participate in the study, approved by the local ethics committee and conducted in accordance with the Declaration of Helsinki and national guidelines (see Supplementary Materials for details). In short, the psychometric function associates the degree of co-alignment Φ with a identification probability so that, to obtain the probability of a contour being identified at time t, with a known degree of co-alignment Φ, we inverse the psychometric function: on average for all participants, with an alignment of $\Phi = 50°$, the contours are identified by chance, which corresponds to 66 ms before the CO event.

DATA RECORDING, PREPROCESSING AND NEURAL SOURCE RECONSTRUCTION

Synchronization of stimulus presentation, eye-tracking, and EEG recordings was controlled via ViSaGe software (Cambridge Research Systems Ltd.). Eye movements were recorded monocularly by EyeLink 1000 (SR Research Ltd.).

Electroencephalogram was recorded via 64 channel ActiCap (Brain Products GmbH). Electrode impedances were kept below 5 kΩ. We averaged referenced the raw EEG data Next, the data were high-pass filtered at 1 Hz by a FIR filter to remove very low frequency and constant trends. Epoching was performed from −1 to 2 s around the behavioral event of interest (i.e., VS, CO, and RC). After epoching, we corrected for baseline drifts by subtracting the mean baseline [(−0.5, 0) s before behavioral event of interest]. Trials with strong muscle activity were identified and removed by visual inspection. While this approach removed severe artifacts, we decided to reduce possible remaining artifacts by rejecting trials with extreme values, linear trends, improbable data and highly negative kurtosis (as suggested in Delorme et al., 2007). To further control for the presence of microsaccade artifacts on our data, we performed microsaccade detection on preprocessed and epoched data by an algorithm published by Engbert and Mergenthaler (2006). Trials with microsaccades were discarded of further analysis.

Preprocessing resulted in 330 ± 20 (mean ± std) contour trials and 210 ± 14 non-contour trials per subject. Sources of neural activity were localized from the Independent Component Analysis (ICA) estimates, computed on preprocessed EEG data an obtaining a total of 64 signal sources per subject (maximum number of IC given the number of EEG electrodes, see Supplementary Materials). Dipole localization of the resulting components topography is performed using DIPFIT2.2 plugin on EEGLab (Delorme and Makeig, 2004), based on a three-shell boundary element model (BEM) on a MNI standard brain template. Source localization on ICs instead of EEG signals reduces several of the factors that add errors on the dipole localization (e.g., environmental noise, non-linear interference between sources, etc.), increasing accuracy on the source localization (Tarkiainen et al., 2003). Note that source localization error of ICA decomposed signals typically extend from 4.1 to 20 mm (Acar and Makeig, 2013), so that the quantitative localization of the dipoles only provides an approximation for the exact location of the underlying source. Non-neural sources (e.g., localized at the scalp) were discarded of further study, leading to an average of 55 ± 5 neural sources per subject.

SPECTRAL DECOMPOSITION AND PHASE LOCKING VALUE

Two spectral decompositions of the ICs were performed. The spectral analysis presented in the spectrograms for high frequency bands (>30 Hz) was computed by a multitaper method, which provides a way to control bias and variance of the spectral estimation by using multiple Slepian tapers (Percival and Walden, 1993). The time-frequency decomposition was computed on epoched data, with a Slepian tapers, in steps of 2 Hz, with a window of 12 cycles per frequency and a spectral smoothing of 1/5 the frequency. The spectral analysis for frequency bands between 5 and 30 Hz was computed using Morlet wavelets, with a width of four cycles per frequency, and steps of 2 Hz. The spectrograms were computed on 90 trials per condition (contour/non-contour) and subject, selected randomly from the available trials. Finally, spectrograms were presented as a power change in respect to the baseline (−0.5 to 0 s relative to event of interest), and then averaged over trials and subjects.

Spectral analysis for the detection of task-relevant neural sources was performed through a discrete multi-scale wavelet transform using Daubechies wavelets of order 4 (DWT). The instantaneous frequency was computed on epoched data, leading to 5 frequency intervals (5.6, 11.16, 22.32, 44.6, and 89.3 Hz mean frequency). The instantaneous phase was extracted by the Hilbert transform. The phase locking value (PLV) (Lachaux et al., 2000), was computed on the instantaneous phase obtained from the DWT spectral decomposition for two different behavioral conditions (contour and non-contour trials). Phase synchronization was estimated between each pairwise combination of neural sources and frequency bands on 90 trials per behavioral condition (contour/non-contour trials, selected randomly from the available trials), with a resolution of 1 ms.

DETECTION OF TASK-RELATED NEURAL SOURCES

The goal of this method is to select neural sources that are associated with our stimulus of interest without any prior assumptions on the data (naive Bayes classifier). Generally, our goal is to compute the likelihood $p(D|c_i)$, namely, the probability that a set of data $D = \{x_1^t, x_2^t, \ldots, x_n^t\}$ belongs to a category $C = \{c_1, c_2\}$ where n is the trial number, t the time point at which the likelihood is computed, and C is a binary behavioral condition of interest. For example, if the goal is to find neural sources that associate with the appearance of stimulus, the classification is a binary classification problem $C = \{0, 1\}$, where 1 indicates the presence of stimulus. Likewise, other behavioral conditions of interest can be reduced to binary classification problems, such as lateralization of visual stimulation ($C = \{'left', 'right'\}$), or with the direction of eye movement ($C = \{'up', 'down'\}$). The likelihood for binary categories was computed via logistic regression (Fahrmeir and Tutz, 2001; Bishop, 2007). In short, logistic regression estimates the relationship between predictors variables and the categorical outcomes c_i, mentioned before. The predictor variables of our logistic regression will be the discrete wavelet transform of the neural sources data, so that $D = \{x_1^t, x_2^t, \ldots, x_n^t\}$ is transformed on the frequency domain such that $\widetilde{D} = \{\widetilde{x}_1^t, \widetilde{x}_2^t, \ldots, \widetilde{x}_n^t\}$. In other words, the logistic regression problem aims to find a set of parameters $\widetilde{w}$ that will establish the following relation: $C = w\widetilde{D}$, where C are the categorical outcomes for a time t and $\widetilde{D}$ is the frequency decomposition of a neural source at time t. To further reduce the dimensionality of our model, we included a L1 or Lasso regularization term on the linear regression (Bishop, 2007). In short, within logistic regression, L1 regularization introduces a penalty term $\alpha|w|$ on the optimization problem, and that results on forcing some of the parameters to have a zero weight. The penalty term is weighted by the hyper-parameter α. To choose the hyper-parameter α, we trained a set of models with α logarithmically spaced between [0.01, 0.3]. We choose the hyper-parameter α that lead to the model with highest likelihood (Friedman et al., 2010). Fitting the data for logistic regression and Lasso regularization is performed by glmnet (Friedman et al., 2007). Evaluation of the classification performance is computed through the Maximum A Posteriori estimate, so that $C_{MAP} = \text{argmax}_C p(\widetilde{D}|c_i)$ (Bishop, 2007). Concatenating the MAP at every time step t is what we call the prediction trace (see **Figure 2A** for an example). The model classification accuracy is validated

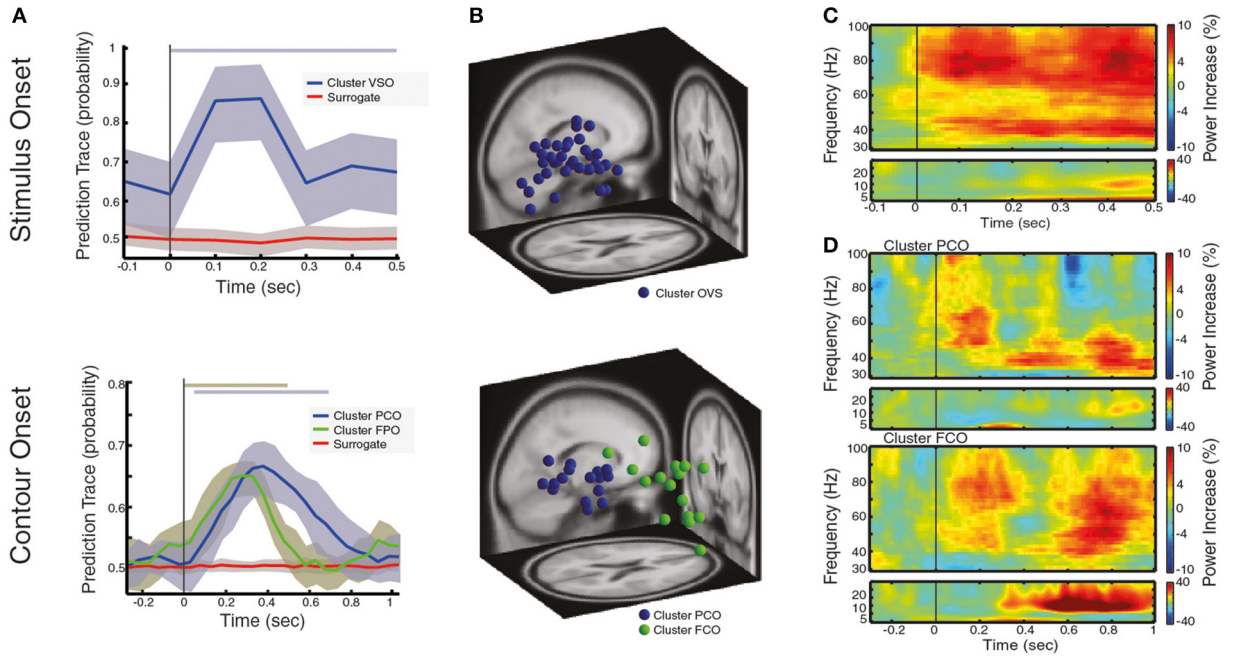

FIGURE 2 | Local oscillatory activity during the processing of visual stimulus and contour categorization. (A) Prediction traces for neural sources that are associated with the processing of visual stimulus after VS onset (left) and for neural sources that associate with correct contour categorization after CO onset (right). The prediction trace of a neural source is the time-resolved probability of a neural source to belong to a behavioral condition of interest (see text for details). Prediction traces of neural sources across subjects are shown in blue/green (mean ± std), while the prediction traces of surrogate data is shown in red (mean ± std). Significance of prediction traces is shown as a shadow in upper part of the plot, colorcoded for different clusters ($p < 0.01$, corrected for multiple comparison). **(B)** Dipole localization of neural sources associated with the processing of visual stimulus (left) and contour categorization (right), across subjects. In **(C,D)** the spectrogram of contour trials reflecting the power increase in respect to baseline, averaged over neural sources and subjects for **(C)** of neural sources associated with visual stimulation at VS onset and **(D)** neural sources associated with contour categorization cluster PCO (upper) and cluster FCO (lower) at CO onset. Note the range of contour visibility spans ± 66 ms around CO onset (the time interval at which subjects identify the contour better than chance).

through repeated random sub-sampling validation, for 100 iterations and a split of the data D into 70% training trials and 30% validation trials, so that for each neural source we estimate 100 prediction traces, which are then averaged as to reduce the bias of the model (Kohavi, 1995). By randomizing categorization labels (random labels were generated through random permutation of the trial number), we obtain the likelihood function of the null-hypothesis, which is, the probability distribution that a dataset $\widetilde{D}$ belongs to a random class c_i (surrogate data, see **Figure 2A** for an example). To this end, repeated random sub-sampling validation, for 100 iterations and a split of the data D into 70% training trials and 30% validation trials, so that for each surrogate source we estimate 100 prediction traces, from which we obtain a probability distribution of the null hypothesis. The probability distribution of the null-hypothesis was used to compute significance level of the categorization performance, so that if $p(\widetilde{D}|c_i)$ is outside the 99% confidence interval of the distribution of the null-hypothesis, the categorization performance is considered significant ($p < 0.01$; Bakeman and Robinson, 2005).

LONG-RANGE SYNCHRONIZATION NETWORKS

Synchronization between distal neural sources was computed on contour and non-contour trials by the PLV (Lachaux et al., 2000) between all pairs of neural sources and frequency intervals obtained by DWT, resulting in $N(N-1) \times f$ phase synchronization values for each behavioral condition (contour and non-contour) where N corresponds to the total number of neural sources, and f corresponds to the different frequency intervals. As the number of trials influences the PLV estimation, the PLV was computed on 90 trials, selected randomly from the available set of trials per subject. To compare PLV across behavioral conditions we performed a cluster-based permutation test where only significant PLV differences are kept for further study ($p < 0.01$; see Maris and Oostenveld, 2007). In short, t-statistics of a phase difference (a pair of neural sources, on a frequency f) were clustered according to functional adjacency between neural sources, or in other words, we analyze the PLV between particular subsets of neural sources. Here, we analyzed PLV between the neural sources PCO-FCO (see **Table 1**) and the PLV between PCO and frontal neural sources that are non-FCO (see Supplementary Materials for details on how we obtain the neural sources that lie within a cortical area of interest). The PLV-t-statistics were accumulated over neural sources (cumulative sum) so that the value of the t-statistics could only be positive/negative if, over all PLV pairs considered, there was a significant positive/negative t-statistics. For example, the PLV of the PCO neural sources at theta

frequency (**Figure 4**) for contours and non-contour trials, was significantly different for 32 connections to FCO neural sources, so that if the visualized t-statistic was positive/negative for a certain time point, it has a significance p-value of $p^{(32)}$. To test whether the difference between contour and non-contour trials arose due to the integration process itself, we estimated whether the t-statistics was significantly different relative to its baseline with z-score (see Supplementary Materials).

RESULTS

BEHAVIORAL ANALYSIS AND NEURAL SOURCE RECONSTRUCTION

Electroencephalographic activity (EEG) and eye movements were recorded from 15 participants who were instructed to identify two different orientations of an oval-like contour (up/down), pairing the possible spatial orientations with a saccadic response in a two-alternative forced choice (2AFC) paradigm (see **Figure 1**). Participants correctly identified the pointing direction of contours on 97.9% of trials when a contour was present. Further analysis revealed no performance differences between trials where the contours appeared on the left/right hemifield, on five different positions in regards to the horizon, and at the three different time onsets in regards to the start of the trial (all with $p > 0.2$).

To this end, several aspects of the behavioral task can be discussed. Firstly, as the presence of spatial cues may lead to an asymmetrical shift of attention before the contour appeared (Summerfield and Egner, 2009), contours appeared on 50% of the trials (on either left/right hemifield, on five different positions in regards of the horizon, see Supplementary Materials), so that the appearance of the contour could not be predicted, as confirmed by the lack of biases on the contour categorization performance. Secondly, as eye movements introduce both amplitude changes on the amplitude of the EEG signal and a broadband increase in gamma oscillatory activity (∼30–100 Hz) (Yuval-Greenberg et al., 2008; Plöchl et al., 2012), subjects were required to maintain fixation until the response cue onset, where they had to report contour identity. Additionally, and to avoid a temporal association between contour and saccadic response (Badler and Heinen, 2006), the response cue appears after a delay period of either 1.03, 1.50, or 1.97 s, once the co-aligned contour disappears. Third, subjects were required to perform an up/down eye movement at every trial (including non-contour trials), so that the trials cannot be solely distinguished based on the planning and execution of an eye movement. Fourth, note that due to their size (∼11° of visual field), the contours could not be detected by individual receptive fields, but rather required the integration of activity across multiple cortical columns (Field et al., 1993; Hess et al., 2001; Mathes et al., 2006). Finally, as contours were continuously morphing, the time at which they were identified typically varied from trial to trial. To account for this variability, we computed the time interval at which the contour is identified with a probability above chance, what we call the range of contour visibility (±66 ms around the CO event). Furthermore, the CO corresponds to the point in time at which subjects identify contour with a probability of 0.70 on average (see Materials and Methods). Finally, through this study we will analyze neural signals associated to three different behavioral events (see **Figure 1**): VS, visual stimulation onset; CO, contour onset (contour and non-contour trials); and RC, response cue onset.

One of the core issues when measuring oscillatory activity within EEG/MEG is the difficulty of attributing scalp signals to the activation of a particular area at cortical level. As a result, synchronization between neural signals across distal locations may reflect the leaking of a single source to several electrodes or several electrodes reflecting a single source (Kujala et al., 2008; Hipp et al., 2011). Here, to improve the spatial specificity of our data and analyze oscillatory activity with higher signal to noise ratio, we performed ICA on the raw EEG data (see Materials and Methods and **Table 1**).

LOCAL SYNCHRONIZATION DURING VISUAL STIMULUS PROCESSING AND CONTOUR PROCESSING

We started by analyzing the neural sources that are generally associated with the processing of visual stimuli. The neural sources of interest were identified though a new analysis approach which selects neural sources based on their ability to predict the behavioral condition of interest, and does not require a pre-selection of recording/analysis sites. The method is based on the hypothesis that the oscillatory activity of neural sources can predict subject perception (see Materials and Methods). In short, the time-frequency decomposition of a neural source is used as a predictor variable in a logistic regression model, such that, for each neural source, we can estimate the probability of a neural source to participate in a behavioral event of interest in a time-resolved fashion, which we call the prediction trace (**Figure 2A** for an example). In other words, the higher the prediction trace, the stronger the association of the neural source to the behavioral event of interest (e.g., contour lateralization). Only neural sources that statistically significantly predicted the behavioral condition of interest were kept for further study (with $p < 0.01$

Table 1 | Coordinates of the cluster centroids in Talariach space and their spatial localization (Lancaster et al., 2000).

Cluster name	Reference on the text	*x, y, z* Talariach coordinates	Anatomical structure	Brodmann area
OVS	Occipital cluster at visual stimulation onset	(4.44, −66.47, 26.87)	Occipital lobe precuneus	Brodmann area 31
PCO	Parietal cluster at contour onset	(−10.47, −57.19, 22.89)	Parietal lobe precuneus	Brodmann area 31
FCO	Frontal cluster at contour onset	(1.85, 35.98, 3.96)	Frontal lobe medial frontal gyrus	Brodmann area 32
OCO	Occipital cluster at contour onset	(−10.99, −76.39, 20.40)	Occipital lobe cuneus	Brodmann area 18
FRC	Frontal cluster at response cue onset	(8.02, 32.06, −17.8)	Frontal lobe medial frontal gyrus	Brodmann area 11
PRC	Parietal cluster at response cue onset	(4.40, −60.69, 14.7)	Parietal lobe posterior cingulate	Broaddman area 23
FNC	Frontal cluster not related with FCO	(−1.47, 47.84, 11.39)	Frontal lobe medial frontal gyrus	Brodmann area 10

based on cluster-based permutation testing, see Materials and Methods). With this process, we obtain a prediction trace for each neural source of each subject. To this end, we clustered the neural sources based on their predictive power (k-means clustering of prediction traces), thus obtaining a pooled prediction trace that reflects the probability of a group of neural sources, across subjects, to predict a behavioral event of interest.

Across all subjects, we found a total of 35 neural sources to be associated with the processing of visual stimuli or, in other words, oscillatory activity within 35 neural sources can be used to predict that a subject is processing visual stimuli on a single trial basis (an average of 2.3 neural sources per subject).These neural sources predicted the presence of a visual stimulus in 87.2% of the trials on average, at 100 ms after visual stimulation onset (VS onset), with time-varying prediction traces that were similar across subjects and across neural sources (**Figure 2A** left). Interestingly, the dipole locations of these sources spread across large areas within the occipital cortex (see **Table 1** for the centroid coordinates of the cluster OVS, and **Figure 2B** left), in accordance with a large body of studies that argue for the involvement of occipital areas on the processing of visual information (Hubel and Wiesel, 1962; Goodale and Milner, 1992; Tallon-Baudry and Bertrand, 1999). For the sake of completeness, we represented the oscillatory activity of these neural sources in form of a spectrogram (**Figure 2C**), showing that visual stimulus onset induces an enhancement of gamma band synchronization that extends over a broad frequency range (30–100 Hz) accompanied with a slight enhancement of oscillatory activity in the low frequency bands (5–30 Hz) within the first 500 ms after VS onset. Taken together, this findings replicate the well-known neural signature associated with the processing of visual stimuli involving the occipital cortex, as reported in human MEG/EEG studies (Lutzenberger et al., 1995; Donner et al., 2007; Volberg et al., 2013) and invasive recordings (Gray et al., 1989; Li et al., 2006), confirming that our analysis method, coupled with ICA source decomposition and the localization of these sources, allows for the reconstruction of local population activity associated with a given behavioral condition of interest.

Next, we analyzed neural activity that associate with contour processing, namely, we identified those neural sources that are predictors of correct contour categorization at CO (see **Figure 1**). Across all subjects we found a total of 31 neural to associate with contour categorization (i.e., average of 2.06 neural sources per subject). Clustering these neural sources based on their prediction traces gave rise to two distinct groups (k-means clustering, see Materials and Methods). The first cluster (PCO) is predictive of contour perception within 50–00 ms, with a correct prediction average of 65.78% trials at 380 ms after CO (±66 ms range of contour visibility **Figure 2A**, right), a comparable performance to other decoding approaches (Rotermund et al., 2011). Dipole localization shows that these neural sources are mainly grouped within parietal cortex (see **Table 1** for the centroid coordinates and **Figure 2B**, right). Concurrently, the second cluster (FCO), is localized within frontal areas (see **Table 1** for the centroid coordinates and **Figure 2B**, right), and is predictive of contour perception for the first 500 ms after CO, with an average correct prediction in 64.26% of trials at 300 ms after CO (**Figure 2A**, right). The spectral decomposition of parietal and frontal neural sources associated with correct contour categorization (cluster PCO and FCO; **Figure 2D**, upper and lower, respectively) shows enhanced oscillatory activity within the theta band (4–8 Hz), co-occurring with a broadband enhancement of gamma oscillatory activity (>30 Hz), especially within low-gamma frequency bands (30–60 Hz). Simultaneously, while beta oscillatory activity (13–30 Hz) seems to be slightly reduced in parietal neural sources, a strong and long-lasting enhancement of beta is present within frontal areas (cluster FCO; **Figure 2D**, lower).

In summary, we have shown that oscillatory activity within parietal/frontal cortices in single trials can be used to predict the subject's ability to correctly classify contours, revealing a crucial involvement of higher visual cortices on the perceptual grouping of local elements onto a coherent percept.

DISSOCIATING THE PROCESSING OF CONTOURS FOR CATEGORIZATION FROM THE CONTOUR LINKING PROCESS AND SACCADIC CONTROL

As perceptual grouping through contour categorization seem to require the processing of contours within parietal/frontal cortices, we continue by testing whether we can disentangle this process from the process of linking the contour elements. In particular, we tested whether oscillatory activity can predict the spatial location of the contour or, in other words, whether the contour appears on the left or right hemifield at a given trial (Contour Lateralization test). The spatial localization of the contour is not a relevant feature for the behavioral task, and we cannot disentangle whether the contour is perceptually available at this stage. Thus, if we can decode the contour spatial location, it is necessarily required that the contour elements have already been linked into a whole.

Oscillatory activity within parietal/frontal neural sources associated with contour processing is assumed to reflect neural processes involved with the processing of contours for further categorization, which may involve top-down attentional selection (Siegel et al., 2008; Van Ede et al., 2012), memory matching (Herrmann et al., 2004) or the targeting of the contour (VanRullen and Thorpe, 2001; Sato and Schall, 2003). However, broadband gamma synchronization within parietal cortex has been proposed to encode motor goals within visuo-motor tasks (Van Der Werf et al., 2008), and enhanced gamma activity within frontal cortex has been associated with eye-motor control, encoding saccadic goals (Schall and Thompson, 1999). To test whether the oscillatory activity within parietal/frontal neural sources arises due to the processing of contours for further categorization or to saccadic control, we tested whether neural sources can predict the saccadic goal, a process associated with saccade planning and execution (Saccade Planning test).

Following the same methodology as in the previous section, we estimated the prediction trace of neural sources associated with each of the three different behavioral events (i.e., VS, visual stimulation onset; CO, contour onset; RC, response cue onset), and identified potential neural sources that are predictors of contour lateralization or saccade planning, see **Figure 3A**. As such, neural activations within VS are used as a double negative control, since they should not associate with either saccade planning or

contour lateralization. Alternatively, we would expect that some neural sources within CO and RC may be predictors of saccade planning.

First, our results show that neural sources that respond to VS do neither predict saccade planning nor contour lateralization (**Figure 3**). Second, we found that neural sources that are active during the CO event are not found to be associated with saccade planning, while a subset of neural sources does predict contour lateralization (cluster name OCO, **Figure 3A**, total of 14 sources, with an average of 0.99 neural sources per subject). At 250 ms after CO (±66 ms range of contour visibility), the spatial localization of the contour within the visual field can be predicted with an average accuracy of 57.7% (significantly different from chance level, $p < 0.01$). Interestingly, dipoles of the neural sources that predict contour lateralization are localized within the occipital lobe and are independent of those neural sources that associate with contour categorization (see **Table 1** for the centroid coordinates and **Figure 3B**). Furthermore, the prediction trace of contour lateralization within higher occipital areas peaks 100 ms earlier than the prediction trace of parietal neural sources associated to contour categorization, FCO. Third, oscillatory activity of neural sources at RC onset were not associated with contour lateralization, suggesting that low-level stimulus properties are not maintained up until the RC event (**Figure 3A**). In contrast, a subset of 32 neural sources (total across subjects, an average of 2.13 neural sources per subject) are associated with saccadic direction, which are separated into two clusters according to its prediction traces: PRC and FRC (**Figure 3C**). Both clusters are predictive of saccadic direction within the first 600 ms after RC onset, with a peak prediction of 85.78 and 74.38% accuracy after 200 and 300 ms after RC, respectively. Dipole localization of the neural sources associated with saccadic planning is presented in **Figure 3C** and **Table 1**. Interestingly, the neural sources of cluster PRC localize within the parietal areas while cluster FRC localize within the frontal cortex. In accordance with recent studies on saccadic control, our results show that both frontal and parietal cortex are involved in saccade preparation and execution (Schall and Thompson, 1999; Sato and Schall, 2003; Van Der Werf et al., 2008). Notably, the set of neural sources within parietal and frontal cortex that associate with saccadic control (PRC and FRC) is not overlapping with the set of parietal and frontal sources that associate with contour integration (PCO and FCO).

In summary, neural sources that are associated with the processing and manipulation of contours to be correctly classified (PCO and FCO) are dissociated from the linking process of local elements into a whole, which can be decoded from oscillatory activity within occipital areas. Furthermore, the neural sources that associated with the overall perceptual grouping process are dissociated from complementary processes that are present during visual processing (e.g., saccade planning). Interestingly, while several behavioral processes can be decoded from neighboring spatial locations (contour categorization and saccadic control), they appear to be segregated neural processes in both time and IC-space.

LONG-RANGE NETWORKS OF OSCILLATORY ACTIVITY DURING CONTOUR PROCESSING

To ascertain whether contour processing and categorization manifests itself within the global synchronization network, we quantified transient phase-synchronization across distant neural sources

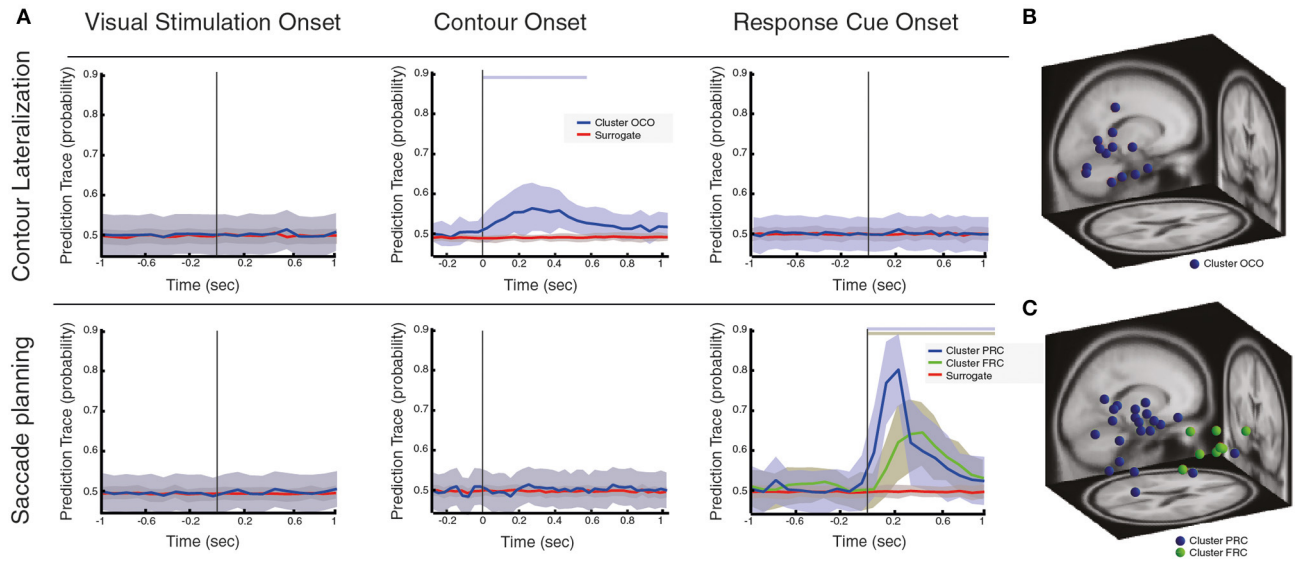

FIGURE 3 | Local oscillatory activity during contour linking process and saccadic control. (A) Prediction traces at three different behavioral events (i.e., VS, visual stimulation; CO, contour onset; RC, response cue), for two different conditions of interest: contour lateralization and saccade planning. Prediction traces of neural sources across subjects are shown in blue/green (mean ± std), while prediction traces of the surrogate data is shown in red (mean ± std). Significance of prediction traces is shown as a shadow in upper part of the plot, colorcoded for different clusters ($p < 0.01$, corrected for multiple comparison). **(B)** Dipole localization of neural sources associated with contour lateralization within CO onset. **(C)** Dipole localization of neural sources associated with saccade planning within RC onset.

(Lachaux et al., 2000) for five different frequencies: theta (5.6 Hz), alpha (11.16 Hz), high beta (22.32 Hz), low gamma (44.6 Hz), and high gamma (89.3 Hz) bands (main frequency within frequency interval, see Materials and Methods).

We first addressed the question of whether the transient synchronization pattern arising during contour trials where the contour is correctly classified differs from the synchronization pattern of non-contour trials. For that, we estimated whether the PLV significantly differs between the two conditions (contour vs. non-contour) by means of a permutation test. The 21.5% of all neural sources show statistically significant synchronization at all frequencies tested ($p < 0.01$), suggesting that there is a dynamic formation of phase-synchronization networks across distal neural sources during cognitive processing (further details in Figure S3).

So far, long-range synchronization between distal neural sources has been identified by grouping neural sources according to their spatial proximity (Palva et al., 2005; Hipp et al., 2011). However, as spatially neighboring neural sources may be involved in more than a single behavioral function, we focus on the properties of long-range synchronization of distal neural sources based on their involvement with the behavioral task of interest rather than on their spatial location. Specifically, we addressed the question of how the neural sources associated with contour processing modulate long-range synchronization networks. For that, we analyzed the connectivity pattern of parietal/frontal areas associated with contour categorization (PCO-FCO) and found that phase-synchronization in contour trials is significantly higher than in non-contour trials at theta between 80 and 985 ms after CO, at alpha within 245–570 ms after CO, and at high gamma between 350 and 720 ms after CO (±66 ms range of contour visibility for all measures, **Figure 4**). In principle, the differences in phase-synchronization between contour and non-contour trials may either reflect neural processes directly related to the perceptual grouping or to secondary processes (e.g., saccade preparation). To differentiate the two possibilities, the significance of t-stats is corrected by the z-score, which estimates whether the t-statistics is significantly different when compared to its baseline (z-score, see Supplementary Methods).

Previous studies report phase locking between frontal and parietal areas while performing visual processing tasks at the beta frequency range (Palva et al., 2005; Phillips et al., 2012), while our analysis found synchronization at theta, alpha, and gamma frequencies. Since our results suggested that different functions can occur in overlapping brain areas, we hypothesize that the coupling between parietal/frontal areas in beta frequency may not be required for the recruitment of neural sources that are enhanced on a behavioral task, but may instead signal a baseline communication or status quo, as proposed by the beta suppression hypothesis (Engel and Fries, 2010; Schroeder et al., 2011). To test this hypothesis, we analyzed the phase-synchronization pattern of PCO neural sources to frontal sources that are not related to contour processing (cluster FNC, see **Table 1** and see Supplementary Materials for details), and found that phase-synchronization of these sources is significantly different between contour and non-contour trials in the theta range (5.5 Hz), starting 80 ms after stimulus onset, at alpha (11 Hz) within 250–550 ms and at high beta (22.6 Hz) within 280–440 ms (±66 ms range of contour visibility for all measures). As such, our results suggest that gamma synchronization between parietal and frontal sources is functionally related to contour processing, while beta synchronization between parietal and frontal non-contour-integration specific sources might reflect secondary processes but not contour processing and categorization itself.

Finally, to further explore the relevance of long-range connections between distal neural sources, we tested whether there is a significantly different number of connections between different sets of neural sources (number of links to other neural sources with significant PLV). We found that parietal sources associated to contour processing -PCO- have a significantly higher number of connections than frontal neural sources -FCO- for any of the tested frequency intervals (Figure S3), suggesting that parietal neural sources may form a hub-like structure underlying coordination of distal neural sources during visual perception. Interestingly, we did not found a significant increase of the number of connections between PCO-FCO, suggesting that phase-synchronization coupling exist but it is not significantly higher than the connectivity that can occur between two random neural sources.

Taken together, these results suggest that the parietal/frontal areas associated with contour processing (PCO/FCO) show

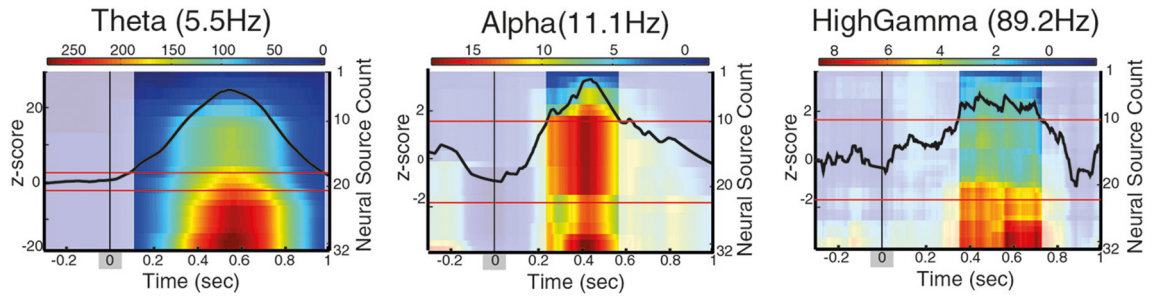

FIGURE 4 | Long-range phase synchronization during contour integration between PCO/FCO neural sources, for different frequency intervals. The images show the cumulative sum of the t-statistics for the Phase Locking Value difference during contour integration process (contour onset at $t = 0 \pm 66$ ms for the range of contour visibility, marked as a shadow gray). Intense color indicates periods of significantly enhanced phase synchronization with distant neural sources (positive t-statistic), corrected for baseline by z-score. A black line indicates the z-score of the neural sources associated with contour integration, red lines indicate z-score significance threshold.

enhanced phase synchronization in theta, alpha and high gamma frequency that arises in trials where the contour is perceptually grouped and classified, while beta synchronization is found between parietal and frontal but non-contour sources (PCO/FNC). Notably, the neural sources localized in the parietal areas and associated to contour processing (PCO) exhibit higher connectivity to distal cortical areas as compared to frontal sources (FCO), therefore forming a hub-like structure underlying the coordination of neural processes involved in contour processing.

DISCUSSION

In this study, we aimed to first determine whether oscillatory activity within early-visual cortical areas predict the perceptual grouping of a visual stimuli; and second, we determined whether this perception process modulates long-range synchronization networks.

To answer those questions, we analyzed EEG activity of subjects performing a contour categorization task, where perceptual grouping can be described as a two-stage process (Roelfsema, 2006; Watt et al., 2008; Mack and Palmeri, 2010; Kourtzi and Connor, 2011; Volberg and Greenlee, 2014) as the successful execution of the task requires the linking of contour boundaries into a coherent contour (Contour Linking Process), as well as a processing of the contour for its correct categorization (Contour Processing). Contour integration follows the Gestalt law of "good continuation" and has been serving as a reference behavioral task to study visual perception as local stimulus features remain constant, thus minimizing variability due to low level stimulus features (Wertheimer, 1923; Field et al., 1993; Hess et al., 2001; Mathes et al., 2006). In other words, given that contour and non-contour stimuli only differ on the co-alignment of a small subset of elements, differences in the oscillatory activity within the neural sources reflect differences between perceptual states. While psychological, psychophysical and neuroimaging studies propose that local interactions within early visual cortex mediate contour integration (Field et al., 1993; Li et al., 2006; Mathes et al., 2006), recent studies report that contour detection and its neural signals can be modulated by the task requirements, including attentional demands (Roelfsema et al., 2004), perceptual learning (Li et al., 2006) or perceptual noise within the contour (Mathes et al., 2006). Here, through the analysis of the EEG signals with a pattern classifier, we decode both the contour linking process as well as the processing of the contour for its correct categorization from a contour categorization task, with no pre-selection of the cortical areas of interest. Furthermore, classical contour integration tasks involve the sudden appearance of a contour and its background elements, so that the contour appearance is inevitable linked to a sudden change in the visual stimulus. Here, the contour integration task was adapted to mitigate the presence of spatial and temporal cues associated to the contour appearance by continuously modulating the orientation of local elements, reducing in turn the possibility of generating an asymmetrical shift of attention before the contour appeared (Summerfield and Egner, 2009, see Video 1 for a contour trial). Notably, the dynamic design allows, for the first time, the dissociation of the neural signatures associated with the onset of the visual stimulus and the appearance of a contour.

Accordingly, in the first part of the study, we aimed to determine whether local oscillatory activity can predict perceptual grouping of a visual stimuli, involving both the linking of local elements into a contour structure (Contour Linking Process) and the further contour processing for its categorization (Contour Processing), which may involve a broad range of secondary processes, such as top-down attentional selection (Siegel et al., 2008; Van Ede et al., 2012), memory matching (Herrmann et al., 2004) or the targeting of the contour (VanRullen and Thorpe, 2001). Our results show that oscillatory activity within occipital cortex allows for the decoding of the spatial location of the contour, indicating that at this stage, the local elements that form the contour are linked into a coherent structure, supporting the idea that occipital areas are classically linked to the processing of visual stimulus in a bottom-up manner (Hubel and Wiesel, 1962; Gross, 1999). Most interesting for this study, oscillatory activity within the frontal and parietal cortex can predict correct categorization of the contour, in line with the idea that top-down control is involved in perceptual grouping (Li et al., 2006; Mathes et al., 2006; Volberg et al., 2013). Whereas occipital sources that reflect the linking of local elements peak at 250 ± 66 ms after CO, frontal cortices better predict contour categorization at 300 ± 66 ms, followed by the parietal neural sources that peak at 380 ± 66 ms, suggesting a dynamics of contour categorization resembling visual search tasks (Buschman and Miller, 2007; Phillips et al., 2012). Our study advocate for a crucial involvement of fronto-parietal areas on a perceptual grouping task that requires contour categorization, areas that are proposed to mediate the formation and selection of behaviorally relevant stimulus (Sato and Schall, 2003), as well as attentional control (Mesulam, 1999; Siegel et al., 2008). Furthermore, our results emphasize the relevance of local oscillatory activity and suggest that enhancement of local synchronization within cortical areas serves as a general mechanism mediating sensory processing (Singer, 1999; Fries, 2009; Hipp et al., 2011). Finally, and most important for the purpose of this study, our results show that several aspects of a behavioral task (e.g., contour categorization and saccade planning) can be decoded within nearby spatial locations (e.g., parietal and frontal cortices). To this end, we argue for the advantage of using pattern classifiers for the analysis of time-resolved brain activity, proposing that this approach increases sensitivity on studying the neural basis of cognitive processes.

The second part of the study aimed to determine whether the integration and categorization of contours manifests itself as a transient synchronization involving distal neural sources. Though the understanding of how cognitive functions modulate synchronization across distributed cortical populations have greatly improved, the measure of such synchronization from EEG/MEG recordings remains difficult. This is mostly due to methodological issues. First, the low spatial resolution of EEG complicates both the cortical localization of neural activations and the computation of long-range synchronization (Kujala et al., 2008; Siegel et al., 2012). To account for this problem, we analyzed EEG signals at the source level, a transformation of electrode data into localized cortical sources, which increased spatial specificity. Secondly, there is a clear lack of statistical tools that allows the analysis of high-dimensional neural signals with no prior assumptions

on the structure and the location of the neural signals associated with the behavioral process of interest (Kilner, 2013). Our method to detect neural signals associated with whichever behavioral conditions of interest may serve as a powerful new tool to analyze high-dimensional neural data, where the selection of neural signals of interest is hypothesis free, with no starting assumptions on functional specialization and localization of neural sources. Instead, the method provides quantification for how well a neural signal predicts the behavioral condition of interest, simultaneously increasing the signal to noise ratio by selection of relevant neural signals. Furthermore, the method corrects for multiple comparisons and in principle, it is not limited to the study of EEG signals, but can be applied to any time-varying signal associated with categorical conditions. As such, our approach complements recent brain-computer applications that quantify structural properties of neural processes (Nicolelis and Lebedev, 2009; Rotermund et al., 2011; King and Dehaene, 2014). Note that the method is constrained to the analysis of neural signals associated with categorical behavioral conditions, where the model itself assumes that the relationship between the behavior and the, potentially non-linear, predictors is linear.

Our analysis show that 21.5% of the neural sources show an intermittent phase synchronization with other neural sources while performing the contour categorization task, supporting recent studies which suggest that there is a dynamic control of information flow across distributed neural sources in a frequency-specific fashion (Engel et al., 2001; Palva et al., 2005; Hipp et al., 2012). Is there a long-range synchronization network specifically associated to the processing of contour percepts for further categorization? For that, we analyzed the phase synchronization between neural sources that are associated to predict the subject's ability to classify contours (clusters PCO/FCO) and found that they synchronize at theta (5.6 Hz, main frequency within interval), alpha (11.6 Hz) and high gamma (89.3 Hz) frequency intervals. Those fluctuations seem to mediate information transmission between parietal/frontal areas which are specifically involved to the processing and manipulation of a contour for its categorization, in congruency with previous studies that report transient synchrony in the high-gamma band to emerge during perceptual binding (Melloni et al., 2007; Phillips et al., 2012), cross-modal integration (Hipp et al., 2012) and attentional control (Mesulam, 1999; Siegel et al., 2008), proposing that task-relevant cortico-cortico communication from between cortical areas may be mediated through gamma synchronization (Fries, 2009). Strikingly, beta synchronization between parietal/frontal areas has been reported in visual processing tasks, such as visual working memory, visual search and visual attention studies, suggesting that long-range beta synchronization may mediate top-down communication between cortical areas are active in tasks involving visual information processing (Munk et al., 2002; Engel and Fries, 2010; Hipp et al., 2011; Morgan et al., 2013; Volberg and Greenlee, 2014). Further, we analyzed phase synchronization between parietal and frontal neural sources that are not associated with contour processing (cluster FNC) and found that they indeed show phase synchronization in the beta frequency range (22.3 Hz). As such, while distal neural sources actively involved in the processing of contours synchronize at gamma frequency, nearby frontal sources synchronize in beta frequency. As observed in studies within the motor control system, where beta is actually replaced by gamma-band oscillatory activity during the preparation and execution of voluntary movements (Pogosyan et al., 2009; Swann et al., 2009), beta synchronization between parietal/frontal sources between neural sources that are recruited for a particular cognitive task at hand may similarly signal the maintenance of baseline activity, facilitating the cross-modal integration of cognitive tasks, allowing for the processing information on different timescales (Engel and Fries, 2010; Schroeder et al., 2011). These results seem to provide further insights on how nearby cortical sources enhance oscillatory in different frequencies in a task-specific manner, emphasizing the relevance on analyzing neural activity based on function rather than analyzing neural activity based on its spatial location.

Taken together, our results suggest that while oscillatory activity within occipital cortex predict the linking of local elements into a contour, oscillatory activity within parietal and frontal cortices play a crucial role in the execution of a contour categorization task, as well as the establishment of transient synchronization among them. In particular, our study reveals a phase locking in alpha, theta and gamma frequencies between frontal and parietal neural sources arising during the correct contour categorization, while a fronto-parietal beta phase locking arises within those neural sources that are not actively recruited in the contour categorization task itself. Finally, we presented a novel method that identifies neural sources based on their ability to predict behavioral conditions of interest, and report that different behavioral functions may involve the activation of cortical areas within nearby spatial locations, suggesting the presence of functionally distinct but spatially overlapping cortical areas.

ACKNOWLEDGMENTS

The project was partially financed by the University of Osnabrück, the Frankfurt Institute of Advanced Studies and the Max Planck Institute for Brain Research, from the Neurophisiology department. We thank specially Wolf Singer, Bill Philips, and Friederike Wiedemann for important and very helpful discussions concerning the design of the experiment and Peter König for supporting the experiments. We thank Tim Kietzman, José Ossandon, and Benedikt Ehinger for their helpful discussions and comments.

SUPPLEMENTARY MATERIAL

The Supplementary Material for this article can be found online at: http://www.frontiersin.org/journal/10.3389/fnint.2014.00064/abstract

REFERENCES

Acar, Z. A., and Makeig, S. (2013). Effects of forward model errors on EEG source localization. *Brain Topogr.* 26, 378–396. doi: 10.1007/s10548-012-0274-6

Altmann, C. F., Bülthoff, H. H., and Kourtzi, Z. (2003). Perceptual organization of local elements into global shapes in the human visual cortex. *Curr. Biol.* 13, 342–349. doi: 10.1016/S0960-9822(03)00052-6

Badler, J. B., and Heinen, S. J. (2006). Anticipatory movement timing using prediction and external cues. *J. Neurosci.* 26, 4519–4525. doi: 10.1016/S0960-9822(03)00052-6

Bakeman, R., and Robinson, B. F. (2005). *Understanding Statistics in the Behavioral Sciences*. Mahwah, NJ: Psychology Press.

Bishop, C. M. (2007). *Pattern Recognition and Machine Learning*. Berkley, CA: Springer.

Buschman, T. J., and Miller, E. K. (2007). Top-down versus bottom-up control of attention in the prefrontal and posterior parietal cortices. *Science* 315, 1860–1862. doi: 10.1126/science.1138071

Delorme, A., and Makeig, S. (2004). EEGLAB: an open source toolbox for analysis of single-trial EEG dynamics including independent component analysis. *J. Neurosci. Methods* 134, 9–21. doi: 10.1016/j.jneumeth.2003.10.009

Delorme, A., Sejnowski, T., and Makeig, S. (2007). Enhanced detection of artifacts in EEG data using higher-order statistics and independent component analysis. *Neuroimage* 34, 1443–1449. doi: 10.1016/j.neuroimage.2006.11.004

Donner, T. H., Siegel, M., Oostenveld, R., Fries, P., Bauer, M., and Engel, A. K. (2007). Population activity in the human dorsal pathway predicts the accuracy of visual motion detection. *J. Neurophysiol.* 98, 345–359. doi: 10.1152/jn.01141.2006

Engbert, R., and Mergenthaler, K. (2006). Microsaccades are triggered by low retinal image slip. *PNAS* 103, 7192–7197. doi: 10.1073/pnas.0509557103

Engel, A. K., and Fries, P. (2010). Beta-band oscillations-signalling the status quo? *Curr. Opin. Neurobiol.* 20, 156–165. doi: 10.1016/j.conb.2010.02.015

Engel, A. K., Fries, P., and Singer, W. (2001). Dynamic predictions: oscillations and synchrony in top-down processing. *Nat. Rev. Neurosci.* 2, 704–716. doi: 10.1038/35094565

Fahrmeir, L., and Tutz, G. (2001). *Multivariate Statistical Modelling Based on Generalized Linear Models*, 2nd Edn. New York, NY: Springer. doi: 10.1007/978-1-4757-3454-6

Field, D. J., Hayes, A., and Hess, R. F. (1993). Contour integration by the human visual system: evidence for a local "association field." *Vision Res.* 33, 173–193. doi: 10.1016/0042-6989(93)90156-Q

Foxe, J. J., and Simpson, G. V. (2002). Flow of activation from V1 to frontal cortex in humans. A framework for defining "early" visual processing. *Exp. Brain Res.* 142, 139–150. doi: 10.1007/s00221-001-0906-7

Friedman, J., Hastie, T., Höfling, H., and Tibshirani, R. (2007). Pathwise coordinate optimization. *Ann. Appl. Stat.* 1, 302–332. doi: 10.1214/07-AOAS131

Friedman, J., Hastie, T., and Tibshirani, R. (2010). Regularization paths for generalized linear models via coordinate descent. *J. Stat. Softw.* 33, 1–22.

Fries, P. (2009). Neuronal gamma-band synchronization as a fundamental process in cortical computation. *Annu. Rev. Neurosci.* 32, 209–224. doi: 10.1146/annurev.neuro.051508.135603

Goodale, M. A., and Milner, A. D. (1992). Separate visual pathways for perception and action. *Trends Neurosci.* 15, 20–25. doi: 10.1016/0166-2236(92)90344-8

Gray, C. M., König, P., Engel, A. K., and Singer, W. (1989). Oscillatory responses in cat visual cortex exhibit inter-columnar synchronization which reflects global stimulus properties. *Nature* 338, 334–337. doi: 10.1038/338334a0

Gross, C. G. (1999). *Brain Vision Memory. Tales in the History of Neuroscience.* Cambridge, MA: A Bradford Book.

Herrmann, C. S., Munk, M. H. J., and Engel, A. K. (2004). Cognitive functions of gamma-band activity: memory match and utilization. *Trends Cogn. Sci.* 8, 347–355. doi: 10.1016/j.tics.2004.06.006

Hess, R., and Field, D. (1999). Integration of contours: new insights. *Trends Cogn. Sci.* 3, 480–486. doi: 10.1016/S1364-6613(99)01410-2

Hess, R. F., Beaudot, W. H., and Mullen, K. T. (2001). Dynamics of contour integration. *Vision Res.* 41, 1023–1037. doi: 10.1016/S0042-6989(01)00020-7

Hipp, J. F., Engel, A. K., and Siegel, M. (2011). Oscillatory synchronization in long-range cortical networks predicts perception. *Neuron* 69, 387–396. doi: 10.1016/j.neuron.2010.12.027

Hipp, J. F., Hawellek, D. J., Corbetta, M., Siegel, M., and Engel, A. K. (2012). Long-range cortical correlation structure of spontaneous oscillatory activity. *Nat. Neurosci.* 15, 884–890. doi: 10.1038/nn.3101

Hoogenboom, N., Schoffelen, J.-M., Oostenveld, R., Parkes, L. M., and Fries, P. (2006). Localizing human visual gamma-band activity in frequency, time and space. *Neuroimage* 29, 764–773. doi: 10.1016/j.neuroimage.2005.08.043

Hubel, D. H., and Wiesel, T. N. (1962). Receptive fields, binocular interaction and functional architecture in the cat's visual cortex. *J. Physiol.* 160, 106–154.

Kilner, J. M. (2013). Bias in a common EEG and MEG statistical analysis and how to avoid it. *Clin. Neurophysiol.* 124, 2062–2063. doi: 10.1016/j.clinph.2013.03.024

King, J.-R., and Dehaene, S. (2014). Characterizing the dynamics of mental representations: the temporal generalization method. *Trends Cogn. Sci.* 18, 203–210. doi: 10.1016/j.tics.2014.01.002

Kohavi, R. (1995). "A study of cross-validation and bootstrap for accuracy estimation and model selection," in *International Joint Conference on Artificial Intelligence IJCAI - Proceedings of the 14th International Joint Conference on Artificial Intelligence* (San Francisco, CA).

Kourtzi, Z., and Connor, C. E. (2011). Neural representations for object perception: structure, category, and adaptive coding. *Annu. Rev. Neurosci.* 34, 45–67. doi: 10.1146/annurev-neuro-060909-153218

Kourtzi, Z., Tolias, A. S., Altmann, C. F., Augath, M., and Logothetis, N. K. (2003). Integration of local features into global shapes: monkey and human FMRI studies. *Neuron* 37, 333–346. doi: 10.1016/S0896-6273(02)01174-1

Kujala, J., Gross, J., and Salmelin, R. (2008). Localization of correlated network activity at the cortical level with MEG. *Neuroimage* 39, 1706–1720. doi: 10.1016/S0896-6273(02)01174-1

Lachaux, J.-P., Rodriguez, E., Van Quyen, M. L., Lutz, A., Martinerie, J., and Varela, F. (2000). Studying single-trials of phase synchronous activity in the brain. *Int. J. Bifurcat. Chaos* 10, 2429–2439. doi: 10.1142/S0218127400001560

Lancaster, J. L., Woldorff, M. G., Parsons, L. M., Liotti, M., Freitas, C. S., Rainey, L., et al. (2000). Automated Talairach atlas labels for functional brain mapping. *Hum. Brain Mapp.* 10, 120–131. doi: 10.1002/1097-0193(200007)10:3%3C120::AID-HBM30%3E3.0.CO;2-8

Li, W., and Gilbert, C. D. (2002). Global contour saliency and local colinear interactions. *J. Neurophysiol.* 88, 2846–2856. doi: 10.1152/jn.00289.2002

Li, W., Piëch, V., and Gilbert, C. D. (2006). Contour saliency in primary visual cortex. *Neuron* 50, 951–962. doi: 10.1016/j.neuron.2006.04.035

Lutzenberger, W., Pulvermüller, F., Elbert, T., and Birbaumer, N. (1995). Visual stimulation alters local 40-Hz responses in humans: an EEG-study. *Neurosci. Lett.* 183, 39–42. doi: 10.1016/0304-3940(94)11109-V

Mack, M. L., and Palmeri, T. J. (2010). Decoupling object detection and categorization. *J. Exp. Psychol. Hum. Percept. Perform.* 36, 1067–1079. doi: 10.1037/a0020254

Maris, E., and Oostenveld, R. (2007). Nonparametric statistical testing of EEG- and MEG-data. *J. Neurosci. Methods* 164, 177–190. doi: 10.1016/j.jneumeth.2007.03.024

Mathes, B., Trenner, D., and Fahle, M. (2006). The electrophysiological correlate of contour integration is modulated by task demands. *Brain Res.* 1114, 98–112. doi: 10.1016/j.brainres.2006.07.068

Melloni, L., Molina, C., Pena, M., Torres, D., Singer, W., and Rodriguez, E. (2007). Synchronization of neural activity across cortical areas correlates with conscious perception. *J. Neurosci.* 27, 2858–2865. doi: 10.1523/JNEUROSCI.4623-06.2007

Mesulam, M. M. (1999). Spatial attention and neglect: parietal, frontal and cingulate contributions to the mental representation and attentional targeting of salient extrapersonal events. *Philos. Trans. R. Soc. Lond. B Biol. Sci.* 354, 1325–1346. doi: 10.1098/rstb.1999.0482

Mishkin, M., Ungerleider, L. G., and Kathleen, A. (1983). Object vision and spatial vision: two cortical pahways. *Trends Neurosci.* 6, 414–417. doi: 10.1016/0166-2236(83)90190-X

Morgan, H. M., Jackson, M. C., van Koningsbruggen, M. G., Shapiro, K. L., and Linden, D. E. J. (2013). Frontal and parietal theta burst TMS impairs working memory for visual-spatial conjunctions. *Brain Stimul.* 6, 122–129. doi: 10.1016/j.brs.2012.03.001

Munk, M. H. J., Linden, D. E. J., Muck, L., Lanfermann, H., Zanella, F. E., Singer, W., et al. (2002). Distributed cortical systems in visual short-term memory revealed by event-related functional magnetic resonance imaging. *Cereb. Cortex* 12, 866–876. doi: 10.1093/cercor/12.8.866

Nicolelis, M. A. L., and Lebedev, M. A. (2009). Principles of neural ensemble physiology underlying the operation of brain-machine interfaces. *Nat. Rev. Neurosci.* 10, 530–540. doi: 10.1038/nrn2653

Oostenveld, R., Fries, P., Maris, E., and Schoffelen, J.-M. (2011). FieldTrip: open source software for advanced analysis of MEG, EEG, and invasive electrophysiological data. *Comput. Intell. Neurosci.* 2011:156869. doi: 10.1155/2011/156869

Palva, J. M., Palva, S., and Kaila, K. (2005). Phase synchrony among neuronal oscillations in the human cortex. *J. Neurosci.* 25, 3962–3972. doi: 10.1523/JNEUROSCI.4250-04.2005

Percival, D. B., and Walden, A. T. (1993). *Spectral Analysis for Physical Applications.* Cambridge, MA: Cambridge University Press.

Phillips, S., Takeda, Y., and Singh, A. (2012). Visual feature integration indicated by pHase-locked frontal-parietal EEG signals. *PLoS ONE* 7:e32502. doi: 10.1371/journal.pone.0032502

Pogosyan, A., Gaynor, L. D., Eusebio, A., and Brown, P. (2009). Boosting cortical activity at beta-band frequencies slows movement in humans. *Curr. Biol.* 19, 1637–1641. doi: 10.1016/j.cub.2009.07.074

Plöchl, M., Ossandón, J. P., and König, P. (2012). Combining EEG and eye tracking: identification, characterization, and correction of eye movement artifacts in electroencephalographic data. *Front. Hum. Neurosci.* 6:278. doi: 10.3389/fnhum.2012.00278

Roelfsema, P. R. (2006). Cortical algorithms for perceptual grouping. *Annu. Rev. Neurosci.* 29, 203–227. doi: 10.1146/annurev.neuro.29.051605.112939

Roelfsema, P. R., Lamme, V. A. F., and Spekreijse, H. (2004). Synchrony and covariation of firing rates in the primary visual cortex during contour grouping. *Nat. Neurosci.* 7, 982–991. doi: 10.1038/nn1304

Rotermund, D., Schipper, M., Fahle, M., and Ernst, U. (2011). High-performance categorization of contour percepts from EEG recordings. *BMC Neurosci.* 12:P94. doi: 10.1186/1471-2202-12-s1-p94

Sato, T. R., and Schall, J. D. (2003). Effects of stimulus-response compatibility on neural selection in frontal eye field. *Neuron* 38, 637–648. doi: 10.1016/S0896-6273(03)00237-X

Schall, J. D., and Thompson, K. G. (1999). Neural selection and control of visually guided eye movements. *Annu. Rev. Neurosci.* 22, 241–259. doi: 10.1146/annurev.neuro.22.1.241

Schroeder, C. E., Wilson, D. A., Radman, T., Scharfman, H., and Lakatos, P. (2011). Dynamics of active sensing and perceptual selection. *Curr. Opin. Neurobiol.* 20, 172–176. doi: 10.1016/j.conb.2010.02.010

Sehatpour, P., Molholm, S., Schwartz, T. H., Mahoney, J. R., Mehta, A. D., Javitt, D. C., et al. (2008). A human intracranial study of long-range oscillatory coherence across a frontal-occipital- hippocampal brain network during visual object processing. *Proc. Natl. Acad. Sci. U.S.A.* 105, 4399–4404. doi: 10.1073/pnas.0708418105

Siegel, M., Donner, T. H., and Engel, A. K. (2012). Spectral fingerprints of long-range neuronal interactions. *Nat. Rev. Neurosci.* 13, 121–134. doi: 10.1038/nrn3137

Siegel, M., Donner, T. H., Oostenveld, R., Fries, P., and Engel, A. K. (2008). Neuronal synchronization along the dorsal visual pathway reflects the focus of spatial attention. *Neuron* 60, 709–719. doi: 10.1016/j.neuron.2008.09.010

Singer, W. (1999). Neuronal synchrony: a versatile code for the definition of relations? *Neuron* 24, 49–65. doi: 10.1016/S0896-6273(00)80821-1

Summerfield, C., and Egner, T. (2009). Expectation (and attention) in visual cognition. *Trends Cogn. Sci.* 13, 403–409. doi: 10.1016/j.tics.2009.06.003

Swann, N., Tandon, N., Canolty, R., Ellmore, T. M., McEvoy, L. K., Dreyer, S., et al. (2009). Intracranial EEG reveals a time- and frequency-specific role for the right inferior frontal gyrus and primary motor cortex in stopping initiated responses. *J. Neurosci.* 29, 12675–12685. doi: 10.1523/JNEUROSCI.3359-09.2009

Tallon-Baudry, C., and Bertrand, O. (1999). Oscillatory gamma activity in humans and its role in object representation. *Trends Cogn. Sci.* 3, 151–162. doi: 10.1016/S1364-6613(99)01299-1

Tallon-Baudry, C., Bertrand, O., and Fischer, C. (2001). Oscillatory synchrony between human extrastriate areas during visual short-term memory maintenance. *J. Neurosci.* 21, 1–5.

Tallon-Baudry, C., Bertrand, O., Delpuech, C., and Permier, J. (1997). Oscillatory gamma-band (30-70 Hz) activity induced by a visual search task in humans. *J. Neurosci.* 17, 722–734.

Tarkiainen, A., Liljeström, M., Seppä, M., and Salmelin, R. (2003). The 3D topography of MEG source localization accuracy: effects of conductor model and noise. *Clin. Neurophysiol.* 114, 1977–1992. doi: 10.1016/S1388-2457(03)00195-0

Uhlhaas, P. J., Pipa, G., Lima, B., Melloni, L., Neuenschwander, S., Nikolic, D., et al. (2009). Neural synchrony in cortical networks: history, concept and current status. *Front. Integr. Neurosci.* 3:17. doi: 10.3389/neuro.07.017.2009

Van Der Werf, J., Jensen, O., Fries, P., and Medendorp, W. P. (2008). Gamma-band activity in human posterior parietal cortex encodes the motor goal during delayed prosaccades and antisaccades. *J. Neurosci.* 28, 8397–8405. doi: 10.1523/JNEUROSCI.0630-08.2008

Van Ede, F., de Lange, F. P., and Maris, E. (2012). Attentional cues affect accuracy and reaction time via different cognitive and neural processes. *J. Neurosci.* 32, 10408–10412. doi: 10.1523/JNEUROSCI.1337-12.2012

VanRullen, R., and Thorpe, S. J. (2001). The time course of visual processing: from early perception to decision-making. *J. Cogn. Neurosci.* 13, 454–461. doi: 10.1162/08989290152001880

Varela, F., Lachaux, J., Rodriguez, E., and Martinerie, J. (2001). The brainweb: phase synchronization and large scale integration. *Nat. Rev. Neurosci.* 2, 229–239. doi: 10.1038/35067550

Volberg, G., and Greenlee, M. W. (2014). Brain networks supporting perceptual grouping and contour selection. *Front. Psychol.* 5:264. doi: 10.3389/fpsyg.2014.00264

Volberg, G., Wutz, A., and Greenlee, M. W. (2013). Top-down control in contour grouping. *PLoS ONE* 8:e54085. doi: 10.1371/journal.pone.0054085

Watt, R., Ledgeway, T., and Dakin, S. C. (2008). Families of models for gabor paths demonstrate the importance of spatial adjacency. *J. Vis.* 8, 1–19. doi: 10.1167/8.7.23

Wertheimer, M. (1923). Untersuchungen zur Lehre von der Gestalt. *Psychol. Forsch.* 4, 301–350. doi: 10.1007/bf00410640

Yuval-Greenberg, S., Tomer, O., Keren, A. S., Nelken, I., and Deouell, L. Y. (2008). Transient induced gamma-band response in EEG as a manifestation of miniature saccades. *Neuron* 58, 429–441. doi: 10.1016/j.neuron.2008.03.027

Conflict of Interest Statement: The authors declare that the research was conducted in the absence of any commercial or financial relationships that could be construed as a potential conflict of interest.

Received: 23 April 2014; accepted: 25 July 2014; published online: 13 August 2014.
*Citation: Castellano M, Plöchl M, Vicente R and Pipa G (2014) Neuronal oscillations form parietal/frontal networks during contour integration. Front. Integr. Neurosci. **8**:64. doi: 10.3389/fnint.2014.00064*
This article was submitted to the journal Frontiers in Integrative Neuroscience.

4.4 Complementary analysis to Paper III: Static vs Dynamic Contour Integration: When Timing Matters

Contour integration is a reference behavioural task for the study of visual perception, as perception relies on the grouping of local elements sharing a common feature [168]. Classically, the task is designed as a pop-out task, where a single frame contains both the contour and distracters.

Simultaneously, it has been proposed that temporal structures within visual stimulation are a key element for the perceptual grouping itself [100]. Unfortunately, little is known on how a dynamic contour formation modulates the neural representation of the contour, as the few studies that use dynamic contour integration do not analyze neural activations [122]. As such, the goal of this study is to investigate whether and how the presence of temporal structure on the contour integration process modulates neural processing, through the analysis of human-EEG performing a contour integration task, where a set of Gabor elements co-align to form a figure.

We first report that perceptual grouping involves activation of both parietal and fontal cortices, regardless of the dynamic structure of the stimulus. Second, our results show that dynamic contour integration involves the activation of more widespread cortical areas than the classical contour integration. Taken together, our results suggest that temporal structure within visual stimuli modulate the neural representation of the perceptual processes associated to contour integration.

Methods

Static Contour Integration

Within the framework of contour integration studies, most of the research explore the spatial properties of contour integration, while little is known about the dynamics of contour integration. To estimate whether our results with morphing contours can be compared to the classical static contour integration tasks, we compared the neural signals of morphing contours to those of static contours. For that, were asked to respond to 100 trials of the mentioned 2AFC visual integration task. All the experimental parameters remained the same except for the frame rate, so that the contour would appear together with a sudden frame change, as in classical contour integration studies.

Results: Temporal structure within contour formation modulates cortical responses

Activity within cortical areas has been reported to be modulated by the temporal structure of the incoming stimulus. For instance, neurons in MT show enhanced activation in response to a specific speed and coherence of moving objects [127, 157], while integration of temporal cues becomes behaviourally relevant for biological motion recognition [99, 111], learning object invariance [240, 284], and sequence learning [93] among others. Within the context of contour integration studies, little is known about the dynamics of contour integration as most of the studies were based on the spatial properties of contour integration [122]. To test whether the temporal structure within stimulus modulates cortical responses and to estimate whether our results with morphing contours can be compared to the classical static contour integration tasks, we compared the neural signals of morphing contours to those of static contours. For that, were asked to respond to 100 trials of the mentioned 2AFC visual integration task where the contour remained static (static trials). All the experimental parameters remained the same except for the frame rate, so that the contour would appear together with a sudden frame change, as in classical contour integration studies (see section 4.4 for details).

On the classical static contour integration task, participants correctly identified the pointing direction of the contours on the 98.2% of the trials, significantly differing from chance level, but not differing from the morphing contour condition. In other words, a difference in the neural signals between the classical static contour integration (static contours) and the morphing contour integration tasks (morphing contours) reflect differences on the processing of temporally structured stimulus, rather than differences in the perception of contour. Following the methodology discussed in the previous sections, we estimated the prediction trace of neural sources associated with perceptual binding with the static trials, and localized them at the scalp level, see Figure 4.3, right column. For the sake of completeness, the neural signals associated to morphing contours presented in Figure 4.3, left column.

A total of 21 neural sources are predictors of contour integration at contour integration onset for static contours. The time-varying prediction traces were clustered (k-means clustering, see section 4.4) in two groups PSC and FSC, see Figure 4.3, right column. The cluster FSC is predictive of contour perception for the first 500 ms, with a correct prediction average of 72.97% trials at 270 ms after contour onset. Dipole localization shows that these neural sources are located within frontal cortex. Concurrently, the cluster PSC (localized within parietal areas) is predictive of contour perception for the first 800 ms after contour onset, with an average correct prediction of 65.16% of trials at 390 ms after contour onset (Figure 4.3, right column). The early activation of frontal cortices at contour onset, replicate previous pop-out studies that propose a frontal-parietal attentional control of neural signals [41]. On a similar fashion, occipital neural sources show an enhanced activation on the perception of contours as reported elsewhere [153, 248], see Figure 4.3 lower plots.

In comparing to the neural sources that are predictors of contour integration for morphing contours, note that the neural sources associated to contour integration localize

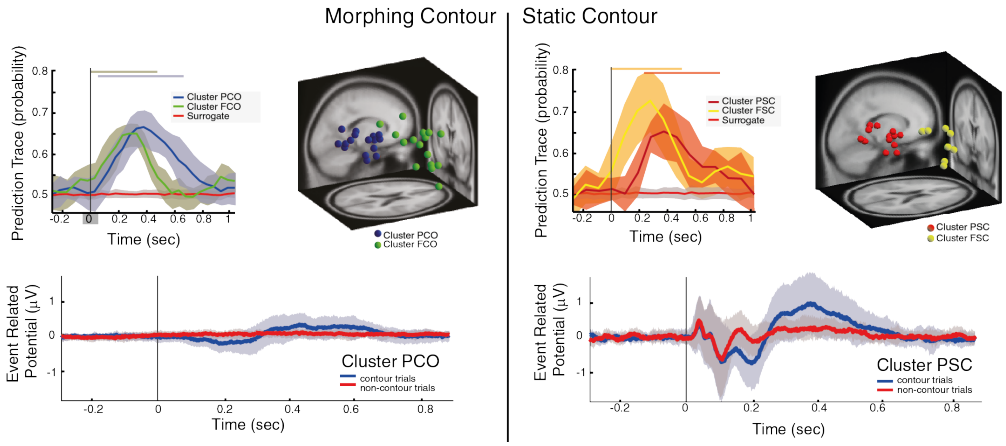

FIGURE 4.3: **Local representation of contour perception: static versus morphing contour integration tasks** Upper plot: Event Related Potential of 90 trials (shadow indicate the standard deviation), locked to contour integration onset ($t = 0$) of contour (blue) and non-contour trials (red) of parietal neural sources PCO and PSC respectively (see below). Lower plots: Prediction traces and dipole localization of the neural sources associated to contour integration.

at parietal-frontal cortices (for both static and morphing contours). While the two processes share a similar spatial localization, the neural sources involved in static and morphing contour integration are independent neural sources. Furthermore, note that the single-trial decoding of perceptual binding in frontal areas improves with static trials (see prediction traces PCO and FCO in Figure 4.3).

In summary, contour perception in both static and morphing contour formation tasks involve parietal/frontal neural sources. Although spatial localization of both processes are rather similar, neural signals associated to contour perception of morphing contours are clearly different, suggesting that the temporal structure of stimulus modulates neural processing. As the morphing of contours allows for the dissociation of visual stimulation onset and contour integration onset, we will proceed on analysing long-range synchronization networks of neural signals associated to morphing signals.

Long-range networks of oscillatory activity during contour processing

To ascertain whether contour processing and categorization manifests itself within the global synchronization network, we quantified transient phase-synchronization across distant neural sources [148] for five different frequency intervals: theta (5.6 Hz), alpha (11.16 Hz), high beta (22.32 Hz), low gamma (44.6 Hz) and high gamma (89.3 Hz) bands (main frequency within frequency interval, see section 4.4). We first addressed the question of whether the transient synchronization pattern arising during contour integration differs from the synchronization pattern of non-contour trials. For that, we estimated whether the difference in the phase locking value (PLV) significantly differs between the two conditions (contour versus non-contour) by means of a permutation

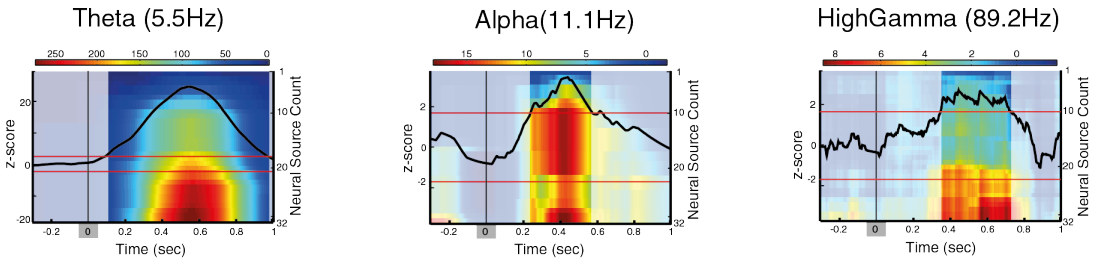

FIGURE 4.4: **Long-range phase synchronization during contour integration for different frequency intervals** between parietal/frontal neural sources associated to contour integration (A) and between parietal and non-frontal neural sources (B). The images show the cumulative sum of the t-statistics for the Phase Locking Value difference during contour integration process (contour integration onset at $t = 0 \pm 66$ ms (range of contour visibility). Intense color indicates periods of significantly enhanced phase synchronization with distant neural sources (positive t-statistic), corrected for baseline by z-score. A black line indicates the z-score of the neural sources associated with contour integration, red lines indicate z-score significance threshold.

test. With that, the differences between PLVs of contour/non-contour trials are described by the t-stats, with a significance threshold of $p<0.01$. The 21.5% of all neural sources show statistically significant synchronization at all frequencies tested, providing evidence that there is a dynamic establishment of phase-synchronization across distal neural sources during cognitive processing (further details in section 4.4).

So far, long-range synchronization between distal neural sources has been identified by grouping neural sources according to their spatial proximity [123, 194]. However, as spatially neighboring neural sources may be involved in more than a single behavioural function, we focus on the properties of long-range synchronization of distal neural sources based on their involvement with the behavioural task of interest rather than on their spatial location. Specifically, we addressed the question of how the neural sources associated with contour processing modulate long-range synchronization networks. For that, we analysed the connectivity pattern of parietal/frontal areas associated with contour categorization (PCO-FCO) and found that phase-synchronization in contour trials is significantly higher than in non-contour trials at theta between 80 and 985 ms after contour onset, at alpha within 245-570 ms after contour onset, and at high gamma between 350-720 ms after contour onset ($\pm$66 ms range of contour visibility for all measures, Figure 4.4). In principle, the differences in phase-synchronization between contour and non-contour trials may either reflect neural processes directly related to the perceptual grouping or to secondary processes (e.g. saccade preparation). To differentiate the two possibilities, the significance of t-stats is corrected by the z-score, which estimates whether the t-statistics is significantly different when compared to its baseline (z-score, see section 4.4).

Previous studies report phase locking between frontal and parietal areas while performing visual processing tasks at the beta frequency range [194, 199], while our analysis found synchronization at theta, alpha, and gamma frequencies. Since our results suggested that different functions can occur in overlapping brain areas, we hypothesize that the coupling between parietal/frontal areas in beta frequency may not

be required for the recruitment of neural sources that are enhanced on a behavioral task, but may instead signal a baseline communication or status quo, as proposed by the beta suppression hypothesis [76, 220]. To test this hypothesis, we analysed the phase-synchronization pattern of PCO neural sources to frontal sources that are not related to contour processing (cluster FNC, see ssection 4.4), and found that phase-synchronization of these sources is significantly different between contour and non-contour trials in the theta range (5.5 Hz), starting 80 ms after stimulus onset, at alpha (11 Hz) within 250-550 ms and at high beta (22.6 Hz) within 280-440 ms ($\pm$66 ms range of contour visibility for all measures). As such, our results suggest that gamma synchronization between parietal and frontal sources is functionally related to contour processing, while beta synchronization between parietal and frontal non-contour-integration specific sources might reflect secondary processes but not contour processing and categorization itself.

Finally, to further explore the relevance of long-range connections between distal neural sources, we tested whether there is a significantly different number of connections between different sets of neural sources. We found that parietal sources associated to contour processing -PCO- have a significantly higher number of connections than frontal neural sources -FCO- for any of the tested frequency intervals, suggesting that parietal neural sources may form a hub-like structure underlying coordination of distal neural sources during visual perception. Interestingly, we did not found a significant increase of the number of connections between PCO-FCO, suggesting that phase-synchronization coupling exist but it is not significantly higher than the connectivity that can occur between two random neural sources. Taken together, these results suggest that the parietal/frontal areas associated with contour processing (PCO/FCO) show enhanced phase synchronization in theta, alpha and high gamma frequency that arises in trials where the contour is perceptually grouped and classified, while beta synchronization is found between parietal and frontal but non-contour sources (PCO/FNC). Notably, the neural sources localized in the parietal areas and associated to contour processing (PCO) exhibit higher connectivity to distal cortical areas as compared to frontal sources (FCO), therefore forming a hub-like structure underlying the coordination of neural processes involved in contour processing.

Discussion: Temporal structure within contour formation modulates cortical responses

Limitations and generalizability

The results obtained in this study rely on the decoding model, which was design to predict a behavioural condition of interest from a linear combination of the EEG frequency decomposition. As such, this study relies on the assumption that a cognitive process can be decoded from a linear combination of EEG features, or in other words, assuming that the relationship between the behaviour and the predictors is linear [22, 78]. To this end, an interesting extension of the current decoding model would be to consider non-linear relationships between the data and the behaviour. From another perspective, and due to the nature of the decoding model, our model can

be generalized to decode categorical variables from neural signals (see section A.1 for more details on regression models). In other words, the method would allow for the decoding of categorical behavioural conditions from neural signals in a time-resolved fashion, shedding light on the temporal organization of information-processing stages.

Additionally, the design of the study assumes that the stimulus-specific activations within and between cortical areas do not change during the recording time. As such, it is assumed that after the warm up time of 40 trials, when their identification performance is stabilized, the subjects are familiar with the task and their neural representations do not adapt. To this end, it may be interesting to perform a longitudinal task where the subject are required to learn stimulus features.

Conclusions

The literature showing that oscillatory activity within visual cortical areas mediate the processing of visual stimulus and perception itself is vast, but the mechanisms by which visual features are integrated into a percept is still unclear, mostly due to the fact that neural signatures and perception itself are modulated by low-level stimulus features and the cognitive requirements of the task.

Through the study of a contour classification task, we provided evidence that it is not only the spatial distribution of contour features, but the temporal structure within the contour that is crucial for perceptual grouping. In particular, we show that the cortical areas recruited for contour classification itself are different as the temporal structure within the stimulus changes, suggesting that temporal continuity of the stimulus crucially modulates neural processing.

Following, we tested whether oscillatory activity within early visual cortex predicts the linking of local elements into a coherent structure and its resulting categorization, and found that, while oscillatory activity within occipital predict the linking of local elements into a contour, oscillatory activity within parietal and frontal cortices play a crucial role in the execution of a contour categorization task, as well as the establishment of transient synchronization among them. In particular, our study reveals a phase locking in alpha, theta and gamma frequencies between frontal and parietal neural sources arising during the correct contour categorization, while a fronto-parietal beta phase locking arises within those neural sources that are not actively recruited in the contour categorization task itself.

Finally, we presented a novel method that identifies neural sources based on their ability to predict behavioural conditions of interest, and report that different behavioural functions may involve the activation of cortical areas within nearby spatial locations, suggesting the presence of functionally distinct but spatially overlapping cortical areas.

5

General Discussion and Conclusions

Cognitive science is the strongest defender of presenting cognition and the brain as information-processing systems, proposing that cognition arises though the manipulation, storage, and retrieval of information, which accurately describe the physical properties of the environment, known as the representationalist framework [84]. This approach has resulted in years of research aiming to associate measurable features of the external world to persistent neural activity, whose results suggest a modular organization of the neural system [89, 109, 137, 178].

However, through this dissertation, we have refereed to recent work that challenges the traditional representationalist framework, an increasing body of experimental evidence which suggests that persistent activations associated to stimulus or cognitive tasks can change systematically. In particular, neural representations have been reported to be modulated by shifts in the physical properties of the stimulus (i.e. low level features), often referred to, in the respective studies, as contextual effects, masking or sequential learning [40, 57, 222, 252]. But those stimulus-specific responses are not only modulated by the stimulus features, but also by the cognitive requirements associated with the task in hand, including attentional selection [41, 208, 227, 262], working memory maintenance [120, 198, 247, 278] or the expectation of a reward [226]. Furthermore, we have reviewed how the sensory representations are altered by experience through the ubiquitous presence of plasticity mechanisms [39, 56, 79, 96, 289].

Altogether, these studies suggest that neural representations are a dynamic process, challenging the classical representationalist framework, where cognition arises through the manipulation of static or persistent neural representations that accurately describe the external world. Most important is that stimulus-specific representations are not only time-dependent responses, but that these time-varying response are as predictive of behaviour as the persistent activation classically reported [14, 205].

The relevance of neural dynamics and their temporal structure become more evident when considering that, at every instance, time-varying stimuli from visual, auditory, olfactory and tactile systems are integrated to produce behaviour [118], in such a way, that timing is intrinsically bound to the completion of cognitive tasks. However, despite the ubiquity of time-varying signals, the impact of temporally-structured stimulus on the neural representations and its interaction with plasticity mechanisms is still not clear.

5.1 Summary of the presented studies

In this dissertation, we have focused on the dynamic aspects of neural representations, studying how time-varying signals modulate the neural responses of an adaptive neural systems. For that, and given the spatial complexity of the neural system, the modulation of neural responses via time-varying signals and other complementary aspects of spatio-temporal processing were discussed at separate spatial scales: at the scale of single neurons, within populations of neurons, and involving activation of distributed large cortical areas.

We started by exploring the impact of the temporal structure of the incoming spike trains on a post synaptic neuron and showed that the temporal structures of pre-synaptic spike trains modulate the spiking structure of the post-synaptic neuron. The relevance of our results lies in the fact, that it is often assumed, that spiking activity can be well approximated as a *Poisson* process, where the time of a spike would not depend on previous spikes, and the distribution of inter-spike intervals would be exponential [81, 115, 193]. While recorded spiking activity of pyramidal neurons typically deviates from *Poisson*-processes [12, 165, 185, 186, 201, 249], it is generally argued, that, when the pre-synaptic spike trains, arriving at a neuron are independent, the temporal structure is washed out [81, 193]. Our computational study shows that those assumptions do not hold, complementing other studies that mathematically disproof it [51, 155, 200]. Through this first chapter, we also introduced the concept of plasticity and activity-dependent plasticity mechanisms, that can be influenced by the precise temporal order between the pre- and post-synaptic spiking [151, 167, 234]. While the relevance of precise spike times for plasticity is recognized experimentally [107, 207, 231, 232, 268], the temporal structure in computational models of plasticity, is usually approximated by a *Poisson* process. Through the modelling of spike-timing dependent plasticity (STDP), we explored how the temporal structure within pre-post synaptic spike trains modulates the synaptic weight that connect the single neuron with its pre-synaptic neurons. In short, our results suggest that the synaptic weight distribution is modulated by the temporal structure at three different temporal scales. First, we described how the fast changes on synaptic weight directly reflect the repetitive structure of the pre-synaptic spike trains. Second, we found that both the regularity of the spiking activity and the relative firing rate of excitatory/inhibitory neurons regulate the speed and the strength at which the synaptic weight change occur due to STDP. Third and finally, our results show that the temporal structure within excitatory pre-synaptic trains modulates the equilibrium distribution of synaptic weights, namely, the resulting persistent changes on a neuron's connectivity. In summary, our first study suggest that the modelling of

real neural firing might require a non-*Poisson* assumption, as structural changes associated to activity-dependent plasticity are modulated by the regularity and frequency of pre-synaptic spiking activity.

In the second study, we focused on characterizing and extending the memory capacity of a cortical circuit model, that processes spatio-temporal stimuli. A fundamental limitation of spiking neural networks, that aim to model generic cortical circuits of spiking neurons, is that a stimulus arriving to a spiking network, will be indistinguishable from its background spiking activity after a few milliseconds [92, 161]. However, critical cognitive phenomena such as sequence learning [57], motor preparation [55, 145] and working memory tasks [72], crucially depend on the retention of information over longer periods of time. While classical short-term memory paradigms argue for a stabilization of short term memory through sustained activity [272], a relatively new paradigm proposes that cortical circuits encode and store information in their transient dynamics, where neural representations become a spatio-temporal pattern of spiking activity that changes over time [38]. Computational studies propose, that the coexistence of several plasticity mechanisms within the cortical circuit are crucial for the stabilization of memory traces [150], while the presence of feedback loops allow for the establishment of memory traces spanning the interval of seconds [159]. In our study, we coupled a generic spiking neural network to an external delayed dynamical system, proposing that stabilization of memory traces may arise through the interaction of the network with an external dynamical system. Although our study did not provide an exhaustive exploration of all the possible coupling paradigms, it is a proof of principle, where the properties of a generic spiking neural network can be modulated through the interaction with an external fluctuating system. To this end, as neurons are embedded in a conducting medium, our study raises the question of whether the electric field fluctuations observed in the neural systems are merely an epiphenomena or whether they have a functional role, in that they modulate the spiking activity of neurons and networks of neurons. Furthermore, within this computational model of spiking neural networks, we have been able to reproduce several essential properties of cortical circuits that have been observed in experiments. First, that network activity is stimulus specific and that stimulus is encoded as a temporally-varying pattern of activity [38, 71, 94]. Second, that the observed stimulus-specific neural trajectories are modulated by the presence of cortical plasticity, in accordance to previous studies [150, 151, 255].

In the final study, we recorded macroscopic cortical activity of human-EEG while performing a contour categorization task, where perceptual grouping is a two stage process where local visual features are integrated into a coherent visual percept and further categorized, and tested three hypothesis. We first tested whether the temporal structure within visual stimulus modulates cortical responses. Secondly, we tested whether oscillatory activity within the visual cortex predicts visual perceptual grouping, hypothesizing that perceptual grouping entails oscillatory activity within distributed cortical areas within visual cortices, not constrained to the early visual cortex. Finally, we tested whether and how this categorization process modulates long-range synchronization, hypothesizing that perceptual grouping may be associated to long-range synchronization in the high frequency range. The relevance of our study lies in the fact that, while the processing of visual stimulus is thought to involve the activation of disperse

cortical areas, including early visual cortices [109, 125], parietal cortex [135, 245], and frontal cortices [83, 180], current models of contour integration argue that the perceptual binding of the different elements of the contour occurs through local mechanisms within early visual areas [77, 82]. Through the study of a contour categorization task, we have provided evidence that the temporal structure within the stimulus is crucial for perceptual grouping, as the neural sources recruited during contour categorization with different temporal structures differ. This suggests that the temporal continuity of the stimulus crucially modulates neural processing. Additionally, our results suggest that, while oscillatory activity within occipital cortex predicts the linking of visual features into a coherent contour, the further manipulation and categorization of the visual stimulus involves both local synchronization within parietal/frontal cortices, as well as a transient synchronization among them. Most importantly, by analysing cortical oscillatory activity, we found, that distinct behavioural processes (i.e. saccadic control and contour categorization) can be decoded from neighbouring cortical areas, suggesting that several stages of behavioural processing may simultaneously occur within nearby cortical areas. Finally, focusing on the processing of temporally structured stimulus, we found that long-range synchronization within functionally associated areas reveal a dynamic phase-locking at disjoint timescales associated with contour categorization. In particular, our study reveals a phase locking in alpha, theta and gamma frequencies arising during perceptual grouping, while beta-synchronization seem to involve secondary processes associated to visual processing itself.

5.2 Dynamic neural responses are stimulus-specific and are modulated by the stimulus dynamics

Studies investigating how neural activity correlates to sensory stimulation, cognitive states, or motor activities, report changes in the firing rates [4, 103], on the synchronization levels [232, 268], or in the phase relations [35, 183] within neural signals. However, most of these studies implicitly assume that the neural responses are stationary, as to characterize the average firing rates, neural synchronization, or phase relations empirically, it is necessary to define an encoding time window and a temporal precision by which those measures are computed [195, 251]. Crucially, the length of the encoding window is estimated by considering periods in which the stimulus-specific response is constant, while the temporal precision determines the temporal resolution at which these measures are computed, considering the minimum time interval at which stimulus-specific response can change. In this stationary framework or attractor-based framework, upon the arrival of a signal, the neural system changes until it settles into one of the patterns or attractor states, and only the steady states to which the system arrives, given a set of initial conditions, matter [202, 209]. Within cognitive science, the stationary framework has been discussed under several schemes that argue about what is the specific physiological substrate where the stimulus-specific symbols occur: within individual neurons as **computationalism**, or within the connections between neurons as **connectionism** [84].

However, through this thesis, we have seen that neurons seem inherently capable of representing information in spatio-temporal patterns of activity. Regardless of the spatial scale, we reported that stimuli or behavioural event generate patterns of activity with rich spatio-temporal structure: spiking activity within single neurons reflect spiking statistics of its incoming spike trains (chapter 2), spiking patterns within networks of neurons reflect incoming stimulus (chapter 3), as well as cortical responses reflect visual stimulus -contours- with different temporal structures (chapter 4). Such observations pose an alternative theoretical framework that aims to explain neural functioning: that neural computations occur within transient dynamics [38, 71, 94], also known as the **dynamicist** framework within the cognitive sciences nomenclature [84] or the reservoir computing framework within the computational neuroscience community [133, 162]. Within this framework, the neural system is a non-equilibrium system which, upon arrival of a signal, generates a high-dimensional transient activity. As such, the brain is an inherently dynamic system, that integrates external signals with its ongoing dynamics in a continuous fashion. With the recent advancement of experimental and computational methods that allow for the recording and decoding of a large number of neural signals in parallel [43, 59], the relevance of spatio-temporal coding in the neural system has become more salient. Transient activity seems to be prominent in olfactory processing [28, 172], visual processing [187] and working memory tasks [14]. Importantly, transient dynamics have been reported to be more informative about the stimulus than its static response [172]. As such, it is becoming clearer, that the temporal structure of neural activity can only be neglected at the cost of loosing information [205].

Here, we argue that, while the stationary framework remains as the best framework to account for a number of neural processes (e.g. long-term memory [70, 174]), the reported studies seem to provide experimental evidence supporting the idea that, at least to some extent, the neural system functions in a non-equilibrium fashion, where neural processing can be seen as a dynamic transition through patterns of activity with rich dynamics.

Interestingly, the transient dynamics that arise in the neural system are specific to the dynamics of the stimulus itself, such that they not only encode a specific stimulus, but also its dynamics. This modulation of neural responses due to the temporal structure of the stimulus has been studied in the field of psychophysics under the name of contextual modulations [222], hysteresis [73], after-effects [252] or sequentail learning [57]. While those studies report behavioural differences that arise due to the presence of temporal structures within the stimulus, a recent body of research report a modulation of neural responses due to the temporal structures in stimulus, ranging from working memory dynamic patterns in parietal cortex [14], to spiking activity within monkey V4 [177], monkey IT [154] or mice early visual cortical areas (V1) [93], that learn temporal dependencies of incoming input. In the context of this thesis, stimulus-specific responses are sensitive to stimulus dynamics in either a simple model of a spiking neural network (chapter 2), where transient spiking activity reflects the statistics of the stimuli; a simple model of a spiking neural network from which we can decode two stimuli with the same firing rate but different temporal structure (chapter 3); or cortical dynamics recorded by EEG, where we were able to decode visual stimulus with different temporal structure (chapter 4).

What are the mechanisms that allow the neural system to process stimuli with rich temporal dynamics? Within the body of research, there are several frameworks that aim to explain the mechanisms by which the neural system processes rich spatio-temporal signals, divided into three classes: dedicated, intrinsic, or stationary [34, 98, 100, 108, 129, 130, 169, 265]. Within the dedicated class, the processing of time is performed through specialized mechanisms that explicitly represent time. Supporting this framework, neuroimaging studies report neural responses to precise temporal structures within the stimulus. For instance, auditory cortex activates specifically to a pair or sequence of tones [19], superior temporal sulcus activate selectively to particular full-body or hand movements [99], while the fusiform gyrus activate to the presence of particular facial expressions in complex viewing situations [15].

In contrast, within the intrinsic framework, the representation of time is considered an inherent property of the dynamics of the system, in hand with the dynamicist framework of neural representations [100]. As such, a stimulus with rich spatio-temporal properties will be encoded within the neural system as a neural signal with rich spatio-temporal dynamics. Some of the most compelling evidence supporting the intrinsic timing framework comes from studies within the olfactory system [28, 172] and the visual system [187], where dynamically changing population activity encode stimuli.

Finally, within the stationary framework, time is ruled out through the processing stages, leading to an invariant representation of stimuli [68]. A broad range of experimental studies report this invariant learning of the temporal dimension, such as activation of the fusiform gyrus to the presence of face expressions in complex viewing situations [15] or the presence of place cells in the hippocampus [182]. Along these lines, several studies presented computational mechanisms where the temporal structure within the stimulus is explicitly ruled out through processing stages, as hierarchical models of invariant object recognition [68], hierarchical models of body movement perception [99] or slow feature analysis [284]. However, despite the variety of studies that aim to understand spatio-temporal processing, there is no unifying theory that explains the mechanisms by which the neural system processes rich spatio-temporal signals [34, 58, 98, 108, 129, 130, 265].

Here, we argue that, understanding how the neural system processes dynamic stimuli is crucial for the further understanding of neural processing itself, and any theory that aims to understand neural processing should consider the processing of dynamic signals.

5.3 Characterizing dynamic neural responses in a time-resolved fashion

Timing is crucial for cognitive processing, as our brain makes sense of complex and continuously changing input stream from the environment. The relevance of the temporal structures for neural processing is evidenced by an overwhelming number of studies such as auditory processing [16, 19, 75, 147], attentional control [41, 176, 227, 262] or visual processing [15, 187] among other cognitive processes [14, 28, 99, 172], involving

specific spike times within a local populations or spike times that mediate intra-cortical communication [213].

Unfortunately, the study of how the brain's responses unfold in time has been largely restricted to cognitive-psychology studies, where the time of different mental operations is analysed by describing the response times of the subject to a stimulus or cognitive task [239]. Although such behaviour-based techniques can provide extensive insights into the dynamics of the neural responses associated to cognitive processing, they cannot provide a complete picture on the link between the neural signals and the behaviours observed. In particular, there is no disentanglement of whether cognitive processes are processed in a single cortical area, or through the interaction of parallel processing streams [142], as well as no indication of what are the intermediate stages involved in the cognitive process. This approach of studying timing is an example of the dearth of experimental methods which allow for the clear segregation of cognitive processes in space and time, so that its segregation has to be done through the simplification of the task to be tested [137].

This approach is usually complemented by standard neuroscience techniques that involve the averaging of neural responses over several repetitions of a stimulus or behaviour. As the variability of cortical responses to repeated stimulation is often as large as the response itself [11], and considering that neural variability reflects the noise of the system, averaging increases the signal to noise ratio (e.g refereed in the literature as Stimulus-Triggered Average, Evoked Responses, etc). However, this approach does not only cancel out the signal variability, but also decreases the possible generalization to neural processing of real-world signals, as the brain processes information based on single events in a time-resolved fashion.

Recently, the advancement of decoding methods provides a framework with which the neural activity can be analysed; both on a single-trial basis and in a time-resolved fashion. As such, it provides access to both the content and the inherent dynamics of neural representations of a stimulus or a cognitive task. It is common to many of these new decoding approaches that they compute the probability of a stimulus being presented given a neural response [49, 50, 143, 275]. This, in turn, provides a quantitative measurement that describes some sort of association between a neural signal and the stimulus [205]. Once the decoding algorithm is trained, the decoding methods quantify the strength of the association between the stimulus and the neural signal on a single trial basis. Additionally, by selecting neural signals based on their strength of association to the stimulus or cognitive task in hand, these decoding algorithms allow for the disentanglement of the location of cognitive processes, i.e. if they occur in a single cortical area or through the interaction of parallel processing streams. If applied in a time-resolved fashion, those same decoding algorithms allow for testing at which moment specific mental content becomes decodable from neural activity [142]. With that, we can characterize the time course of neural representations, shedding light on the temporal organization of cognitive processing.

In light of these advances, it is now possible to decode low-level stimulus features such as the spatial orientation of visual stimulus [116], or its color [29] from high resolution fMRI, up to the point that it is now possible to reconstruct which static images [184], moving objects [184], or which movies the subject is watching [189].

Despite the intrinsic low spatial resolution of the method, low-level features can be similarly decoded from EEG/MEG activity, where several studies report the successful decoding of motor [275], auditory [143] or visual stimuli [49, 50]. Various studies have also shown that it is also possible to decode higher processing stages such as perceptual expectation of a known visual stimuli [144] or the categorical classification of a visual stimuli [50, 212].

In this dissertation, we have focused both on decoding low-level stimulus features (spatial location of visual stimuli) and on the decoding of higher cognitive stages (categorical classification of a stimuli), as well as on the decoding of stimulus-specific spiking activity that arises in a generic spiking neural network. In doing so, we have shown that the decoding of time-varying neural signals can be applied to a broad range of neural signals, ranging from spiking activity within neural networks, to the neural activity recorded through EEG that arises in response to visual stimulation. Through the establishment of time-resolved decoders, we reported how neural representations of a specific stimulus unfold over time, providing a novel methodology to understand how a stimulus is represented, manipulated, and transformed.

Altogether, the development of decoding methods, that can be applied to successive time points, can be used to quantify where and for how long specific information can be decoded from neural activity (either stimulus or behaviourally related). However, it must be noted that these decoding approaches can be used to further understand the mechanisms through which the brain encodes information. In particular, this methodology paves the way for new and interesting questions, such as, which features in a neural signal would be better predictors of the information of interest? A decoder could be trained on the raw neural data, on its time-frequency transformation, or in any linear or non-linear transformation that we could imagine. By examining how well we can predict the presence of a stimulus/behaviour, we can find out which features were carrying the relevant information, bringing us closer to the question of how the neural system encodes information. In a similar manner, comparing the features within the decoders that are used to predict different stimuli, we may disentangle what features are used by the neural system to encode stimulus-specific features. Furthermore, by testing the ability of a trained decoder to generalize over time, we may be able to explore the stability of such neural representations and, eventually, disentangle whether and how neural signals are transformed over time. In a similar manner, one could test the generalization capability of a trained decoder across experimental conditions, in effect describing how neural representations generalize across stimulus or behavioural tasks. A few studies have already explored the temporal generalization of the visual and auditory systems, reporting that stimulus-specific patterns can be modulated by the specific cognitive task at hand (see [142] for review). Finally, the further development of decoding methods has advanced, and will continue to advance, the field of brain computer interfaces (BCI), that bridge direct communication between the neural system and an external device [270].

5.4 Perspectives and open issues

In this thesis we have focused on exploring the impact of spatially-structured stimulus on neural representations and processing, describing the neural system as a self-organizing system that interacts and adapts to environmental changes. There are several directions in which the work presented here could be extended.

First, since our study on single-neuron shows that the temporal structure of incoming spike trains modulate the speed at which the synaptic weight change, it would be interesting to extend these results by investigating this aspect on recurrent neural networks and to study a) whether and how temporally structured activity propagates within recurrent networks of balanced excitation inhibition, as suggested by [51] and b) whether the speed and strength of synaptic weight changes are modulated by temporally structured activity within recurrent neural networks.

Second, our study on a generic spiking neural network proposed that the limited memory trace of a spiking neural network can be extended by both the presence of ongoing plasticity or through the coupling with an external delayed dynamical system. Although our study did not provide an exhaustive exploration of all the possible coupling paradigms, it is a proof of principle where the properties of a generic spiking neural network can be modulated through the interaction with an external fluctuating system. Given that neurons are embedded in a conducting system, it may be interesting to experimentally test whether the electric field fluctuations observed in the brain are merely an epiphenomena or whether they have a functional feedback role that affects the spiking activity of the neurons. Furthermore, our study reported the emergence of stimulus-specific dynamic patterns within a generic spiking neural network. Within this context, there are at least two important follow up questions. The first, what are the neural mechanisms that allow for the delineation of stimulus-specific patterns? Computational studies on recurrent neural networks propose that plasticity mechanisms enable the generation of stimulus-specific representations [151]. To this end, it would be interesting to test the behavioural limits of such pattern learning, and exploring whether these behavioural limits can be fully explained by the network dynamics of a plastic spiking neural networks. Secondly, how specific these transient dynamics are to different stimuli? Experimental studies report that while those transient dynamics are stimulus-specific, they are also resistant to noise, so that reproducible trajectories are obtained despite small variations in the stimulus [28, 172]. Recent computational studies suggest that the presence of activity-dependent plasticity mechanisms enables for the generation of neural representations from a noisy environment [255]. To this end, it would be interesting to explore what are the limits in the noise signals that would allow for the creation of this stimulus-specific boundaries, with the goal of answering the broader question of whether the neural system can learn to associate a meaning or representation to any spatio-temporal pattern.

Third, our study on contour integration reports that oscillatory activity within parietal and frontal cortices predicts perceptual grouping of a contour, as well as its phase locking in theta, alpha and gamma frequencies. While occipital cortical areas that involve early visual cortices are active during visual stimulation, they do not seem to be involved in the identification of particular contours. To this end, it would be

interesting to extend our work in several directions. First, we can test whether our findings generalize under perceptual variability, so that the orientation of local elements that form the contour do not perfectly co-align. As current models of contour integration argue for the presence of a local mechanism where the different elements of the contour are combined within early cortical areas [77, 82], we would expect that perceptual variability does not modulate cortical activity within parietal and frontal cortical areas. Note that this data has been already recorded and analysed, and there is a poster and journal article in preparation. Second, we can test whether our findings are generalizable when modulating the cognitive demands of the task: as our task requires the grouping and classification of two contours, would our findings generalize to three or ten contours? The relevance of this task relies on challenging the framework of perceptual decision making, where the decision between two alternatives is classically modelled as a competition process between the two neural representations [102]: as the competition process is thought to be locally implemented, within the cortical areas that perform the integration of sensory information, we would expect a differential activity within both parietal and frontal cortical areas. Third, while the current decoding algorithm allows to establish a correlative association between oscillatory activity within parietal and frontal cortices and perceptual grouping, it would be highly interesting to test for a causative association through the implementation of on-line decoding: what are the exact features of the recorded EEG activity that predict the contour perception of a subject? The implementation of on-line decoding for a single trial and in a subject specific manner is particularly relevant to determine the behavioural relevance of those neural features that have a high signal to noise ratio, whose trial-to-trial and between subject variability is so high that it cannot be detected by methods that require averaging.

APPENDIX A

Appendices

A.1 Appendix I: Regression models

Given a set of observations $D = (x_1, y_1), (x_2, y_2), \ldots (x_n, y_n)$ for $x_i \in \mathbb{R}^d$ and $y_i \in \mathbb{R}$, the goal of regression models is to find a set of parameters w so that we can establish a relationship between variables x_i and y_i such as $Y = W \cdot X$, for $Y = y_1, y_2, \ldots, y_n$ and $X = x_1, x_2, \ldots, x_n$.

For example, given a set of time series x_i describing the change of temperatures (covariates x_i) in two different cities (response variables y_i), the goal of a regression model is to find a set of parameters w that relate the time series x_i to the response variables y_i.

With this goal in mind, the process by which a regression model is implemented can be divided into five major steps: acquiring data, obtaining the set of weights w (parameter estimation or training phase), estimating whether the model has learnt data structure (model validation and generalization) and, finally, once the regression model

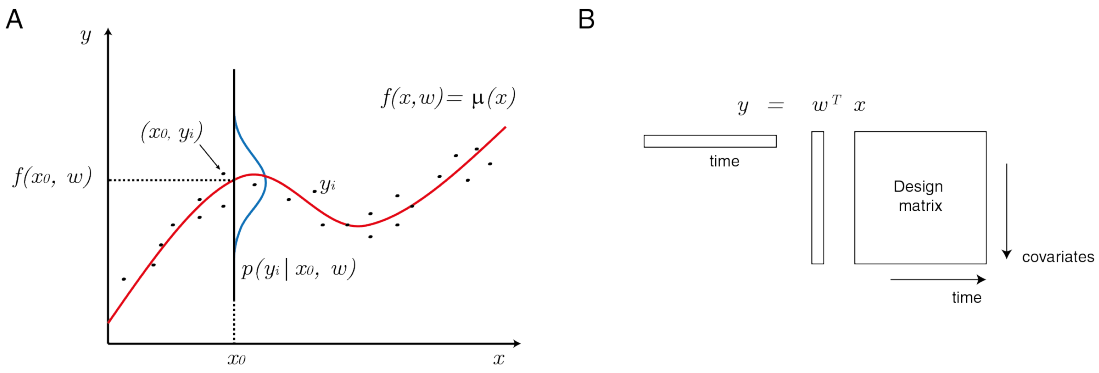

FIGURE A.1: Visualization of a graphical (A) and matrix (B) representation of a regression problem

has been validated and checked for generalization, we may aim to compare different models (model comparison). This annex will be discussing the latter four, with a final remark on regularization methods. Note that this whole section is based on information collected from several references listed at the end of the appendix itself.

Further clarifications

Before continuing, I would like to make some more clarifications on regression models. Consider that we have computed a set of parameters W that establish the best relationship between predictors X and the response variables Y. This process can be compared with a mapping from data such that every observation x_i with a trained w can be transformed into a variable y_i so that $y_i = f(x_i, w)$.

This mapping function $y_i = f(x_i, w) = \mu(x)$ is the underlying function $\mu(x)$ of the data D (see Figure A.1 A). If the observed data D is a randomly drown sample of a Gaussian process with mean μ and variance σ, and if the variance is constant over time, the resulting underlying function $\mu(x)$ corresponds to the expected value of the covariates, so that:

$$\mu(x) = f(x_i, w) + \varepsilon_i \text{ where } \varepsilon_i \; \mathcal{N}(\mu, \sigma^2)$$

Once the relationship w between observations x_i and target values y_i, we can also use this model as a **generative model**, so that we can predict the value of y_i for a new set of observations x_i.

A last remark about nomenclature of the observation: within the regression model context, x_i can be refereed as covariates or predictors, while y_i are the model outcomes, response variables or target values. In this section, those labels will be used intermingled.

Model Assumptions

Given the previous definition of a regression model, consider the assumptions that of the model upon data to analyse:

- **Linearity** The mean of the response variable y_i is a linear combination of the parameters w and the predictor variables x_i or a transformation of predictor variables $\Phi_i(x)$.
- **Independence of errors** Observations are independent and identically distributed random variables drawn from a Gaussian distribution $y_i \; \mathcal{N}(\mu, \sigma^2)$, so that at each instance i data will be distributed according to a Gaussian distribution with mean μ and variance σ^2.

- **Known variance** The variance σ^2 of the covariates y_i is known, so that the regression problem is reduced to find the underlying function $\mu(x)$.
- **Constant variance** Observations x_i are weakly stationary, whose second moments (variance σ^2) do not change over time.

What can be modelled?

Given this set of assumptions, which data can be analysed by regression models?

The simplest model of regression is the one that involves a linear dependency between predictors x_i and the outcomes y_i (linear regression), given that both predictors and outcomes are i.i.d. samples drawn of a Gaussian distribution with constant variance.

How can we then model dependencies between observations that are not linear?

The predictors x_i can be arbitrarily transformed by basis functions. In fact, multiple copies of the same predictor x_i can be transformed by a different basis functions, making them linearly independent for the regression model to be solved. This process leads to a General Linear Model, a powerful tool to analyse data dependencies.

The outcomes y_i can be transformed by a link function, basically a function that will relate the non-Gaussian error distribution error of y to the regression model. This mapping leads to the Generalized Linear Models.

Linear regression

The simplest model of regression is the one that involves a linear dependency between predictors x_i and the outcomes y_i so that:

$$\begin{aligned} y &= f(x,w) = w_0 + w_1 x_1 + w_2 x_2 + \ldots + w_d x_d \\ y &= f(x,w) = \sum_{i=0}^{n} w_i x = W^T X \end{aligned} \tag{A.1}$$

The matrix representation of linear regression can be visualized in Figure A.1 B. Linear regression will only be able to find linear relationships between observations and covariates. In this case, computing the parameters w is reduced to an algebraic problem of $Y = W^T X$, where both Y and X are given by the data. As such, computing the parameters W is reduced to solving the following inverse problem: $W = X^+ Y$, where X is referred as the **design matrix** and the notation $^+$ indicates the Moore–Penrose pseudoinverse (see section A.1.1).

General Linear Models

As mentioned, predictors x_i can be arbitrarily transformed by basis functions mapping them to a higher non-linear space, while being still linear within the regression model itself.

Basis functions are a set of linearly independent vectors that, in a linear combination, can represent every vector in that vector space. For instance, the vectors $a = [001]$, $b = [010]$ and $c = [100]$ are basis functions of a 3 dimensional vector space.

$$\begin{aligned} y &= f(x, w) = w_0 + \sum_{i=1}^{n-1} w_i \Phi_i(x) \\ y &= f(x, w) = \sum_{i=0}^{n} w_i \Phi_i(x) = w^T \Phi_i(x) \end{aligned} \tag{A.2}$$

where $\Phi_i(x)$ are known basis functions. The computation of these parameters W is equivalent on maximizing the likelihood that a set of parameters describes the data best, namely, maximizing $W_{ML} \arg\max p(D|W)$.

The simplest basis expansion that can be used is a polynomial regression:

$$\begin{aligned} y &= f(x, w) = w_0 + w_1 x + w_2 x^2 + \ldots + + w_d x^n \\ y &= f(x, w) = \sum_{i=0}^{n} w_i x^i = w^T \Phi_i(x) \end{aligned} \tag{A.3}$$

This transformation makes regression models powerful, with he ability to estimate non-linear dependencies from observations. Note that with this generalization, the estimation of the parameters W still reduced to solving the inverse problem: $W = A^+ Y$, where $A = \Phi(X)$ is referred as the **design matrix** and the notation $^+$ indicates the Moore–Penrose pseudoinverse (see section A.1.1).

Generalized Linear Models

The Generalized Linear models are a generalization of linear regression that allows outcomes y_i to have error distributions other than Gaussian, via mapping the outcomes y_i by the link function.

The link function establishes a relationship between the distribution of the observed y_i and the Normal distribution that is required to solve the regression problem.

For instance, a linear regression model can be seen as the simplest case of a generalized linear model, where the link function is the identity and the outcomes y_i have already a Gaussian distribution with constant variance.

Distribution of y_i	Link Function	Usage
Normal	Identity: $\mu = W^T X$	Data that has a linear response (real values within $-\inf, +\inf$))
Exponential or gamma	Inverse: $-\mu^-1 = W^T X$	Data that has an exponential or gamma-like response (real values within $(0, +\inf)$)
Poisson	Log: $ln(\mu) = W^T X$	Counting occurrence data, like, sales per minute (integer values within $[0, +\inf)$)
Bernoulli, Binomial or Categorical	Logit: $ln(\frac{\mu}{1-\mu} = W^T X$	a single yes/no occurrence, counting of k type 1 occurrences out of N, counting of k occurrences of type K, respectively (integer values within $[0, 1]$, $[0, N]$ and $[0, K)$ respectively)

Regardless on the modifications that can be applied on the observations $D = (x_1, y_1), (x_2, y_2), \ldots (x_n, y_n)$, the regression problem is solved based on the linear dependency between predictors x_i and outcomes y_i. No difference between linear models, general linear models or generalized linear models is made in further sections.

A.1.1 Parameter Estimation

Parameter Estimation: Least-squares

Several methods have been developed to estimate those parameters w, differing on the complexity of the algorithm, robustness towards heavy-tailed distributions and presence of closed form solution.

The most common of the parameter estimation methods is the least-squares estimation, which can be derived towards the maximum likelihood approach. Intuitively, in the least-squares estimation, the goal is to minimize the error term between the observed variable Y and its approximation $w^T x_i$, namely, E is the error function to minimize and our goal is $E = min \sum (y_i - w^T x_i)^2$. Note that the squared distance between to vectors corresponds to the squared Euclidean distance between two points, a distance measure between two variables. Similarly, within maximum likelihood approach, our goal is to find a set of parameters w that describe our data D the best. Namely, we aim to find the maximum likelihood that data D can be described by a set of parameters w so that $\arg\max_w p(D|w)$.

In this section, we are going to describe regression models from the mentioned parameter estimation methods, finishing by making a link between the two approaches (see section A.1.1).

Ordinary least squares

The method minimizes the squared error between the observed outcomes y_i and the computed approximation $w^T x_i$, so that the estimated parameters $\hat{w}$ are the ones that lead to the minimum error:

$$\hat{W} = \arg\min ||Y - W^T X|| \tag{A.4}$$

Parameter Estimation: Maximum Likelihood (MLE)

Formally, given a set of observations $D = x_1, x_2, \ldots x_n$ for $x_i \in \mathbb{R}^d$ and an assumed set of distributions $\rho_\theta : \theta \in \Theta$, we assume that D is a randomly drown sample of an underlying distribution ρ_θ, our goal is to estimate the true distribution ρ_θ where the data comes from, namely, find the maximum probability $p(D|\theta)$. θ_{ML} is the maximum likelihood estimator over Θ, also denoted $\mathcal{L}$.

Definition:

θ_{ML} is the maximum likelihood estimator over $\theta \in \Theta$ so that $\theta_{ML} = \arg\max_\theta p(D|\theta)$, where $p(D|\theta) = p(x_1, x_2, \ldots, x_n|\theta) = \prod_{i=1}^n p(x_i|\theta) = \sum_{i=1}^n log(p(x_i|\theta))$.

Properties of the Maximum Likelihood Estimation

A maximum likelihood estimator θ_{ML} may not be unique. If the likelihood function $p(D|\theta)$ is strictly concave in θ, then the θ_{ML} is unique when it exists. The solution to an optimization problem exists if the parameter space Θ is compact and if the likelihood function $p(D|\theta)$ is continuous on that space.

The estimator is easy to compute and invariant under scaling parameters, so that $\prod_{i=1}^n p(x_i|\theta) = \sum_{i=1}^n log(p(x_i|\theta))$.

Likelihoods of can be linearly combined so that:

$$\begin{aligned} \mathcal{L}(\theta) &= \mathcal{L}_1(\theta) + \mathcal{L}_2(\theta) \\ Ln\mathcal{L}(\theta) &= Ln\mathcal{L}_1(\theta) + Ln\mathcal{L}_2(\theta) \end{aligned}$$

Maximum Likelihood Estimator for Gaussian Processes

If the set of parameters w that we want to estimate are Gaussian, so that $\theta = (\mu, \sigma^2)$ where μ is the mean and σ^2 is the standard deviation of the Gaussian, we can analytically obtain the maximum likelihood values by the following derivations:

$$\begin{aligned}
\mathcal{L}(\theta) = p(D|\theta_{ML}) &= \max_{\theta} p(D|\theta) \\
&= \max_{\theta} p(x_1, x_2, \ldots, x_n|\theta) = \max_{\theta} \prod_{i=1}^{n} p(x_i|\theta)
\end{aligned}$$

Logarithm of the Likelohood

$$\begin{aligned}
\ln\ p(D|\theta) &= \ln\ p(D|\mu, \sigma^2) = \ln \prod_{i=1}^{n} \mathcal{N}(x_i|\mu, \sigma^2) \\
&= \sum_{i=1}^{n} \ln \mathcal{N}(x_i|\mu, \sigma^2) \\
&= \sum_{i=1}^{n} \ln \left[\frac{1}{\sqrt{2\pi\sigma^2}} exp\left(-\frac{1}{2\sigma^2}(x_i - \mu)^2 \right) \right] \\
&= \ln \left(\left(\frac{1}{\sqrt{2\pi\sigma^2}} \right)^n \right) - \frac{1}{2\sigma^2} \sum_{i=1}^{n} (x_i - \mu)^2 \\
&= -\frac{n}{2} \ln \sigma^2 - \frac{n}{2} 2\pi - \frac{1}{2\sigma^2} \sum_{i=1}^{n} (x_i - \mu)^2
\end{aligned} \tag{A.5}$$

This is the logarithmic form of the likelihood, given that the observations of interest follow a Gaussian distribution. Next, minimize over both of the parameters of interest.

Minimize over μ

$$\begin{aligned}
\frac{\partial}{\partial \mu} \ln\ p(D|\theta) &= -\frac{\partial}{\partial \mu} \frac{n}{2} \ln \sigma^2 - \frac{\partial}{\partial \mu} \frac{n}{2} 2\pi - \frac{\partial}{\partial \mu} \frac{1}{2\sigma^2} \sum_{i=1}^{n} (x_i - \mu)^2 \\
&= \frac{1}{2} \sum_{i=1}^{n} 2(x_i - \mu) \Rightarrow \sum_{i=1}^{n} x_i = \sum_{i=1}^{n} \mu \\
&\Rightarrow \mu_{ML} = \frac{1}{n} \sum_{i=1}^{n} x_i
\end{aligned} \tag{A.6}$$

Minimize over σ^2

$$\begin{aligned}
\frac{\partial}{\partial\sigma}\ln\ p(D|\theta) &= -\frac{\partial}{\partial\sigma}\frac{n}{2}\ln\sigma^2 - \frac{\partial}{\partial\sigma}\frac{n}{2}2\pi - \frac{\partial}{\partial\sigma}\frac{1}{2\sigma^2}\sum_{i=1}^{n}(x_i-\mu)^2 \\
&= -\frac{n}{2}\frac{1}{\sigma^2} + \frac{1}{2}\frac{1}{(\sigma^2)^2}\sum_{i=1}^{n}(x_i-\mu)^2 \\
&= \frac{1}{\sigma^2}\left[\frac{1}{2\sigma^2}\sum_{i=1}^{n}(x_i-\mu)^2 - \frac{n}{2}\right] \\
&= \frac{1}{2\sigma^2}\left[\frac{1}{\sigma^2}\sum_{i=1}^{n}(x_i-\mu)^2 - n\right] \\
&\Rightarrow \quad \sigma_{ML} = \frac{1}{n}\sum_{i=1}^{n}(x_i-\mu)^2
\end{aligned} \tag{A.7}$$

Maximum Likelihood Estimator for Regression Models

The computation of parameters w of the regression model is equivalent on maximizing likelihood, so that $\mu_{ML}(x) = \mu(x) = f(x,\theta)$. First consider that our observations $D = (x_1, y_1), (x_2, y_2), \ldots (x_n, y_n)$ have the following likelihood function:

$$\begin{aligned}
\mathcal{L}(\theta) = p(D|\theta_{ML}) &= \max_{\theta} p(D|\theta) \\
&= \max_{\theta} p(y_1, y_2, \ldots, y_n | x_1, x_2, \ldots, x_n, \theta) = \max_{\theta}\prod_{i=1}^{n} p(y_i|x_i,\theta)
\end{aligned}$$

Start on logarithmic form of the likelihood presented in equation A.5 and consider that the observations y_i are the ones that we want to model. The variability σ^2 of the observations is constant over time, so that we do not need to make any estimation on the regression problem. This means, that the parameters that we aim to estimate are concentrated on the μ, and according to equation A.1 $\mu = f(x,\theta) = W^T X$.

$$\begin{aligned}
\ln\ p(D|\theta) &= -\frac{n}{2}\ln\sigma^2 - \frac{n}{2}2\pi - \frac{1}{2\sigma^2}\sum_{i=1}^{n}(y_i-\mu)^2 \\
&= -\ln\left(\frac{1}{\sqrt{2\pi\sigma^2}}\right)^n - \frac{1}{2\sigma^2}\sum_{i=1}^{n}(y_i - w^T x_i)^2
\end{aligned}$$

The first term is constant. In order to maximize $p(D|\theta)$ we will have to minimize the second term. In other words, maximum likelihood estimation of a linear regression problem is reduced to the following minimization problem:

$$\min \sum_{i=1}^{n} (y_i - w^T x_i)^2 \tag{A.8}$$

Define $A = W^T$ as the **design matrix** and rewrite:

$$\begin{aligned} \min \sum_{i=1}^{n} (y_i - w^T x_i)^2 &= \max(p(D\theta)) \\ &= (Y - AX)^T (Y - AX) \\ &= ||Y - AX||^2 \end{aligned} \tag{A.9}$$

The resulting equation A.9 is by definition the squared error. In summary, minimizing the squared error leads to the maximum likelihood estimators.

Furthermore, we can similarly rewrite this equations to understand why regression models can be solved through solving the inverse problem:

$$\begin{aligned} \max(p(D\theta)) &= \min \sum_{i=1}^{n} (y_i - w^T x_i)^2 \\ &= \min((Y - AX)^T (Y - AX)) \\ &= \min(Y^T Y - 2Y^T AW + W^T A^T AW) = \min(Y^T Y - 2W^T A^T Y + W^T A^T AW) \end{aligned}$$

In order to minimize, take the gradient or partial derivative with respect to the parameters W:

$$\begin{aligned} \frac{\partial}{\partial W}(\min(Y^T Y - 2W^T A^T Y + W^T A^T AW)) & \\ -A^T Y + A^T AW &= 0 \Leftrightarrow W = (A^T A)^{-1} A^T Y \\ \text{where } A^+ &= (A^T A)^{-1} A^T \text{ is the pseudoinverse} \\ \text{then } W &= A^+ Y \end{aligned}$$

In other words, when the regressors are normally distributed y_i $\mathcal{N}(\mu, \sigma^2)$ with a constant σ^2, then the maximum likelihood estimate of those parameters are those arrived by least-squared estimators or by the Monroe-Penrose pseudoinverse.

Relation to Bayes rule

Very importantly, I would like to explicitly mention a link between linear regression and the Bayes theorem.

Note that the outcome of a regression model is $\mu(x) = \arg\max p(D|\theta)$, namely, the likelihood of the observed data D being drown from an underlying function with parameters θ.

Note that the prior probability of occurrence of a parameter θ is equal for all parameters (so that $p(\theta) = p(\theta_i)$).

This leads to the following simplification:

$$\begin{aligned} p(D|\theta) &= \frac{p(\theta|D)p(D)}{p(\theta)} \\ p(D|\theta) &\simeq p(\theta|D) \end{aligned} \tag{A.10}$$

Namely, by computing a regression model we obtain the likelihood $p(D|\theta)$ of that model, which is equal to the posterior probability $p(\theta|D)$.

A.1.2 Model Validation - Goodness of Fit

Within regression model context, model validation is concerned with the process of deciding whether the results obtained from the regression model are, indeed, describing a relationship between variables that can be observed in data.

Generalizing, measures that estimate how well a statistical model g_i fits a set of observations D are grouped under the concept of goodness of fit. **Goodness of fit** measures can be used in statistical hypothesis testing, e.g. to test for normality of residuals, to test whether two samples are drawn from identical distributions (see Kolmogorov–Smirnov test), or whether outcome frequencies follow a specified distribution (see Pearson's chi-squared test).

This section contains a simplified sample of goodness of fit measures, and can be divided into two parts: the estimation of the error of the model on approximating the real data dependencies, and the predictive capabilities of the model, or whether and how well the model is able to predict new data.

Error Estimation

Once the model has been trained and the parameters θ estimated, how well does the parameters describe my data? Regression models are supervised learning algorithms,

so that within the supervised data itself $D = (x_1, y_1), (x_2, y_2), \dots (x_n, y_n)$, we have already information about variable of interest y_i .

From a set of observations $D = (x_1, y_1), (x_2, y_2), \dots (x_n, y_n)$, we have trained a model $g(x|D)$. How well the model represents the data can be computed by the **mean squared error**, estimated as in A.11. Similarly, we can define the mean or expected error when we train several realizations of the same model as in equation A.12.

$$MSE = \frac{1}{n}\sum_{i=1}^{n}(y_i - g(x_i|D))^2 \tag{A.11}$$

$$E[MSE] = \frac{1}{n}\sum_{i=1}^{n}E[(y_i - g_i(x_i|D))^2] \tag{A.12}$$

Note that in this case, the distance measure between estimated and true model is computed through the Euclidean distance. The actual implementation of the distance measure on the MSE will depend on the data statistics.

Bias-Variance decomposition Crucial to the understanding of how well an estimated model g_i describes the real underlying data dependencies f is the bias-variance decomposition: any model g_i approximating the real function f have three unavoidable sources of noise.

Until now, the MSE has been used to estimate how far our model g_i stands from the observed outcomes y_i. This process can be brought slightly further. The set of observations D have come about from an underlying real data model f, the one we aim to approximate by computing g_i. What we are going to do is to extend the MSE so that we can understand whether and how well we can ever approximate the real underlying function f. For that, we can simply rewrite the MSE as follows:

$$\begin{aligned} E[(y_i - g_i)^2] &= E[(y_i - f_i + f_i - g_i)^2] \\ &= E[(y_i - f_i)^2] + E[(f_i - g_i)^2] + 2E[(f_i - g_i)(y_i - f_i)] \\ &= E[\epsilon^2] + E[(f_i - g_i)^2] + 2\left(E[f_i y_i] - E[f_i^2] - E[g_i y_i] + E[g_i f_i]\right) \end{aligned}$$

We decompose the third term as follows: consider that f is constant and $E[y_i] = f_i$. In this way $E[f_i y_i] = f_i^2$ and $E[f_i^2] = f_i^2$. Further $E[g_i y_i] = E[g_i(f_i + \epsilon)] = E[g_i f_i + g_i \epsilon] = E[g_i f_i] + 0$. With these reformulations, the third term above is reduced to zero, so that $E[(y_i - g_i)^2] = E[\epsilon^2] + E[(f_i - g_i)^2] + 0$

The second term can be decomposed similarly: $E[(f_i - g_i)^2] = E[(f_i - E[g_i])^2] + E[(E[g_i] - g_i)^2] + 0$.

Thus, the MSE can be rewritten as:

$$\begin{aligned} E[(y_i - g_i)^2] &= E[\epsilon^2] + E[(f_i - E[g_i])^2] + E[(E[g_i] - g_i)^2] \\ &= \text{Var}(\epsilon) + (\text{bias})^2 + \text{Var}(g_i) \end{aligned}$$

Very importantly, the mean squared error is composed of three types of errors: variance of the noise of the data ϵ, bias and variance.

The **bias** is the systematic deviation of the model g_i from the real underlying function f, representing how accurate the model is across different training instances. The **variance** represents whether the model predicts or represents the particular realization of this data, in other words, how sensitive the model is to small changes in the training set.

Generally, the bias and variance of an estimated model parameter $\hat{\theta}$ can be defined:

$$\text{Bias} \quad : \quad bias(\hat{\theta}) = E(\hat{\theta}) - \theta = E[\hat{\theta} - \theta] \tag{A.13}$$

$$\text{Variance} \quad : \quad \text{Var}(\hat{\theta}) = E[(\hat{\theta} - \theta)^2] \tag{A.14}$$

Predictive Power: Training and Testing

Further, once the model has been trained and the parameters θ estimated, how well can the model generate predictors y_i for a set of observations? Namely, we are testing the predictive power of our model.

There are several methods to estimate the predictive power, few of them are going to be covered here. This section aims to provide an introduction and intuition about the process.

Essentially, observed data $D = (x_1, y_1), (x_2, y_2), \ldots (x_n, y_n)$ is divided into training and testing sets: the one in which the parameters θ are going to be computed, and the one in which an estimation of $\hat{y_i}$ is going to be made and compared to the observed y_i. The simplest form of splitting the data can be visualized in A.2 A. For further information, see (REF).

Overfitting Further, we can also conceptualize the model accuracy by two measures: overfitting and underfitting. Overfitting occurs when the model describes the random noise ϵ rather than the dependencies f between the observations $y = f(x) + \varepsilon$. In other words, the model will have a poor predictive performance on test data.

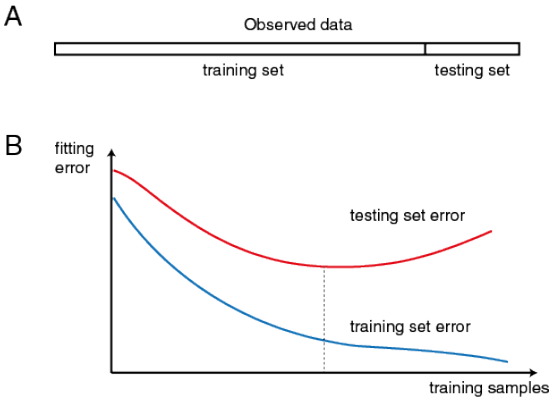

FIGURE A.2: Visualization of A) data partition on training and testing sets and B) overfitting of an estimated model

Overfitting occurs when the model is too complex (has too many parameters) and tries to fit all small variations on the data. As such, the error of the model if checked on training data, will keep reducing as the complexity of the model increases (see Figure A.2B). However, if we use the model to generate new observations y_i and test those observations against some unseen testing data, the error may as well increase.

We could also present the same problem by asking: what is the 'appropriate' number of parameters in our model so that we get the minimum error and higher predictive power? Once we have estimated the goodness of fit of our model, we can solve this question by comparing different models g_i.

A.1.3 Model Comparison and Model Selection

There are several methods for choosing among the set of candidate models, based on several quantitative measures that can be used to describe the model g_i. Model comparison and selection is not the focus of this annex, we will rather refer to other sources (see A.1.5 section for references).

A.1.4 Regularization Methods

Generalizations of the linear regression makes regression models an extremely powerful inference method. In fact, we have presented overfitting as the case in which regression models are too complex and model noisy variations of data rather than the underlying structure. Another way of avoiding over-complex models is by applying regularization to the parameter estimation process.

Regularization consists on introducing additional constraints when solving ill-posed problems. Ill posed problems are the ones where either the existence or the uniqueness of a solution are not ensured, i.e. regularization, or when the solution depends on the initial conditions.

Common examples of regularization are lasso regularization (L1-norm), ridge or Tikhonov regularization (L2-norm), which differ on the additional constraints imposed on the solution. In fact, if described from the point of view of Bayesian statistics, different

regularization methods can be viewed as special cases of the same regression problem. Regularization methods are not the focus of this annex, we will rather refer to other sources (see A.1.5 section for references).

A.1.5 References

Bishop, C.M. (2007). Pattern Recognition and Machine Learning (Springer).

Fahrmeir, L., and Tutz, G. (2001). Multivariate Statistical Modelling Based on Generalized Linear Models (Springer; 2nd edition).

Bakeman, R., and Robinson, B.F. (2005). Understanding statistics in the behavioral sciences (Cengage Learning).

Friedman, J., Hastie, T., and Tibshirani, R. (2010). Regularization Paths for Generalized Linear Models via Coordinate Descent. J. Stat. Softw. 33, 1–22.

Bibliography

[1] Abbott, L. F., and Nelson, S. B. Synaptic plasticity: Taming the beast. *Nature* (2000), 1178–1183.

[2] Abraham, W. C. Metaplasticity: tuning synapses and networks for plasticity. *Nature reviews Neuroscience 9*, 5 (May 2008), 387.

[3] Adrian, E. The Electrical Activity of the Mammalian Olfactory Bulb. *Electroencephalography and clinical neurophysiology 2* (1950), 377–388.

[4] Adrian, E., and Zotterman, Y. The impulses produced by sensory nerve endings. Part 2. The response of a single End-Organ. *J. Physiol. 61* (1926), 151–171.

[5] Ahissar, E., and Zacksenhouse, M. Temporal and spatial coding in the rat vibrissal system. *Progress in brain research 130* (Jan. 2001), 75–87.

[6] Allen, N. J., and Barres, B. A. Glia — more than just brain glue. *Nature 457*, February (2009), 675–677.

[7] Alvarez-Maubecin, V., Fernando Garcia-Hernandez, Williams, J. T., Bockstaele, E. J. V., Garcia-Hernandez, F., Williams, J. T., and Van Bockstaele, E. J. Functional Coupling between Neurons and Glia. *The Journal of neuroscience : the official journal of the Society for Neuroscience 20*, 11 (June 2000), 4091–4098.

[8] Andrew, B., and Ketiner, R. E. Neuronal population coding of movement direction. *Science 233* (1986).

[9] Araque, A., and Navarrete, M. Glial cells in neuronal network function. *Philosophical transactions of the Royal Society of London. Series B, Biological sciences 365*, 1551 (Aug. 2010), 2375–81.

[10] Arenas, a., Diazguilera, a., Kurths, J., Moreno, Y., and Zhou, C. Synchronization in complex networks. *Physics Reports 469*, 3 (Dec. 2008), 93–153.

[11] Arieli, A., Sterkin, A., Grinvald, A., and Aertsen, A. Dynamics of Ongoing Activity: Explanation of the Large Variability in Evoked Cortical Responses. *Science 273* (1996).

[12] Averbeck, B. B. Poisson or not Poisson: differences in spike train statistics between parietal cortical areas. *Neuron 62*, 3 (May 2009), 310–1.

[13] Averbeck, B. B., Latham, P. E., and Pouget, A. Neural correlations, population coding and computation. *Nature Reviews Neuroscience 7*, 5 (2006), 358–366.

[14] Baeg, E. H., Kim, Y. B., Huh, K., Mook-Jung, I., Kim, H. T., and Jung, M. W. Dynamics of population code for working memory in the prefrontal cortex. *Neuron 40*, 1 (Sept. 2003), 177–88.

[15] Bartels, A., and Zeki, S. Functional brain mapping during free viewing of natural scenes. *Human brain mapping 21*, 2 (Feb. 2004), 75–85.

[16] Bartlett, E. L., and Wang, X. Long-lasting modulation by stimulus context in primate auditory cortex. *Journal of neurophysiology 94*, 1 (July 2005), 83–104.

[17] Bartos, M., Vida, I., Frotscher, M., Meyer, A., Monyer, H., Geiger, J. R. P., and Jonas, P. Fast synaptic inhibition promotes synchronized gamma oscillations in hippocampal interneuron networks. *Proceedings of the National Academy of Sciences of the United States of America 99*, 20 (Oct. 2002), 13222–7.

[18] Bartos, M., Vida, I., and Jonas, P. Synaptic mechanisms of synchronized gamma oscillations in inhibitory interneuron networks. *Nature reviews. Neuroscience 8*, 1 (Jan. 2007), 45–56.

[19] Bendixen, A., Roeber, U., and Schröger, E. Regularity extraction and application in dynamic auditory stimulus sequences. *Journal of cognitive neuroscience 19*, 10 (Oct. 2007), 1664–77.

[20] Bertschinger, N., and Natschläger, T. Real-time computation at the edge of chaos in recurrent neural networks. *Neural Computation 16* (2004), 1413–1436.

[21] Bi, G. Q., and Poo, M. M. Synaptic modifications in cultured hippocampal neurons: dependence on spike timing, synaptic strength, and postsynaptic cell type. *The Journal of Neuroscience 18*, 24 (Dec. 1998), 10464–72.

[22] Bishop, C. M. *Pattern Recognition and Machine Learning*. Springer, 2007.

[23] Blake, D. T., Byl, N. N., and Merzenich, M. M. Representation of the hand in the cerebral cortex. *Behavioural brain research 135*, 1-2 (Sept. 2002), 179–84.

[24] Bliss, T. V. P., Lø mo, T., and Physiol, J. Long-lasting potentiation of synaptic transmission in the dentate area of the anaesthetized rabbit following stimulation of the perforant path This information is current as of April 3 , 2008 This is the final published version of this article ; it is ava. *Journal of Physiology* (1973).

[25] Boedecker, J., Obst, O., Mayer, N. M., and Asada, M. Initialization and self-organized optimization of recurrent neural network connectivity. *HFSP journal 3*, 5 (Oct. 2009), 340–9.

[26] Bosking, W. H., Zhang, Y., Schofield, B., and Fitzpatrick, D. Orientation selectivity and the arrangement of horizontal connections in tree shrew striate cortex. *The Journal of neuroscience : the official journal of the Society for Neuroscience 17*, 6 (Mar. 1997), 2112–27.

[27] Brincat, S. L., and Connor, C. E. Dynamic shape synthesis in posterior inferotemporal cortex. *Neuron 49*, 1 (Jan. 2006), 17–24.

[28] Broome, B. M., Jayaraman, V., and Laurent, G. Encoding and decoding of overlapping odor sequences. *Neuron 51*, 4 (2006), 467–82.

[29] Brouwer, G. J., and Heeger, D. J. Decoding and reconstructing color from responses in human visual cortex. *The Journal of neuroscience : the official journal of the Society for Neuroscience 29*, 44 (Nov. 2009), 13992–4003.

[30] Brown, E. N., Kass, R. E., and Mitra, P. P. Multiple neural spike train data analysis: state-of-the-art and future challenges. *Nature neuroscience 7*, 5 (May 2004), 456–61.

[31] Brunel, N., and Wang, X.-J. What determines the frequency of fast network oscillations with irregular neural discharges? I. Synaptic dynamics and excitation-inhibition balance. *Journal of neurophysiology 90*, 1 (July 2003), 415–30.

[32] Buckley, M. J., and Sigala, N. Is top-down control from prefrontal cortex necessary for visual categorization? *Neuron 66*, 4 (May 2010), 471–3.

[33] Buehlmann, A., and Deco, G. The neuronal basis of attention: rate versus synchronization modulation. *The Journal of neuroscience : the official journal of the Society for Neuroscience 28*, 30 (July 2008), 7679–86.

[34] Buhusi, C. V., and Meck, W. H. What makes us tick? Functional and neural mechanisms of interval timing. *Nature reviews. Neuroscience 6*, 10 (Oct. 2005), 755–65.

[35] Bullmore, E., and Sporns, O. Complex brain networks: graph theoretical analysis of structural and functional systems. *Nature reviews. Neuroscience 10*, 3 (Mar. 2009), 186–98.

[36] Buonomano, D. V. The biology of time across different scales. *Nature Chemical Biology 3*, 10 (2007), 594–597.

[37] Buonomano, D. V., and Karmarkar, U. R. How do we tell time? *The Neuroscientist : a review journal bringing neurobiology, neurology and psychiatry 8*, 1 (Feb. 2002), 42–51.

[38] Buonomano, D. V., and Maass, W. State-dependent computations: spatiotemporal processing in cortical networks. *Nature Reviews Neuroscience 10* (2009), 113–125.

[39] Buonomano, D. V., and Merzenich, M. M. Cortical plasticity: from synapses to maps. *Annual review of neuroscience 21* (Jan. 1998), 149–86.

[40] Busch, N. a., Debener, S., Kranczioch, C., Engel, A. K., and Hermann, C. S. Size matters: effects of stimulus size, duration and eccentricity on the visual gamma-band response. *Clinical Neurophysiology 115*, 8 (Aug. 2004), 1810–20.

[41] Buschman, T. J., and Miller, E. K. Top-Down Versus Bottom-Up Control of Attention in the Prefrontal and Posterior Parietal Cortices. *Science 315* (2007), 1860–1862.

[42] Buzsáki, G. Theta Oscillations in the Hippocampus. *Neuron 33*, 3 (Jan. 2002), 325–340.

[43] Buzsáki, G. Large-scale recording of neuronal ensembles. *Nature Neuroscience 7*, 5 (2004), 446–51.

[44] Buzsáki, G. *Rhythms of the Brain*. Oxford University Press, 2011.

[45] Buzsáki, G., Anastassiou, C. a., and Koch, C. The origin of extracellular fields and currents–EEG, ECoG, LFP and spikes. *Nature reviews Neuroscience 13*, 6 (June 2012), 407–20.

[46] Buzsáki, G., Llinás, R. R., Singer, W., Berthoz, A., and Christen, Y. *Temporal Coding in the Brain*. 1994.

[47] Buzsáki, G., and Wang, X.-J. Mechanisms of gamma oscillations. *Annual review of neuroscience 35* (Jan. 2012), 203–25.

[48] Caporale, N., and Dan, Y. Spike Timing–Dependent Plasticity: A Hebbian Learning Rule. *Annual Review of Neuroscience 31*, 1 (2008), 25–46.

[49] Carlson, T. A. High temporal resolution decoding of object position and category. *Journal of Vision 11* (2011), 1–17.

[50] Castellano, M., Plöchl, M., Vicente, R., and Pipa, G. Decoding contour categorization from parietal/frontal cortical areas : does perceptual grouping becomes a global process ? *under review* (2014).

[51] Câteau, H., and Reyes, A. Relation between Single Neuron and Population Spiking Statistics and Effects on Network Activity. *Physical Review Letters 96*, 5 (Feb. 2006), 1–4.

[52] Cavanaugh, J. R., Bair, W., and Movshon, J. A. Selectivity and spatial distribution of signals from the receptive field surround in macaque V1 neurons. *Journal of neurophysiology 88*, 5 (Nov. 2002), 2547–56.

[53] Chapin, J. K. Using multi-neuron population recordings for neural prosthetics. *Nature Neuroscience 7*, 5 (2004), 452–5.

[54] Chow, C. C., White, J. a., Ritt, J., and Kopell, N. Frequency control in synchronized networks of inhibitory neurons. *Journal of computational neuroscience 5*, 4 (Dec. 1998), 407–20.

[55] Churchland, M. M., Cunningham, J. P., Kaufman, M. T., Foster, J. D., Nuyujukian, P., Ryu, S. I., and Shenoy, K. V. Neural population dynamics during reaching. *Nature 487*, 7405 (July 2012), 51–6.

[56] Citri, A., and Malenka, R. C. Synaptic plasticity: multiple forms, functions, and mechanisms. *Neuropsychopharmacology 33*, 1 (2008), 18–41.

[57] Conway, C. M., and Christiansen, M. H. Sequential learning in non-human primates. *Trends in cognitive sciences 5*, 12 (2001), 539–546.

[58] Coull, J. T., Cheng, R.-K., and Meck, W. H. Neuroanatomical and neurochemical substrates of timing. *Neuropsychopharmacology: official publication of the American College of Neuropsychopharmacology 36*, 1 (Jan. 2011), 3–25.

[59] Csicsvari, J., Henze, D. a., Jamieson, B., Harris, K. D., Sirota, A., Barthó, P., Wise, K. D., and Buzsáki, G. Massively parallel recording of unit and local field potentials with silicon-based electrodes. *Journal of neurophysiology 90*, 2 (Aug. 2003), 1314–23.

[60] Dan, Y., and Poo, M.-M. Spike timing-dependent plasticity: from synapse to perception. *Physiological Reviews 86*, 3 (2006), 1033–48.

[61] Davis, G. W. Homeostatic control of neural activity: from phenomenology to molecular design. *Annual review of neuroscience 29* (Jan. 2006), 307–23.

[62] Davis, G. W., and Bezprozvanny, I. Maintaining the stability of neural function: a homeostatic hypothesis. *Annual review of physiology 63* (Jan. 2001), 847–69.

[63] Dayan, P., and Abbott, L. *Theoretical Neuroscience: Computational and Mathematical Modeling of Neural Systems*. The MIT Press, 2001.

[64] de Ruyter van Steveninck, R. R. Reproducibility and Variability in Neural Spike Trains. *Science 275*, 5307 (Mar. 1997), 1805–1808.

[65] DeCharms, R. C., and Zador, a. Neural representation and the cortical code. *Annual review of neuroscience 23* (Jan. 2000), 613–47.

[66] Desai, N. S., Rutherford, L. C., and Turrigiano, G. G. Plasticity in the intrinsic excitability of cortical pyramidal neurons. *Nature Neuroscience 2* (1999), 515–520.

[67] D'Huys, O., Vicente, R., Erneux, T., Danckaert, J., and Fischer, I. Synchronization properties of network motifs: influence of coupling delay and symmetry. *Chaos 18*, 3 (Sept. 2008), 037116.

[68] DiCarlo, J. J., and Cox, D. D. Untangling invariant object recognition. *Trends in cognitive sciences 11*, 8 (Aug. 2007), 333–41.

[69] Dolan, R. J., and Dayan, P. Goals and habits in the brain. *Neuron 80*, 2 (Oct. 2013), 312–25.

[70] Dudai, Y. The neurobiology of consolidations, or, how stable is the engram? *Annual review of psychology 55* (Jan. 2004), 51–86.

[71] Durstewitz, D., and Deco, G. Computational significance of transient dynamics in cortical networks. *The European journal of neuroscience 27*, 1 (Jan. 2008), 217–27.

[72] Durstewitz, D., Seamans, J. K., and Sejnowski, T. J. Neurocomputational models of working memory. *Nature*, november (2000).

[73] Eisler, H., and Ottander, C. On the problem of hysteresis in psychophysics. *Journal of Experimental Psychology 65*, 6 (1963).

[74] Elman, J. Finding structure in time. *Cognitive Science 14* (1990), 179–211.

[75] Elman, J. L., and Zipser, D. Learning the hidden structure of speech. *J. Acoust. Soc. Am. 83*, 4 (1988), 1615–1626.

[76] Engel, A. K., and Fries, P. Beta-band oscillations-signalling the status quo? *Current opinion in neurobiology* (Mar. 2010), 156–165.

[77] Ernst, U. a., Mandon, S., Schinkel-Bielefeld, N., Neitzel, S. D., Kreiter, A. K., and Pawelzik, K. R. Optimality of human contour integration. *PLoS computational biology 8*, 5 (Jan. 2012), e1002520.

[78] Fahrmeir, L., and Tutz, G. *Multivariate Statistical Modelling Based on Generalized Linear Models*. Springer; 2nd edition, 2001.

[79] Feldman, D. E. Synaptic Mechanisms for Plasticity in Neocortex. *Annu. Rev. Neurosci. 32* (2009), 33–55.

[80] Felleman, D. J., and Van Essen, D. C. Distributed hierarchical processing in the primate cerebral cortex. *Cerebral cortex 1*, 1 (1991), 1–47.

[81] Fellous, J., Rudolph, M., Destexhe, A., and Sejnowski, T. J. Synaptic Background Noise Controls the Input/output Characteristics of Single Cells in an in-vitro Model of in-vivo Activity. *Neuroscience 122*, 3 (2003), 811–829.

[82] Field, D. J., Hayes, a., and Hess, R. F. Contour integration by the human visual system: evidence for a local "association field". *Vision research 33*, 2 (Jan. 1993), 173–93.

[83] Foxe, J. J., and Simpson, G. V. Flow of activation from V1 to frontal cortex in humans. A framework for defining "early" visual processing. *Experimental brain research. Experimentelle Hirnforschung. Expérimentation cérébrale 142*, 1 (Jan. 2002), 139–50.

[84] Frankish, K., and Ramsey, W. *The Cambridge Handbook of Cognitive Science*. Cambridge University Press, 2012.

[85] Freeman, W. J. The Physiology of Perception. *Scientific American 264*, 2 (1991), 78–85.

[86] Fries, P. A mechanism for cognitive dynamics: neuronal communication through neuronal coherence. *Trends in Cognitive Sciences 9*, 10 (Oct. 2005), 474–80.

[87] Fries, P. Neuronal gamma-band synchronization as a fundamental process in cortical computation. *Annual review of neuroscience 32* (2009), 209–24.

[88] Fries, P. The model- and the data-gamma. *Neuron 64*, 5 (Dec. 2009), 601–2.

[89] Friston, K. A theory of cortical responses. *Philosophical transactions of the Royal Society of London. Series B, Biological sciences 360*, 1456 (Apr. 2005), 815–36.

[90] Friston, K. J. Functional and effective connectivity in neuroimaging: A synthesis. *Human Brain Mapping 2*, 1-2 (1994), 56–78.

[91] Froemke, R. C., and Dan, Y. Spike-timing-dependent synaptic modification induced by natural spike trains. *Nature 416*, 6879 (Mar. 2002), 433–8.

[92] Ganguli, S., Huh, D., and Sompolinsky, H. Memory traces in dynamical systems. *PNAS 105* (2008), 18970–18975.

[93] Gavornik, J. P., and Bear, M. F. Learned spatiotemporal sequence recognition and prediction in primary visual cortex. *Nature Neuroscience*, March (Mar. 2014).

[94] Gerard, H., Boyd, R., Goldstein, N. J., Liberman, A., Principles, B., Higgins, E. T., Kruglanski, A. W., Shachar, R., Mens, G. L., Juslin, P., Rabinovich, M., Huerta, R., and Laurent, G. Neuroscience. Transient dynamics for neural processing. *Science 321*, 5885 (July 2008), 48–50.

[95] Gerhard, F., Pipa, G., Lima, B., Neuenschwander, S., and Gerstner, W. Extraction of Network Topology From Multi-Electrode Recordings: Is there a Small-World Effect? *Frontiers in computational neuroscience 5*, February (Jan. 2011), 4.

[96] Gerstner, W., and Kistler, W. M. *Spiking Neuron Models. Single Neurons, Populations, Plasticity.* Cambridge University Press, 2002.

[97] Gerstner, W., Kreiter, a. K., Markram, H., and Herz, A. V. Neural codes: firing rates and beyond. *PNAS 94*, 24 (Nov. 1997), 12740–1.

[98] Gibbon, J., Malapani, C., Dale, C. L., and Gallistel, C. Toward a neurobiology of temporal cognition: advances and challenges. *Current opinion in neurobiology 7*, 2 (Apr. 1997), 170–84.

[99] Giese, M. a., and Poggio, T. Neural mechanisms for the recognition of biological movements. *Nature reviews Neuroscience 4*, 3 (Mar. 2003), 179–92.

[100] Goel, A., and Buonomano, D. V. Timing as an intrinsic property of neural networks : evidence from in vivo and in vitro experiments. *Philosophical transactions of the Royal Society B*, January (2014).

[101] Gold, C., Henze, D. a., Koch, C., and Buzsáki, G. On the origin of the extracellular action potential waveform: A modeling study. *Journal of neurophysiology 95*, 5 (May 2006), 3113–28.

[102] Gold, J. I., and Shadlen, M. N. The neural basis of decision making. *Annu. Rev. Neurosci. 30* (Jan. 2007), 535–74.

[103] Goldstein, B. *Cognitive Psychology.* Thomson Wadsworth, 2008.

[104] Golledge, H. D. R., Panzeri, S., Zheng, F., Pola, G., Scannell, J. W., Giannikopoulos, D. V., Mason, R. J., Tovée, M. J., and Young, M. P. Correlations, feature-binding and population coding in primary visual cortex. *Neuroreport 14*, 7 (May 2003), 1045–50.

[105] Goodale, M. a., and Milner, a. D. Separate visual pathways for perception and action. *Trends in neurosciences 15*, 1 (Jan. 1992), 20–5.

[106] Gordon, I. E. *Theories of Visual Perception.* Psychology Press, Sept. 2004.

[107] Gray, C. M., König, P., Engel, A. K., and Singer, W. Oscillatory responses in cat visual cortex exhibit inter-columnar synchronization which reflects global stimulus properties. *Nature 338* (1989), 334–337.

[108] Grondin, S. Timing and time perception: A review of recent behavioral and neuroscience findings and theoretical directions. *Attention, Perception & Psychophysics 72*, 3 (2010), 561–582.

[109] Gross, C. G. *Brain Vision Memory. Tales in the History of Neuroscience.* A Bradford Book, 1999.

[110] Gross, C. G., Rocha-Miranda, E., and Bender, D. B. Visual Cortex Properties of Neurons in Inferotemporal of the Macaque. *J Neurophysiology 35*, 1 (1972), 96–111.

[111] Gu, Y., Dremstrup, K., and Farina, D. Single-trial discrimination of type and speed of wrist movements from EEG recordings. *Clinical Neurophysiology 120*, 8 (Aug. 2009), 1596–600.

[112] Guitart-Masip, M., Duzel, E., Dolan, R., and Dayan, P. Action versus valence in decision making. *Trends in cognitive sciences 18*, 4 (Apr. 2014), 194–202.

[113] Haken, H. *Principles of Brain Functioning.* Springer, 1996.

[114] Hammer, B., and Steil, J. J. Tutorial : Perspectives on Learning with RNNs. *Neural Networks*, April (2002), 357–368.

[115] Hanson, F. B., and Tuckwell, H. C. Difussion Approximations for Neuronal Activity Including Synaptic Reversal Potentials. *J. Theoret. Neurobiol 2* (1983), 127–153.

[116] Haynes, J.-D., and Rees, G. Predicting the orientation of invisible stimuli from activity in human primary visual cortex. *Nature neuroscience 8*, 5 (May 2005), 686–91.

[117] Hebb, D. *The Organization of Behavior: A Neuropsychological Theory.* New York: Wiley & Sons., 1949.

[118] Helmholtz, H. *Handbuch der physiologischen optik.* New York: Dover, 1890.

[119] Henn, F. a. Neurotransmission and glial cells: a functional relationship? *Journal of neuroscience research 2*, 4 (Jan. 1976), 271–82.

[120] Herrmann, C. S., Lenz, D., Junge, S., Busch, N. A., and Maess, B. Memory-matches evoke human gamma-responses. *BMC Neuroscience 8* (2004), 1–8.

[121] Herz, A. V. M., Gollisch, T., Machens, C. K., and Jaeger, D. Modeling single-neuron dynamics and computations: a balance of detail and abstraction. *Science 314*, 5796 (Oct. 2006), 80–5.

[122] Hess, R. F., Beaudot, W. H., and Mullen, K. T. Dynamics of contour integration. *Vision research 41*, 8 (Apr. 2001), 1023–37.

[123] Hipp, J. F., Engel, A. K., and Siegel, M. Oscillatory synchronization in large-scale cortical networks predicts perception. *Neuron 69*, 2 (Jan. 2011), 387–96.

[124] Hopfield, J. J. Neural Networks and Physical Systems with Emergent Collective Computational Abilities. *Proceedings of the National Academy of Sciences 79* (1982), 2554–2558.

[125] Hubel, D. H., and Wiesel, T. N. Receptive Fields, Binocular Interaction and Functional Architecture in the cat's Visual Cortex. *J. Physiol. 160* (1962), 106–154.

[126] Hubel, D. H., and Wiesel, T. N. Early Exploration of the Visual Cortex. *Neuron 20* (1998), 401–412.

[127] Huk, A. C., and Heeger, D. J. Task-Related Modulation of Visual Cortex. *J. Neurophysiol.* (2000), 3525–3536.

[128] Huys, Q. J. M., Zemel, R. S., Natarajan, R., and Dayan, P. Fast population coding. *Neural computation 19*, 2 (Feb. 2007), 404–441.

[129] Ivry, R. B., and Schlerf, J. E. Dedicated and intrinsic models of time perception. *Trends in cognitive sciences 12*, 7 (July 2008), 273–80.

[130] Ivry, R. B., and Spencer, R. M. C. The neural representation of time. *Current opinion in neurobiology 14*, 2 (Apr. 2004), 225–32.

[131] Izhikevich, E. M. Large scale model of the human brain. *BMC Neuroscience 10*, Suppl 1 (2009), L3.

[132] Jacobs, A. L., Fridman, G., Douglas, R. M., Alam, N. M., Latham, P. E., Prusky, G. T., and Nirenberg, S. Ruling out and ruling in neural codes. *PNAS 106*, 14 (Apr. 2009), 5936–41.

[133] Jaeger, H. The "echo state" approach to analysing and training recurrent neural networks. *GMD Report* (2001), 1–47.

[134] Jensen, O. Maintenance of multiple working memory items by temporal segmentation. *Neuroscience 139*, 1 (2006), 237–49.

[135] Johnson, J. S., Kundu, B., Casali, A. G., and Postle, B. R. Task-dependent changes in cortical excitability and effective connectivity: a combined TMS-EEG study. *Journal of neurophysiology 107*, 9 (May 2012), 2383–92.

[136] Joshi, P., and Triesch, J. Rule for Firing Rate Homeostasis. *ICANN* (2008), 567–576.

[137] Kandel, E. R., Schwartz, J. H., and Jessell, T. M. *Principles of Neural Science*, 54th editi ed. McGraw-Hill Professional, 2012.

[138] Kauer, J. a., and Malenka, R. C. Synaptic plasticity and addiction. *Nature reviews. Neuroscience 8*, 11 (Nov. 2007), 844–58.

[139] Kayser, C., Logothetis, N. K., and Panzeri, S. Millisecond encoding precision of auditory cortex neurons. *Proceedings of the National Academy of Sciences of the United States of America 107*, 39 (Sept. 2010), 16976–81.

[140] Ken-Ichi, F., and Nakamura, Y. Approximation of Dynamical Systems by Continuous Time Recurrent Neural Networks. *Neural Networks 6* (1993), 801–806.

[141] Kim, S. J., and Linden, D. J. Ubiquitous plasticity and memory storage. *Neuron 56*, 4 (Nov. 2007), 582–92.

[142] King, J.-R., and Dehaene, S. Characterizing the dynamics of mental representations: the temporal generalization method. *Trends in cognitive sciences* (Mar. 2014), 1–8.

[143] King, J. R., Faugeras, F., Gramfort, a., Schurger, a., El Karoui, I., Sitt, J. D., Rohaut, B., Wacongne, C., Labyt, E., Bekinschtein, T., Cohen, L., Naccache, L., and Dehaene, S. Single-trial decoding of auditory novelty responses facilitates the detection of residual consciousness. *NeuroImage 83* (Dec. 2013), 726–38.

[144] Kok, P., Jehee, J. F. M., and Lange, F. P. D. Less Is More : Expectation Sharpens Representations in the Primary Visual Cortex. *Neuron* (2012), 265–270.

[145] Körding, K. P., and Wolpert, D. M. Bayesian integration in sensorimotor learning. *Nature 427*, 6971 (Jan. 2004), 244–7.

[146] Kourtzi, Z., and Connor, C. E. Neural representations for object perception: structure, category, and adaptive coding. *Annual review of neuroscience 34* (Jan. 2011), 45–67.

[147] Kuhl, P., and Rivera-Gaxiola, M. Neural substrates of language acquisition. *Annual review of neuroscience 31* (2008), 511–34.

[148] Lachaux, J.-P., Rodriguez, E., Quyen, M. L. V., Lutz, A., Martinerie, J., and Varela, F. Studying single-trials of phase synchronous activity in the brain. *International Journal of Bifurcation and Chaos 10* (2000), 2429–39.

[149] Lapicque, L. Recherches quantitatives sur l'excitation 'electrique des nerfs trait'ee comme une polarisation. *J. Physiol. Pathol. Gen. 9* (1907), 620–635.

[150] Lazar, A., Pipa, G., and Triesch, J. Fading memory and time series prediction in recurrent networks with different forms of plasticity. *Neural Networks 20*, 3 (Apr. 2007), 312–22.

[151] Lazar, A., Pipa, G., and Triesch, J. SORN: a self-organizing recurrent neural network. *Frontiers in Computational Neuroscience 3*, October (2009), 23.

[152] Leopold, D. A., and Logothetis, N. K. Multistable phenomena: changing views in perception. *Trends in Cognitive Sciences 3*, 7 (1999), 254–264.

[153] Li, L., Gratton, C., Yao, D., and Knight, R. T. Role of Frontal and Parietal Cortices in the Control of Bottom-up and Top-down Attention in Humans. *Brain Research 1344* (2010), 173–184.

[154] Li, N., and DiCarlo, J. J. Unsupervised natural visual experience rapidly reshapes size-invariant object representation in inferior temporal cortex. *Neuron 67*, 6 (Sept. 2010), 1062–75.

[155] Lindner, B. Superposition of many independent spike trains is generally not a Poisson process. *Physical Review E 73*, 2 (2006), 1–4.

[156] Lindsey, B. G., Morris, K. F., Shannon, R., and Gerstein, G. L. Repeated patterns of distributed synchrony in neuronal assemblies. *Journal of neurophysiology 78*, 3 (Sept. 1997), 1714–9.

[157] Liu, J., and Newsome, W. T. Functional organization of speed tuned neurons in visual area MT. *Journal of neurophysiology 89*, 1 (Jan. 2003), 246–56.

[158] Lukoševičius, M., and Jaeger, H. Reservoir computing approaches to recurrent neural network training. *Computer Science Review 3*, 3 (Aug. 2009), 127–149.

[159] Maass, W., Joshi, P., and Sontag, E. D. Computational aspects of feedback in neural circuits. *PLoS Comput. Biol. 3*, 1 (2007), e165.

[160] Maass, W., and Markram, H. On the computational power of circuits of spiking neurons. *Journal of Computer and System Sciences 69*, 4 (Dec. 2004), 593–616.

[161] Maass, W., Natschläger, T., and Markram, H. Fading memory and kernel properties of generic cortical microcircuit models. *Journal of Physiology 98*, 4-6 (2004), 315–30.

[162] Maass, W., Natschläger, T., Markram, H., Maass, W., and Markram, H. Real-time computing without stable states : a new framework for neural computation based on perturbations. *Neural Computation 14*, 11 (2002), 2531–2560.

[163] Mack, M. L., and Palmeri, T. J. Decoupling object detection and categorization. *Journal of experimental psychology. Human perception and performance 36*, 5 (Oct. 2010), 1067–79.

[164] Mack, M. L., and Palmeri, T. J. The timing of visual object categorization. *Frontiers in psychology 2*, July (Jan. 2011), 165.

[165] Maimon, G., and Assad, J. a. Beyond Poisson: increased spike-time regularity across primate parietal cortex. *Neuron 62*, 3 (May 2009), 426–40.

[166] Mainen, Z. F., and Sejnowski, T. J. Reliability of spike timing in neocortical neurons. *Science 268*, 5216 (June 1995), 1503–6.

[167] Markram, H. Regulation of Synaptic Efficacy by Coincidence of Postsynaptic APs and EPSPs. *Science 275*, 5297 (Jan. 1997), 213–215.

[168] Mathes, B., Trenner, D., and Fahle, M. The electrophysiological correlate of contour integration is modulated by task demands. *Brain research 1114*, 1 (Oct. 2006), 98–112.

[169] Mauk, M. D., and Buonomano, D. V. The neural basis of temporal processing. *Annual review of neuroscience 27* (Jan. 2004), 307–40.

[170] Maurer, A. P., and McNaughton, B. L. Network and intrinsic cellular mechanisms underlying theta phase precession of hippocampal neurons. *Trends in neurosciences 30*, 7 (July 2007), 325–33.

[171] Mayor, J., and Gerstner, W. Signal buffering in random networks of spiking neurons: microscopic vs. macroscopic phenomena. *Integration The Vlsi Journal 72*, 1 (Nov. 2008), 1–5.

[172] Mazor, O., and Laurent, G. Transient dynamics versus fixed points in odor representations by locust antennal lobe projection neurons. *Neuron 48*, 4 (Nov. 2005), 661–73.

[173] McCormick, D. a., and Bal, T. Sleep and arousal: thalamocortical mechanisms. *Annual review of neuroscience 20* (Jan. 1997), 185–215.

[174] McGaugh, J. L. Memory–a Century of Consolidation. *Science 287*, 5451 (Jan. 2000), 248–251.

[175] Melloni, L., Schwiedrzik, C. M., Wibral, M., Rodriguez, E., and Singer, W. Response to: Yuval-Greenberg et al., "Transient Induced Gamma-Band Response in EEG as a Manifestation of Miniature Saccades." Neuron 58, 429-441. *Neuron 62*, 1 (Apr. 2009), 8–10; author reply 10–12.

[176] Mesulam, M. M. Spatial attention and neglect: parietal, frontal and cingulate contributions to the mental representation and attentional targeting of salient extrapersonal events. *Philosophical transactions of the Royal Society of London. Series B, Biological sciences 354*, 1387 (July 1999), 1325–46.

[177] Meyer, T., and Olson, C. R. Statistical learning of visual transitions in monkey inferotemporal cortex. *Proceedings of the National Academy of Sciences of the United States of America 108*, 48 (Nov. 2011), 19401–6.

[178] Milner, a. D., and Goodale, M. a. Two visual systems re-viewed. *Neuropsychologia 46*, 3 (Feb. 2008), 774–85.

[179] Mishkin, M., Ungerleider, L. G., and Kathleen, A. Object vision and spatial vision: two cortical pahways. *TINS* (1983), 414–417.

[180] Morgan, H. M., Jackson, M. C., van Koningsbruggen, M. G., Shapiro, K. L., and Linden, D. E. J. Frontal and parietal theta burst TMS impairs working memory for visual-spatial conjunctions. *Brain stimulation 6*, 2 (Mar. 2013), 122–9.

[181] Morrison, A., Diesmann, M., and Gerstner, W. Phenomenological models of synaptic plasticity based on spike timing. *Biological cybernetics 98*, 6 (June 2008), 459–78.

[182] Moser, E. I., Kropff, E., and Moser, M.-B. Place cells, grid cells, and the brain's spatial representation system. *Annual review of neuroscience 31* (Jan. 2008), 69–89.

[183] Nadasdy, Z. Binding by asynchrony: the neuronal phase code. *Frontiers in Neuroscience 4*, September (Sept. 2010), 1–11.

[184] Naselaris, T., Prenger, R. J., Kay, K. N., Oliver, M., and Gallant, J. L. Bayesian reconstruction of natural images from human brain activity. *Neuron 63*, 6 (Sept. 2009), 902–15.

[185] Nawrot, M. P., Boucsein, C., Rodriguez Molina, V., Aertsen, A., Grun, S., and Rotter, S. Serial interval statistics of spontaneous activity in cortical neurons in vivo and in vitro. *Neurocomputing 70*, 10-12 (2007), 1717–1722.

[186] Nawrot, M. P., Boucsein, C., Rodriguez Molina, V., Riehle, A., Aertsen, A., and Rotter, S. Measurement of variability dynamics in cortical spike trains. *Journal of Neuroscience Methods 169*, 2 (2008), 374–90.

[187] Nikolić, D., Häusler, S., Singer, W., and Maass, W. Distributed fading memory for stimulus properties in the primary visual cortex. *PLoS biology 7*, 12 (Dec. 2009), e1000260.

[188] Nir, Y., Staba, R. J., Andrillon, T., Vyazovskiy, V. V., Cirelli, C., Fried, I., and Tononi, G. Regional slow waves and spindles in human sleep. *Neuron 70*, 1 (Apr. 2011), 153–69.

[189] Nishimoto, S., Vu, A. T., Naselaris, T., Benjamini, Y., Yu, B., and Gallant, J. L. Reconstructing visual experiences from brain activity evoked by natural movies. *Current Biology 21*, 19 (Oct. 2011), 1641–6.

[190] Nunez, P. L., and Srinivasan, R. *Electric Fields of the Brain.* 2006.

[191] Oberlaender, M., de Kock, C. P. J., Bruno, R. M., Ramirez, A., Meyer, H. S., Dercksen, V. J., Helmstaedter, M., and Sakmann, B. Cell type-specific three-dimensional structure of thalamocortical circuits in a column of rat vibrissal cortex. *Cerebral cortex 22*, 10 (Oct. 2012), 2375–91.

[192] Okatan, M., Wilson, M. A., and Brown, E. N. Analyzing Functional Connectivity Using a Network Likelihood Model of Ensemble Neural Spiking Activity. *Neural Computation 17* (2005), 1927–1961.

[193] Ostojic, S., Brunel, N., and Hakim, V. How connectivity, background activity, and synaptic properties shape the cross-correlation between spike trains. *The Journal of Neuroscience 29*, 33 (Aug. 2009), 10234–53.

[194] Palva, J. M., Palva, S., and Kaila, K. Phase synchrony among neuronal oscillations in the human cortex. *The Journal of Neuroscience 25*, 15 (Apr. 2005), 3962–72.

[195] Panzeri, S., Brunel, N., Logothetis, N. K., and Kayser, C. Sensory neural codes using multiplexed temporal scales. *Trends in Neurosciences 33*, 3 (2010), 111–120.

[196] Panzeri, S., Petersen, R. S., Schultz, S. R., Lebedev, M., and Diamond, M. E. The role of spike timing in the coding of stimulus location in rat somatosensory cortex. *Neuron 29*, 3 (Mar. 2001), 769–77.

[197] Pascual-Leone, A., Amedi, A., Fregni, F., and Merabet, L. B. The plastic human brain cortex. *Annual review of neuroscience 28* (Jan. 2005), 377–401.

[198] Pesaran, B., Pezaris, J. S., Sahani, M., Mitra, P. P., and Andersen, R. a. Temporal structure in neuronal activity during working memory in macaque parietal cortex. *Nature neuroscience 5*, 8 (Aug. 2002), 805–11.

[199] Phillips, S., Takeda, Y., and Singh, A. Visual feature integration indicated by pHase-locked frontal-parietal EEG signals. *PloS one 7*, 3 (Jan. 2012), e32502.

[200] Pipa, G., Vreeswijk, C., and Grun, S. Impact of spike-train autostructure on probability distribution of joint-spike events. *Neural Computation* (2013).

[201] Pipa, G., Wheeler, D. W., Singer, W., and Nikolić, D. NeuroXidence: reliable and efficient analysis of an excess or deficiency of joint-spike events. *Journal of computational neuroscience 25*, 1 (Aug. 2008), 64–88.

[202] Poucet, B., and Save, E. Attractors in Memory. *Science 308* (2005).

[203] Pouget, A., Dayan, P., and Zemel, R. S. Inference and computation with population codes. *Annual review of neuroscience 26* (Jan. 2003), 381–410.

[204] Prut, Y., Vaadia, E., Bergman, H., Haalman, I., Hamutal, S., and Abeles, M. Spatiotemporal Structure of Cortical Activity: Properties and Behavioral Relevance. *J. Neurophysiol. 79*, 6 (1998), 2857–2874.

[205] Quian Quiroga, R., and Panzeri, S. Extracting information from neuronal populations: information theory and decoding approaches. *Nature reviews. Neuroscience 10*, 3 (Mar. 2009), 173–85.

[206] Ramón y Cajal, S. *Studien über die Hirnrinde des Menschen.* Johann Ambrosius Barth, 1906.

[207] Riehle, A., Grün, S., Diesmann, M., and Aertsen, A. Spike Synchronization and Rate Modulation Differentially Involved in Motor Cortical Function. *Science 278*, 5345 (Dec. 1997), 1950–1953.

[208] Roelfsema, P. R., Lamme, V. a. F., and Spekreijse, H. Synchrony and covariation of firing rates in the primary visual cortex during contour grouping. *Nature neuroscience 7*, 9 (Sept. 2004), 982–91.

[209] Rolls, E. T., Grabenhorst, F., and Deco, G. Decision-making, errors, and confidence in the brain. *Journal of neurophysiology 104*, 5 (Nov. 2010), 2359–74.

[210] Romo, R., and Salinas, E. Flutter discrimination: neural codes, perception, memory and decision making. *Nature reviews. Neuroscience 4*, 3 (Mar. 2003), 203–18.

[211] Roozendaal, B., McEwen, B. S., and Chattarji, S. Stress, memory and the amygdala. *Nature reviews. Neuroscience 10*, 6 (June 2009), 423–33.

[212] Rotermund, D., Schipper, M., Fahle, M., and Ernst, U. a. High-performance classification of contour percepts from EEG recordings. *BMC Neuroscience 12*, Suppl 1 (2011), P94.

[213] Salinas, E., and Sejnowski, T. J. Correlated neuronal activity and the flow of neural information. *Nature Reviews Neuroscience 2*, 8 (Aug. 2001), 539–50.

[214] Sanei, S., and Chambers, J. *EEG Signal Processing.* John Wiley & Sons, 2007.

[215] Sanger, T. Neural population codes. *Current Opinion in Neurobiology 13*, 2 (2003), 238–249.

[216] Scannell, J. W., Blakemore, C., and Young, M. P. Analysis of connectivity in the cat cerebral cortex. *The Journal of neuroscience : the official journal of the Society for Neuroscience 15*, 2 (Feb. 1995), 1463–83.

[217] Schmidhuber, J., Wierstra, D., Gagliolo, M., and Gomez, F. Training recurrent networks by Evolino. *Neural computation 19*, 3 (Mar. 2007), 757–79.

[218] Schmolesky, M. T., Wang, Y., Hanes, D. P., Thompson, K. G., Leutgeb, S., Schall, J. D., Leventhal, A. G., Morand, S. M., Harvey, M., Grosbras, M.-h., Patterson, C. A., Duijnhouwer, J., Wissig, S. C., Krekelberg, B., Kohn, A., Brostek, L., Büttner, U., Mustari, M. J., and Glasauer, S. Signal Timing Across the Macaque Visual System. *Journal of Neurophysiology* (1998), 3272–3278.

[219] Schrauwen, B., Buesing, L., and Legenstein, R. On Computational Power and the Order-Chaos Phase Transition in Reservoir Computing. *NIPS* (2008).

[220] Schroeder, C. E., Wilson, D. A., Radman, T., Scharfman, H., and Lakatos, P. Dynamics of Active Sensing and Perceptual Selection. *Curr Opin Neurobiol. 20*, 2 (2011), 172–176.

[221] Schuett, S., Bonhoeffer, T., and Hübener, M. Pairing-induced changes of orientation maps in cat visual cortex. *Neuron 32*, 2 (Oct. 2001), 325–37.

[222] Schwartz, O., Hsu, A., and Dayan, P. Space and time in visual context. *Nature reviews. Neuroscience 8*, 7 (July 2007), 522–35.

[223] Schwarzlose, R. F., Swisher, J. D., Dang, S., and Kanwisher, N. The distribution of category and location information across object-selective regions in human visual cortex. *Proceedings of the National Academy of Sciences of the United States of America 105*, 11 (Mar. 2008), 4447–52.

[224] Shadlen, M. N., and Newsome, W. T. Is there a signal in the noise? *Current Biology* (1995), 248–250.

[225] Shen, K., and Scheiffele, P. Genetics and Cell Biology of Building Specific Synapse Connectivity. *Annual review of neuroscience 33* (Apr. 2010), 473–509.

[226] Shuler, M. G., and Bear, M. F. Reward timing in the primary visual cortex. *Science 311*, 5767 (Mar. 2006), 1606–9.

[227] Siegel, M., Donner, T. H., Oostenveld, R., Fries, P., and Engel, A. K. Neuronal synchronization along the dorsal visual pathway reflects the focus of spatial attention. *Neuron 60*, 4 (Nov. 2008), 709–19.

[228] Silfverhuth, M. J., Hintsala, H., Kortelainen, J., and Seppänen, T. Experimental comparison of connectivity measures with simulated EEG signals. *Medical & biological engineering & computing 50*, 7 (July 2012), 683–8.

[229] Singer, W. Synchronization of Cortical Activity and its Putative Role in Information Processing and Learning. *Annual Rev. Phisiol. 55* (1993), 349–74.

[230] Singer, W. Neuronal Synchrony : A Versatile Code for the Definition of Relations? *Neuron 24* (1999), 49–65.

[231] Singer, W. Distributed processing and temporal codes in neuronal networks. *Cognitive neurodynamics 3*, 3 (2009), 189–96.

[232] Singer, W., and Gray, C. M. Visual Feature Integration and the Temporal Correlation Hypothesis. *Annu. Rev. Neurosci.* (1995).

[233] Softky, W. R. Simple codes versus efficient codes. *Current opinion in neurobiology 5*, 2 (Apr. 1995), 239–47.

[234] Song, S., and Abbott, L. F. Cortical Remapping through Spike Timing-Dependent Plasticity. *Neuron 32* (2001), 1–12.

[235] Song, S., Miller, K. D., and Abbott, L. F. Competitive Hebbian learning through spike-timing-dependent synaptic plasticity. *Nature Neuroscience 3*, 9 (2000), 919–926.

[236] Sparks, D. L., Holland, R., and Guthrie, B. L. Size and distribution of movement fields in the monkey superior colliculus. *Brain Research 113* (1976), 21–34.

[237] Spiers, H. J., and Maguire, E. a. Decoding human brain activity during real-world experiences. *Trends in cognitive sciences 11*, 8 (Aug. 2007), 356–65.

[238] Stern, E. A., Kincaid, A. E., and Wilson, C. J. Spontaneous Subthreshold Membrane Potential Fluctuations and Action Potential Variability of Rat Corticostriatal and Striatal Neurons In Vivo. *J. Neurophysiol. 77* (1997), 1697–1715.

[239] Sternberg, S. The discovery of processing stages: extensions of donders' method. *Acta Psychologica 30* (1969), 276–315.

[240] Stone, J. V. Learning perceptually salient visual parameters using spatiotemporal smoothness constraints. *Neural computation 8*, 7 (Oct. 1996), 1463–92.

[241] Stratton, P., Cheung, A., Wiles, J., Kiyatkin, E., Sah, P., and Windels, F. Action potential waveform variability limits multi-unit separation in freely behaving rats. *PloS one 7*, 6 (Jan. 2012), e38482.

[242] Strogatz, S. H. *Nonlinear Dynamics and Chaos*. Westview Press, 2000.

[243] Strogatz, S. H. Exploring complex networks. *Nature 410*, 6825 (Mar. 2001), 268–76.

[244] Summerfield, C., and Egner, T. Expectation (and attention) in visual cognition. *Trends in cognitive sciences 13*, 9 (Sept. 2009), 403–9.

[245] Tallon-Baudry, C., and Bertrand, O. Oscillatory gamma activity in humans and its role in object representation. *Trends in cognitive sciences 3*, 4 (Apr. 1999), 151–162.

[246] Tallon-Baudry, C., Bertrand, O., Delpuech, C., and Permier, J. Oscillatory gamma-band (30-70 Hz) activity induced by a visual search task in humans. *The Journal of neuroscience : the official journal of the Society for Neuroscience 17*, 2 (Jan. 1997), 722–34.

[247] Tallon-Baudry, C., Bertrand, O., and Fischer, C. Oscillatory synchrony between human extrastriate areas during visual short-term memory maintenance. *The Journal of Neuroscience 21*, 20 (Oct. 2001), 1–5.

[248] Tanskanen, T., Saarinen, J., Parkkonen, L., and Hari, R. From local to global : Cortical dynamics of contour integration. *Journal of Vision 8* (2008), 1–12.

[249] Teich, M. C., Heneghan, C., Lowen, S. B., Ozaki, T., and Kaplan, E. Fractal character of the neural spike train in the visual system of the cat. *Journal of the Optical Society of America. A, Optics, image science, and vision 14*, 3 (Mar. 1997), 529–46.

[250] Tetko, I. V., and Villa, a. E. A pattern grouping algorithm for analysis of spatiotemporal patterns in neuronal spike trains. 1. Detection of repeated patterns. *Journal of neuroscience methods 105*, 1 (Jan. 2001), 1–14.

[251] Theunissen, F., and Miller, J. P. Temporal Encoding in Nervous Systems: A Rigorous Definition. *Journal of computational neuroscience 162* (1995), 149–162.

[252] Thompson, P., Burr, D., and Addams, R. Visual aftereffects. *Current Biology 19*, 1 (2009), 11–14.

[253] Thorn, C. a., Atallah, H., Howe, M., and Graybiel, A. M. Differential dynamics of activity changes in dorsolateral and dorsomedial striatal loops during learning. *Neuron 66*, 5 (June 2010), 781–95.

[254] Tiesinga, P. H. E., and Sejnowski, T. J. Rapid temporal modulation of synchrony by competition in cortical interneuron networks. *Neural computation 16*, 2 (Feb. 2004), 251–75.

[255] Toutounji, H., and Pipa, G. Spatiotemporal Computations of an Excitable and Plastic Brain: Neuronal Plasticity Leads to Noise-Robust and Noise-Constructive Computations. *PLoS Computational Biology 10*, 3 (Mar. 2014), e1003512.

[256] Traub, R. D., Bibbig, A., LeBeau, F. E. N., Buhl, E. H., and Whittington, M. a. Cellular mechanisms of neuronal population oscillations in the hippocampus in vitro. *Annual review of neuroscience 27* (Jan. 2004), 247–78.

[257] Traub, R. D., Kopell, N., Bibbig, a., Buhl, E. H., LeBeau, F. E., and Whittington, M. a. Gap junctions between interneuron dendrites can enhance synchrony of gamma oscillations in distributed networks. *The Journal of neuroscience : the official journal of the Society for Neuroscience 21*, 23 (Dec. 2001), 9478–86.

[258] Turrigiano, G. G. Homeostatic plasticity in neuronal networks: the more things change, the more they stay the same. *Trends in neurosciences 22*, 5 (May 1999), 221–7.

[259] Turrigiano, G. G., and Nelson, S. B. Homeostatic plasticity in the developing nervous system. *Nature Reviews Neuroscience 5* (2004), 97–107.

[260] Uhlhaas, P. J., Pipa, G., Neuenschwander, S., Wibral, M., and Singer, W. A new look at gamma? High- (¿60 Hz) γ-band activity in cortical networks: function, mechanisms and impairment. *Progress in biophysics and molecular biology 105*, 1-2 (Mar. 2011), 14–28.

[261] Van Der Werf, J., Jensen, O., Fries, P., and Medendorp, W. P. Gamma-band activity in human posterior parietal cortex encodes the motor goal during delayed prosaccades and antisaccades. *The Journal of Neuroscience 28*, 34 (Aug. 2008), 8397–405.

[262] van Ede, F., de Lange, F. P., and Maris, E. Attentional cues affect accuracy and reaction time via different cognitive and neural processes. *The Journal of neuroscience : the official journal of the Society for Neuroscience 32*, 30 (July 2012), 10408–12.

[263] van Rossum, M. C., Bi, G. Q., and Turrigiano, G. G. Stable Hebbian learning from spike timing-dependent plasticity. *Journal of neuroscience 20*, 23 (Dec. 2000), 8812–21.

[264] Van Vreeswijk, C., Abbott, L. F., and Ermentrout, G. B. When inhibition not excitation synchronizes neural firing. *Journal of computational neuroscience 1*, 4 (Dec. 1994), 313–21.

[265] van Wassenhove, V. Minding time in an amodal representational space. *Philosophical transactions of the Royal Society of London. Series B, Biological sciences 364*, 1525 (July 2009), 1815–30.

[266] VanRullen, R., Guyonneau, R., and Thorpe, S. J. Spike times make sense. *Trends in neurosciences 28*, 1 (Jan. 2005), 1–4.

[267] VanRullen, R., and Thorpe, S. J. The time course of visual processing: from early perception to decision-making. *Journal of Cognitive Neuroscience 13*, 4 (May 2001), 454–61.

[268] Varela, F., Lachaux, J.-p., Rodriguez, E., and Martinerie, J. The brainweb: phase sunchronization and large scale integration. *Nature Reviews Neuroscience 2*, April (2001).

[269] Vida, I., Bartos, M., and Jonas, P. Shunting inhibition improves robustness of gamma oscillations in hippocampal interneuron networks by homogenizing firing rates. *Neuron 49*, 1 (Jan. 2006), 107–17.

[270] Vidal, J. Toward direct brain-computer communication. *Annual Rev. Biophys. Bioeng. 2* (1973), 157–180.

[271] Villa, a. E., Tetko, I. V., Hyland, B., and Najem, a. Spatiotemporal activity patterns of rat cortical neurons predict responses in a conditioned task. *Proceedings of the National Academy of Sciences of the United States of America 96*, 3 (Feb. 1999), 1106–11.

[272] Vogels, T. P., Rajan, K., and Abbott, L. F. Neural network dynamics. *Annu. Rev. Neurosci. 28*, c (2005), 357–76.

[273] Volberg, G., and Greenlee, M. W. Brain networks supporting perceptual grouping and contour selection. *Frontiers in psychology 5*, April (Jan. 2014), 264.

[274] Wade, N. J., and Swanston, M. T. *Visual Perception. An Introduction*, 2nd ed. 2001.

[275] Waldert, S., Preissl, H., Demandt, E., Braun, C., Birbaumer, N., Aertsen, A., and Mehring, C. Hand movement direction decoded from MEG and EEG. *The Journal of neuroscience : the official journal of the Society for Neuroscience 28*, 4 (Jan. 2008), 1000–8.

[276] Wang, X.-j. Neurophysiological and Computational Principles of Cortical Rhythms in Cognition. *Physiological Reviews* (2010), 1195–1268.

[277] Watt, A. J., and Desai, N. S. Homeostatic plasticity and STDP: keeping a neuron's cool in a fluctuating world. *Frontiers in Synaptic Neuroscience 2*, June (2010), 1–16.

[278] Watt, R., Ledgeway, T., and Dakin, S. C. Families of models for gabor paths demonstrate the importance of spatial adjacency. *Journal of Vision 8*, 23 (2008), 1–19.

[279] Weinberger, N. M. Associative representational plasticity in the auditory cortex: a synthesis of two disciplines. *Learning & memory (Cold Spring Harbor, N.Y.) 14*, 1-2 (2007), 1–16.

[280] Werbos, P. J. Backpropagation Through Time : What It Does and How to Do It. *Proceedings of the IEEE 78*, October (1990), 1550–1560.

[281] Whittington, M. A., Traub, R. D., Kopell, N., Ermentrout, B., and Buhl, E. H. Inhibition-based rhythms: experimental and mathematical observations on network dynamics. *International Journal of Psychophysiology 38* (2000), 315–336.

[282] Wiesel, T. N., and Hubel, D. H. Effects of Visual Deprivation on Morphology and Physiology of Cells in the Cat's Lateral Geniculate Body. *J Neurophysiology* (1963).

[283] Wikipedia. Two-streams hypothesis.

[284] Wiskott, L., and Sejnowski, T. J. Slow feature analysis: unsupervised learning of invariances. *Neural computation 14*, 4 (Apr. 2002), 715–770.

[285] Womelsdorf, T., Schoffelen, J.-M., Oostenveld, R., Singer, W., Desimone, R., Engel, A. K., and Fries, P. Modulation of neuronal interactions through neuronal synchronization. *Science 316*, 5831 (June 2007), 1609–12.

[286] Yao, H., and Dan, Y. Stimulus timing-dependent plasticity in cortical processing of orientation. *Neuron 32*, 2 (Oct. 2001), 315–23.

[287] Yuval-Greenberg, S., Keren, A. S., Tomer, O., Nelken, I., and Deouell, L. Y. Response to Letter: Melloni et al., "Transient Induced Gamma-Band Response in EEG as a Manifestation of Miniature Saccades." Neuron 58, 429–441. *Neuron 62*, 1 (Apr. 2009), 10–12.

[288] Yuval-Greenberg, S., Tomer, O., Keren, A. S., Nelken, I., and Deouell, L. Y. Transient induced gamma-band response in EEG as a manifestation of miniature saccades. *Neuron 58*, 3 (May 2008), 429–41.

[289] Zhang, W., and Linden, D. J. The other side of the engram: experience-driven changes in neuronal intrinsic excitability. *Nature reviews. Neuroscience 4*, 11 (Nov. 2003), 885–900.

Curriculum Vitae

Schlagvorderstrasse 10
Osnabrück 49074 Deutschland
+49 176 82181967
m@martacastellano.eu
Date of Birth: April 28, 1986

Marta Castellano

Education

01.11 – Present **PhD in Cognitive Science**, *University of Osnabrück, Department of Neuroinformatics*, Osnabrück, Germany.

10.08 – 11.10 **MSc in Computational Science**, *Max Plank Institute for Brain Research, Department of Neurophysiology*, J. W. Goethe University, Frankfurt am Main, Germany.

09.04 – 06.08 **BSc in Biotechnology**, *University of Vic*, Barcelona, Spain, *Rank: 1st of 82*.

PhD Thesis

Working Title *Computational Principles of Neural Processing: modulating neural systems through temporally structured stimuli.*

Description The thesis aims to explore the computational basis of neural systems, focusing on how plasticity modulates neural processing. Specifically, through both computational and experimental studies, this thesis explores the effects of temporally structured stimulus on neural processing at the single neuron level, within networks of neurons, and within cortical areas.

Publications

Castellano, M.; Plöchl, M; Vicente, R. and Pipa, G. (2014). Neuronal Oscillations during contour integration of dynamic visual stimuli form parietal/frontal networks (under review)

Castellano, M., Pipa, G (2013). Memory trace in spiking neural networks. *In Artificial Neural Networks and Machine Learning – ICANN 2013, Lecture Notes in Computer Science*(Springer Berlin Heidelberg), pp. 264–271

Scheller, B., Castellano, M., Vicente, R., and Pipa, G. (2011). Spike train auto-structure impacts post-synaptic firing and timing-based plasticity. Front. Comput. Neurosci. 5, 60.

Other Publications Castellano, M. *Criticality in self-organized recurrent neural networks.* Master's thesis. Johann Wolfgang Goethe University of Frankfurt am Main, Germany, 2010

Conferences and Workshops Attended

05.14 **Poster presentation**, 4th Osnabrück Computational Cognition Alliance Meeting (OCCAM)., Osnabrück, Germany.

09.13 **Invited talk**, 23rd International Conference on Artificial Neural Networks, Sofia, Bulgaria.

08.13 36th European Conference on Visual Perception, Bremen, Germany

03.13 10th German Neuroscience Society Meeting, Göttinguen, Germany

07.12 INCF training course on "Advanced Statistical Modelling of Neuronal Data". Osnabrück, Germany

12.11 **Invited talk**, International Workshops on Higher Education, Vic, Barcelona, Spain.

11.11 Workshop on Learning and Plasticity at the CIRM, Marseille, France

09.11 The Fate of the Memory Trace: Learning, Remembering and Forgetting. ECE Summer School in Neuroscience at the Ruhr-University Bochum, Germany

08.10 **Poster presentation**, 3rd International Neuroinformatics Coordinating Facility Congress (INCF). Kobe, Japan .

02.10 **Poster presentation**, Computational and Systems Neurosciences Meeting (COSYNE). Salt Lake City, UT, USA .

01.10 Brain Clocks and Rhythms Summer School, Santiago de Chile, Chile

11.09 Trends in Complex Systems. International Workshop on Synchronization and Multiscale Complex Dynamics in the Brain (BSYNC09), Dresden, Germany.

10.09 Bernstein Conference on Computational Neuroscience (BCCN 2009), Frankfurt am Mainz, Germany

Referee Activities

since 2014 International Conference on Artificial Neural Networks (conference)

since 2014 Biologically Inspired Cognitive Architectures (journal)

Theses Supervised

Master's Theses

07.13 – 05.14 *Ernesto Lopez Montecinos.* Modelling Local Field Potential through delayed dynamical systems

Bachelor's Theses

05.14 – Present *Lukas Röd* Do task requirements modulate visual binding?.

04.14 – Present *Jan Boelts* On-line decoding of visual perception through EEG.

02.11 – 05.12 *Felix Breuninger.* Social games in virtual reality.

02.12 – 05.13 *Alex Meier.* Multi-scale Reservoir Computing Using SORN and Mackey-Glass Systems.

02.11 – 05.12 *Sarah Schaechtelin.* Computational performance and memory capability in a liquid state machine using a critical reservoir.

Teaching Experience

10.11-02.12 *Modelling with spiking neurons*

The course aimed to provide a basis for modelling single neurons and population of neurons. Through discussions of recent publications, the students were introduced to theoretical neurosciences.

Research Positions

10.08 – 10.09 **Department of Neurophysiology**, *Max Plank Institute for Brain Research.*, Frankfurt, Germany.

12.07 – 02.08 **Department of Psychology**, University of Vic, Barcelona.
- ☐ Gender perception in adolescents by survey analysis (SPSS).

07.07 – 10.07 **Neurobiology of Learning and Memory Research Group**, *Sumantra Chattarji's Lab, National Center for Biological Sciences (NCBS)*, TATA Institute of Fundamental Research, Bangalore, India.
- ☐ Protective effects of Estrogen on acute stress, an approach to study PTSD
- ☐ Implementation of the Novelty-Induced Hypophagia Test for the detection of chronic antidepressant treatments on animal models.

02.07 – 07.07 **Medical Statistics and Bioinformatics Research Group**, University of Vic, Barcelona.
- ☐ Single Nucleotide Polymorphisms (SNPs) effects on alternative splicing and its correlation to prostate cancer

09.05 – 02.07 **Bank for Genetic Resources, Genomics lab**, University of Vic, Barcelona.
- ☐ Analysis and evaluation of different procedures for extraction and purification of DNA from composting samples.
- ☐ Analysis and study of the development of microbial diversity during composting process by PCR.

02.04 – 10.05 **Bank for Genetic Resources, Microbiology lab**, University of Vic, Barcelona.
- ☐ Study of microbial communities in the composting process and creation of a microorganism's collection.

Personal Skills and Competences

Languages

Spanish	**Native language**	
Catalan	**Native language**	
English	**Fluent**	*Cambridge Advanced Exam (CAE)*
German	**Beginner**	

Computer skills

Programming	Matlab, Perl, SPSS

Miscelaneous

Other Courses	Health Monitoring on Laboratory Animals (Category C FELASA)